Ph.D. Program in Civil, Chemical and Environmental Engineering

Curriculum in Chemical, Materials and Process Engineering

Department of Civil, Chemical and Environmental Engineering

Polytechnic School, University of Genoa, Italy

Extraction and encapsulation of Bio-components from Tomato Waste for Food and Biomedical Applications

Junyang Li

EXTRACTION AND ENCAPSULATION OF BIO-COMPONENTS FROM TOMATO WASTE FOR FOOD AND BIOMEDICAL APPLICATIONS

BY

JUNYANG LI

Dissertation discussed in partial fulfillment of
the requirements for the Degree of

DOCTOR OF PHILOSOPHY

Civil, Chemical and Environmental Engineering
curriculum in Chemical, Materials and Process Engineering,
Department of Civil, Chemical and Environmental Engineering, University of Genoa, Italy

October 2023

Adviser and co-adviser:

Prof. Patrizia Perego – Department of Civil, Chemical and Environmental Engineering, University of Genoa

Dr. Margherita Pettinato – Department of Civil, Chemical and Environmental Engineering, University of Genoa

External Reviewers:

Prof. Gianpiero Pataro – Department of Industrial Engineering, University of Salerno

Prof. Bahar Aliakbarian – Department of biosystem & agricultural engineering, Michigan State University

Examination Committee:

Prof. José Manuel Domínguez González – Department of Chemical Engineering, University of Vigo

Prof. Massimo Santarelli – Department of Energy, Polytechnic University of Milan

Prof. Elisabetta Finocchio – Department of Civil, Chemical and Environmental Engineering, University of Genoa

Ph.D. program in Civil, Chemical and Environmental Engineering

Curriculum in Chemical, Materials and Process Engineering

Cycle XXXVI

“Strive not to be a success, but rather to be of value.”

[Albert Einstein]

AIM AND CONTENTS OF THE Ph.D. THESIS

The main purpose of this work is to study innovative extraction techniques for extracting bioactive substances, especially lycopene, from tomato waste (peels and seeds) and to study the stability of lycopene under different encapsulation techniques. The main challenge faced by this work is the selection of extraction technology. The guiding idea is to use green extraction technologies to extract lycopene to ensure high efficiency, low energy consumption and reducing pollution to the environment, in order to cope with the increasing demand for lycopene. The severe food safety environment and increasingly serious environmental pollution. The second major aspect is to find a strategy to protect from the environmental of lycopene. Due to the extremely unstable nature of lycopene to external factors such as light, heat, and pH, it is necessary to use a suitable embedding method to protect lycopene. The challenge in this case is how to select an appropriate, simple-to-operate, low-energy, efficient encapsulation technology based on the end use of the product. In this study, three techniques (oil-in-water nanoemulsion, spray drying and supercritical carbon dioxide drying method) were used to encapsulate and protect lycopene.

The topic addressed by this thesis is organized and subdivided into chapters as follows.

Chapter 1 - State of the Art - the source of tomato waste, the economic value associated to the compounds still contained in tomato waste and the technical methods for extracting bioactive substances from tomato waste were elaborated in detail. Different encapsulation methods of lycopene were introduced and applications were briefly analyzed.

Chapter 2 - Raw Materials Characterization - the tomato waste was analyzed in terms of physical-chemical characteristics such as moisture content, active water, particle size distribution, ash and lycopene content.

Chapter 3 - The effects of different extraction methods such as SLE, UAE, and MASE on the extraction yield of lycopene from tomato waste were evaluated. The extraction kinetics of SoLVE extraction, a new extraction method was analyzed.

Chapter 4 - The lycopene-rich extract was encapsulated and protected using the homogeneous nanoemulsion embedding method, spray drying, and supercritical carbon dioxide drying method. The analysis evaluated the stability of the emulsion droplets and lycopene in the nanoemulsions during prolonged storage at different temperatures. The particle characteristics of the solid powder were analyzed.

NOMENCLATURE

ABS	Absorbance
$ABTS^{\bullet+}$	2,2′-azino-bis (3-ethylbenzothiazolin-6-sulfonic acid
$AdjR^2$	Adjusted coefficient of determination
ASE	Accelerated Solvent Extraction
ARP	Antiradical power
atm	Atmosphere
ANOVA	Analysis of variance
a_w	Water activity
BBD	Box–Behnken design
C	Cooler system
CCD	Central Composite Design
C_0	Concentration of analyte (mg g^{-1}) at time t = 0
COSE	Conventional organic solvent extraction
C_t	Concentration of analyte (mg g^{-1}) at time t (min)
D	Average diameter
DB	Dried biomass
DM	Dry test meter
DSD	Droplet size distribution
$d_{3,2}$	Sauter mean diameter
d_{bottom}	Bottom diameter (mm)
d_k	Mean diameter of each interval
d_{top}	Top diameter (mm) and the
d_j	Diameter interval
$d_{(x,o.5)}$	The size of droplet below 50 % of the samples
EC	Extraction cell
EE	Encapsulation efficiency
Emu	Emulsion
EnE	Encapsulation efficiency
ESE	Enhanced solvent extraction
EtOH	Ethanol

ETS	Evaluate the total solids
F	The cumulative mass fraction of the undersize
F’	The cumulative mass fraction of oversize
FAO	Food and Agriculture Organization of the United Nations
FESEM	Field Emission Scanning Electron Microscopy
F_i	Cumulative mass fraction of undersize at the current sieve
FI	Flow indicator
$f(x)$	Relative frequency
GA	Gum arabic
$g(d)_m$	Generic mean value of the distribution
h	Hour
HB	Heating bath
HE	Heat exchanger
HPLC	High-performance liquid chromatography
HPTE	High pressure and temperature-assisted extraction
i	Index
I	Inulin
INV	Inlet needle valve
K_1	Peleg’s rate constant (min g mg^{-1})
K_2	Peleg’s capacity constant (g mg^{-1})
LE	Lycopene equivalents
L/S	Liquid-to-solid ratio
LY	Lycopene yield
M	Manometer
m	Mass
Ma	Maltodextrin
MAE	Microwave-assisted extraction
mg	Milligrams
mL	Milliliters
$mass_{final}$	Total mass at the end of the drying process
$mass_{Ceramic\ Cup}$	Mass of the tare

m_c	Final mass collected
m_f	Initial mass fed
m_{free}	Mass of free lycopene in the nanoemulsions
$m_{initial}$	Mass of lycopene contained in the extract loaded to the nanoemulsions
m_{total}	Mass of total lycopene in the nanoemulsions
N_2	Nitrogen
n_i	The number of droplets with the size of d_i
nm	Nanometers
OV	Outlet needle valve
O/W	Oil-in-water
P	Operating pressure
P_0	The vapor pressure of pure water
P1, P2	Pump
PC	Precipitation chamber
PeC	Pectin citrus
PEF	Pulsed electric field
PFE	Pressurized fluid extraction
PI	Pressure indicator
PLE	Pressurized Liquid Extraction
PR	product recovery
PSE	Pressurized solvent extraction
PSD	Particle Sizes Distributions
PV	Pressure valve
PVP	Polyvinylpyrrolidone
R	Restrictor
R^2	Coefficient of determination
RB	Refrigerating bath
RSM	Response surface methodology
RSMD	Root mean square deviation
S	Saturator
S1	CO_2 supply
S2	Nitrogen supply

S3	Liquid solution supply
SAA	Supercritical assisted atomization
sc-CO_2	Supercritical carbon dioxide
SD	Standard deviation
SE	Solvent extraction
SEM	Scanning electron microscope
SoLVE	Solid-Liquid Multivariable Extractor
SLE	Solid-liquid extraction
SR	Solvent reservoir
SV	Selecting valve
Sub	Subcritical
SWC	Swelling capacity
T	Temperature
t	Time
TC	Total carotenoid yield
TE	Trolox equivalent
TW	Tomato waste
UAE	Ultrasound-assisted extraction
V	Total extraction volume
W	watt
WA	Water activity
WAI	Water absorption indexes
Wh	whey
W/O/W	Water-in-oil-in-water emulsions
WPTC	World Tomato Processing Council
WSI	Water solubility indexes
wt	Weight
x_i	Mass fraction
X_i	Input variable
X_j	Input variable
Y	Generic response variable
°C	Celsius degree
Δ_φ	Variable variation rage

µg	Micrograms
µL	Microliters
φ_i, φ_{min}	Generic variable and minimum variable value
β_0, β_j, β_{jj} and β_{ij}	Model coefficients
L*	Lightness
a*	Redness
b*	Yellowness

ABSTRACT

Tomato waste (TW), the solid residue left after the industrial processing of tomatoes, is considered as one of the most promising candidates to recovery the lycopene. It consists mainly of tomato peels and seeds making up about 3 % to 5 % of the total weight of processed tomatoes which depends on their specific production process. The World Processing Tomato Council (WPTC) estimates that the annual production of tomatoes in Italy is around 5.5 million tons and at a global more than 40 million tons, resulting in the overall production of large quantities of waste after industrial processing of the tomato. Discarding TW directly not only results in a huge loss of valuable materials, but also poses serious management problems from both the economic and environmental point of view. Considering its nutritional properties, however, it is a promising source of biocompounds according to previous studies. Tomato waste consists mainly of pericarp and seeds, of which fiber is the major compound accounting for 25.4 - 50.0 % of the dry matter. The other components are 15.4 - 23.7 % of total protein, 5.4 - 20.5 % of total fat, and 4.4 - 6.8 % of mineral. More importantly, this by-product contains valuable antioxidants which can be extracted by means of proper extraction methods. Effective utilization of food by-products/wastes as a secondary source for new products has been an emerging research topic in recent years. Tomato processing wastes have been the subject of significant research, especially the recovery of lycopene through efficient extraction methods. Unfortunately, lycopene is nonpolar and readily degradable, so lycopene extraction, processing, and analysis must be performed under controlled conditions to minimize oxidative degradation and isomer formation. Conventional methods of lycopene extraction have non-negligible drawbacks such as time-consuming, toxic chemicals and low efficiency. In recent years, a variety of high efficient extraction techniques have emerged, including microwave, ultrasonic, supercritical fluid and pressurized liquid extraction. These non-conventional techniques exhibit several advantages for the extraction of bioactive molecules, such as a shorter processing time, reduction in the use of organic solvents as well as mild operating parameters to avoid thermal degradation. Therefore, they are environmentally friendly and usually result in higher yields and high-quality final extracts.

In this thesis, a preliminary characterization of TW was carried out and different extraction techniques (solid-liquid extraction, ultrasound-assisted extraction, microwave-assisted extraction under pressure and solid-liquid multivariable extractor) were investigated with ethanol and water or their mixed solutions as green solvents. One of the objectives of this research project was to recover lycopene from TW using ethanol solutions as green solvents and to improve the extraction rate by modulating process variables. In this study, response surface modeling and kinetic studies were used as tools for processing optimization and the extracts were evaluated as total lycopene yield and antiradical power.

Since it is rapidly susceptible to degradation and isomerization upon exposure to heat, light or oxygen, lycopene can lose its activity and medical effects without proper protection. Accordingly, the second research objective of this thesis was to analyze and evaluate the protective effect on lycopene by using different methods (oil-in-water nanoemulsion, spray drying method and supercritical CO_2). Among xxx, the oil-in-water nanoemulsion method was carried out with isopropyl myristate as oil phase and Pluronic F-127 as emulsifier. The stability of the nanoemulsion particles and the lycopene content in nanoemulsion were initially characterized at different temperatures. Further, TW extracts as well as oil-in-water nanoemulsions were directly microencapsulated by spray drying and supercritical CO_2 using inulin and maltodextrin as wall materials. The encapsulation process was optimized by modulating different parameters (e.g., coating agent composition, inlet temperature, feed flow rate, feed flow rate of CO_2 and feed flow rate of N_2) and was analyzed using the Response Surface Methodology.

The results about the characterization of TW showed on initial moisture content, approximately 84.3 ± 0.83 %. After the drying process, a final moisture of approximately 6 % of residual moisture. Particularly, after the drying process, the TW exhibited a water activity of 0.101 ± 0.042, resulting as suitable for long-term storage in water-proof containers and in the dark for extraction experiments. After crushing, the average diameter of the particles is smaller (732 ± 67 µm), making it possible to directly use TW for extraction. The biomass showed an ash content of 4.1 ± 0.8 %. SLE using hexane as solvent was carried out for the quantification of lycopene as reference. The total lycopene content was 1438.24 ± 44.3 µg/g (dry solid), measured via HPLC. SLE using sunflower seed oil as solvent was carried out for a general

traditional extraction. The results showed that the optimal conditions were T = 45 °C, L/S = 20/3 mL/g, stirring speed = 900 rpm, t = 45 min. The total lycopene content was 1237.32 ± 4.80 µg lycopene equivalent/g (dry solid) measured by UV-vis spectrophotometer. UAE extraction using ethanol as solvent as advanced extraction method was carried out. Response Surface Methodology was used to investigate the effect of the ultrasound-assisted extraction parameters on the extract bioactive content. The optimal conditions found by the desirability method (T = 65 °C, t = 20 min, L/S = 72 mL/g, *A* = 65 %, *on*/*off* = 33/30 s/s, V = 90 mL) were experimentally verified and the total lycopene content was 1536 ± 53 µg/g (dry solid), measured via HPLC. It was also found that the frequency of ultrasonic vibration studied (40kHz, 80kHz, 120kHz) did not significantly improve the lycopene extraction yield. SoLVE extraction using ethanol as solvent as the focus of this chapter was carried out. The optimal conditions also found by the desirability method (CCD) (T = 65 °C, t = 41 min, L/S = 27 mL/g, *A* = 39 %, *on*/*off* = 32/30 s/s) were experimentally verified. Under optimal conditions, the trans-lycopene yield was of 546.7 µg/g and the total lycopene yield was 1193.0 µg lycopene equivalents/g. In addition, the extraction kinetic model was found to be consistent with the Peleg's model through the study of the extraction kinetics during the extraction process. Finally, microwave-assisted subcritical extraction method was used to study and compare the extraction of lycopene with the extraction conditions of UAE and SoLVE. The optimal conditions were T = 100 °C, L/S = 72 mL/g, V = 30 mL, t = 15 min. The maximum total lycopene content was 962.97 ± 42.87 µg/g (dry solid), the *trans*-lycopene yield was of 662.84 ± 24.55 µg/g (dry solid), measured via HPLC. Due to the instability of lycopene, it is easily degraded under the influence of external factors (temperature, light, oxygen, pH). Therefore, further research on the protection of lycopene is necessary. This study used different technologies to encapsulate and protect lycopene through solid and liquid formulations. In the part of encapsulation, nanoemulsions were found stable for up to three months at the optimal storage temperature (4 °C) as no significant agglomeration was observed. The addition of extracted solution was found to significantly reduce the droplet size and increase the stability of nanoemulsions. The spray drying technology was found efficient for transferring the nanoemulsion to solid powder. The operating conditions at which spray drying reached the highest recovery were the input temperature 170 °C, the gas flow rate 35 m^3/h, the flow rate of the nanoemulsion 6 mL/min and the coating agent

(maltodextrin) at 40 % w/w. Under the optimal conditions, the recovery of the product reached 80.3 %. Furthermore, as a comparison, a feasibility evaluation of the encapsulation of the obtained extract by spray drying was carried out, investigating the possibility to add inulin in the composition of the wall material. The best results were obtained at the lowest percentage of inulin (21.7 % inulin and 78.3 % of maltodextrins). Finally, a SAA laboratory apparatus was adopted to dry the nanoemulsions, and different coating agents, CO_2 flow rate, temperature, feed flow rate, and production recovery were evaluated.

INDEX

NOMENCLATURE 9

ABSTRACT 15

1 STATE OF THE ART 1

1.1 Tomato waste 1

1.2 Chemical value – bioactive components in TW 4

1.3 Extraction techniques of bioactive components from TW 5

1.3.1 Conventional extraction 7

1.3.2 Microwave-assisted extraction 8

1.3.3 Ultrasound-assisted extraction 9

1.3.4 Pressure-assisted extraction 9

1.3.5 Combined extractions 16

1.4 Micro-/Nano-encapsulation of extracted bioactive components 17

1.4.1 Emulsion 18

1.4.2 Spray drying 19

1.5 Application of encapsulated lycopene 21

2 RAW MATERIAL CHARACTERIZATION 23

2.1 Materials and Methods 23

2.1.1 Tomato waste samples 23

2.1.2 Determination of the moisture of TW 24

2.1.3 Determination of the water activity of TW 24

2.1.4 Determination of the particles size distribution of dry TW 25

2.1.5 Determination of the ash content of TW 27

2.1.6 Determination of the total lycopene content of TW 27

2.1.7 Lycopene yield by HPLC 28

2.2 Results and Discussion 29

2.2.1 Physical Characterization of TW 29

2.2.2 Chemical Characterization of TW 30

2.3 Conclusions 30

3 EXTRACTION OF LYCOPENE FROM TW BY NON-CONVENTIONAL METHODS . 33

3.1 Chemicals and Sample Preparation 33
3.2 Solid-liquid extraction (SLE) 34
3.3 Ultrasound-assisted extraction (UAE) 34
3.4 Experimental Design of UAE 35
3.4.1 Numerical Optimization 36
3.4.2 Evaluation of the effects of frequency in UAE 36
3.5 Solid-liquid Multivariable Extractor extraction (SoLVE) methods 37
3.5.1 SoLVE system equipment 37
3.5.2 Lycopene extraction and analysis optimization using the Central Composite Design 38
3.5.3 Kinetic models for SoLVE process 39
3.5.4 Optimization of the process 40
3.5.5 Color measurements as a tool of quantitative determination of lycopene 40
3.6 Microwave-Assisted Subcritical Extraction (MASE) Methods 41
3.6.1 MASE system equipment 41
3.6.2 Microwave-Assisted Subcritical Water and Ethanol 20% (v/v) Extraction 41
3.6.3 UAE combined with MASE 42
3.7 Analytical methods 42
3.7.1 Total Carotenoid yield by UV-vis spectrophotometer 42
3.7.2 Lycopene yield by HPLC 43
3.7.3 Antiradical power 44
3.7.4 Antiradical Power through its radical inhibition ability 44
3.7.5 Determination of total solids 44
3.8 Results and discussion 44
3.8.1 SLE 44
3.8.2 UAE 47
3.8.2.1 Ultrasound-assisted Extraction Modelling by RSM 47
3.8.2.2 Process Optimization 54
3.8.2.3 Evaluation of the effects of frequency in UAE 60
3.8.3 SoLVE 61
3.8.3.1 Lycopene content 61
3.8.3.2 Antiradical power 63
3.8.3.3 Relationship of inhibition and concentration of lycopene 65
3.8.3.4 Extraction Kinetics Curves 66
3.8.3.5 Effect of parameters on the K_1 and K_2 69

3.8.3.6 *Trans*-lycopene and *cis*-lycopene content 72
3.8.3.7 Desirability 73
3.8.3.8 Color measurement 76
3.8.4 Microwave-assisted subcritical extraction 79
3.8.4.1 Effect on lycopene yield of different solvents and times 79
3.8.4.2 *Trans*-lycopene and *cis*-lycopene content 82
3.8.4.3 Effect of biomass for different methods at different concentrations 84
3.9 Conclusion 86
4 ENCAPSULATION OF BIOACTIVE EXTRACTED FROM TW 91
4.1 Encapsulation by Oil-in-water nanoemulsions methods 92
4.1.1 Apparatus, Chemicals, Standards and Solvents 92
4.1.1.1 Chemical and sample preparation 92
4.1.1.2 Apparatus 92
4.1.2 Preparation of aqueous phase and O/W emulsion 93
4.1.2.1 Emulsification of Alcohol Extracts 93
4.1.2.2 Emulsification of Oil Extracts 94
4.1.3 Analytical methods 94
4.1.3.1 Droplet size distribution 94
4.1.3.2 Lycopene content 95
4.1.3.3 Stability test 96
4.1.3.4 Emulsions total and free lycopene content in nanoemulsions 96
4.1.3.5 Lycopene encapsulation rate in nanoemulsions 96
4.1.4 Statistical analysis 97
4.1.5 Results and discussion 97
4.1.5.1 Emulsion production with ethanol 97
4.1.5.2 Stability of nanoemulsion 101
4.1.5.3 Emulsion production with sunflower seed oil 103
4.2 Encapsulation by Spray Drying 106
4.2.1 Materials and Methods 106
4.2.1.1 Apparatus, chemicals, standards and solvents 106
4.2.1.2 Extract stabilization by Spray drying 107
4.2.1.3 O/W nanoemulsions stabilization by Spray drying 108
4.2.2 Analytical methods 109
4.2.2.1 Product recovery 109
4.2.2.2 Determination of particle sizes 109

4.2.2.3 Determination of moisture content 110
4.2.2.4 Determination of water activity 110
4.2.2.5 Determination of lycopene content in powders 110
4.2.2.6 Determination of lycopene content in powders 110
4.2.2.7 Water solubility index and water absorption index 111
4.2.3 Results and discussion 112
4.2.3.1 Extract stabilization by Spray drying 112
4.2.3.2 Encapsulation of nanoemulsion with different coating agent by spray drying 114
4.3 Encapsulation by supercritical assisted atomization (SAA) 120
4.3.1 Materials and Methods 120
4.3.1.1 Apparatus, chemicals, Standards and Solvents 120
4.3.1.2 SAA Apparatus and Procedure 121
4.3.1.3 Process description 122
4.3.1.4 Product recovery 123
4.3.1.5 Determination of particle sizes 123
4.3.1.6 Determination of moisture content 124
4.3.1.7 Determination of water activity 124
4.3.2 Results and Discussion 124
4.4 Conclusion 126
CONCLUSIONS 131
Figure 135
Table 141
References 143
RINGRAZIAMENTI 165

1 STATE OF THE ART

1.1 Tomato waste

Tomato (*Lycopersicon esculentum*), as one of the most popular vegetables in the world, enriches lycopene, phenolics, organic acids, vitamins, and many other beneficial components [1]. According to the Food and Agriculture Organization of the United Nations (FAO), tomato is the second most produced vegetable crop after potato in the world, with an annual production of 190 million tons of fresh fruit in 144 countries, and it ranks 6th compared to other agricultural sectors (potatoes, onions, pumpkins, etc.) in Italy, leading to an overall high profitability with regards to the tomato processing industry. Furthermore, it is one of the most expensive vegetable crops as well [2]. Tomato can be consumed as fresh or after processing. The global production of processed tomato has fluctuated between 150 M and 200 M tons over the last two decades (Figure 1), and in the Northern Hemisphere accounts for about 85% of the total. Asia, America, Europe and Africa share about 54.9 %, 17.3 %, 15.5 % and 11.9 % of the total production, respectively, contributed mainly by China, USA, India, Turkey, Egypt, Italy, Iran, and Spain [3] (Figure 2).

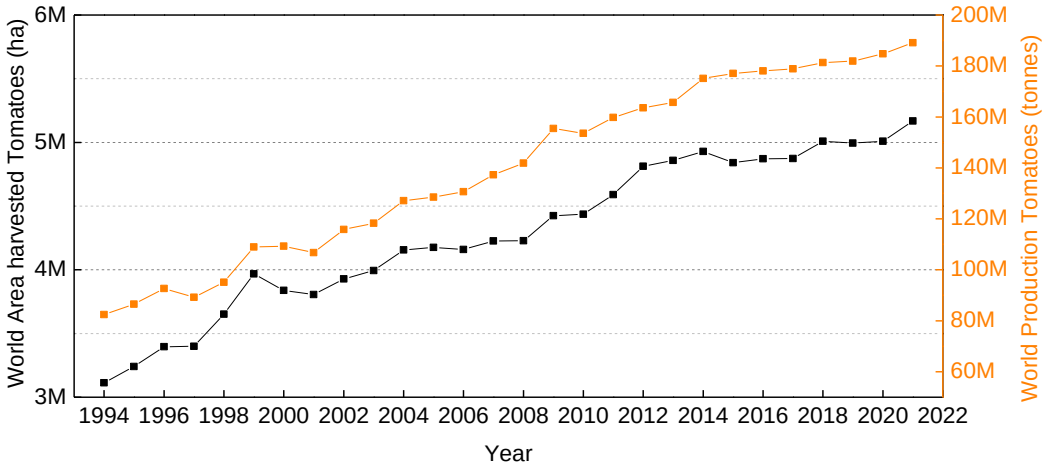

Figure 1. Production/yield quantities of tomatoes in world 1994-2021 (FAO).

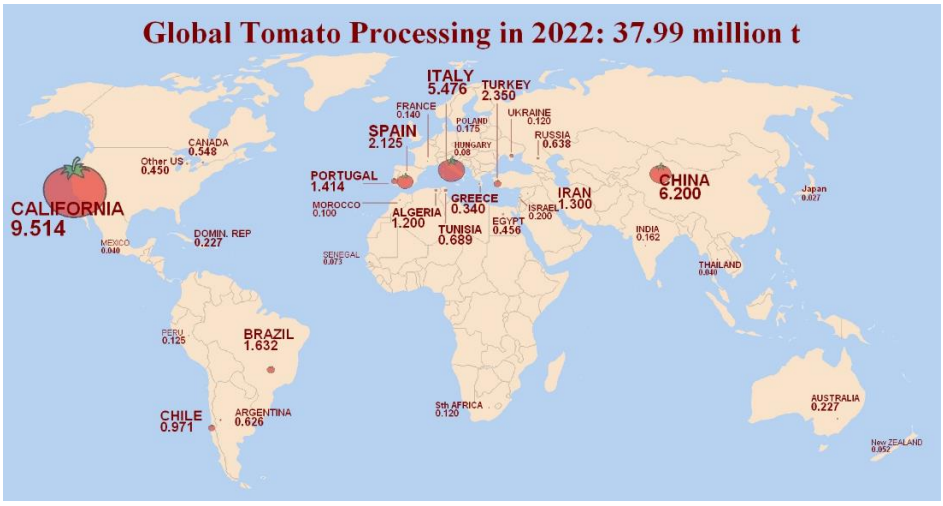

Figure 2. Average production quantities of tomatoes by country in 2022 [3].

For the industrial tomato processing, the activities involve the processing of raw tomatoes into semi-processed products (concentrated tomato pulp) and semi-processed products to the final products (ketchup, sauces, etc.) which can be used directly by consumers [2,4-6]. Some definitions related to concentrated tomato juice, tomato pulp, tomato puree, and tomato paste can be found in literatures [4], as shown below:

- **Tomato pulp** is crushed tomatoes either before or after peeling and deseeding.
- **Tomato juice** refers to the finely screened juice obtained by crushing whole tomatoes, removing the skin and seeds, and can be used without dilution or concentration.
- **Tomato paste** is the product of concentrated tomato pulp after removal of the skin and seeds, containing 24% or more of natural tomato soluble solids. Ketchup, marketed to consumers in small packages and sold as a condiment, could also be described as tomato puree.
- **Tomato puree** applies to lower concentrations of tomato paste (containing 8% to less than 24%.
- **Tomato serum** that has been filtered or centrifuged to completely remove suspended solids.
- **Pulp** is the suspended solid matter in tomato juice, puree or paste. Can be separated by centrifugation.
- **Tomato syrup** is concentrated tomato liquid.

After the industrial processing of tomatoes, the solid residue is called tomato waste (TW) and is considered as one of the most promising candidates for bioactive components recovery. TW consists mainly of tomato skins and seeds making up of about 3 % to 5 % of total weight of processed tomato which depends on their specific production process [7,8]. By-products of tomato processing represent a major disposal problem for the industry concerned, but they are also promising sources of chemical compounds which may be reused because of their favorable technological or nutritional properties [9]. One of the representative compounds is lycopene which has been investigated for many years. However, the available lycopene on the market is commercially produced by extraction and concentration from whole tomato fruits or synthetic with significant differences upon the costs involved to obtain, and is relatively expensive [10,11]. For the produced of synthetically lycopene, the Wittig reaction has been used as a main shortcut to introduce newly conjugated carbon-carbon double bonds [12]. The process of synthetical is long and complex and involves, in the final stages, the condensation of two intermediate products, phospho methanesulfonate and C10-dialdehyde, dissolved in toluene in the presence of sodium methyloxide to form lycopene crystals. Afterwards crystals must be subsequently purified by filtration and recrystallization, to obtain a red crystalline powder with large crystals and regular shape. Synthetic lycopene is a mixture of geometric isomers of lycopene and consists mainly of all-trans lycopene, 5-cis-lycopene and small amounts of other isomers. It must be at least 96 % total lycopene, of which not less than 70 % is all-trans-lycopene and the remainder is predominantly 5-cis-lycopene [13], it can contain low concentrations of reaction by-products, such as triphenyl phosphine oxide (TPPO; not more than 0.01 %) and apo-12'- lycopene (not more than 0.15 %) [14]. This has simulated plenty of research looking for low-cost alternative sources of lycopene. Food by-products/waste, as a second choice for new product development, has been given more attention for producing low-cost ingredients. Baysal, Ersus, and Starmans reported that significant amounts of carotenoids were lost as waste during tomato processing [15]. Discarding these wastes can not only cause a huge loss of valuable materials, but also raises serious management issues from both economic and environmental perspectives. Therefore, a further investigation on the recovery and protection of lycopene from TW is highly considerable to support the sustainable development, and the technique for recovering lycopene need to be improved.

1.2 Chemical value – bioactive components in TW

Valuable biologically active compounds (carotenoids, mainly lycopene (80 - 90 %) and beta-carotene, as well as lutein, vitamin C, vitamin E and various phenolic compounds) in tomatoes have been fully reported by many researches [16]. It is noteworthy that TW from industry enrichs considerable chemical values as well that mainly come from pericarp and seeds, in which fiber is the major compound accounting for 25.4 - 50.0 % of the dry matter, with 15.4 - 23.7 % of proteins, 5.4 - 20.5 % of fats, and 4.4 - 6.8 % of minerals [7,17,18]. This TW contains important antioxidants (mainly lycopene and other carotenoids) which can be extracted by means of proper extraction methods [19-22]. Carotenoids are a group of phytochemicals that are responsible for yellow, orange and red colors of foods and vegetables [23]. They can be classified in two broad sub-categories: carotenes (such as α-carotene, β-carotene and lycopene) and xanthophylls (such as lutein, astaxanthin and cryptoxanthin). From the chemical point of view, xanthophylls are carotenes' oxygenated derivatives; indeed, they differ for the presence of oxygen atoms in the structure: carotenes are purely hydrocarbons (for example, α-carotene, β-carotene and lycopene formula is $C_{40}H_{56}$), whereas xanthophylls are formed by carbon, hydrogen and oxygen (lutein formula is $C_{40}H_{56}O_2$, astaxanthin is $C_{40}H_{52}O_4$ and cryptoxanthin is $C_{40}H_{56}O$).

The lycopene content of fresh tomatoes ranges from 43 to 181 mg/kg, with an average level between 55 and 80 mg/kg. However, the lycopene of tomato mainly come from tomato skins which represents more than 80 % of the total [24], while in tomato pulp it is lower than 20%, depending on the cultivar, season and region of cultivation [21,25]. George et al. [21] found that tomato skin contained high amounts of polyphenols and ascorbic acid, and lycopene content was about 2.5 times higher than that of tomato pulp. A similar chemical population but with significant different content was found between whole tomato and TW. Other studies reported a higher ratio of biocomponents (carotenoids, phenolic content) in TW as compared with whole tomato on a wet base [26-30]. Unfortunately, even though the above mentioned advantages, the current use of industrial tomato waste (seeds and peels) is mainly for animal feeding or as fertilizers [31,32]. However, the high chemical value in TW indicates its potential commercial application for extracting antioxidants [33].

1.3 Extraction techniques of bioactive components from TW

Food industry by-products/wastes are believed as a cheap raw material for the recovery of bioactive components with commercial value, for development of food additives, new functional foods, nutra-/pharmaceuticals, cosmeceuticals, and beauty products, as well as for innovative and more sustainable packaging [34]. Metabolites in food industrial by-products was reported to has an enormous potential for producing sustainable additives, chemicals, biofuels, and energy [35]. By now, many molecules of interest for the industrial application have been documented to be recovered from agri-food waste like caffeine from spent coffee grounds [36,37], lycopene and carotenoids from TW [38], astaxanthin from crustacean and shrimp waste [39,40], polyphenols from fruit waste and rice [41], lipids and protein from the waste of olive or microalgae [42-44]. These active substances have potential health benefits as ingredients or additives in medical products as well as in food and cosmetic industries. The most vital process from industrial food waste to isolate bioactive compounds are extraction and purification. Thanks to the enabled use of green and food-grade solvents, pressure-assisted extraction has been successfully applied to extract bio-substances such as proteins, polysaccharides (lignans), lipids, polyphenolic compounds (carotenoids and tocopherols) and essential oils from food waste [45]. However, the recovery of lycopene from this material is not straightforward and traditional solvent extraction procedures give low yields [46-48] due to the compactness of plant tissue that hinders solvent penetration and transport of lycopene from chromoplasts, as well as the possible degradation during extraction. Indeed, lycopene is very susceptible to degradation once released from the protective chromoplast environment [5,49]. To overcome these problems, green solvents combined with emerging technologies such as low-temperature microwave-assisted extraction, ultrasound-assisted extraction, pulsed electric field (PEF), supercritical fluid extraction, enzyme-assisted extraction, pressurized liquid extraction, microemulsion and their combinations have attracted much attention in the effective extraction of lycopene, and many extraction methods have been reported to have overwhelming advantages (such as low energy consumption, short extraction times, improved yields, and supporting environmental sustainability) but also some disadvantages [50,51] as shown in Table 1.

Table 1. The advantages and disadvantages of various methods for lycopene extraction [52].

Technology	Technique	Principle	Advantages	Disadvantages
Solvent Extraction (SE)	Solvent	Solvent dissolution	• Easy scale up • Easy operation • Maturity in industrial application • Wide applicability	• Consuming solvent / time / energy • Low yields • Affecting substances stability • Degradation of target substances
Ultrasound Assisted Extraction (UAE)	Ultrasounds	Cavitation and physiochemical effects disrupted cell wall	• High efficiency • Saving energy and time • Reducing organic solvent use • Wide applicability • Easy operation • Less impurity • Low temperature • Low cost	• High device requirements and wastage • Difficult to enlarge • Probably affecting substances • Noise
Microwave Assisted Extraction (MAE)	Microwaves	Thermal effects disrupted cell wall	• High efficiency • Saving energy and time • Reducing organic solvent use • Uniform heating • Selective • Wide applicability	• High device requirements and wastage • Difficult to enlarge • Probably affecting substances
Supercritical Fluid Extraction (SFE)	Supercritical fluid	Solubility changes of solutes near critical point of supercritical fluid	• High efficiency • High solubility • No organic solvent use • Nontoxicity • Mild temperature • Stability • Easy operation • High purity • No pollution	• High device requirements and wastage • Difficult to enlarge • Probably affecting substances • Low solubility • Difficult to clean device • High device cost
Pulsed Electric Field Assisted Extraction (PEF)	Electric field	Pulsed electric field increased the permeability and disrupt the cell wall	• High efficiency • Saving energy and time • Reducing organic solvent use	• High device requirement and wastage • Difficult to enlarge • Probably affecting substances
High Pressure Extraction (HPE)	Pressure	High pressure disrupted cell wall	• High efficiency • Saving energy • Reducing organic solvent use • Uniform treatment	• High device requirements and wastage • Difficult to enlarge • Safety concerns at high pressure

The combined technique was found to improve extract yield of lycopene from tomato waste (pericarp) compared to conventional extraction techniques [52]. In particular, the use of extraction performed at high-pressure conditions, such as supercritical fluids and pressurized liquid extraction, favored the process with important benefits as short processing times, reduced use of organic solvent and mild operative conditions that avoided thermal degradation of bio-compounds [53]. These technologies are considered environmentally friendly and are generally able to result in higher yields and high-quality final extracts.

Considering both conventional solid-liquid extraction and non-conventional techniques, the overall aim is to improve extraction yield of targeted compounds, avoid deterioration and loss of functionality during processing, and to produce a food-grade final product [54]. Therefore, this part presents the latest findings on UAE, MAE, SFE and pressure-assisted extraction processes, as well as the possibility of combining different extraction processes.

1.3.1 Conventional extraction

Conventional extractions (including maceration, percolation, squeezing, counter-current extraction, extraction through Soxhlet, and distillation, from unconventional (or innovative) ones) have been used for many years, although they have many drawbacks: they require the use of large amounts of expensive pure solvents; have low extraction selectivity; have high solvent evaporation rates during processing; and are generally characterized by long extraction times and thermal decomposition of thermolabile compounds [55]. Conventional methods for the extraction of lycopene from various sources have used pure solvents such as dichloromethane or a mixture of polar and non-polar solvents (e.g., hexane, acetone, and ethanol) [56]. For example, Soxhlet extraction as one of the conventional techniques which is carried out by extracting lycopene-containing food samples using different organic solvents at boiling point temperatures, and it was reported to provide the highest carotenoid recovery [57,58]. This method is often used as a control to check the performance efficiency of other extraction methods. However, this technique is quite time-consuming and expensive, using a large amount of solvent during the extraction process, and it is usually accompanied by lycopene isomerization and oxidation because of the elevated temperature and prolonged extraction time [59]. The solvents

used to extract lycopene are often toxic (hexane and methanol), making even trace amounts of these solvents in the final extracts unsuitable for food products [60]. To overcome all the limitations of conventional extraction, new and promising extraction techniques, which are defined as non-conventional, have been developed, mainly in the industrial field, such as ultrasound-assisted extraction (UAE) [61], supercritical fluid extraction (SFE) [46], microwave-assisted extraction (MAE) [62], enzyme-assisted extraction[63,64], and rapid solid-liquid extraction dynamic via the Naviglio extractor [65].

1.3.2 Microwave-assisted extraction

Microwave-Assisted Extraction (MAE) is relatively simple, economical, and fast to conduct, requiring less extraction time and less solvent than other methods. In this technique, microwaves induce rapid heating of the polar components of cells, facilitating the drift of lycopene into the extraction solvent, thereby increasing the yield of lycopene [66]. For example, Ho et al. [67] investigated the effect of MAE on lycopene yield at hexane-ethyl acetate ratio 0:1 mL/mL and solid–liquid ratio 1:20 g/mL at 400 W to achieve the required energy transfer to the sample. In their study, the maximum yield of *all-trans*-lycopene was found to be 13.592 mg/100 g, and ethyl acetate was better as solvent for the extraction of lycopene than hexane.

As a time-saving technique, MAE is a very promising method with regards to efficient lycopene recovery. To optimize lycopene extraction process, extraction time, solvent type, temperature, solid-to-liquid ratio, microwave power, and delivered energy equivalents are usually considered as key factors. The MAE technique induces a rapid heating primarily to polar components due to dipole rotation and ion drift [68], so in theory, superheating of polar cellular components would improve the migration of lycopene into the extraction solvent, while a shorter processing time could limit thermal exposure of non-polar components. That is, MAE may have an impact on the yield of *cis*- and *trans*- isomers. However, MAE was found to have no significant effect on the extraction ratio of *cis*-isomers and *trans*-lycopene in experiments carried out by Ho et al. [67]. So, more studies are still needed to better investigate the effect of this technique on the recovery of carotenoids from wastes.

1.3.3 Ultrasound-assisted extraction

Ultrasound-Assisted Extraction (UAE) is a fairly efficient extraction method for lycopene recovery from TW, due to its special properties for the application of green chemistry in food processing [69]. In addition, its extraction rate and bioactive compounds yield can be increased by decreasing extraction volume, and its ultra-short extraction time can help to reduce energy consumption. Many related studies reported the investigations about the reuse of TW using UAE method. The mechanical action of UAE was reported to enhance cell wall disruption and improve solvent penetrability for maximum lycopene yield [70], which is in line with one study conducted by Silva et al. [71] who found a lycopene yield up to 1334.8 µg/g in presence of ethyl acetate as solvent in UAE process. Kumcuoglu et al. [72] also reported a shorter extraction time, a lower temperature and less solvent volume for UAE compared with the conventional organic solvent extraction (COSE) method. In another study, some interesting properties (total carotenoids 1408 ± 14 µg/g, lycopene yield 1536 ± 53 µg/g, antiradical capacity 36.1 ± 0.9 $\mu g_{trolox\ equivalent}/g$) was found in bio-active compounds extracted via UAE with ethanol as solvent [38]. Thus, considering the mentioned advantages reported above, UAE can be a good candidate to obtain remarkable amount of thermosensitive compounds from natural products.

1.3.4 Pressure-assisted extraction

In recent years, as a consequence of the deepening of research on biologically active natural substances, many extraction methods have been developed in order to obtain active compounds directly from natural sources.

Among the emerging extraction technologies that can enhance the performance of conventional extraction techniques the pressured liquid extraction (PLE) is considered environmental-friendly, efficient, generating a small amount of waste and reducing cost and time [73,74]. The methodology is based on the use of solvents below their critical point in order to keep the liquid phase during the extraction. Firstly, PLE was introduced by Dionex Corporation [73] in 1995 at the Pittcon Conference, as Accelerated Solvent Extraction (ASE) technology. It is also known as pressurized solvent extraction (PSE); enhanced solvent extraction (ESE) or pressurized fluid extraction (PFE) [75-78].

At the beginning, this technology was used for trace analysis of organic contaminants [73,79,80]. However, in recent years, due to the advantages of PLE, such as significantly shortened extraction time and low solvent volume required, easy operation and good performance, this technology is being applied to different fields, including biology, pharmaceuticals and food industry [45,80-82].

Regarding the mechanism of extraction, PLE combines elevated pressure and temperature with liquid solvents, without exceeding the critical points of the solvent or solvent mixtures, which remains in a liquid state. In this way, it is possible to increase the mass transfer rate of compounds from the matrix to the extraction solvent to achieve a fast and efficient solid-liquid extraction. PLE often demonstrated better recovery if compared with other extraction techniques such as microwave-assisted extraction (MAE), or ultrasound-assisted extraction (UAE) [83,84]. Other significant advantages of PLE include the elimination of post-extraction steps, such as filtration and centrifugation, the high level of automation, and the possibility of coupling with different techniques, such as ultrasound [73,85,86].

Regarding the operation mode, there are three possible different modalities for applying the PLE process: static [87-89], dynamic [90] and static-dynamic. In the static mode, a fixed volume of extracting solvent is used; in the dynamic mode, the extracting solvent flows continuously through the sample; and in the static-dynamic layout a combination of the two modes is proposed. As shown in Figure 3a, static pressurized liquid extraction generally consists of the following components: (1) a pump to feed the solvent through the system; (2) an extraction vessel. The extractor consists of an extraction cell (EC) in which the solid matrix is contained, surrounded by a heating system. The layout is completed by (3) a system cooling the fluid from oven temperature to room temperature or even lower; (4) an on/off pressure needle valve located after the cooler to maintain pressure during static extraction; (5) N_2 flushing system, located between the high-pressure pump and the extraction system. The dynamic pressurized liquid extraction system is improved on the basis of the static pressurized extraction system, as shown in Figure 3b: (1) the selector valve connected to the N_2 flow is replaced by the inlet valve, because in dynamic mode, there is no need to purge the system; (2) the extraction vessel ; (3) a restrictor connected to the outlet of the cooler (in place of the on/off valve) is used to maintain constant the pressure in the system [91].

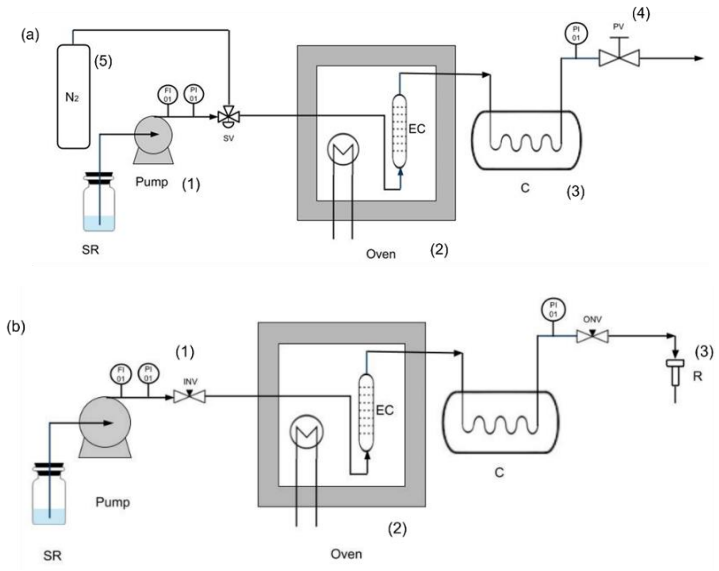

Figure 3. PLE system adapted from [91-93]. (a) Static mode; (b) Dynamic mode. SR, solvent reservoir; FI, flow indicator; PI, pressure indicator; SV, selecting valve; EC, extraction cell; C, cooler system; PV, pressure valve; INV, inlet needle valve; OV, outlet needle valve; R, restrictor.

Other configurations of pressure-assisted process are also proposed in literature.

Extractor Naviglio is based on the application of pressure (about 8 - 9 bar) and decompressions up to atmospheric values, creating a suction effect and a mechanical transport of target compounds from the solid to the solvent phase. The system is composed of two cylinders in which extraction is performed, which communicate through a tube on which an electro-valve is intercepted. A pneumatic system, with compressed air, moves two pistons to provide a pressure rise during a static stage, during which pressure is maintained constant for a while, improving the penetration of the solvent within the solid and a dynamic stage. Then, when the pistons are removed from the equilibrium position and alternately work generating negative pressure gradient between the inside and the outside of the solid matrix and promoting the dragging effect of the extraction [94]. This system is designed to work at room or low temperatures reducing the thermal stress for thermo-sensitive compounds [95].

Moreover, high pressure and temperature-assisted extraction (HPTE), similarly to PLE, exploits the effects of pressure to work at high temperature for the mass transfer improvements, but a different setup of the extraction cell is employed. Indeed, extraction is carried out in a stainless-steel vessel and a stirrer equipped by impellers provides an excellent and homogeneous mixing action [96]. The extractor can work up

to 350 °C and up to 200 bar and the two variables are monitored by a thermocouple and a pressure gauge, respectively. The thermal sensor is connected to a temperature which maintains the variable at the desired set point value by an external electrical jacket. Before the extraction, an inert atmosphere is created inside the extraction vessel by bubbling inert gases for air removal with the aim of limiting degradation reactions of thermo-sensitive compounds. In HPTE, temperature and pressure are strictly related since the second one corresponds to the vapor pressure of the solvent at the set point temperature [36].

Some authors use a combination of static and dynamic [76,97,98] layout to optimize the extraction process. Both modes have their own advantages and disadvantages. The most significant negative feature of dynamic pressurized extraction is that the solute in the extract is diluted, which requires a concentration step as post-processing. Whereas, for the static extraction mode, the extraction efficiency depends on the solute mass transfer balance between the matrix and the extracting solvent [99]. The critical factors are the temperature and time of the extraction. Furthermore, in the static extraction mode complete extraction might not be achieved due to the limited volume of the extraction fluid.

In order to improve the extraction efficiency of an active substance, the key parameters that can affect the efficiency of the extraction process must be investigated. For pressurized liquid extraction, the factors that affect the extraction include the type of residue, solvent type, extraction time, pressure, temperature, pH, liquid-to-solid ratio, stirring speed, particle size, and sample moisture [100,101].

Pressure-assisted extractions can employ wide range of extraction temperatures, usually from room temperature to 200 °C, and pressures up to 200 bar [76]. Temperature is a very important parameter to improve the mass transfer rate of the target compound from the solid matrix to the extraction solvent. Due to the non-compressibility of the liquid (the change in density with pressure is usually insignificant), in some cases the effect of pressure does not have a direct effect on solubility of analyte. However, operating at higher pressures can ensure that the solvent remains in a subcritical liquid state while pressure forces the solvent to penetrate into the matrix pores and facilitate the desorption of the target compound due to a synergistic effect with temperature. The combined effect of high temperature and high pressure provides conditions able to significantly increase the solubility and

diffusivity of the solute, to perform the rupture of the solute-matrix bond, and to reduce the surface tension and viscosity of the solvent [102-105].

Indeed, as reported by Aliakbarian et al. [106], subcritical water extraction ($100 \leq T \leq 140$ °C and $8 \leq P \leq 15$ MPa, for 130 min), provided a total flavonoid and polyphenol 12 and 19 folds higher than conventional solid liquid extraction performed with water at 25 °C for 19 h, and with a higher antiradical power. In addition, polyphenol extraction from *Teucrium montanum* L. carried out by subcritical water gave higher concentrations of total phenolics in comparison to aqueous, methanolic, acetone, ethyl acetate and petroleum ether extracts obtained by conventional solid/liquid extraction [107]. At the same time, the comparison of HPTE with other extraction technique, using ethanol as solvent, showed the best performance of the former on the recovery of bioactive compounds from *Arthrospira platensis*, while conventional solid-liquid extraction provided the worst performance [108].

A particular extraction technique under pressure is supercritical fluid extraction (SFE). SFE is an emerging clean technique that was developed in the late 70s/early 80s of the last millennium and represents the most studied supercritical carbon dioxide-based technique [109,110]. Most of the published work focuses on the extraction of compounds of interest from plant matrices such as seeds, fruits, or leaves. The SFE process exploits the advantages of the use of carbon dioxide in the supercritical state: mild critical values of temperature and pressure (Tc = 31.1 °C; Pc = 73.8 bar), partial elimination of the use of organic solvents that could remain present in traces in the extract (with consequent limitation of the environmental impact of the extraction process), the possibility of simply modulating the solvent power of CO_2 which changes significantly with pressure and temperature, ease in the scale-up of the process up to the industrial scale [111-115]. It is important to underline that carbon dioxide in the supercritical state is a "hybrid" between a gas and a liquid; indeed, it has some properties typical of gases (such as the high diffusivity, which guarantees a better transport of matter with consequent extraction times drastically reduced than the ones of the classic solvent extraction), others comparable to those of liquids (such as the density, to which the solvent power is directly connected). Moreover, carbon dioxide is non-toxic, non-flammable, available in large quantities and cheap. The main disadvantage of supercritical carbon dioxide(sc-CO_2) based techniques is linked to the investment costs (for the design of equipment that operate at high pressures) and

operational costs (for pumping CO_2). The fundamental elements in an extraction plant are sketched in Figure 4, a) the carbon dioxide vessel; b) the pump (with refrigerated head to avoid cavitation phenomena); c) a heat exchanger to pre-heat the carbon dioxide; d) an extraction vessel in which the matrix from which to extract the compounds of interest is loaded; e) one or more separators at lower pressures than the extractor's one.

In some cases, due to the low polarity of carbon dioxide, a polar cosolvent can be added to increase the solvent power of the mixture. With this strategy, however, one of the advantages of SFE, which is the complete elimination of organic solvents, is lost.

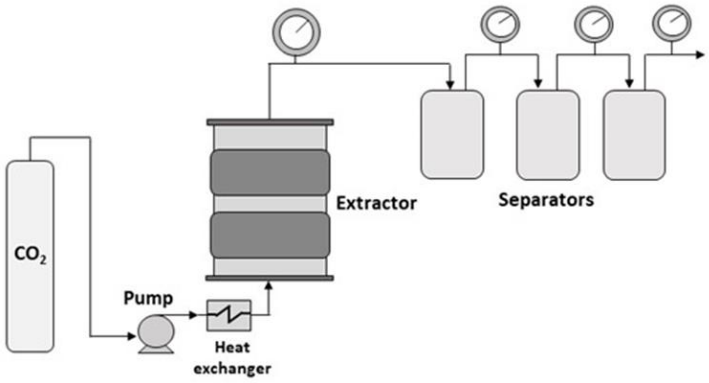

Figure 4. Sketch of the SFE plant.

Although PLE has been sometimes used to extract carotenoids, the non-polar nature of some of these components makes SFE using sc-CO_2 the most suitable extraction technique for this category of compounds [82]. Supercritical carbon dioxide has been used alone or with low quantities of ethanol as cosolvent to extract those substances from different sources, such as tomato, vegetables or see-food waste. Table 2 provides an overview of studies focused on the supercritical carbon dioxide extraction of carotenoids from food wastes. The source from which the active principle has been extracted, the eventual amount of co-solvent added to sc-CO_2, the operating conditions in terms of pressure, temperature and extraction time and the recovery of the carotenoid are reported. The recovery reported in the table are the ratios between the dry weight of the carotenoid in the extracts and the dry weight of the carotenoid contained in the original sample.

Table 2. Extraction of carotenoids by supercritical carbon dioxide. EtOH = ethanol; P = operating pressure; T = operating temperature; t = extraction time.

Carotenoid	Source	EtOH %	P bar	T °C	t min	Recovery %	Ref
α-carotene	Apricot peels	15.5	350	59	30	97.9	[116]
β-carotene	Tomato paste waste	5	300	65	120	50	[117]
β-carotene	Tomato processing waste	/	300	80	/	88	[118]
β-carotene	Sweet potato peels	15.5	350	59	30	99.8	[116]
β-carotene	Tomato peels	15.5	350	59	30	96.9	[116]
β-carotene	Apricot peels	15.5	350	59	30	99	[116]
β-carotene	Pumpkin peels	15.5	350	59	30	88.2	[116]
β-carotene	Peach peels	15.5	350	59	30	99.2	[116]
lycopene	Tomato paste waste	5	300	55	120	54	[117]
lycopene	Tomato processing waste	/	300	80	/	80	[118]
lycopene	Tomato processing waste	/	450	70	420	75	[119]
lycopene	Tomato peels	15.5	350	59	30	92.5	[116]
lycopene	Apricot peels	15.5	350	59	30	83.2	[116]

It is possible to note that for the extraction of this class of compounds, in some cases CO_2 alone is used; in most cases, the addition of a co-solvent is required, which in all of reported cases is ethanol. The amount of ethanol (when present) varies from 5 to 15.5 %. Carotenes are extracted in general at 300 - 350 bar (only in one case a pressure of 450 bar has been adopted to extract lycopene [117]), whereas in the case of xanthophylls a wider range of pressures can be observed (astaxanthin is extracted from crustacean waste at 200 bar [39], and fucoxanthin is extracted from brown seaweed waste at 400 bar) [119]. From the point of view of operating temperatures, carotenes are extracted at higher values of temperature (from 55 to 80 °C) than xanthophylls (for which temperatures in the range 40 - 59 °C are sufficient). The recovery's values are generally high, confirming that the sc-CO_2 extraction is the proper technique for carotenoids.

1.3.5 Combined extractions

Industries are always paying attention to the optimization of extraction methods to achieve the highest recoveries of by-products. Because of various physicochemical barriers in different food matrix, it is critical to choose a method or a combined method that can efficiently extract lycopene from raw materials. Prior to the extraction process, different factors need to be considered in order to get efficient recovery of the product. The high-water content in raw food matrix is considered to be detrimental to extraction process, especially for SFE [120]. To eliminate water from materials, thermal dehydration processes was found to have a negative effect because thermal treatment can cause lycopene isomerization or destruction. To overcome this problem, lyophilization is suggested as a better option to remove water from raw materials [121]. Following which, different extraction techniques can be combined typically found in the combinations of ultrasound-enzyme, ultrasound-microwave, microwave-pressure, SFE-enzyme, PEF-ultrasound, and ultrasound-enzyme-microemulsion. Konwarh and Ladole [122,123] extracted and isolated lycopene from TW using ultrasound-enzyme method, in which, the extraction yield of lycopene was greatly improved, and the co-immobilized biocatalyst showed excellent reusability. Kha [124] combined microwave drying with ultrasonic-assisted water extraction to modulate lycopene extraction rate by varying ultrasonic power, extraction time, powder particle size, and the ratio of water to activated carbon powder. By means of SEM analysis, it was observed that this combined method resulted in severe disruption to the cellular structure of the wood turtle aril, which supported its high extraction yields of oil, β-carotene and lycopene in this study. Manosonication-assited extraction is an example of pressure-assisted process coupled with other extraction aid, particularly the cavitation effects induced by ultrasounds. The system involves a double-jacket reaction chamber, a sensor and PID controller for temperature control, an ultrasonic generator and nitrogen gas controlled by a manometer was supplied to adjust the amount of external pressure applied to the reaction chamber through an inlet fitting [125]. Amiri-Rigi et al. [70] explored extraction of microemulsions after ultrasound-enzyme pretreatment aiming to achieve deep separation of lycopene with using only low amount of surfactant. Regardless of the advantages of combined extraction methods, proper pretreatment is also highly suggested to reduce the use of chemical reagents and avoid the use of harmful reagents.

1.4 Micro-/Nano-encapsulation of extracted bioactive components

Due to the special chemical structure of lycopene, the molecule is unstable to the presence of light, oxygen, and heat [126,127]. These problems limited the use of natural TW extract as a source of lycopene. In order to overcome these drawbacks, encapsulation techniques can be employed. Indeed, encapsulation of bioactive substances (flavors, drugs, enzymes, vitamins, essential oils and carotenoids) is used to protect them from external denaturizing agent, control their release and improve bioavailability [128].

There are many encapsulation techniques for bioactive substances, such as vacuum freeze drying [129,130], spray drying [130,131], and nanoemulsions [132,133]. And each has its own advantages (Table 3). When choosing the final method, the choice should be based on the form and use of the product combined with the unique advantages of each method. Among them, nanoemulsions, have been widely used in food industry [134,135] due to its various advantages, for example the potential to improve the solubility and bioavailability of many foods active compounds. Nanoemulsions have been applied as carriers for lipid active compounds and pharmaceuticals using the ability to dissolve non-polar active compounds for drug delivery, etc. [136-138]. In cosmetics, nanoemulsions can be used in the synthesis of skin and hair care products, [139], and also in petroleum [140] and paints and coatings, [141,142] etc.

Table 3. The advantages and disadvantages of various methods for lycopene encapsulation.

Technology	Principle	Advantages	Disadvantages	References
Spray drying	Use hot air at high temperature to dry the sample	More economicalOperated in batch or continuous modeAble to produce good quality powdered products with small particle size	Products face thermal degradation issue since need to be operated at high temperature, i.e. 150 - 220 °C Not suitable for high viscous solution since it will cause clog at the nozzle	[143,144]
Freeze drying	Use sublimation and freezing concept at low temperature and vacuum pressure to dry the sample	Operated in batch modeAble to produce powdered products that are highly porous and light weightCan preserve most of the initial properties of compounds such as colour, flavours, dimensions, shape, taste, texture and biological	Products have tendency to shrink and crack since operated at very low freezing temperature, for example -40 °CHigh operating costRequire longer operating timeFormed high porous wall between bioactive compounds and its	[145]

		activityProducts have higher entrapment efficiency	surrounding that cause prolong release of bioactive compounds	
Emulsion	Interfacial tension; droplet deformation	Cover up the unpleasant taste. Increase the bioavailability of the dose. Sustained release medication. Very cost-effective	Storage conditions may affect stability. Bulky, difficult to transport, and prone to container breakages. Liable to microbial contamination which can lead to cracking.	[146]
Supercritical assisted atomization (SAA)	The solubility in $scCO_2$	Can obtain smaller particles with narrower PSD and with fewer solvent residues and a reduced use of organic solvents.	The possibility of processing only principles that are soluble in scCO2, the production of particles with broad PSDs or even agglomerates, and the need for high processing pressures, and sometimes, temperatures.	[147]

1.4.1 Emulsion

In recent years, a large number of studies has been carried out for increasing the bioavailability and solubility of lycopene. Moreover, the emulsifier layer surrounding the oil droplets that containing lipophilic lycopene can be designed to protect the lycopene against oxidation and degradation by reducing them exposure to oxygen, interact with metal ions such as Fe^{2+}, heat, and light, including the development of emulsions [148-150]. Emulsions consist in a non-equilibrium system formed by a mixture of two or more liquids stabilized by surfactants. They can be of two types single oil-in-water (O/W) or double water-in-oil-in-water (W/O/W) emulsions [151]. Indeed, the oil-in-water emulsion can be used to encapsulate lipophilic lycopene molecule, and also can be conveniently incorporated into water-based food system such as beverages, and food products. Homogeneous mixtures in which droplets are formed in the size range of 10-500 nm are called nanoemulsions [141]. Compared with other traditional emulsions, nanoemulsions have ultra-low interfacial tension, due to the continuous Brownian motion of the droplets [152], which slows down the emulsion destabilization processes including coalescence, flocculation and Ostwald ripening, etc. However, although the improved thermodynamically stability, nanoemulsions are

still sensitive to the environment stresses, such as heat, freezing and thawing, and altering pH which would further destabilizes the encapsulated compounds.

Lycopene encapsulation into nanoemulsion based systems showed problems of precipitation and separation under prolonged storage, thus losing their protective effect on the active substance. For example, Kim et al. [153] showed that the retention of lycopene extract in nanoemulsions varied between 2.58 % and 52.35 % after 16 weeks of storage away from light, and the oxidized lycopene exceeded 50 %. Also, Zhao et al. [133] investigated the stability of nanoemulsions of lycopene at different temperatures and showed that the rate of lycopene degradation was much lower at 4 °C storage than at 37 °C. Therefore, in the case of sensible compounds, further manipulation is needed for more effective protection of active compounds.

1.4.2 Spray drying

Spray drying is a low-cost industrial consolidated technique, providing dry and good-quality products [154]. Spray drying works by pumping the liquid to be atomized through a nozzle. Hot air is then used to remove water from the initial solution and a dry powder is obtained at the bottom of the cyclone. Encapsulation efficiency depends on many process parameters such as feed flow rate, air inlet/outlet temperature, feed temperature, and wall material used [155]. Microencapsulation is a process by which molecules of an unstable bio-compound are stored inside an envelope to be protected or released in a controlled way. In this way they appear to be surrounded or covered by a continuous film of polymeric material, with this technique it is possible to produce particles having dimensions in a range from micrometers to millimeters [156]. Depending on the final use, various characteristics of the microcapsules can be modified to obtain the desired final product. The size and shape of the particles, the compatibility, the physic and chemical properties of the shell and the permeability are some of the main parameters to consider in the choice of materials and process parameters. This technique allows to protect and increase the shelf-life of many active substances that are chemically fragile, volatile, or unstable. Lycopene is easily subjected to degradation during storage, especially in presence of oxygen and light. The encapsulation of carotenoids has shown a significant improvement in their stability compared to the non-encapsulated ones during storage [157]. The powder

obtained moreover, can be stored at room temperature and this represent a cheaper and less polluting storage technique respect to the freezing one.

Generally, the wall materials for encapsulation are being divided into three main groups: carbohydrates, proteins, and lipids / waxes. However, the first two groups are being utilized more commonly in spray drying encapsulation, and the third group is being used for other encapsulation methods [158]. For food products different encapsulating materials may be used, as maltodextrin, whey protein isolate, modified starch, gum [159], gelatine [160], sucrose [161] and polysaccharide. In recent years, several studies have shown how the combination of maltodextrin with other amphiphilic (molecule containing both a hydrophilic and a hydrophobic group) materials can be a promising wall material to encapsulate lipophilic compounds, such as lycopene, improving its protection and retention in the particles [162]. The selection of a suitable wall material is critical to a microencapsulation spray drying process, that avoids changes due to oxidation, chemical interactions, or volatilization [163] and maximizes the retention of the biomolecules after the drying process is completed. Research on microencapsulation by spray drying has concentrated on improving the encapsulation efficiency and extending the shelf life of the product to produce high quality encapsulated powders. The main factors that affect the encapsulation efficiency are the properties of the wall and core materials [164].

The composition of the wall material during the drying process often consists of maltodextrins [165,166]. Maltodextrins are commonly used in the spray-drying encapsulation process due to their high-water solubility, low-cost, mild flavor, and good encapsulation performances [165]. Nevertheless, other encapsulation agents can improve properties of the produced for instance, several health benefits are related to the consumption of the dietary fiber inulin, which facilitates intestinal regularity and prevents the development of tumors. It also seems to reduce total and low-density lipoprotein cholesterol absorption and improve calcium absorption in the intestine [166]. This technique protects and increases the shelf-life of many active substances that are chemically fragile and unstable, and modulates their properties according to the coating agent selection [154].

1.5 Application of encapsulated lycopene

Lycopene, a bright red carotenoid hydrocarbon, is considered a very potent antioxidant due to the presence of conjugated double bonds, which protect cells from oxidative damage and reduce the risk of chronic diseases [167,168]. As a food fortifier, lycopene is widely added to various functional foods in the form of capsules and nanoemulsions [169,170]. However, lycopene is highly sensitive to chemical degradation and is easily oxidized during storage, transportation, and ingestion, resulting in low bioavailability [171]. In recent years, several encapsulation methods have been developed as delivery system, such as protein-based nanoparticles [172], emulsions [173], liposomes [174,175], and microcapsules [176]. These techniques aim mainly to expand the application of lycopene in food with the goal of maximizing lycopene stability. Among which, nanoemulsion is an effective delivery system that has received increasing attention because of its simplicity of preparation, high safety, and easy industrialization [177]. The average droplet diameter of nanoemulsions is usually less that 500 nm [178]. In this process, precipitation and coalescence can be avoided because the Brownian motion of droplets in nanoemulsions is strong enough to counteract gravity- or viscosity-induced dynamic instabilities with long-term stability [179].

Thanks to these outcomes, many functional foods with extra inclusion of lycopene have been developed. In which, functional beverage is one of the fastest growing segments of functional food [180]. Kim et al. [170] prepared lycopene nanoemulsion by using emulsification-evaporation technology and optimized the preparation procedure using BBD through RSM, with taking droplet size, emulsification efficiency and emulsion stability as response surfaces and, consequently, evaluating the shelf life of lycopene beverages under accelerated storage conditions. Kinetic modeling at different storage temperatures indicated that the degradation of lycopene trapped in nanoemulsions in beverage systems followed first-order kinetics, with stable encapsulated lycopene in beverages at both 4 and 20 °C.

The concept of nano-encapsulation originated from the cellular model, which encapsulates active substances in a semipermeable membrane to protect them from external media and inappropriate exposures, while also controlling the entry and exit of intracellular substances [181,182]. Microcapsules have been successfully used in food industry to protect substances sensitive to temperature, light, oxygen, as well as humidity. Rocha et al. [176] prepared nanocapsules-containing cake with special

functionality by mixing microcapsules with milk at 50 °C. It was found that cake made with lycopene-rich microcapsules had an even distribution of dye compared to cake with free lycopene which generated a lot of pigmentation. In such products, lycopene bioaccessibility can be enhanced when companied with dietary fat intake as it helps lycopene bind to chylomicrons and lipoproteins that carry lycopene from intestinal cells to the lymph or portal circulation [183]. On the other hand, improving the physicochemical properties of nanocapsules could also increase the bioaccessibility or bioavailability of capsuled bioactive compounds [184-187].

Therefore, the main purpose of this study is to recover bioactive substances, especially lycopene, from TW using different extraction techniques and to evaluate the processing conditions and optimal operating parameters of different extraction techniques. Different encapsulation technologies are used to further protect lycopene to prevent lycopene from being affected by external factors, thereby degrading and losing its biological activity.

Parts of this section were already published in ***"High-Pressure Technologies for the Recovery of Bioactive Molecules from Agro-Industrial Waste"*** *by Junyang Li, Margherita Pettinato, Roberta Campardelli, Iolanda De Marco, Patrizia Perego, Applied Sciences 12.7 (2022): 3642. doi.org/10.3390/app12073642.*

2 RAW MATERIAL CHARACTERIZATION

ABSTRACT

The main purpose of this section is to analyze the physicochemical properties of tomato waste as useful information to better analyze extraction performance in next chapters. The physical analysis includes determination of moisture, water activity, particles size and ash content of tomato waste. For the chemical analysis, the total lycopene content was determined.

2.1 Materials and Methods

2.1.1 Tomato waste samples

Organic tomatoes were produced in the northern Italy, harvested, and used to produce tomato sauce. The TW resulting from this process was then collected in once time, separated, and stored at -20 °C for all the tests. This batch of biomass was used in the entire study of this thesis. Before the Ultrasound-Assisted Extraction TW were thawed, dried and ground (Figure 5).

Figure 5. Tomato waste (peels and seeds) thawed, dried and ground.

The drying process was carried out by placing the thawed matrix inside an oven, at a constant temperature (60 °C), for 3 days. This process allowed to make a comparison with other materials or with the same material from other varieties of tomato to establish correctly whether the matrix is a suitable source of bio compounds. Furthermore, water removal allowed to have a greater stability of the product, to have no water-solvent interference and to facilitate storage operations. The dried product,

in fact, can be stored at room temperature inside a watertight container away from light. This method of storage is cheaper from an economic point of view than the freezing method, which requires energy and appropriate equipment. After, the grinding process was carried out to increase the available exchange surface and to have a more homogeneous particle size.

2.1.2 Determination of the moisture of TW

The TW moisture content was obtained by drying approximately 3.0 g of fresh sample at 110 °C until a constant weight was observed. The amount of moisture was calculated by the Equation (1).

$$Moisture = \frac{m_{initial} - m_{final}}{m_{initial}} \qquad (1)$$

Where $m_{initial}$ is the mass of the sample at the beginning of the drying process and m_{final} is the mass of the sample at the end of the thermal treatment after two days. Tests were done in triplicate and reported as mean value ± standard deviation.

2.1.3 Determination of the water activity of TW

Water activity (a_w) is an important parameter for microbiological and chemical stability of foods. It is defined as the ratio of the vapor pressure of water in the product to the vapor pressure of pure water at the same temperature, as shown by the Equation (2).

$$a_w = \frac{P}{P_0} \qquad (2)$$

Where P is the vapor pressure of water in the product and P_0 is the vapor pressure of pure water. Activity water can assume values between 0 and 1. The TW water activity was detected by HygroPalm -HP23-AW-A (Rotronic, Crawley, UK). Tests were done in triplicate and reported as mean value ± standard deviation.

2.1.4 Determination of the particles size distribution of dry TW

Particle size analysis is the fractionation of a set of solid particles of different sizes. So, sieving analysis was performed on TW to determine the particle size distribution of the dried material, using a series of sieves (Table 4) composed of wires whose distance and diameter are defined. Approximately 40 g of sample were used to guarantee that even fine particles for the lower mesh sizes could be collected. Sieving is probably the most used technique to carry out particle size analyses, due to its simplicity. Test were performed using a vibratory sieve shaker machine (Giuliani, Technology, Torino, Italy), that gives an oscillatory and wavy movement to the sieve stack. Sieves with different diameters were used (Table 4), a lid was placed on top of the first sieve and a bottom pan under the last one. Tests were done in triplicate.

Table 4. Screen opening used during the test on particle size distribution.

Sieve number [-]	**Sieve openings** [mm]
1	3.327
2	2.794
3	1.981
4	1.651
5	1.168
6	1.000
7	0.840
8	0.701
9	0.500
10	0.420
11	0.355
12	0.250

The cumulative mass fraction of oversize is the mass fraction of particles retained from the biggest to a given sieve opening and was calculated by Equation 3.

$$F' = 1 - F = 1 - \int_0^x f(x)dx \qquad (3)$$

Where F' is the cumulative mass fraction of oversize and F is the cumulative mass fraction of the undersize, that is the fraction of the total weight of particles that passes through each individual screen. $f(x)$ is the relative frequency.

The inflection points of the undersize function and that of the oversize function coincide and correspond to the maximum of the function $f(x)$, as shown in Equation 4.

$$f(x) = \frac{dF(x)}{dx} \qquad (4)$$

Where, as mentioned before, F is the cumulative mass fraction of the undersize. F has been calculated up to a diameter value j using Equation 5.

$$F_i(d_j) = \sum_{i=1}^{i=j} x_j \qquad (5)$$

Where i is the sieve number, and its numeration goes from the smallest to the largest sieve, F_i is the cumulative mass fraction of undersize at the current sieve, x_i is the mass fraction related to the single diameter interval d_j, calculated by Equation 6.

$$x_i = \frac{mass}{total\ mass} \qquad (6)$$

Where mass is the mass of the particle fraction at a given diameter (d_j) and total mass is the total mass fed.

The generic mean value of the distribution $g(d)_m$ can be calculated through the discretized Equation 7.

$$g(d)_m = \int_0^1 g(d)dF = \sum_k [g(d_k) + g(d_{k-1})] \cdot [F(d_k) - F(d_{k-1})] \cdot \frac{1}{2} \qquad (7)$$

Then the mean diameter of each interval was calculated by the arithmetic mean of the two sieve openings, according to the Equation 8.

$$d_k = \frac{d_{top} - d_{bottom}}{2} \qquad (8)$$

Where d_k is the mean diameter of each interval, d_{top} is the top diameter (mm) and the d_{bottom} is the bottom diameter (mm).
The area subtended to the graph was calculated using trapezoids method.
Finally, the percentage loss of the test was calculated using the final mass collected and the initial mass fed, as shown in Equation 9.

$$loss = \frac{m_f - m_c}{m_f} \cdot 100 \qquad (9)$$

Where loss is the percentage of material lost during the test, m_f is the initial mass fed and m_c is the final mass collected.

2.1.5 Determination of the ash content of TW

The TW ashes were obtained by treating approximately 0.5 g of the sample at 650 °C for 4 hours. The mass of ashes was calculated basing on the dry initial sample and it was expressed as reported in the Equation 10.

$$mass_{ashes} = \frac{mass_{final} - mass_{Ceramic\ Cup}}{mass\ of\ initial\ sample} \qquad (10)$$

Where $mass_{final}$ is the total mass at the end of the process and $mass_{Ceramic\ Cup}$ is the mass of the tare. Then, the ratio of ashes to dried sample mass was calculated.
Tests were done in triplicate and reported as mean value ± standard deviation.

2.1.6 Determination of the total lycopene content of TW

For the total lycopene of TW, it was extracted by using conventional SLE with *n*-hexane [188]. The extraction was performed in a 100 mL bottle on magnetic stirrer plate (LLG-uniSTIRRER3, magnetic stirrer with heating, EU-plug, 515W) at room

temperature in the dark. The extraction was repeated 5 times until the solvent 30 mL resulted colorless. Total carotenoids were determined by UV-vis spectrophotometer (model Lambda 25, Perkin Elmer, Wellesley, MA, USA), and triplicate analyses were carried out on samples of obtained extracts, whose absorbance (ABS) was read at a wavelength of 470 nm.

The concentration of total carotenoids was calculated using the calibration curve (R^2 = 0.986), obtained from the standard solutions of *all-trans*-lycopene (C = 0.001-0.01 mg/mL) reported in Equation 11.

$$ABS_{470nm} = 85.547 \cdot C \qquad (11)$$

Total carotenoid yield (TC) was obtained by the Equation 12 as milligrams of lycopene equivalents (LE) per gram of dried biomass (DB):

$$TC\left(\frac{mg_{LE}}{g}\right) = \frac{C \cdot V \cdot D}{m_{DB}} \qquad (12)$$

Where V is the volume of the solvent used for the extraction (mL), D is the sample dilution factor (-) and m_{DB} is the mass of dried tomato seeds and peels used for the extraction (g).

2.1.7 Lycopene yield by HPLC

The method reported by Anguelova et al. [189] was applied for the investigation of lycopene in the extracts, with some modifications. The analyses were carried out using a High-Performance Liquid Chromatographer (Agilent 1100 series, Palo Alto, CA, USA), equipped with a C18 (5 µm, 4.6 x 250 mm) reversed phase column (Vydac, Hesperia, CA, USA), and a diode array detector (DAD). Before the analysis, samples were filtered through a 0.22 µm membrane filter, then injected samples (100 µL, without dilution) were detected at 470 nm. An isocratic mobile phase (flow rate = 1 mL/min) of acetonitrile (44 % v/v), methanol (54 % v/v), and isopropanol (2 % v/v) was used. Lycopene content in the sample was calculated by peak area integration (A, mAU) and according to the calibration curve (R^2 = 0.982), obtained from the standard solution of all-trans-lycopene (C = 100 - 2700 µg/mL), reported in Equation (13).

$$A = 131.47 \cdot C \qquad (13)$$

Lycopene yield (LY) was given through Equation (8), where V is the volume of the solvent used for the extraction (mL) and m_{DB} is the mass of dried tomato seeds and peels used for the extraction (14).

$$LY(\frac{\mu g}{g}) = \frac{C \cdot V}{m_{DB}} \qquad (14)$$

2.2 Results and Discussion

2.2.1 Physical Characterization of TW

Fresh TW showed a moisture of 84.3 ± 0.83 %, which was reduced after drying (60 °C) up to about 6 % of residual moisture. After grinding, the dried biomass was analyzed in terms of water activity, ash, and mean size. Particularly, after the drying process, the TW exhibited a water activity of 0.101 ± 0.042, resulting as suitable for long-term storage in water-proof containers and in the dark for extraction experiments. The biomass showed an ash content of 4.1 ± 0.8 % and the obtained value agreed with those reported in literature [190-192], while the mean size of ground particles was of 732 ± 67 µm (Equation 8). Figure 6 shows the cumulative mass fraction of the overflow respect to the mean diameter of the interval. From the cumulative mass fraction, it is possible to see that most of the particles were collected for diameters lower than 1 mm and, in particular, lower than 0.500 mm.

The grinding phase allows to have a greater quantity of fine particles than those of large size, as we can see by the distribution. A small particle size of the sample allows to increase the surface contact and, consequently, to improve the extraction process thanks to the enhanced mass transfer.

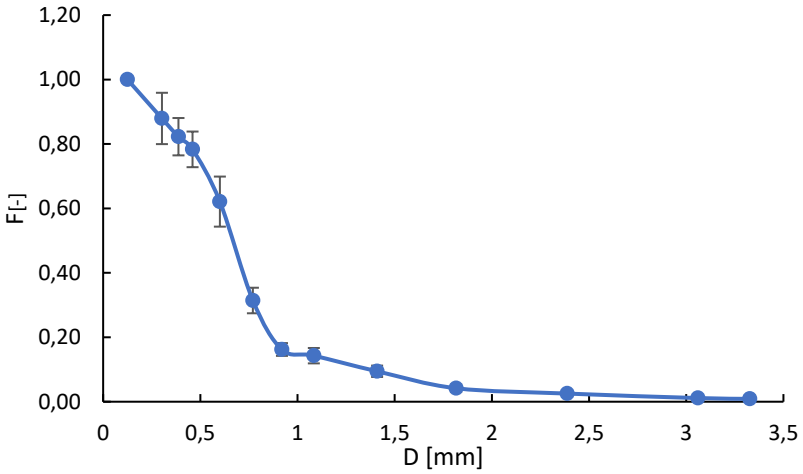

Figure 6. Mean of cumulative mass fraction (F) of overflow as function of the mean diameter of each interval (D).

The percentage losses were calculated using Equation (10). As can be seen from the results, during the tests there were no significant losses of material.

2.2.2 Chemical Characterization of TW

SLE using hexane as solvent was carried out for the quantification of lycopene as reference values to be compared with performance of non conventional extraction. Three consecutive extractions were performed. The results shows that the total lycopene content was 1438.24 ± 44.3 µg/g (dry solid), measured via HPLC. This total lycopene content of tomato processing waste shows much higher than the 5.32 ± 0.15 mg/100 g reported by Poojary et al. [193] and the 510.6 mg/kg reported by Nour et al [194].

2.3 Conclusions

The purpose of this section on TW characterization is to obtain indispensable data on TW characteristics for further studies on the extraction of antioxidants from this feedstock. Initial moisture data at the time of collection were obtained, confirming that TW sampled at different dates and periods presented the same moisture content, approximately 84.3 ± 0.83 %. This information allowed the determination that drying for 3 days at 60 °C provided a starting material suitable for antioxidant extraction, with a final moisture of approximately 6 % of residual moisture. Particularly, after the

drying process, the TW exhibited a water activity of 0.101 ± 0.042, resulting as suitable for long-term storage in water-proof containers and in the dark for extraction experiments. After crushing, the average diameter of the particles is smaller (732 ± 67 μm), making it possible to directly use TW for extraction. The biomass showed an ash content of 4.1 ± 0.8 % and the obtained value agreed with those reported in literature [190-192]. Furthermore, the high content of lycopene in TW confirms the potential applications of TW beyond the production of food dietary supplements and cosmetic uses.

Parts of this section were already published in ***"A Comprehensive Optimization of Ultrasound-Assisted Extraction for Lycopene Recovery from Tomato Waste and Encapsulation by Spray Drying" by Junyang Li,*** *Margherita Pettinato, Alessandro Alberto Casazza, Patrizia Perego.* ***Processes 10.2 (2022): 308.*** *doi.org/10.3390/pr10020308****,*** *and partially presented as "Ultrasound-assisted Extraction of Lycopene from Industrial Tomato Waste", in the international congress "6th Green and Sustainable Chemistry Conference - GREEN2020", online, as poster presentation.*

3 EXTRACTION OF LYCOPENE FROM TW BY NON-CONVENTIONAL METHODS

ABSTRAT

The main purpose of this section was to study the improvement of extraction efficiency of lycopene from TW using different extraction methods. The main challenge of this section was to utilize green (even food-grade solvents), environmentally friendly, and sustainable solvents and extraction techniques in order to guarantee the high recovery and extraction efficiency of lycopene. In fact, in conventional technologies, the solvent usually lies on harmful organic chemicals, cumbersome and equipment with high energy consumption. In this part of the study, water, ethanol and mixtures of water and ethanol were used as green solvents to compare the extraction efficiency of lycopene, applying extraction techniques considered highly innovative such as ultrasonic-assisted extraction, microwave-assisted extraction, and the latest Solid-liquid multivariable extractor. The particular extraction method presented in this section is the Solid-liquid Multivariable Extractor [195], a new semi-automated continuous extractor capable of exploit several variables (temperature, pressure, ultrasonic frequency, solvent flow rate, etc.) at the same time, as described in Section 3.5 and Section 3.8.3. The optimum process conditions were analyzed to obtain maximum extraction efficiency and the highest antioxidant activity of lycopene using Response Surface Methodology. The extraction kinetics using the Solid-liquid multivariable extractor method for lycopene recovery was investigated and the key factors affecting the extraction efficiency were analyzed.

3.1 Chemicals and Sample Preparation

Ethanol (analytical grade, Sigma Aldrich, St. Louis, MO, USA); 2,2′-azino-bis (3-ethylbenzothiazoline-6-sulphonic acid) diammonium salt (Sigma Aldrich, Milan, Italy); potassium persulfate, iso-propanol, acetonitrile, methanol (Carlo Erba, Cornaredo, Italy), *all-trans*-lycopene and the standards (Sigma Aldrich, Milan, Italy) employed in this study were of analytical grade and used without further purification. The water was obtained with a Milli-Q system (Merck-Millipore, Darmstadt,

Germany). Tomato peels and seeds were kindly provided by a producer of tomato sauce in northern Italy. The Ultrasonic probe (Sonicator Vibra cell 75115, 700 W, Bioblock Scientific Co., Stras-bourg, France) High-Performance Liquid Chromatographer with a diode array detector (Agilent 1100 series, Palo Alto, CA, USA) were used.

3.2 Solid-liquid extraction (SLE)

Lycopene extraction from TW was carried out by SLE. The apparatus used was made by an magnetic stir plate (LLG-uniSTIRRER3, magnetic stirrer with heating, EU-plug, 515W) equipped with a speed 900 rpm, working at different temperature (25 °C, 35 °C, 45 °C, 55 °C, 65 °C), with a solid-to-liquid ratio from 4 mL/g to 20 mL/g, for different times (5 min, 15 min, 25 min, 35 min, 45 min). The extraction was performed directly in a 100 mL beaker, which hosted dried TW and the solvent (Sunflower seed oil). Temperature was detected by a thermocouple and controlled by a thermostatic bath. After the extraction, the liquid was separated from the exhausted solid by centrifugation (6036 x g for 15 min) (MF-20-R, Alliance Bio Expertise, Guipry, France) and stored at -20 °C for further analyses.

3.3 Ultrasound-assisted extraction (UAE)

Lycopene extraction from TW was carried out by UAE. This method allows the extraction of bioactive compounds in very short time, at a low temperature, with low energy and solvent requirement, and it is particularly suitable for the recovery of the thermosensitive bioactive compounds [196]. The apparatus used was made by an ultrasonic probe (Sonicator Vibra cell 75115, 700 W, Bioblock Scientific Co., Strasbourg, France) equipped with a tip of 13 mm, working at 20 kHz of frequency. The probe was directly submerged into a 150 mL beaker, which hosted dried TW and the solvent (ethanol). Temperature was detected by a thermocouple and controlled by a thermostatic bath. After the extraction, the liquid was separated from the exhausted solid by centrifugation (6036 x g for 10 min) (MF-20-R, Alliance Bio Expertise, Guipry, France) and filtration (0.45 µm filter) and stored at -20 °C for further analyses.

3.4 Experimental Design of UAE

Response Surface Methodology (RSM) [197] was used to investigate the effect of the ultrasound-assisted extraction parameters on the extract bioactive content. A Central Composite Design (CCD) was employed as the experimental design. The CCD consisted of factorial points, each having two levels (±1), a set of central points (level 0), and a set of star points, where experimental runs were in the same level as the centre points, except for one factor, whose distance from the centre of the design space was ±α where $|\alpha| \geq 1$. The setting of the α value (1.565) and the number of trials at the centre of the domain influence the accuracy of the estimation [198].

The factors investigated included extraction temperature (35 - 65 °C), time (20 - 50 min), volume of the extraction system (45 - 90 mL), liquid-to-solid ratio (27 - 80 mL/g), amplitude (30 – 65 %) and on/off pulsed ratio (on) (30 - 70 s). The last was defined as the time of applied ultrasounds in a cycle where the relaxation time (ultrasounds were not applied) was fixed to 30 s. Ranges of variation of each input variable were coded according to Equation (15), in such a way that they could vary from -1 to 1:

$$X_i = \frac{\varphi_i - \varphi_{min}}{\Delta_\varphi / 2} - 1 \qquad (15)$$

Where X_i is the input variable, φ_i, φ_{min}, and Δ_φ are the actual variable value, the minimum variable value and variable range, in original units.

The experimental plan consisting of 33 experiments was used to optimize the content of active substances in the extract.

The individual and interaction effects of independent variables (X_j) on the generic response (Y) were mathematically fitted through a second order polynomial (Equation 16):

$$Y = \beta_0 + \sum_{j=1}^{k} \beta_{jj} X_j^2 + \sum_{j=1}^{k} \sum_{i=1}^{k} \beta_{ij} X_i X_j \qquad (16)$$

Where β_0 is a constant and β_j, β_{jj} and β_{ij} are the coefficients of the terms of the equation. The model adequacy was determined by means of the analysis of variance

(ANOVA) using the Design Expert Software (Stat-Ease, Inc., Minneapolis, MN, USA).

The influence of the process operating conditions was evaluated on total carotenoid yield, lycopene yield, and antiradical power of the extract, which were selected as the response variables.

3.4.1 Numerical Optimization

Numerical optimization of the process was carried out by the Desirability function [199] built through the optimization tool of Design Expert software. Desirability (Equation 17) is a multiple response method, which provides an overall objective function starting from fitting equations obtained for each response variable (the total desirability, D). D ranges from 0 to 1, as a geometric mean of the desirable range of each response (d_i), which varies from 0 (undesirable value) to 1 (the most desirable value), as well.

$$D = (\prod_{i=1}^{n} {d_i}^{r_i})^{1/\sum r_i} \qquad (17)$$

In Equation 17, r_i represents the importance that can be assigned by the user (in the software from 1 to 5) for each response variable [200]. The definition of d_i used in this study, where the purpose is the maximization of the response variables, is given by Equation 18, where Y_i is the response variable, and $Y_{i,min}$ and $Y_{i,max}$ are the lower and upper value of Y_i [201].

$$d_i = \begin{cases} 0, & Y_i \leq Y_{i,min} \\ \left(\frac{Y_1 - Y_{1,min}}{Y_{1,max} - Y_1}\right), & Y_{i,min} < Y_i < Y_{i,max} \\ 1, & Y_i > Y_{i,max} \end{cases} \qquad (18)$$

3.4.2 Evaluation of the effects of frequency in UAE

The ultrasound-assisted extraction under different frequency was performed flasks at room temperature (no more than 30 °C after the process). The extraction conditions, based on previously best conditions found for UAE at 20 kHz, and the effect of three different frequencies (40 kHz, 80 kHz and 120 kHz) were be evaluated on extraction

performances. After the extraction, the liquid was separated from the exhausted solid by filtration (0.45 µm) and stored at -20 °C for further analyses.

3.5 Solid-liquid Multivariable Extractor extraction (SoLVE) methods

3.5.1 SoLVE system equipment

Solid-Liquid Multivariable Extractor (SoLVE) was used to extract lycopene from TW. Briefly, The system (Figure 7) consists of the following components: 1) An HPLC pump capable of delivering different flow rates (1-10 mL/min); 2) A computer that can display and adjust pressure and flow; 3) Able to provide different frequencies (1-500 Hz) ultrasonic reactor; 4) a reaction vessel connected to a constant temperature water bath; 5) two parallel cylinders (2 cm in diameter, up to 20 cm in length) as reaction cells, etc.

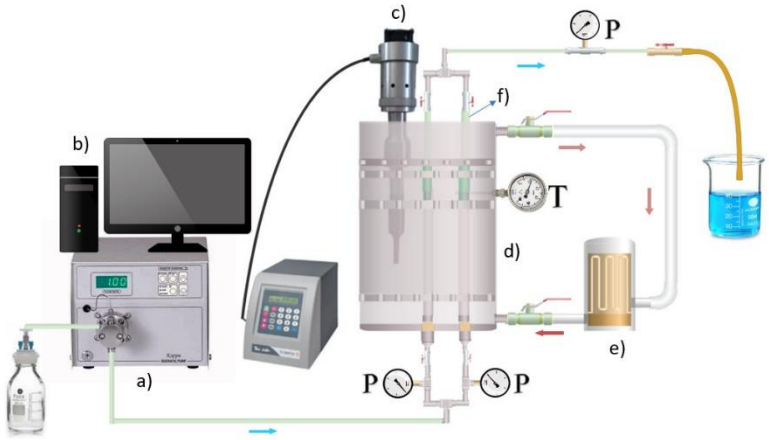

Figure 7. Solid-liquid multivariate extractor. a) HPLC pump b) A computer that can display and adjust pressure and flow; c) Ultrasonic reactor; d) Reaction vessel; e) Constant temperature water bath; f) Reaction cells. P, pressure sensor; T, temperature sensor.

The technique was patented by the team of the laboratory [202]. The solid-liquid multivariable extractor is a new type of extraction system that can achieve high temperature through a heat exchanger, high pressure through a feeding pump, and is supplemented by ultrasonic equipment. SoLVE can simultaneously control temperature, pressure, ultrasound and solvent gradients, allowing it to mix more solvents and change their composition over time. A micrometric mesh filter located in the outlet section of the column also allows simultaneous separation of the liquid

extract from the solids after extraction. The column length is 30 cm and the inner diameter is 7.8 mm. The system can operate in intermittent, semi-intermittent or continuous mode.

3.5.2 Lycopene extraction and analysis optimization using the Central Composite Design

Response Surface Methodology (RSM) was used to investigate the effect of the ultrasound-assisted extraction parameters on the extract bioactive content. A Central Composite Design (CCD) was employed as experimental design. The CCD consisted of factorial points, each having two levels (± 1), a set of central points (level 0), and a set of star points, where experimental runs were in the same level as the center points, except for one factor, whose distance from the center of the design space was ± α where |α| ≥1. The setting of the α value (1.565) and the number of trials at the center of the domain influence the accuracy of the estimation.

The lycopene extraction from TW was carried out by SoLVE exploiting ethanol as a substitute solvent. Factors studied included extraction temperature (27 - 73 °C), extraction time (12 - 58 min), liquid-to-solid ratio (12 - 95 mL/g), feed flow rate (0.34 - 4.64 mL/min) and on/off pulse ratio (19 - 81/30 s/s). The last was defined as the time of applied ultrasounds in a cycle where the relaxation time (ultrasounds were not applied) was fixed to 30 s. Ranges of variation of each input variable were coded according to Equation (19), in such a way that they could vary from -1 to 1:

$$X_i = \frac{\varphi_i - \varphi_{min}}{\Delta_\varphi / 2} - 1 \qquad (19)$$

Where X_i is the input variable, φ_i, φ_{min}, and Δ_φ are the actual variable value, the minimum variable value and variable range, in original units.

The experimental plan consisting of 26 experiments was used to optimize the content of active substances in the extract.

The individual and interaction effects of independent variables (X_j) on the generic response (Y) were mathematically fitted through a second order polynomial (Equation 20):

$$Y = \beta_0 + \sum_{j=1}^{k} \beta_j X_j + \sum_{j=1}^{k} \beta_{jj} X_j^2 + \sum_{j=1}^{k} \sum_{i=1}^{k} \beta_{ij} X_i X_j \qquad (20)$$

Where β_0 is a constant and β_j, β_{ij} and β_{jj} are the coefficients of the terms of the equation. The model adequacy was determined by means of the analysis of variance (ANOVA) using the Design Expert Software (Stat-Ease, Inc., Minneapolis, MN, USA).

The influence of the process operating conditions was evaluated on total lycopene yield, which were selected as the response variables.

3.5.3 Kinetic models for SoLVE process

Three different mathematical have been successfully applied to describe the kinetic modelling of solid-to-liquid phase extraction of lycopene, namely, the first order kinetic model, the mass transfer model, and Peleg's model [193,203]. These three models were compared by fitting the experimental data obtained from lycopene extraction into each model. Fitting of the proposed model was essential by coefficient of determination and root-mean-square deviation (RMSD).

Peleg's model (Equation 21) is a non-exponential empirical equation proposed by Peleg (1988) as:

$$C_t = C_0 + \frac{t}{K_1 + K_2 \cdot t} \qquad (21)$$

Where C_t is the concentration of analyte (mg g^{-1}) at time t (min), C_0 is the concentration of analyte (mg g^{-1}) at time t = 0, K_1 is Peleg's rate constant (min g mg^{-1}) and K_2 is Peleg's capacity constant (g mg^{-1}). The term C_0 can be omitted from Peleg's equation, as the initial concentration of target solute is zero in the extraction solvent. Therefore, Equation 21 was used in the final form as Equation 22.

$$C_t = \frac{t}{K_1 + K_2 \cdot t} \qquad (22)$$

Peleg's K_1 parameter refers to extraction rate (B_0, mg g^{-1} min^{-1}) at the beginning ($t = t_0$) according to Equation 23:

$$B_0 = \frac{1}{K_1} \qquad (23)$$

Peleg's capacity constant K_2 refers to the maximum extraction yield, that is, the equilibrium concentration of total extracted analyte when $t \to \infty$ (C_{eq}, mg g^{-1}), as indicated in Equation 24.

$$C_{t\to\infty} = C_{eq} = \frac{1}{K_2} \qquad (24)$$

3.5.4 Optimization of the process

The approach for optimization of the parameters from the developed models based on RSM coupled with numerical optimization consisted on the desirability function. The numerical optimization technique of the "Design-Expert" software was used. The criteria selected for optimization was maximization of all the responses i.e., lycopene yield, and inhibition, so obtaining the corresponding bast kinetic parameters, which were modeled by RSM as function of the considered input variables.

3.5.5 Color measurements as a tool of quantitative determination of lycopene

Color can be used as a direct estimate or as an indirect estimate of lycopene content. Color measurement can also be used as an estimate of chemical composition as a quality and quantity indicator [204]. The color measurement was described in terms of L*, a*, and b* values for TW before and after extraction. Color measurements were performed following the CIELab international method using a Color Meter (CM-2500d) (Konica Minolta optics, Inc. Japan). Measurements were performed directly on the samples to be analyzed, prepared so that they have a uniform surface for investigation. The values obtained have a Luminosity range from 0 to 100. For this purpose, a preliminary calibration of the instrument was carried out using two targets, one (black) gives the value 0, the other (standard white) the value 100. The light source mode/viewing angle for the CIE Standard Daylight Illuminant D65/10° is chosen and set measurement mode to reflectance. Each measurement was made on a chosen

portion of sample with a diameter of 8 mm. All measurements were automatically repeated three times, processed and the average was given as the result.

3.6 Microwave-Assisted Subcritical Extraction (MASE) Methods

3.6.1 MASE system equipment

MW multimodal reactor (Figure 8) (SynthWAVE, Milestone, Bergamo, Italy) able to exploit an external inert gas feeding (N_2) was used to perform the extraction from TW. The reaction chamber can be pressurized with the necessary amount of N_2 to avoid solvent phase change (5 - 25 bars). The samples can be heated at different temperatures with a maximum irradiation power of 1500 W.

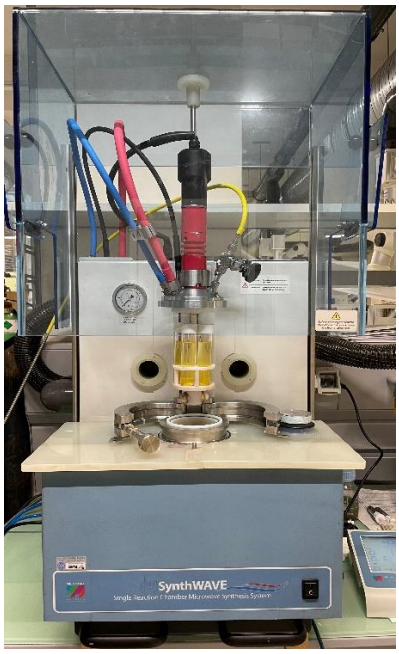

Figure 8. MW multimodal reactor: SynthWAVE, Milestone, Bergamo, Italy.

3.6.2 Microwave-Assisted Subcritical Water and Ethanol 20% (v/v) Extraction

According to the method described by Cravotto and Ferreira [205,206], TW (0.42 g) were mixed with the desired amount of solvent (30 mL) at a 1:72 solid-to-liquid ratio. Then the mixture was introduced into an MW multimodal reactor working at 2.45 GHz able to exploit an external inert gas feeding (N_2). For each test, an appropriate purging with N_2 was performed three times to remove oxygen traces from the system, reducing

oxidative stress on the biomass. The reaction chamber was then pressurized with the necessary amount of N_2 to maintain the solvent in the liquid phase. The samples were heated at 160 °C with a maximum irradiation power of 1500 W. The temperature was maintained for the desired amount of time (10, 15, and 20 min under magnetic stirring at 650 rpm). Three different solvents were tested, i.e., water, ethanol 20 %, and ethanol. The samples with ethanol further tested were at three different temperatures (80, 90, and 100 °C). the temperature was maintained for the desired amount of time (10, 15, and 20 min under magnetic stirring at 650 rpm). The resulting solution was filtered under a vacuum. The dry extract was recovered by freeze-drying (LyoQuest-85, Telstar, Madrid, Spain), weighed, and stored at -20 °C for further analyses. Each extraction was performed in triplicate to validate the reproducibility of the experimental results and the percentage standard deviation was consequently calculated and reported as error bars in graphs.

3.6.3 UAE combined with MASE

In order to extract lycopene by a combination of two non-conventional extraction technologies, TW (0.42 g) were mixed with the desired amount of ethanol (30 mL) at a 1:72 solid-to-liquid ratio. The apparatus used was made by an ultrasonic probe (Sonicator Vibra cell 75115, 500 W, Bioblock Scientific Co., Strasbourg, France) equipped with a tip of 13 mm, working at 20 kHz of frequency. The probe was directly put into test tube, containing dried TW and the solvent (ethanol) for 5 min. Then, the method described in section 3.6.2. was used for MASE.

3.7 Analytical methods

3.7.1 Total Carotenoid yield by UV-vis spectrophotometer

Total carotenoids were determined by UV-vis spectrophotometer (model Lambda 25, Perkin Elmer, Wellesley, MA, USA), and triplicate analyses were carried out on samples of obtained extracts, whose absorbance (ABS) was read at a wavelength of 470 nm.

The concentration of total carotenoids was calculated using the calibration curve (R^2 = 0.986), obtained from the standard solutions of *all-trans*-lycopene (C = 0.001 - 0.01 mg/mL) reported in Equation (25).

$$ABS_{470nm} = 85.547 \cdot C \qquad (25)$$

Total carotenoid yield (TC) was obtained by the Equation (26) as milligrams of lycopene equivalents (LE) per gram of dried biomass (DB):

$$TC\left(\frac{mg_{LE}}{g}\right) = \frac{C \cdot V \cdot D}{m_{DB}} \qquad (26)$$

Where V is the volume of the solvent used for the extraction (mL), D is the sample dilution factor (-) and m_{DB} is the mass of dried tomato seeds and peels used for the extraction (g).

3.7.2 Lycopene yield by HPLC

The method reported by Anguelova et al. [189] was applied for the investigation of lycopene in the extracts, with some modifications. The analyses were carried out using a High-Performance Liquid Chromatographer (Agilent 1100 series, Palo Alto, CA, USA), equipped with a C18 (5 µm, 4.6 x 250 mm) reversed phase column (Vydac, Hesperia, CA, USA), and a diode array detector (DAD). Before the analysis, samples were filtered through a 0.22 µm membrane filter, then injected samples (100 µL, without dilution) were detected at 470 nm. An isocratic mobile phase (flow rate = 1 mL/min) of acetonitrile (44 % v/v), methanol (54 % v/v), and isopropanol (2 % v/v) was used. Lycopene content in the sample was calculated by peak area integration (A, mAU) and according to the calibration curve (R^2 = 0.982), obtained from the standard solution of all-trans-lycopene (C = 100 - 2700 µg/mL), reported in Equation (27).

$$A = 131.47 \cdot C \qquad (27)$$

Lycopene yield (LY) was given through Equation (8), where V is the volume of the solvent used for the extraction (mL) and m_{DB} is the mass of dried tomato seeds and peels used for the extraction (28).

$$LY\left(\frac{\mu g}{g}\right) = \frac{C \cdot V}{m_{DB}} \qquad (28)$$

3.7.3 Antiradical power

The ability of extracts to scavenge free radicals was evaluated by $ABTS^{\bullet+}$ (2,2′-azino-bis (3-ethylbenzothiazolin-6-sulfonic acid)) assay [207]. The working solution (7 mM $ABTS^{\bullet+}$) was prepared by adding 0.0959 g of 2,2′-azino-bis (3-ethylbenzothiazoline-6-sulphonic acid) diammonium salt in deionized water up to a final volume of 25 mL and 440 µL of 140 mM potassium persulfate solution. After 16 h of reaction under dark conditions, the working solution was used to assess extract antiradical power. Then, 50 µL of properly diluted sample of the extract was added to 1 mL of $ABTS^{\bullet+}$ working solution, and its absorbance was read after 2 min at 734 nm by a UV-vis spectrophotometer (model Lambda 25, Perkin Elmer, Wellesley, MA, USA). Antiradical power (ARP) was expressed as micrograms of Trolox equivalents (TE) per kg of dried biomass (DB), through the calibration curve reported by Aliakbarian [106].

3.7.4 Antiradical Power through its radical inhibition ability

Following the method reported by [208]. Absorbance of samples was read after 6 min at 734 nm by using a UV-vis spectrophotometer (model Lambda 25, Perkin Elmer, Wellesley, MA, USA). Inhibition (%), which was calculated according to equation (29).

$$Inhibition = \left(\frac{A_{blank} - A_{sample}}{A_{blank}}\right) \cdot 100 \qquad (29)$$

3.7.5 Determination of total solids

To evaluate the total solids (ETS) of the extract by gravimetric analysis, 1 mL of the extract was placed in an oven at 105 °C until a constant weight was reached. The ETS was finally expressed in milligrams of total solids per milliliter of extract (mg/mL).

3.8 Results and discussion

3.8.1 SLE

Though solid-liquid extraction is a technique that has been known for a long time and is still widely used there are still many unknown aspects that require further investigation to fully understand the mechanism. For the extraction of lycopene using sunflower seed oil, when the extraction time and liquid-to-solid ratio are constant,

within a certain temperature range, the yield of lycopene increases as the temperature increases (Figure 9). This result is consistent with the previous study of the effect of operating parameters on the extraction rate of lycopene through UAE using ethanol as the extraction agent [38]. Kumcuoglu et al. [72] also obtained the same results when studying parameters on lycopene extraction efficiency. This shows that temperature is indeed a key factor affecting lycopene extraction efficiency. As can be seen from Figure 9, when the error range is considered, there is no significant improvement in the extraction yield of lycopene when the temperature is increased to 65 °C compared to 45 °C. Therefore, from the perspective of energy conservation, in the following extraction experiments, the extraction temperature was set at 45 °C.

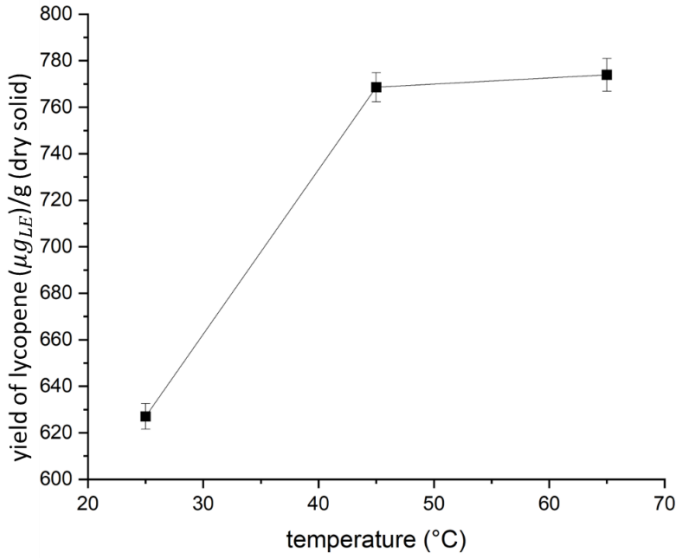

Figure 9. Yield of lycopene vs temperature with 25 min of extraction time using sunflower seed oil and liquid-to-solid ratio equal to 20/3 mL/g by SLE. LE, lycopene equivalents.

Figure 10 shows the effect of liquid-to-solid ratio (L/S) on lycopene extraction yield. The curve also shows that as the liquid-to-solid ratio increases, the lycopene extraction rate increases accordingly. Higher solvent to material ratios results in larger driving force, which accelerates mass transfer and promotes diffusion of lycopene into the medium. However, when the mass transfer process reaches its maximum, further increasing the ratio of solid-to-liquid will extend the diffusion distance of the solvent to the internal matrix and will hardly improve the lycopene yield [209]. This phenomenon was also observed by Ying et al [210]. It can be seen from Figure 10 that

when the liquid-to-solid ratio increases from 6.67 mL/g to 20 mL/g, the liquid-to-solid ratio increases by 3 times, but the lycopene extraction yield only increases by 14 %. On the other hand, due to the larger proportion of solvent, it may lead to higher consumption of organic solvents and energy. It is a waste in terms of liquid consumption, so this experiment uses 6.67 mL/g as the liquid-to-solid ratio for the next experimental analysis.

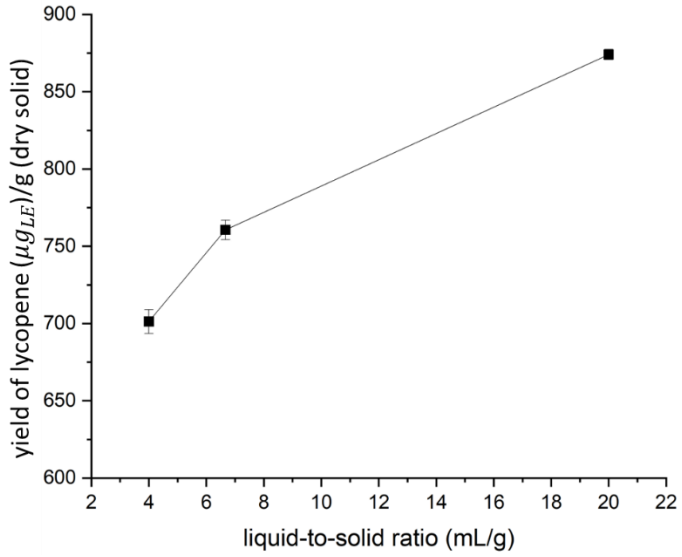

Figure 10. Yield of lycopene vs liquid-to-solid ratio with 25 min of extraction time and at 45 °C using sunflower seed oil by SLE. LE, lycopene equivalents.

Extraction time is undoubtedly a key factor affecting extraction results. But for a substance like lycopene, which is very sensitive and easily affected by the external environment, reasonable extraction time is crucial. Long-term extraction means that the exposure time of lycopene to the environment increases, so lycopene is easily degraded by the action of light and oxygen [211]. Figure 11 clearly shows that the extraction yield of lycopene increases with the increase of extraction time, but when the extraction time is extended from 45 minutes to 65 minutes, the extraction yield of lycopene does not improve with the increase of time. Therefore, based on all factors, the parameters for optimal extraction of maximum lycopene yield using sunflower oil as the extraction agent are: T = 45 °C, L/S = 20/3 mL/g, t = 45 min, and stir = 900 rpm.

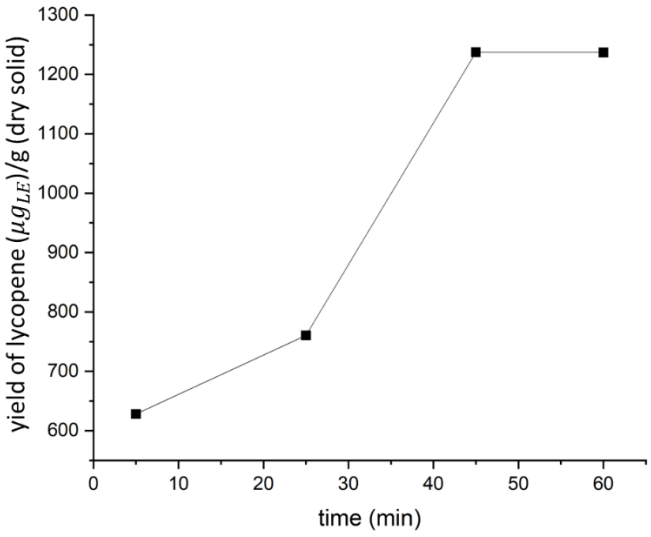

Figure 11. Yield of lycopene vs time that extracted at 45 °C using sunflower seed oil and liquid-to-solid ratio was 20/3 mL/g by SLE. LE, lycopene equivalents.

3.8.2 UAE

3.8.2.1 Ultrasound-assisted Extraction Modelling by RSM

The simultaneous influence of independent variables on the UAE of total carotenoids and lycopene yields, and on the antiradical power of the obtained extracts, was evaluated through the design of experiments. Table 5 reports the value of the input variables for the 33 runs of the experimental plan and the values of the response variables, reported as the mean value of triplicate analyses ± standard deviation.

Table 5. Values of the input variables (T = temperature; t = time; L/S = liquid-to-solid ratio; on = time during which ultrasounds were applied in a cycle (ultrasounds off = 30 s); V = total extraction volume) in the Central Composite Design of the ultrasound-assisted extraction process, and experimental results of the response variables (TC = total carotenoid yield; LY = lycopene yield; ARP = antiradical power). Data are reported as mean value of triplicate analyses ± standard deviation.

T **(°C)**	***t*** **(min)**	***L/S*** **(mL/g)**	***A*** **(%)**	**on (s)**	***V*** **(mL)**	**TC** $(\mu g_{LE}/g_{DB})$	**LY** $(\mu g/g_{DB})$	**ARP** $(\mu g_{TE}/kg_{DB})$
50	35	54	48	50	32	1268 ± 7	788 ± 3	41.31 ± 1.48
35	50	80	30	30	45	1223 ± 60	579 ± 6	35.83 ± 2.62
35	20	80	30	30	90	845 ± 11	257 ± 5	28.22 ± 2.25
50	35	54	48	50	68	890 ± 26	523 ± 21	30.28 ± 0.98
35	20	80	65	70	90	761 ± 11	442 ± 15	31.07 ± 1.45
65	20	27	65	30	45	1252 ± 15	655 ± 6	25.90 ± 1.77
35	20	27	30	30	45	700 ± 24	391 ± 20	16.69 ± 0.58
65	20	80	65	30	90	1206 ± 21	1008 ± 41	39.16 ± 1.80
50	35	54	20	50	68	818 ± 26	510 ± 14	29.43 ± 1.34
50	35	54	48	50	68	991 ± 11	665 ± 0	32.42 ± 2.74
27	35	54	48	50	68	764 ± 28	587 ± 26	23.76 ± 0.85
35	50	80	65	70	45	1093 ± 75	770 ± 10	40.27 ± 2.44
50	35	54	48	81	68	1038 ± 31	806 ± 12	37.78 ± 1.34
50	35	54	75	50	68	1206 ± 25	1011 ± 16	39.59 ± 2.18
65	50	27	65	30	90	1553 ± 20	1035 ± 48	34.14 ± 2.60
65	20	80	30	70	90	1155 ± 51	801 ± 54	28.85 ± 2.39
35	50	27	30	30	90	826 ± 24	556 ± 41	14.98 ± 0.65
50	58	54	48	50	68	1217 ± 8	1016 ± 39	27.82 ± 2.25
50	12	54	48	50	68	1112 ± 13	818 ± 23	23.86 ± 0.81
50	35	54	48	19	68	1174 ± 42	785 ± 23	25.90 ± 0.98
65	50	80	65	30	45	1024 ± 28	704 ± 8	36.15 ± 2.39
50	35	54	48	50	103	856 ± 23	693 ± 39	26.11 ± 1.21
50	35	54	48	50	68	752 ± 5	723 ± 45	23.65 ± 0.18
50	35	12	48	50	68	751 ± 4	344 ± 2	9.51 ± 0.30
50	35	54	48	50	68	796 ± 8	531 ± 39	24.93 ± 1.03
65	20	27	30	70	45	817 ± 33	476 ± 13	17.01 ± 1.43
35	20	27	65	70	45	555 ± 4	312 ± 12	16.9 ± 1.07
50	35	95	48	50	68	787 ± 37	532 ± 0	25.23 ± 1.63
50	35	54	48	50	68	732 ± 36	493 ± 5	23.65 ± 1.21
35	50	27	65	70	90	648 ± 10	242 ± 47	19.42 ± 1.12
65	50	80	30	70	45	723 ± 12	552 ± 10	30.60 ± 1.37
65	50	27	30	70	90	700 ± 16	473 ± 0	21.78 ± 0.33
73	35	54	48	50	68	895 ± 35	710 ± 11	33.92 ± 0.98

LE = lycopene equivalents; DB = dried biomass; TE = trolox equivalents.

The total carotenoid yields ranged from 555 to 1553 $\mu g_{LE}/g_{DB}$ showing a strong variability as a function of the investigated input variables. A previous study [48], concerning the recovery of carotenoids from waste of tomato industry, investigated the effect of different solvents by conventional extraction process, obtaining a TC of 17.57 mg_{LE}/kg dry TW using ethanol as solvent, while the maximum TC of 243.00 mg_{LE}/kg dry TW was provided by ethyl lactate (three solid-to-liquid extractions in series, liquid-to-solid ratio 1:10 w/v, temperature 70 °C, time 30 min). Therefore, it can be noted that the reported yields were much lower than those obtained in the present study by UAE. In fact, the use of ultrasounds allows an increase in the extraction yield, and a reduction in the use of solvent and process times, with respect to the conventional solvent extraction (SE). Luengo et al. [212] used manosonication-assisted extraction to improve carotenoids extraction yields, and a maximum TC of 14.08 mg_{LE}/100 g dry solid was obtained at 45 °C, using hexane/ethanol 50/50 v/v as solvent, showing the effect of ultrasounds in being able to reduce the temperature needed for the extraction compared to the conventional process. However, positive effects of pressure should be also considered, as reported for the recovery of lycopene by supercritical fluid extraction using ethanol 5 % as co-solvent (up to 77.2 % lycopene recovery) [213], and pressurized liquid extraction [214] with lycopene yields up to 41.74 ± 3.38 mg/100 g using ethanol 75 % as solvent.

TC was modeled according to a reduced quadratic model (Equation 30) and analysis of variance (ANOVA) was performed (Table 4) to assess the significance of the model and equation terms.

$$\sqrt{TC} = 0.96 + 0.023 \cdot T + 0.016 \cdot t + 6.46 \cdot 10^{-3} \cdot \frac{L}{S} + 0.040 \cdot A - 0.021 \cdot on - 0.064 \cdot V - 0.048 \cdot T \cdot t - 0.046 \cdot \frac{L}{S} \cdot T + 0.048 \cdot T \cdot A + 0.036 \cdot T \cdot V + 0.032 \cdot \frac{L}{S} \cdot on - 0.034 \cdot A \cdot on + 0.042 \cdot t^2 - 0.041 \cdot (\frac{L}{S})^2 \quad (30)$$

A, *T*·*t*, *T*·*L*/*S*, t^2 were the most significant terms (p-value < 0.05) of the model, which resulted as significant (p = 0.0032) with no significant lack of fit (p = 0.3020), and adequately represented the experimental data within the design space (R^2 = 0.8081). AdjR^2 presented a lower value, due to the number of not significant terms which were still present in the equation to support the hierarchy. *A* presented a positive value of

the coefficient, indicating that the higher its value, the higher the TC, while the interaction terms of *T*·*t* and *T*·*L*/*S* showed a negative value of the coefficients, as well as the quadratic term of the *L*/*S*.

The highest value of TC was experimentally found at 65 °C, with 50 min as the extraction time, low *L*/*S* (27), high *A* (65 %) and *V* (90 mL), and low on (30 s).

Table 6. Model coefficients and significance for total carotenoid yield (TC) as a function of input variables and analysis of variance.

Source	**Coefficient Coded Value**	**Cofficient -95% C.I.**	**Cofficient +95% C.I.**	***P*-value**
Model				0.0032
Intercept	0.96	0.92	1.01	
T	0.023	-0.047	0.093	0.4965
t	0.016	-0.018	0.050	0.3317
L/*S*	6.464×10^{-3}	-0.064	0.077	0.8480
A	0.040	5.532×10^{-3}	0.074	0.0254
on	-0.021	-0.091	0.050	0.5430
V	-0.064	-0.13	6.222×10^{-3}	0.0712
T·*t*	-0.048	-0.087	-8.696×10^{-3}	0.0196
T·*L*/*S*	-0.046	-0.085	-7.073×10^{-3}	0.0234
T·*A*	0.048	-0.033	0.13	0.2249
T·*V*	0.036	-2.667×10^{-3}	0.075	0.0658
T ·*L*/*S*	-0.074	-0.15	6.224×10^{-3}	0.0682
t·*V*	-0.031	-0.11	0.050	0.4293
L/*S*· *on*	0.032	-7.062E × 10^{-3}	0.071	0.1019
A ·*on*	-0.034	-0.11	0.046	0.3764
t^2	0.042	6.013×10^{-4}	0.083	0.0471
L/S^2	-0.041	-0.082	5.692×10^{-4}	0.0529
R^2	0.8081			
AdjR^2	0.6162			
Lack of Fit				0.3020

Lycopene content was found in the range 242 - 1035 µg/g_{DB}, and the highest value was found under the same conditions maximizing TC. The regression equation

showing the dependence of LY from input variables (Equation 31) reported in Table 7, where the results of ANOVA indicated that the model was significant with no significant lack of fit, and in good agreement with experimental data. *L*/*S*, *A*, *TV*, *L*/*S* on and $(L/S)^2$ were the terms which more significantly affected the response variable, exhibiting positive coefficients, with exception given for the quadratic term of *L*/*S*.

$$\sqrt{LY} = 25.79 + 0.77 \cdot T + 0.86 \cdot t + 1.34 \cdot \frac{L}{S} + 1.61 \cdot A - 0.12 \cdot on + 0.035 \cdot V - 1.25 \cdot T \cdot A + 1.85 \cdot \frac{L}{S} \cdot on - 2.10 \cdot A \cdot on + 1.09 \cdot t^2 - 0.19 \cdot (\frac{L}{S})^2 \quad (31)$$

Table 7. Model coefficients and significance for lycopene yield (LY) as a function of input variables and analysis of variance.

Source	Coefficient Coded Value	Cofficient -95% C.I.	Cofficient +95% C.I.	P-value
Model				0.0001
Intercept	25.79	24.40	27.18	
T	0.77	-1.50	3.05	0.4855
t	0.86	-0.24	1.97	0.1174
L/*S*	1.34	0.24	2.45	0.0194
A	1.61	0.51	2.71	0.0065
on	0.12	-2.16	2.39	0.9147
V	0.035	-1.07	1.14	0.9482
T·*t*	-1.25	-2.51	0.014	0.0523
T·*A*	1.50	-1.10	4.10	0.2426
T·*V*	1.85	0.59	3.11	0.0062
L/*S* · *on*	1.66	0.40	2.92	0.0125
A · *on*	-2.10	-4.70	0.50	0.1077
t^2	1.09	-0.25	2.42	0.1052
L/S^2	-2.77	-4.10	-1.43	0.0004
R^2	0.8226			
AdjR^2	0.7013			
Lack of Fit				0.3792

Rahimi and Mikani [61] carried out a study on the process parameters of UAE using sunflower oil as solvent, evaluating the lycopene recovery by varying the solid to liquid ratio, the process time, and the ultrasound intensity. The highest extraction yield (87.25 %, 91.49 $mg_{LE}/100\ g_{dried}$ TW) was provided by an ultrasound intensity of 70 W/m^2, an extraction time of 10 min, and a ratio of dried TW to oil equal to 20. Their results only partially agreed with the findings of the present study, since the ratio of dried TW to oil was the less significant parameter, while a strong dependence was found in this study on the liquid-to-solid ratio. However, it could depend on an increased total extraction volume as the ratio of dried TW to oil was decreased, a factor which can potentially influence the extraction performances, and which was considered as a further variable in this study. Indeed, results reported by Kumcuoglu et al. [72] showed the significant influence of the lycopene ultrasound-assisted extraction yield from the liquid-to-solid ratio, which was changed by maintaining the total extraction volume constant at 40 mL.

The ARP model (Equation 32) and the related ANOVA are shown in Table 8.

$$\sqrt{ARP} = 5.25 + 0.22 \cdot T + 0.16 \cdot t - 0.63 \cdot \frac{L}{S} + 0.29 \cdot A - 0.26 \cdot on - 0.42 \cdot V - 0.21 \cdot \frac{L}{S} + 0.40 \cdot T \cdot A - 0.17 \cdot T \cdot V - 0.42 \cdot \frac{L}{S} \cdot t - 0.51 \cdot \left(\frac{L}{S}\right)^2 + 0.23 \cdot A^2 + 0.19 \cdot V^2 \quad (32)$$

The model was significant, with not significant lack of fit. All the linear terms of the equation exhibited a *p*-value < 0.05 as well as the reported interactive and quadratic terms. The absence of not significant terms in the reduced quadratic model enabled very good experimental data fitting (R^2 = 0.9448; $AdjR^2$ = 0.9070).

Table 8. Model coefficients and significance for antiradical power (ARP) as a function of input variables and analysis of variance.

Source	Coefficient Coded Value	Cofficient -95% C.I.	Cofficient +95% C.I.	*P*-value
Model				<0.0001
Intercept	5.25	5.11	5.40	
T	0.22	0.11	0.33	0.0004
t	0.16	0.051	0.27	0.0064
L/S	0.63	0.52	0.74	<0.0001
A	0.29	0.18	0.40	<0.0001
on	0.26	0.032	0.48	0.0273
V	-0.42	-0.65	-0.19	0.0010
T·L/S	-0.21	-0.33	-0.081	0.0027
T·A	0.40	0.15	0.66	0.0040
T·V	0.17	0.047	0.30	0.0098
t·L/S	-0.42	-0.68	-0.16	0.0029
L/S^2	-0.51	-0.64	-0.37	<0.0001
A^2	0.23	0.097	0.37	0.0019
V^2	0.19	0.060	0.33	0.0069
R^2	0.9448			
AdjR^2	0.9070			
Lack of Fit				0.9885

The ARP of extracts obtained under different operating conditions can be ascribed not only to extracted carotenoids, but also to polyphenols (mainly p-coumaric and chlorogenic acid derivatives) [215] and amino acids, whose synergistic effects and interactions are able to provide enhanced bioactivity over single compounds [216]. The obtained values of ARP ranged between 9.51 ± 0.30 and 41.31 ± 1.48 $\mu g_{TE}/kg_{DB}$, exhibiting a strong variability with respect to the selected operating variables.

3.8.2.2 Process Optimization

By means of Equations (26) - (28) it was possible to build the desirability function in order to investigate the combined effects of all the operating conditions investigated. The response variables were maximized by assigning the highest importance to (5/5) to LY, followed by ARP (4/5) and TC (3/5), while the values of the input variables where the best solution was found were in the same range of the experimental session, with exception given for the total volume. Indeed, process optimization was also imposed to maximize this variable (importance 3/5) in order to understand the maximum volume treatable with the same energy input without significant losses in extraction yields. The desirability function dependence on input variables is reported in Figure 12. Surface plots on the same row (e.g., Figure 12a, d, g) show the same input variables on the axes, while the columns report the minimum (Figure 12a-c), optimal (Figure 12d-f,) and maximum (Figure 12g-i) values of the operating conditions in the selected design space. The strong interdependence of the operating conditions was revealed by the shape changes of the surface in correspondence with the minimum (Figure 12a-c,) and maximum (Figure 12g-i) values of the variables. Extraction time is one of the most important variables in this kind of separation process, and the higher the contact time between the solid particles and the solvent, the higher the mass transfer achieved. In Figure 13 the chromatogram is shown. Nevertheless, extraction kinetics often show a plateau, and times longer than the critical value do not provide a significant enhancement in extraction yields. Furthermore, when thermo-sensitive compounds are involved in the process, degradation kinetics should be taken into account. Conflicting effects of extraction times were reported by several authors. For instance, positive effects of prolonged time in UAE were found for the recovery of polyphenols and phlorotannin from brown seeds [217] and lycopene from tomato [192,218], as well as for flavonoids from *Lycium barbarum* up to 90 min [219], while a reduced concentration of polyphenols from mango residues was observed by prolonging the time from 20 to 30 min [220], of anthocyanins from pigmented rice after 20 min [221], and a slight decrease in lycopene yield from tomato was also observed in improved ultrasound-assisted extraction after 20 min of sonication [222].

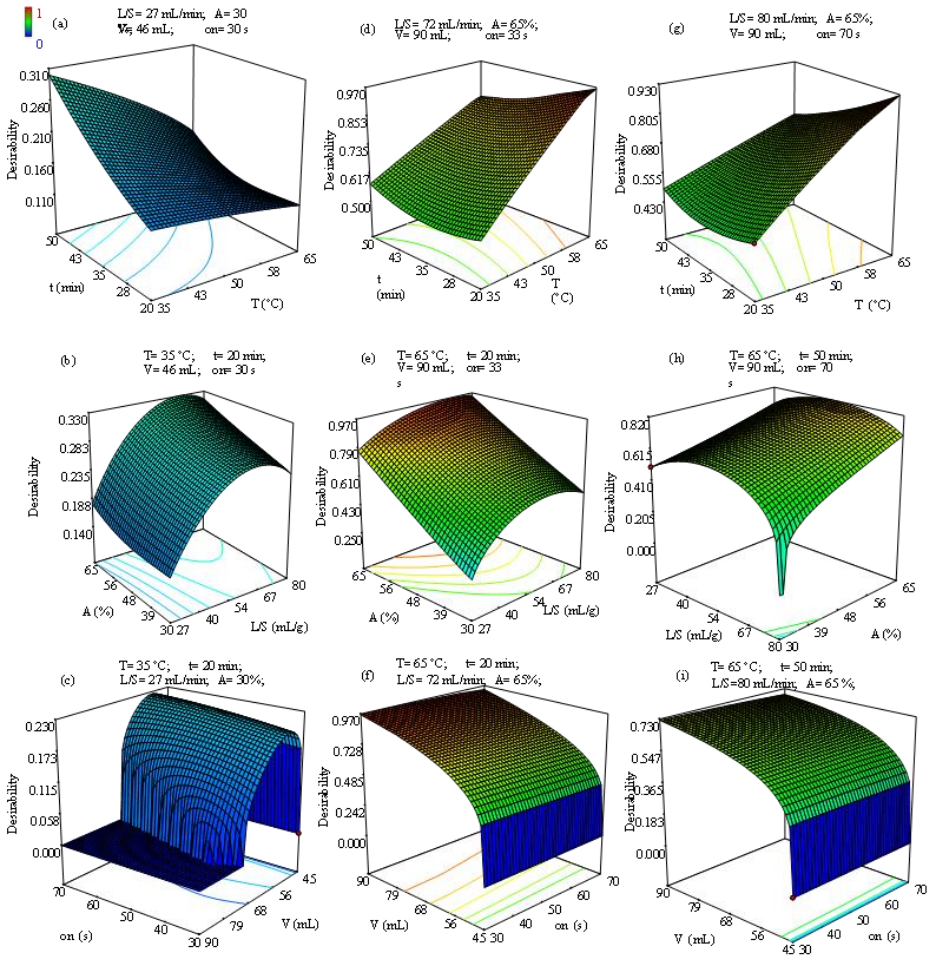

Figure 12. Surface plots of desirability as a function of the input variables: temperature (T), time (t), ultra-sound amplitude (A), on/off pulsed ratio (on), liquid-to-solid ratio (L/S), and volume (V).

Moreover, no significant effects of time were reported by Grassino et al. [223] in the recovery of polyphenols and flavonoids from TW. Generally, the increase in sonication time initially shows positive effects, then the yields tend to decrease at long times [196]. However, both degradation and extraction kinetics parameters are always functions of the other operating conditions, such as temperature and ultrasound amplitude, so the system behavior over time can strongly change by varying UAE parameters, as observed in this study.

Temperature's ability to improve mass transfer in solid-liquid extraction is well known in literature [224]. However, in UAE, other contributions of this parameter are involved. Indeed, if an increase in system temperature initially provides a higher extraction yield due to the higher solubility and diffusivity of compounds in the liquid medium and the lower solvent viscosity, on the other hand, it causes a rise in solvent vapor pressure and a reduction in solvent surface tension. Consequently, more solvent

vapor enters in the bubble cavity, and numerous cavitation bubbles are generated, so the violence of the collapse is reduced, weakening the sonochemical effects [196,225]. Moreover, lycopene stability and antioxidant activity can be negatively impacted by the higher temperature adopted. The structure of lycopene makes it susceptible to degradation because of its conjugated double bonds. However, it has been reported that the compound is quite stable at temperatures below 60 °C [52,226]. Liao et al. [222] obtained the highest LY at 25 °C, and lower values were attained at higher temperatures, whereas Lianfu and Zelong [66] reported an increase in LY as temperature rose from 54 to 84 °C. The need to ensure both high extraction yields and the preservation of the biological activity of the compounds often requires finding the right compromise by an optimization process.

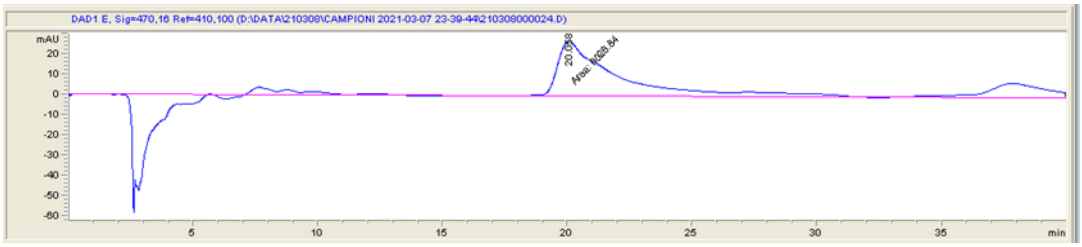

Figure 13. Chromatogram under optimal condition of UAE analysed by using HPLC Agilent 1100 series.

Amplitude is a measure of the power delivered. Usually, the yield of extraction increases with power, due to the larger amplitude of ultrasound traveling through the solvent which provokes more intense bubble implosion and sonochemical effects on the solid particles [196], including particle fragmentation which increases the surface area [227], enhancing the process performance. However, after reaching a peak, sometimes extraction yields tend to decrease with the further increase in amplitude [227]. When the power increases to a very high level, it leads to an increase in the number of bubbles formed, and the collapse occurs non-spherically, decreasing the impact of the implosion. Furthermore, the layer of cavitation bubbles around the tip of the probe hinders the transmission of energy in the extraction medium, reducing the yield [196,220,225]. An increase from Figure 15b, e, h can be observed as the positive effect of amplitude rise throughout the investigated design space. This result is in agreement with the findings of other studies [212,222]. The on/off pulsed ratio was a

useful parameter to control temperature inside the system. Compared to continuous ultrasound application, the process operating in pulsed mode decreases the number of cavitation bubbles but increases the intensity of their implosion [196]. However, this was the parameter that less affected the response variables (Table 4, Table 5 and Table 6) and the desirability, as can be observed in Figure 12c, f, i. The larger the liquid-to-solid ratio, the higher the mass of compounds that can be transferred in the liquid solvent, due to a favorable concentration gradient during the diffusion and the lower viscosity of the system enhancing the cavitation effect [196]. As can be seen in the desirability surface plots (Figure 12b, e, h), the objective function value initially increased with L/S up to a maximum value, beyond which it decreased. This effect can be traced back to the maximum of mass transfer reached, as well as to the degradation effects precisely due to the high cavitation effect resulting in degradation of the desirable solute [72,196]. Total extraction volume is an important parameter for UAE, since it is related to the power density. The importance of this parameter is highlighted by some troubles encountered in the ultrasound-assisted process scale-up [228], also related to the industry-available sonic probes [225]. Keeping a constant liquid-to-solid ratio with the other investigated parameter, all the extraction yields decreased as the system volume increased (Figure 14a - c). Indeed, as reported by Kulkarni and Rathod [229], the lower extraction yields with the increase in the liquid volume could be due to a decrease in power density and ultrasound efficiency due to the scatter of ultrasonic energy in bulk solution, while low sonication volume leads more collisions among particles, increasing the total area exposed to solvent extraction. The only exception was given by LY which, at low temperatures, agreed with the other response variables (Figure 14c) despite showing an opposite shape when temperature was increased above 50 °C (Figure 14d). This evidence could be related to the selectivity toward lycopene induced by the variation volume, and therefore to the power applied [225].

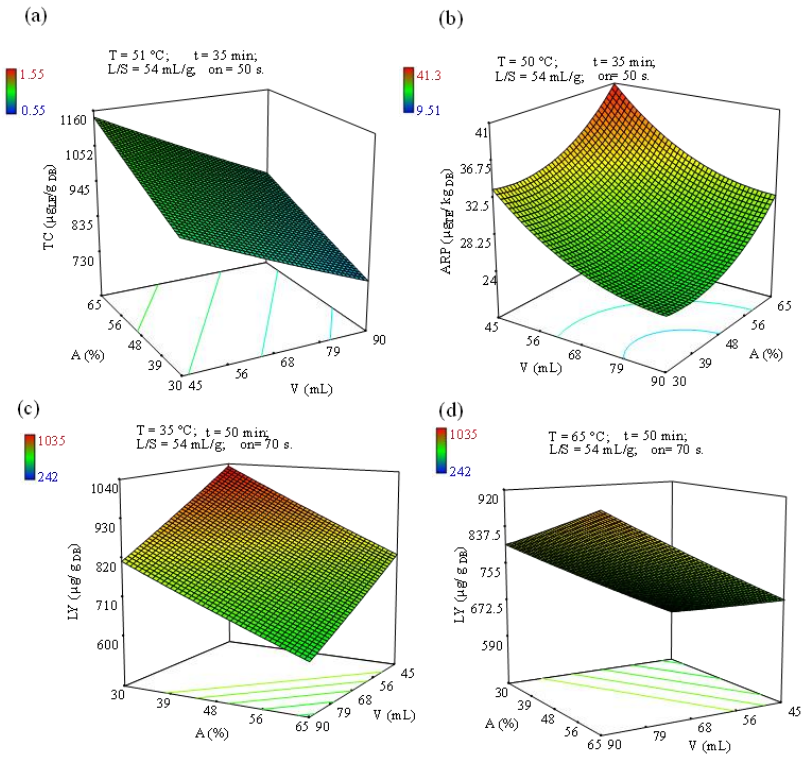

Figure 14. Surface plots of: (a) total carotenoid yield (TC); (b) antiradical power (ARP); and (c,d) lycopene yield as functions of amplitude (A) and total volume (V).

Numerical optimization under the abovementioned constraints led to the optimum values of the input variables reported in Table 9. As shown in Figure 15, the optimal solution numerically found allowed the obtainment of a global desirability of 0.964, being particularly favorable in maximizing LY and ARP. The optimal point was experimentally verified, and results were very close to those predicted by the model. Only the LY result was significantly higher than the value mathematically predicted. This discrepancy could be due to the non-homogeneous lycopene content in the matrix.

Table 9. Results of numerical optimization and experimental verification. T, temperature; t, time; L/S, liquid to solid ratio; A, amplitude; on, time working of UAE probe; V, volume; TC, carotenoid content; LY, lycopene content; ARP, antiradical power.

Variables	Optimized Values	Response Variable Values Predicted by Model	Response Variable Values Experimentally Verified
T (°C)	65		
t (min)	20		
L/S (mL/g)	72		
A (%)	65		
on (s)	33		
V (mL)	90		
TC (μg_{LE}/g)		1402	1408 ± 14
LY (µg/g)		1140.39	1536 ± 53
ARP (μg_{TE}/kg)		39.8	36.1 ± 0.9

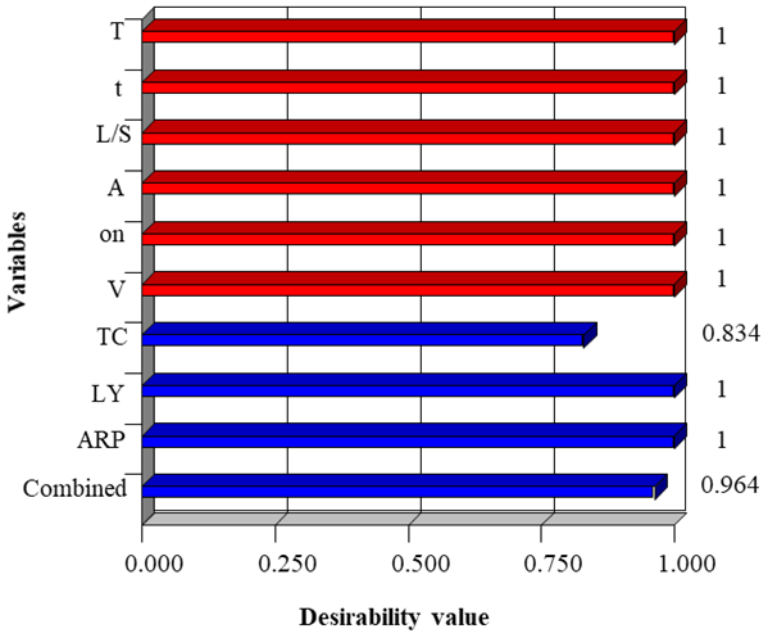

Figure 15. Desirability values for the input and response variables. T, temperature; t, time; L/S, liquid to solid ratio; A, amplitude; on, time working of UAE probe; V, volume; TC, carotenoid content; LY, lycopene content; ARP, antiradical power.

3.8.2.3 Evaluation of the effects of frequency in UAE

There have been different opinions on whether ultrasonic frequency has an impact on the extraction rate of lycopene. In order to study the ultrasonic frequency and evaluate its effect on the yield of extracted lycopene, three different session frequencies (40 kHz, 80 kHz, 120 kHz) were evaluated in this experiment (Figure 16). In this study, when frequency is 40 kHz the yield of lycopene is the highest (Figure 16), but the total yield of lycopene is still low. When measurement errors are also considered, the data obtained at the three different frequencies indicate almost the same value. In addition, there are many studies showed that the maximum yield of lycopene can be obtained with low frequency. Liao et al. [222] studied the effects of different ultrasonic frequencies on the extraction rate of lycopene using an extraction temperature of 25 °C, an ultrasonic power of 200 W, a *S*/*L* ratio of 2:1 mL/g, and a time of 45 minutes. The results showed that the higher ultrasonic frequency, the extraction efficiency of lycopene initially. The maximum extraction efficiency was 77 % in the range of 34 - 50 kHz. However, when the ultrasonic frequency is greater than 50 kHz, the extraction efficiency gradually decreased as the ultrasonic frequency increases. Mizrach et al. [230] obtained consistent results when studying the effect of ultrasonic frequency on the extraction efficiency of biocomponents from agricultural crops, and according to research report, ultrasonic frequencies below 100 kHz produced relatively good results when used to extract raw materials.

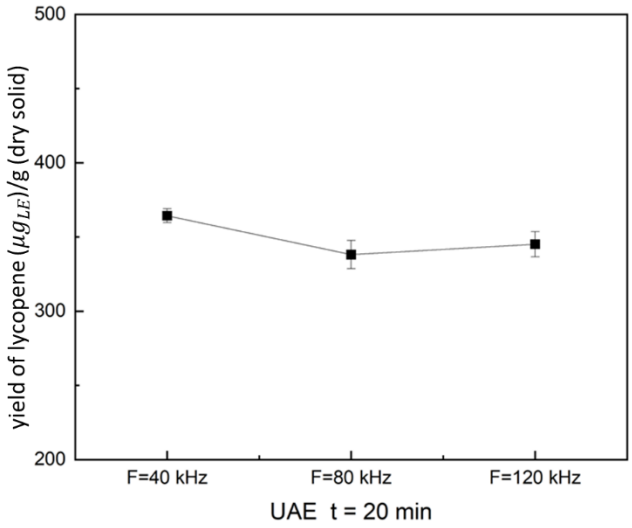

Figure 16. Yield of total lycopene extracted with ultrasound-assisted extraction (UAE) at different frequencies for 20 min.

3.8.3 SoLVE

3.8.3.1 Lycopene content

Another extraction technique under evaluation to recovery lycopene from TW was SoLVE. Statistical analysis of lycopene extraction yield obtained by the experimental plan indicated that the temperature, liquid-to-solid ratio, and the on/off pulsed ratio (on = 30 s) are significant on lycopene yield (Table 10). The surface plot showed that lycopene yield increased as the temperature and the on/off pulsed ratio (on = 30 s) decreased (Figure 17a and 17b). The data also show that when the extraction was conserved out for a long time, the extraction efficiency remains at a high level, and there was no significant by difference changing liquid-to-solid ratio and temperature (Figure 17c). This may be due to the fact that the extraction efficiency has reached the maximum after reaching a certain time. It can also be shown that almost no degradation reaction of lycopene occurred within the extraction time range of this experiment. The *trans*-lycopene yield ranged from 92.5 - 546.7 µg/g, and the maximum value was comparable with those reported in other studies, showing yields ranging from 0.639 to 73.40 mg/100 g [33,231,232]. Kaul et al. found that when TW (0.15 mm particle size) was treated with hexane: acetone: alcohol (2:1:1 mL: mL: mL), 1:30 using as solid-to-liquid ratio (w/v) at 50 °C, the maximum recovery of lycopene/100 g was 1.98 mg in four extractions in 8 minutes. The results presented in this study, using SoLVE were satisfying, so the method can be considered a remarkable non-conventional extraction method. It should also be noted that same different in the yield of different lycopene recovered could depend both on the extraction method and on the type of raw material. The chromatogram was shown in Figure 18.

Table 10. Analysis of variance (ANOVA) for reduced quadratic model for optimization of extraction parameters based on yield of lycopene.

Source	Sum of Squares	df	Meam Square	F-value	P-value	
Model	2.57E+05	12	21411.27	11.16	0.0005	significant
A-*T*	30283.76	1	30283.76	15.78	0.0032	
B-*t*	2286.65	1	2286.65	1.19	0.3033	
C-*L*/*S*	1.12E+05	1	1.12E+05	58.1	< 0.0001	
D-*A*	549.74	1	549.74	0.2865	0.6054	
E-*on*	36195.33	1	36195.33	18.86	0.0019	
AB	22531.83	1	22531.83	11.74	0.0075	
AE	10368.07	1	10368.07	5.4	0.0452	
BE	14795.41	1	14795.41	7.71	0.0215	
CE	37640.65	1	37640.65	19.62	0.0016	
DE	31987.58	1	31987.58	16.67	0.0027	
A^2	8015.18	1	8015.18	4.18	0.0713	
C^2	10068.1	1	10068.1	5.25	0.0477	
Residual	17269.21	9	1918.8			
Lack of Fit	15784.83	7	2254.98	3.04	0.2699	Not significant
Pure Error	1484.38	2	742.19			
Cor Total	2.74E+05	21				
R^2	0.937					
Adjusted R^2	0.853					

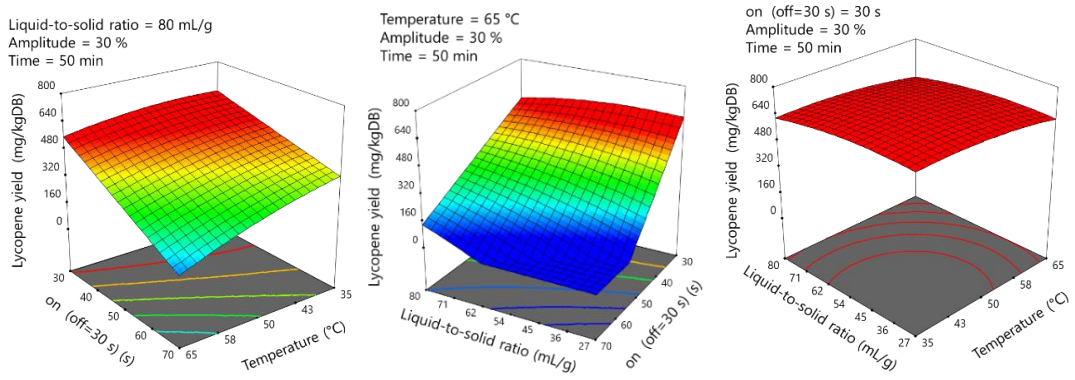

Figure 17. Surface plots of lycopene yield as function of the input variables: a) on/off pulsed ratio (on, s) and temperature (°C), b) liquid-to-solid ratio (mL/g) and on/off pulsed ratio (on, s), c) liquid-to-solid ratio (mL/g) and temperature (°C).

Lycopene yield was modeled according to a reduced quadratic model (Equation 33) and analysis of variance (ANOVA) was performed (Table 11) to assess the significance of the model. The Model F-value of 11.16 and P-values 0.0005 (p-value < 0.05) indicate model terms are significant. The temperature, liquid-to-solid ratio, and on/off pulsed ratio (on) were the most significant terms (p-value < 0.05) of the model, which resulted significant (p = 0.0005) with no significant lack of fit (p = 0.2699).

$$Lycopene\ yield = -513.73 + 46.07 \cdot T + 41.53 \cdot t - 4.04 \cdot \frac{L}{S} - 18.51 \cdot A - 21.28 \cdot on - 0.61 \cdot T \cdot t - 0.17 \cdot T \cdot on + 0.0012 \cdot t \cdot \frac{L}{S} - 0.20 \cdot t \cdot on + 0.26 \cdot \frac{L}{S} \cdot on + 0.36 \cdot A \cdot on - T^2 - 0.045 \cdot (\frac{L}{S})^2 \qquad (33)$$

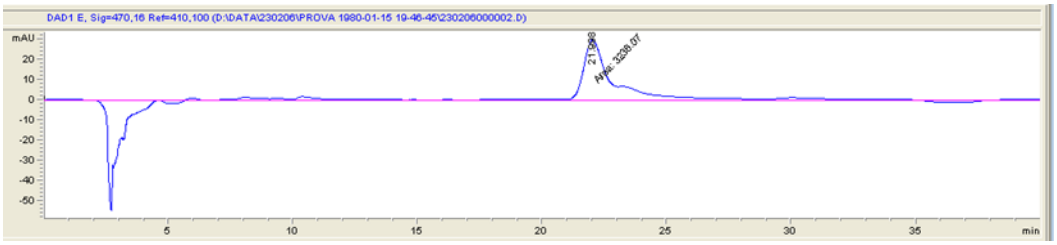

Figure 18. Chromatogram of Optimal condition of SoLVE analysed by using HPLC Agilent 1100 series.

3.8.3.2 Antiradical power

Figure 19 shows the effects of two extraction parameters (liquid-to-solid ratio and temperature) on the antioxidant activities of the extracts as determined by ABTS assay. When the temperature is increasing and liquid-to-solid ratio is decreasing, the extracts showed a maximum antioxidant activity. On the other hand, lycopene content in extracts increased with increasing the temperature. Lycopene as an antioxidant, so, the antioxidant activity can be increased with its concentration in the extract. As can be seen from Table 11, the antioxidant activity showed significant correlation (p-value < 0.05) with single parameters such as temperature, time and liquid-to-solid ratio.

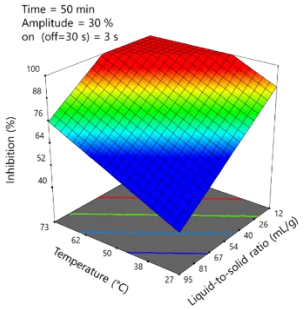

Figure 19. Surface plots of inhibition as function of liquid-to-solid ratio (L/S) and temperature (°C).

Table 11. Analysis of variance (ANOVA) for reduced quadratic model for optimization of extraction parameters based on inhibition.

Source	Sum of Squares	df	Mean Square	F-value	P-value	
Model	1227.09	14	87.65	31.54	<0.0001	significant
A-*T*	29.77	1	29.77	10.71	0.0096	
B-*t*	16.79	1	16.79	6.04	0.0363	
C-*L*/*S*	489.71	1	489.71	176.25	<0.0001	
D-*A*	3.12	1	3.12	1.12	0.3167	
E-*on*	4.9	1	4.9	1.76	0.2169	
AB	12.35	1	12.35	4.44	0.0643	
AD	88.09	1	88.09	31.7	0.0003	
AE	123.19	1	123.19	44.34	<0.0001	
BC	18.17	1	18.17	6.54	0.0308	
CD	21.14	1	21.14	7.61	0.0222	
CE	134.79	1	134.79	48.51	<0.0001	
DE	20.22	1	20.22	7.28	0.0245	
B^2	17.03	1	17.03	6.13	0.0352	
D^2	34.13	1	34.13	12.28	0.0067	
Residual	25.01	9	2.78			
Lack of Fit	16.92	7	2.29	0.5089	0.7898	Not significant
Pure Error	8.99	2	4.5			
Cor Total	1252.1	23				
R^2	0.98					
Adjusted R^2	0.949					

3.8.3.3 Relationship of inhibition and concentration of lycopene

a

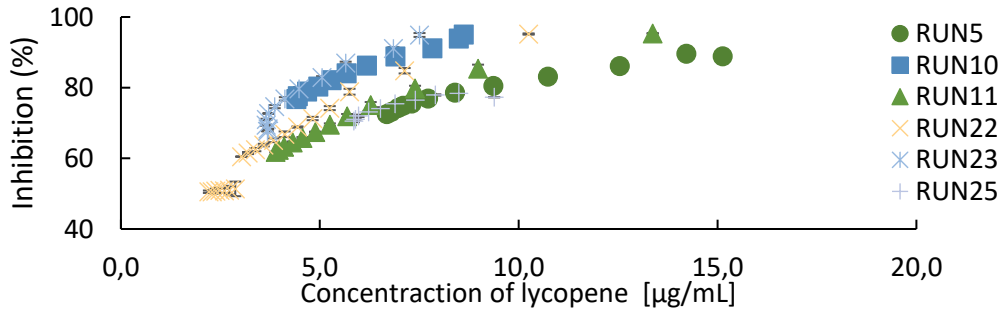

b

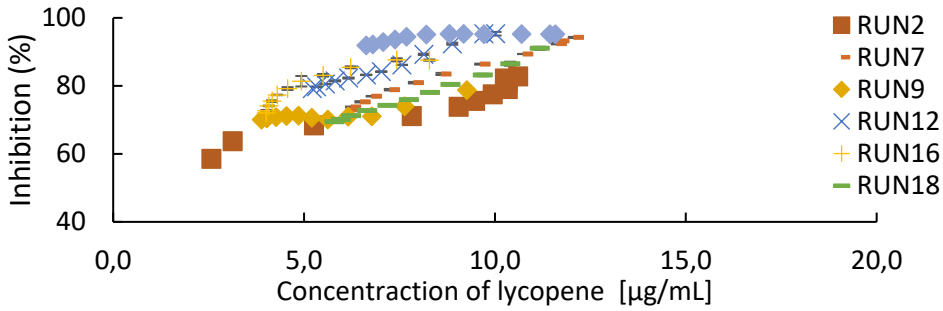

c

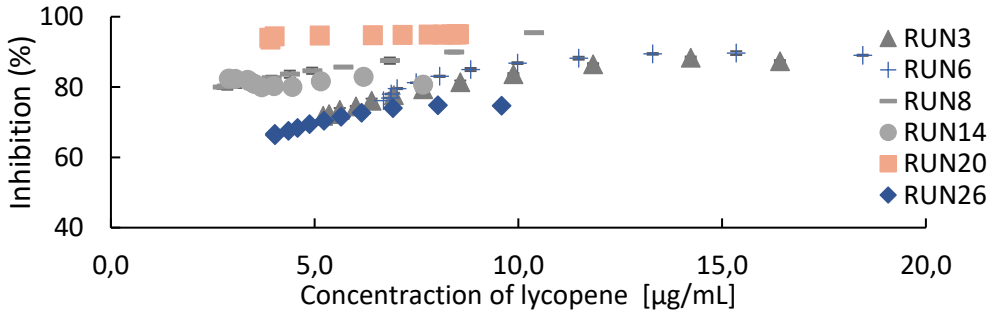

d

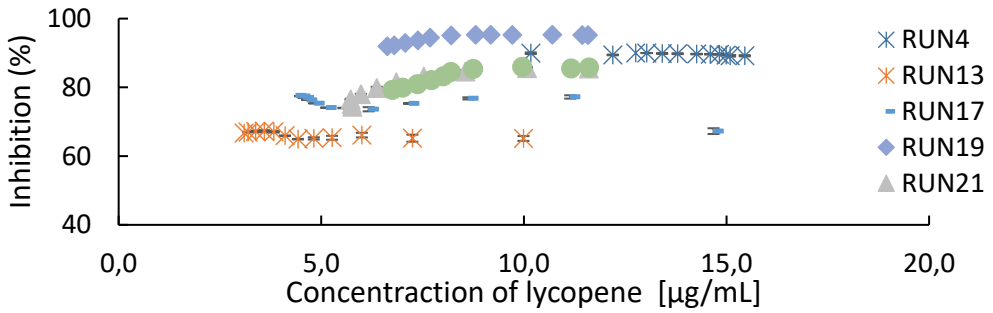

Figure 20. Relationship between inhibition and lycopene concentration under different conditions.

Research shows that lycopene detected in the tomato samples was found to be significantly related with the antioxidant capacity of the extract. Dewanto et al. [233] found that thermal processing increased the total antioxidant activity of tomato after 30 min of heating at 88 °C. The total antioxidant activity increased because larger amounts of lycopene were released from the matrix during thermal processing. Figure 18 showed the relationship between inhibition and lycopene concentration. From Figure 20 it can be seen that almost all the antioxidant activity of the RUNs increased with the increase of lycopene concentration. According to the literature, generally, the change of antioxidant activity in lycopene-rich extracts was mainly influenced by lycopene content, proportions of the isomers of lycopene, and the synergistic effects of carotenoid in the extract [5]. However, It can be seen from Figure 20d that the antioxidant activity of RUN13 and RUN17 did not increase with the increase of lycopene concentration. According to the research of Hackett et al. [234], when the temperatures up 50 °C, the antioxidant activity was influenced because of the lycopene degraded [235]. From Figure 20a, 20c and 20d, it can be seen that for the RUN4, RUN8, RUN13, RUN25, and RUN26, the extraction temperature is 65 °C, which is consistent with the results of Hackett's research. When the temperature is higher than 50 °C, it may cause the degradation of lycopene and reduce the antioxidant activity. Although the extraction temperature of RUN14 and RUN17 is lower than 50 °C, the working time of the ultrasonic probe is 70 s and 81 s respectively after each 30 s of pause. The long ultrasonic cycle released a lot of heat when it is working, which may have caused the local temperature to be higher than 50 °C, thus causing the degradation of lycopene. thereby affecting antioxidant activity.

3.8.3.4 Extraction Kinetics Curves

So far, by fitting experimental data obtained from lycopene extraction to each model. Among the proposed models, the Peleg's model was found to be suitable to describe the extraction kinetics of lycopene. According to findings of Poojary and Passamonti [193], the extraction kinetics data of lycopene concentration in solvent (ethanol) were mathematically described using the empirical equation (Equation 21) proposed by Peleg (1988), whose applicability on the extraction kinetics of intracellular compounds from different food matrices has been extensively demonstrated [236,237].

Table 12. Calculated parameters of Peleg's model at different extraction conditions.

Sample	Time	Lycopene yield	Dev. st	t/lycopene yield	K_1	K_2	R^2	Lycopene yield calc	RMSD
	[min]	[µg/g]	[µg/g]	[min g/µg]	[min g/µg]	[µg/g]	[-]	[µg/g]	
Center	35	368.0	1.07	0.10	0.0499	0.0012	0.9775	380.8	7.4
RUN2	50	326.3	0.18	0.15	0.138	0.0003	0.9806	282.0	3.5
RUN4	50	360.3	0.64	0.14	0.1101	0.0006	0.9308	356.9	8.8
RUN6	50	546.7	1.00	0.09	0.0316	0.0012	0.9648	545.9	16.3
RUN8	20	452.7	4.70	0.04	0.0181	0.0013	0.9991	453.5	4.5
RUN9	20	537.2	4.22	0.04	0.0231	0.0007	0.9381	539.1	12.0
RUN10	35	302.7	0.56	0.12	0.0548	0.0017	0.9879	306.2	11.6
RUN11	35	459.5	2.47	0.08	0.0311	0.0012	0.963	478.8	19.3
RUN12	35	353.9	1.05	0.10	0.0571	0.0012	0.9919	353.2	3.0
RUN13	20	421.2	3.10	0.05	0.0252	0.001	0.9859	442.5	14.7
RUN14	35	196.8	1.10	0.18	0.069	0.0028	0.9473	209.6	9.4
RUN16	35	243.6	0.44	0.14	0.0706	0.0018	0.9442	262.0	17.9
RUN17	50	362.8	0.74	0.14	0.046	0.0019	0.9336	354.6	4.2
RUN18	20	259.0	0.26	0.08	0.0545	0.0013	0.9868	248.4	4.7
RUN19	50	189.7	0.24	0.26	0.1463	0.0023	0.9045	191.4	2.6
RUN20	35	92.5	0.12	0.38	0.6044	0.0067	0.8293	45.4	18.1
RUN21	35	363.7	0.62	0.10	0.0401	0.0014	0.9631	392.8	12.9
RUN22	12	291.4	1.37	0.04	0.023	0.0014	0.9935	306.9	9.2
RUN23	35	205.1	0.84	0.17	0.0918	0.0018	0.8754	226.1	7.9
RUN24	58	354.2	0.37	0.16	0.0779	0.0015	0.9741	351.7	7.4
RUN25	20	229.1	0.38	0.09	0.0569	0.0013	0.9585	241.3	4.9
RUN26	50	346.7	0.46	0.14	0.0514	0.0019	0.9928	341.5	5.2

Table 12 shows the results of the kinetic study of the extraction process as function of the input variable. The experimental data are well described; Being R^2 in the range 0.8293 - 0.9991. The yield of lycopene is in the range 92.5 - 546.7 µg/g, values comparable with the results described in Li et al [38]. The kinetic model curves of lycopene extraction at different conditions are shown in Figure 21. Among them, the highest yield was obtained in the case of RUN6. The effective diffusion coefficients are the highest for condition of RUN14. Figure 21 reports the extraction kinetic curves of lycopene by SoLVE. Only due to the limited extraction time and plateau did not appear.

a

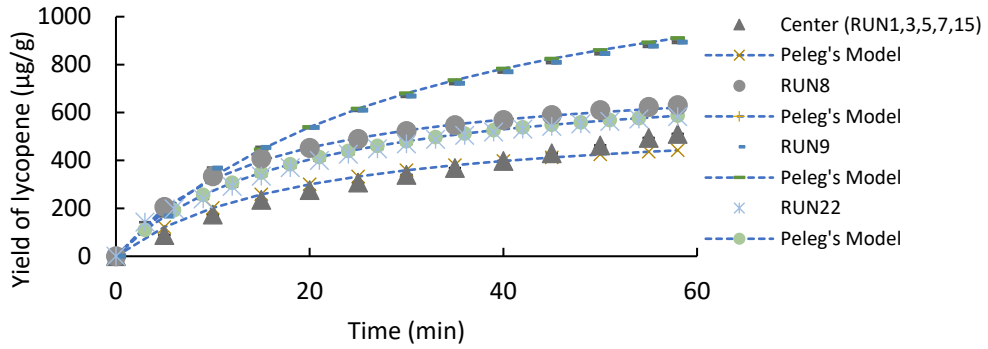

b

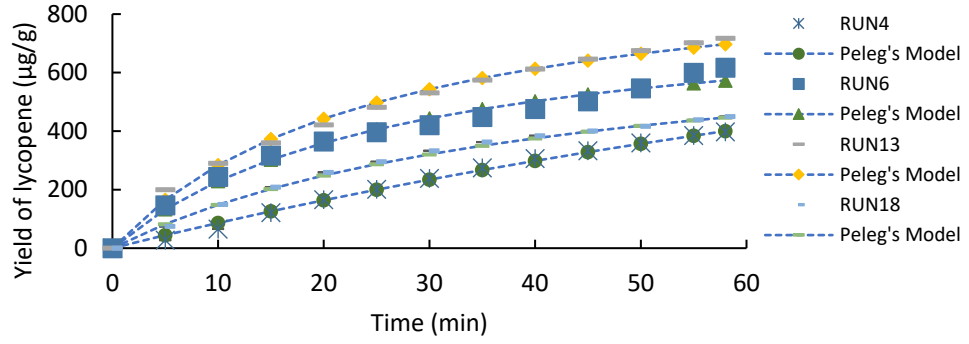

c

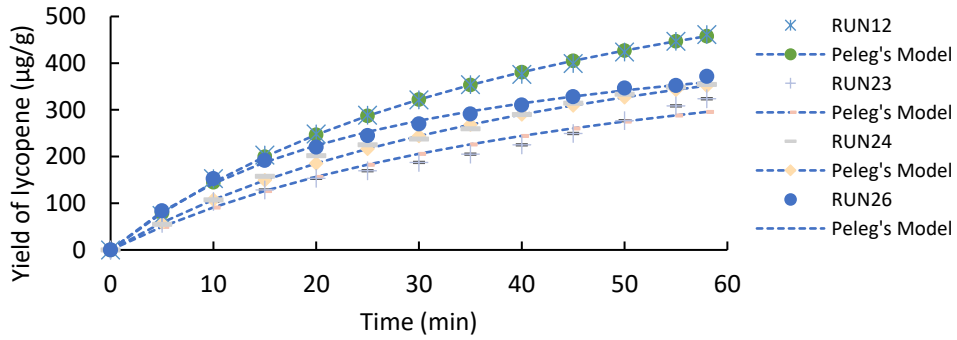

d

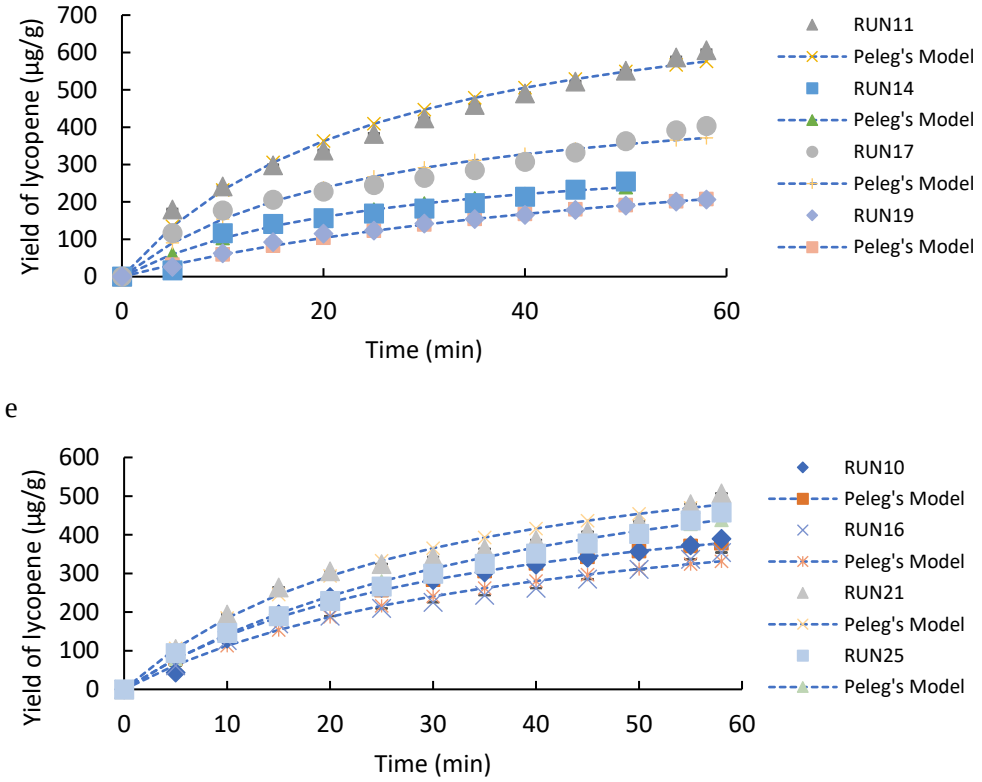

e

Figure 21. Extraction kinetics of lycopene under different experimental conditions fitted by the Peleg's model.

3.8.3.5 Effect of parameters on the K_1 and K_2

Table 13 shows that extraction temperature and time affect significantly the K_1 parameter. The constant K_1 of the Peleg's model has higher values at relatively short extraction times and lower temperature, indicating a higher reaction rate at low temperatures and initial extraction times (Figure 22). Similarly, the reaction rate was lower after a long extraction at time high temperature. On the contrary, the Peleg's model constant K_2 did nit show a significant dependence on the extraction time and temperature (Table 14), while was significantly affect to by the on/off pulsed ratio (on) and amplitude, indicating that the reaction rate was lower at long extraction time, high temperature and high *on*/*off* pulsed ratio (*on*) (Figure 23a and 23b).

Table 13. Analysis of variance (ANOVA) for reduced quadratic model for optimization of extraction parameters based on K_1.

Source	Sum of Squares	df	Meam Square	F-value	P-value	
Model	0.0201	16	0.0013	33.6	0.0005	significant
A-*T*	0.0015	1	0.0015	41.38	0.0013	
B-*t*	0.0025	1	0.0025	68.1	0.0004	
C-*L*/*S*	0	1	0	0.9148	0.3828	
D-*A*	6.65E-06	1	6.65E-06	0.1777	0.6908	
E-*on*	0.0001	1	0.0001	1.94	0.2225	
AB	0.0008	1	0.0008	20.88	0.006	
AC	0.0007	1	0.0007	18.94	0.0073	
AE	0.0011	1	0.0011	28.46	0.0031	
BC	0.0021	1	0.0021	56.08	0.0007	
BE	0.001	1	0.001	25.85	0.0038	
CD	0.0014	1	0.0014	36.75	0.0018	
CE	0.0012	1	0.0012	31.57	0.0025	
A^2	0.001	1	0.001	26.47	0.0036	
B^2	0.0002	1	0.0002	4.45	0.0886	
D^2	0.0004	1	0.0004	10.16	0.0243	
E^2	0.0013	1	0.0013	34.79	0.002	
Residual	0.0002	5	0			
Lack of Fit	0.0001	3	0	1.42	0.4392	Not significant
Pure Error	0.0001	2	0			
Cor Total	0.0203	21				
R^2	0.9908					
Adjusted R^2	0.9613					

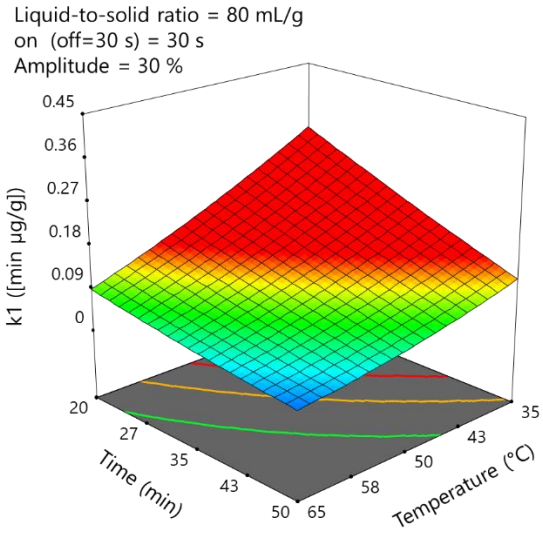

Figure 22. Surface plots of k1 as functions of the input variable of time (min) and temperature (°C).

Table 14. Analysis of variance (ANOVA) for reduced 2FI model for optimization of extraction parameters based on K_2.

Source	Sum of Squares	df	Meam Square	F-value	P-value	
Model	1.91	11	0.1736	7.81	0.0023	significant
A-T	0.0609	1	0.0609	2.74	0.1321	
B-t	0.0078	1	0.0078	0.3516	0.5678	
C-L/S	0.079	1	0.079	3.56	0.0919	
D-A	0.0794	1	0.0794	3.57	0.0912	
E-*on*	0.1484	1	0.1484	6.68	0.0295	
AC	0.1614	1	0.1614	7.26	0.0246	
AD	0.5065	1	0.5065	22.79	0.001	
AE	0.4083	1	0.4083	18.38	0.002	
BD	0.4794	1	0.4794	21.57	0.0012	
BE	0.5643	1	0.5643	25.39	0.0007	
CD	0.095	1	0.095	4.27	0.0687	
Residual	0.2	9	0.0222			
Lack of Fit	0.0737	7	0.0105	0.1666	0.9697	Not significant
Pure Error	0.1263	2	0.0632			
Cor Total	2.11	20				
R^2	0.9052					
Adjusted R^2	0.7893					

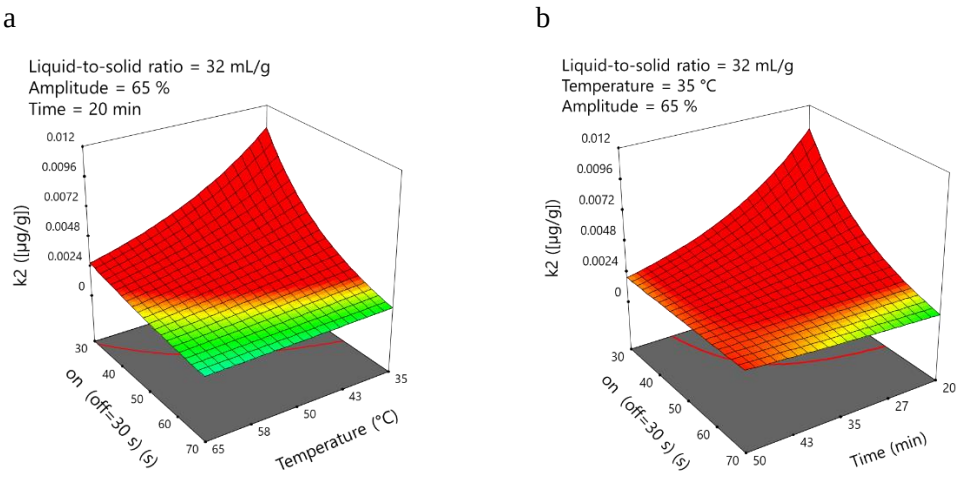

Figure 23. Surface plots of k2 as functions of the input variables: a) temperature (°C) and on/off pulsed ratio (on), b) time (min) and on/off pulsed ratio (on).

3.8.3.6 *Trans*-lycopene and *cis*-lycopene content

According to some studies, the bioavailability of *cis*-isomers of lycopene and trans-lycopene are different. According to the reach of Boileau [238], *cis*-isomers of lycopene are more bioavailable than *trans*-lycopene, as demonstrated by two studies involving bile acid micelles and ferrets. Different methods can get different composition of *cis*-lycopene and *trans*-lycopene, for example, according to the research of Vallecilla-Yepez and Ciftci [239] extraction from tomato peels and seeds using supercritical carbon dioxide (sc-CO_2) and compare it with conventional hexane extraction, with sc-CO_2 extraction producing higher yields of *cis*-lycopene. From the Figure 24, it can be seen that almost all RUNs have a high content of *trans*-lycopene about 80 %. This experimental result is consistent with the findings obtained by Ho's [67], using low ethyl acetate microwave-assisted extraction, but slightly lower than the *cis*-content obtained by using high ethyl acetate microwave-assisted extraction. The maximum content of *cis*-lycopene is 30 % a little lower than the *cis*-lycopene content 34 % obtained using traditional hexane extraction methods and the *cis*-lycopene content 67 % using sc-CO_2 extraction methods [240].

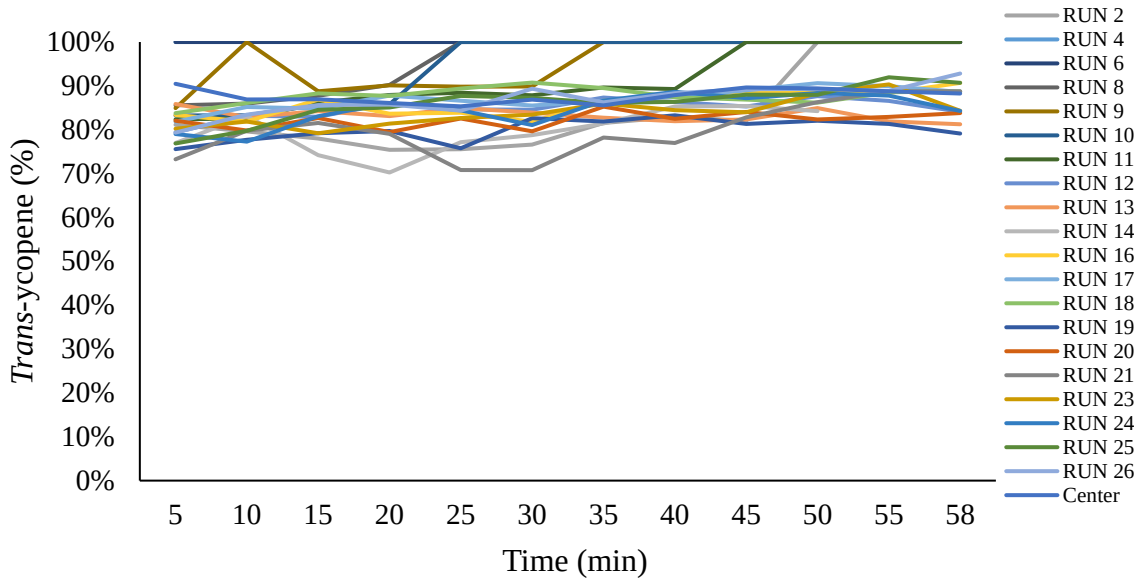

Figure 24. *Trans*-lycopene isomer percentage in the extract composition and extraction time under different conditions.

3.8.3.7 Desirability

The search for the optimum point was carried out through a numerical optimization using the software Design Expert (Stat-Ease, Inc., Minneapolis, United States). For the calculation, different levels of importance and the limit values of the interval were attributed to the independent variables. The variable values temperature, time, liquid-to-solid ratio, amplitude, on/off pulsed ratio (on=30 s), K_1 and K_2 were in range, while lycopene yield and antiradical power were maximized. Figure 25 shows all responses about the optimum point. The optimum point obtained had the following coordinates: T = 64 °C, t = 41 min, L/S = 40 mL/g, A = 39 %, on/off = 32/30 s/s, K_1 = 0.024 min µg/g, K_2 = 0.001 µg/g, inhibition = 95.68 %, yield of lycopene 567.3 µg/g. This point had a desirability of 1. Under the optimal conditions obtained, the extraction experiment was carried out for 3 hours, after substituting the data obtained from the extraction into the Peleg's model, it was found that a high adhesion of R^2 = 0.9985 was obtained (Figure 26). From Figure 27 also can be seen that the experimental data and the calculated data have reached a high degree of agreement, and after 3 h extraction the plateau appeared. From Figure 28 it is clear that the concentration of lycopene has a great influence on the extract properties, since the intensity of antioxidant activity increases with the increase of lycopene concentration. This is consistent with Shi's experiment [5] which indicated that lycopene is the main influencing factor of extract activity. It can be seen from Figure 29 that the content of

cis-lycopene is about 22 % when the extraction time reaches 20 minutes. When the extraction time exceeds 80 minutes, the obtained lycopene is all *trans*-lycopene.

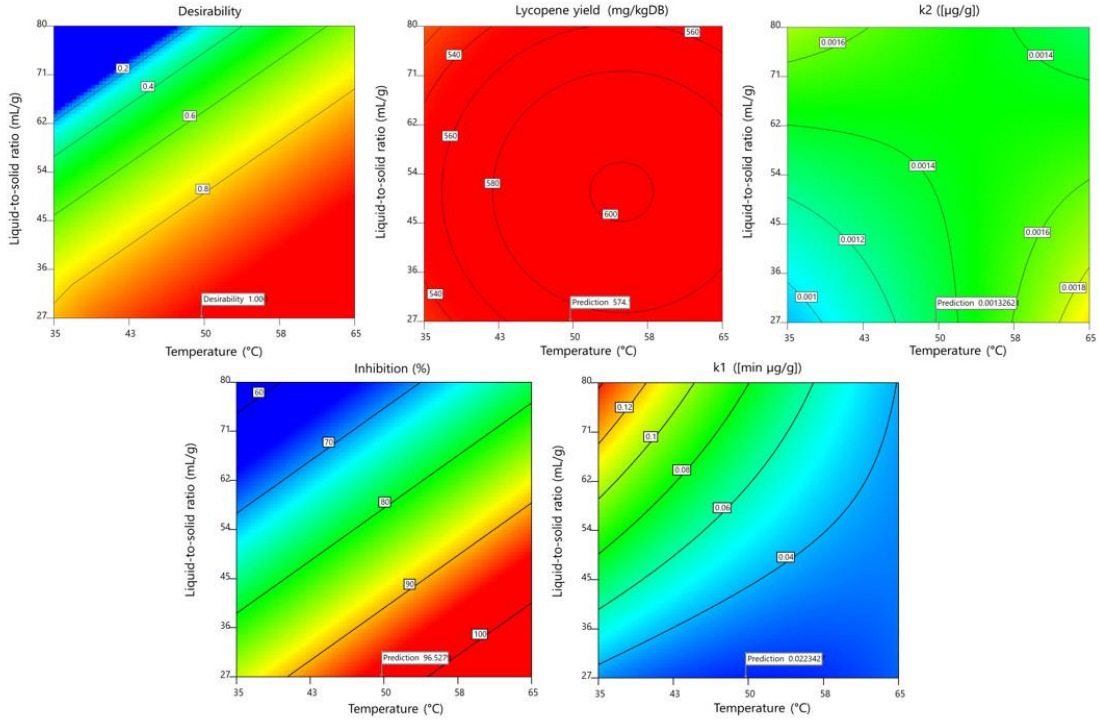

Figure 25. *Trans*-lycopene conditions.

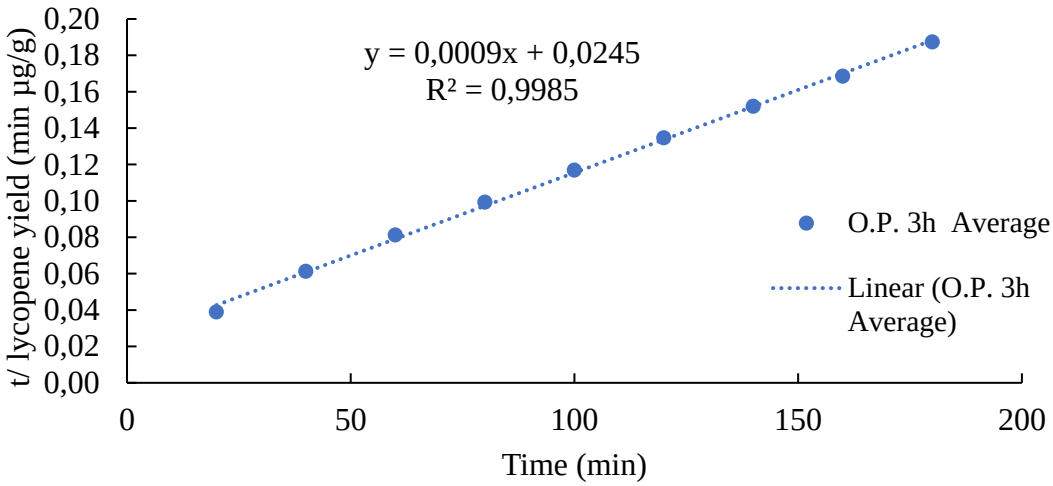

Figure 26. The calculation of parameters K_1 and K_2 of Peleg's model and fit the extraction kinetic model R^2.

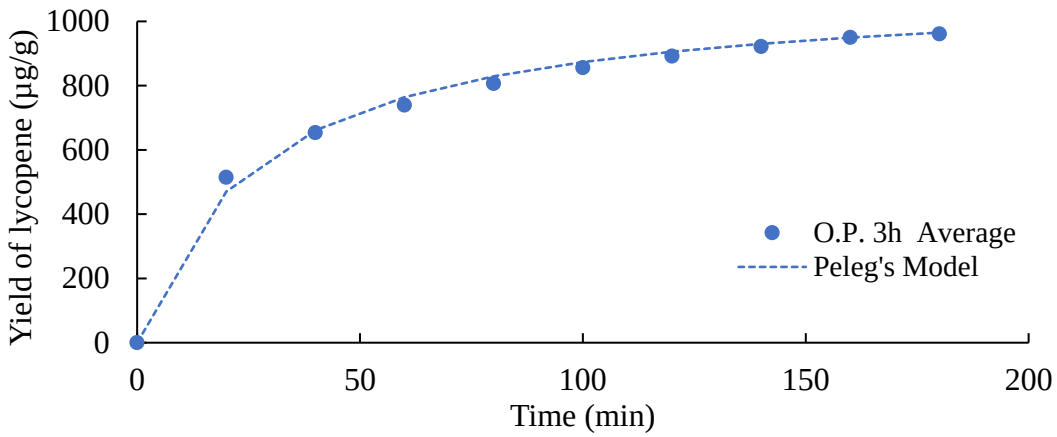

Figure 27. Extraction kinetics of lycopene at the best conditions for 3h fitted to the Peleg's model.

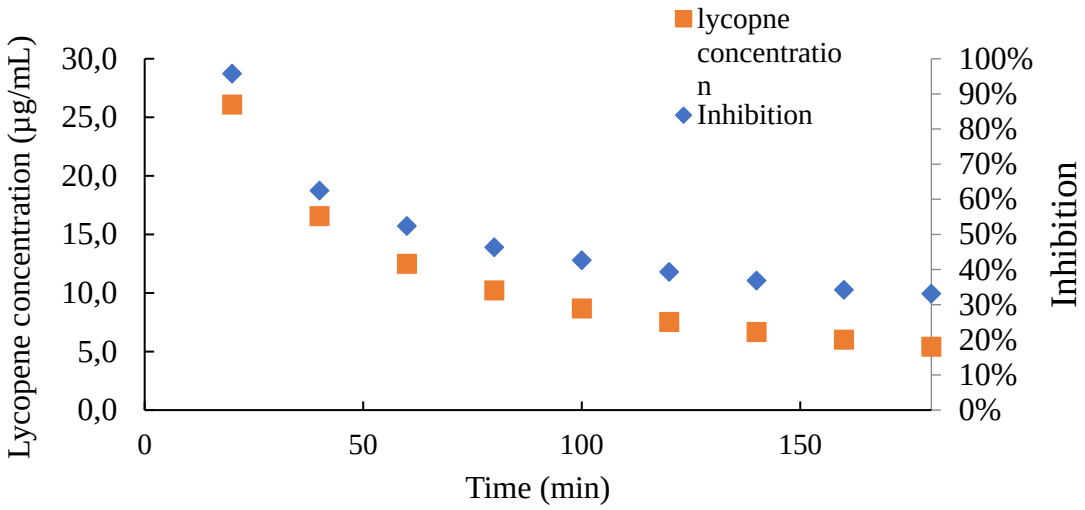

Figure 28. Relationship between inhibition and lycopene concentration under the best conditions for 3h.

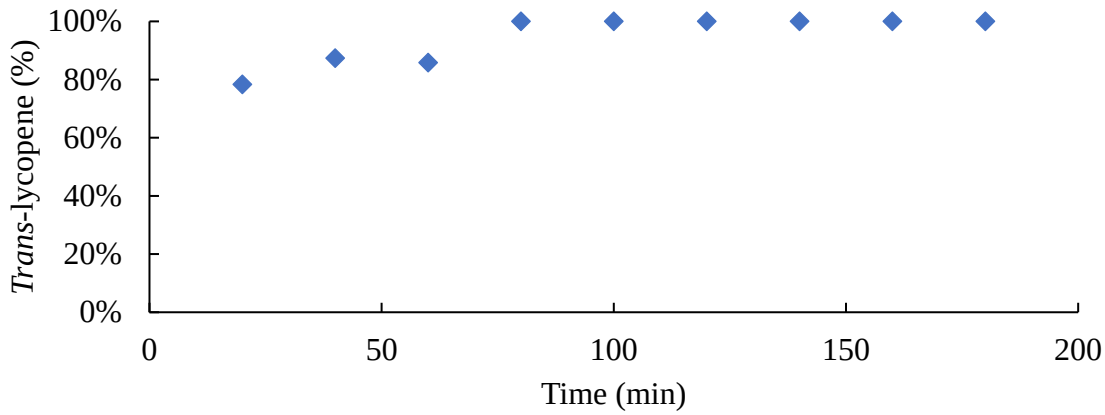

Figure 29. *Trans*-lycopene content and extraction time under the best conditions for 3h.

3.8.3.8 Color measurement

From Figure 30, it can be seen that the TW presents an evident discoloration after three hours of extraction. Visually the color changes from red to yellow. In addition, it can be clearly seen from Figure 30b that after 3 hours the pure ethanol passes the column from in to out, the color of the residue has varied. Furthermore, the color of the residue of the inlet of the extraction column is lighter than the color of the outlet. This phenomenon is consistent with the fact that the solvent enters pure from the column inlet and has the maximum capacity to absorb lycopene. As it passes through the column towards the exit, its ability to absorb lycopene decreases. So, the outlet is redder than the inlet of the column with a certain amount of lycopene remaining. The results of the color measurements, shown in Figures 31a, 31b and 31c, give a numerical value to the visual perception. In particular, Figure 31a reflects the progressive decrease of lightness; the Figure 31b shows an increase in the red component; Figure 31c a simultaneous decrease in the yellow component. In particular, Figure 31b indicates that more lycopene remained at the column outlet than at the column inlet.

a

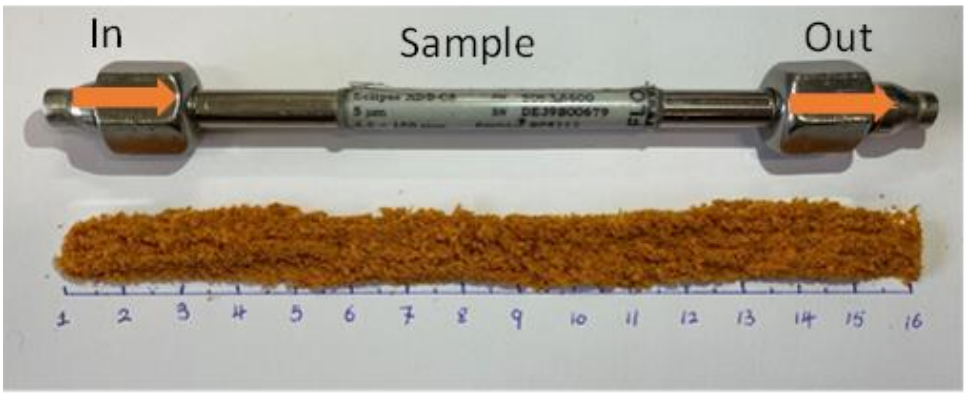

b

Figure 30. Tomato waste. a) without extraction, b) after 3 hours extraction with ethanol.

a

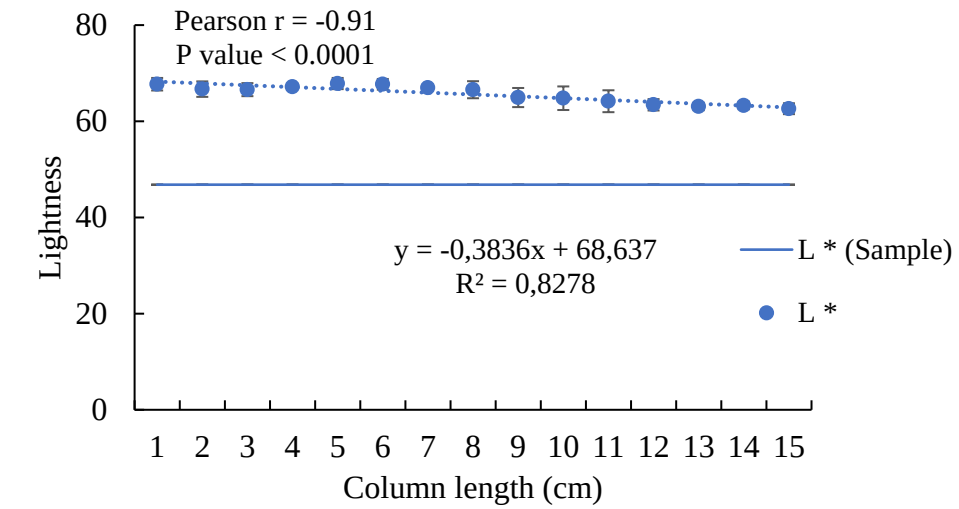

b

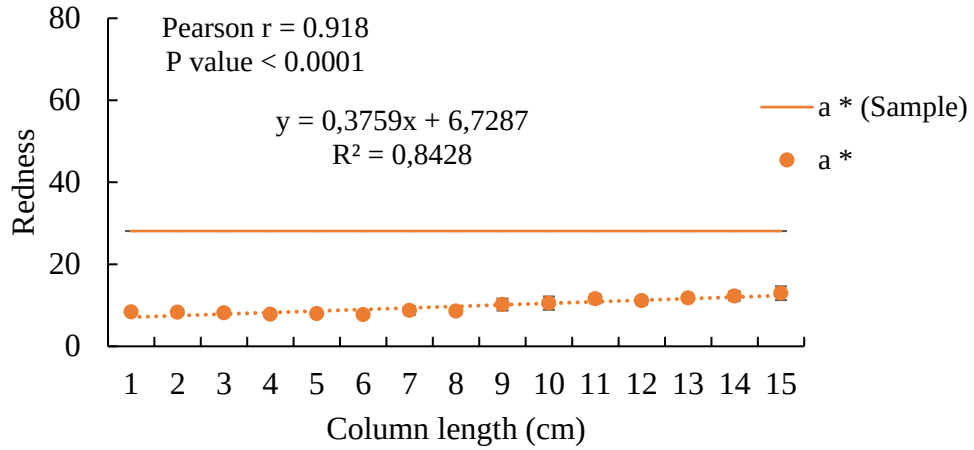

c

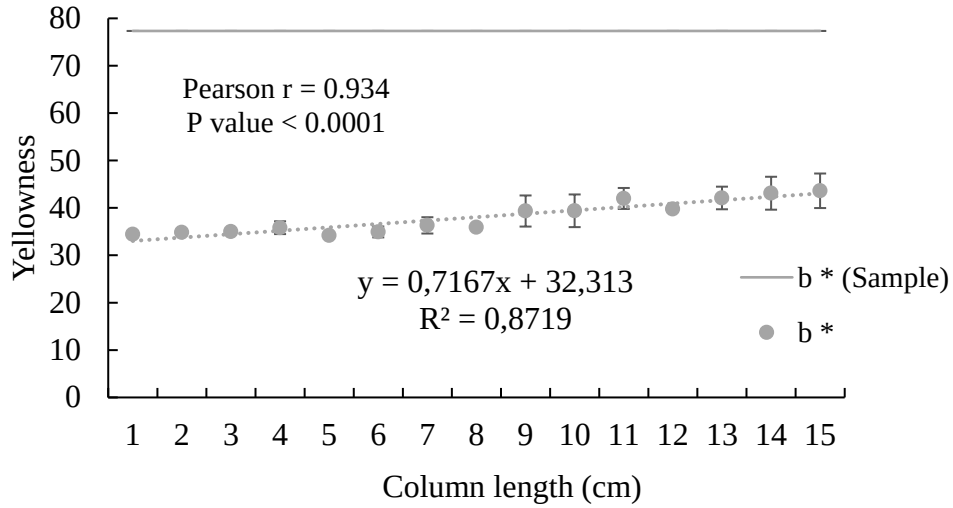

Figure 31. The lightness, redness and yellowness of TW before (a) and after extraction (b) (The X-axis is the solvent flow direction from 1 [in] to 15 [out]).

In order to fully prove that there is a correlation between the color of the extraction residue and the content of lycopene, it was performed a correlation analysis on the obtained data of the concentration of lycopene and the color of the extraction residue. As shown in Figure 32, the Pearson correlation coefficients indicated a negative correlation of lightness (r = -0.8844), and a positive correlation of redness (r = 0.8764) and yellowness (r = 0.8838) with lycopene concentration at a significant level of p < 0.0001. It can be considered that there is a strong linear correlation between the color of the extraction residue of the samples in this study and the concentration of lycopene. This linear correlation lays a theoretical foundation for judging the content of lycopene in the extraction residue through the determination of color in the future.

a

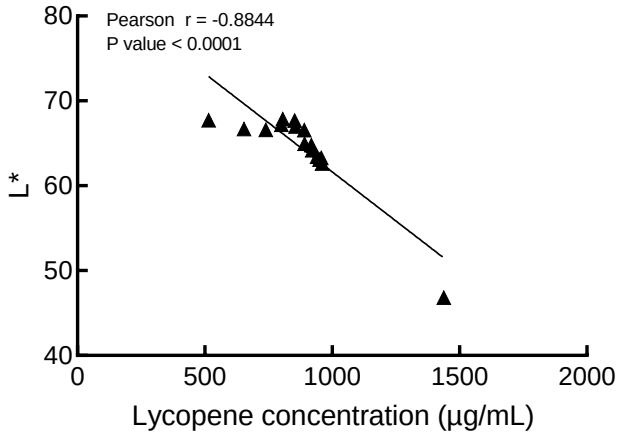

b

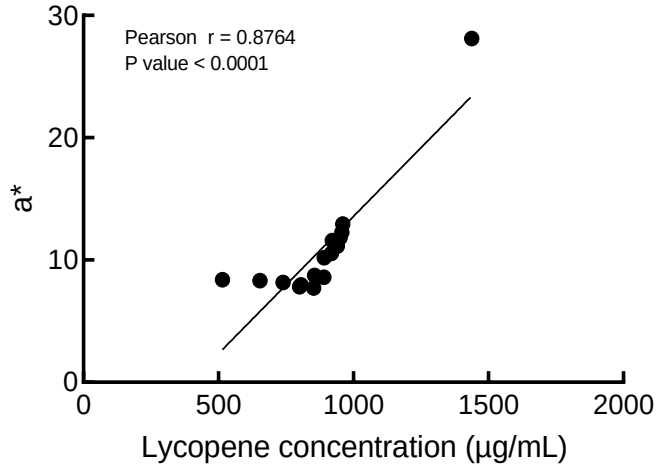

c

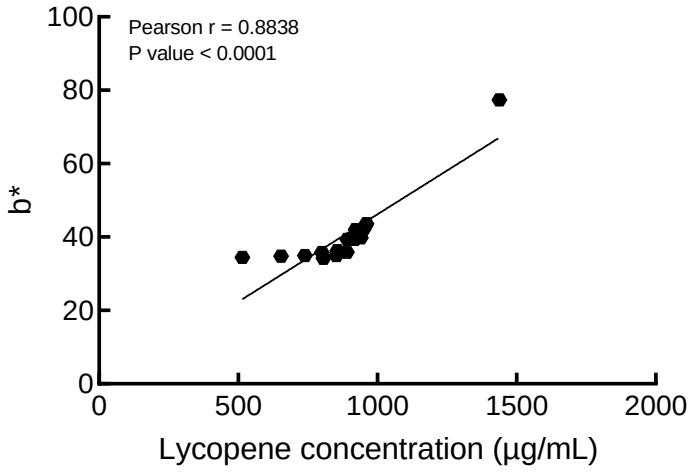

Figure 32. Association between color parameters and lycopene concentration. a) L* vs lycopene concentration, b) a* vs lycopene concentration, c) b* vs lycopene concentration.

3.8.4 Microwave-assisted subcritical extraction

3.8.4.1 Effect on lycopene yield of different solvents and times

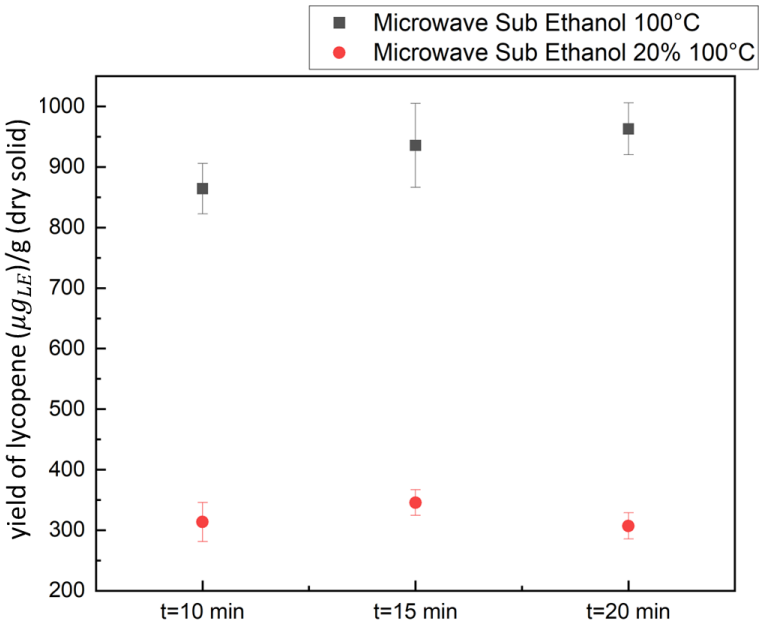

Figure 33. Yield of total lycopene by microwave-assisted extraction under pressure with two different solvents at different times by MASE.

Figure 33 shows the variation of lycopene yield as a function of time and solvent composition. Adding ethanol in the solvent composition can improve the extraction efficiency of lycopene. When the ethanol content was 20 %, the extraction efficiency of lycopene slightly increased with the increase of extraction time. The two extraction lines also show that the extraction rate of lycopene is higher for the mixture of water

and ethanol at 10 minutes than that of pure water as solvents (Figure 34). When the solvent is ethanol 20 %, the lycopene yield did not show a dependence on time in the investigated range.

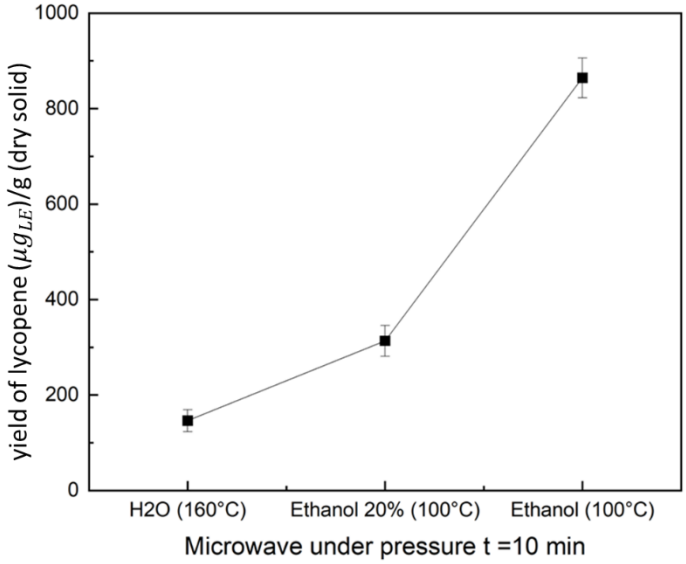

Figure 34. Yield of total lycopene by microwave-assisted extraction under pressure with three different solvents for 10 min by MASE.

Figure 34 shows that under the same conditions, when increase the percentage of ethanol the yield of lycopene also can be increased. The study is similar with the study of Shi et al. [232]. In Shi's study he has found that when the ethanol percentage increased from 5 % to 15 %, the extraction rate of lycopene increased from 37.7 to 55.8 μg/g (45 °C) and from 45.3 to 67.1 μg/g (75 °C). As can be seen from Figure 34, although increasing the proportion of ethanol can improve the extraction rate of lycopene, there is still a relatively large gap compared with pure ethanol. This is because lycopene is fat-soluble and extremely difficult to dissolve in water [241], and ethanol is an organic solvent. Therefore, the extraction yield of lycopene with ethanol as solvent is much greater than that of water as solvent. This is consistent with the results shown in Figure 34.

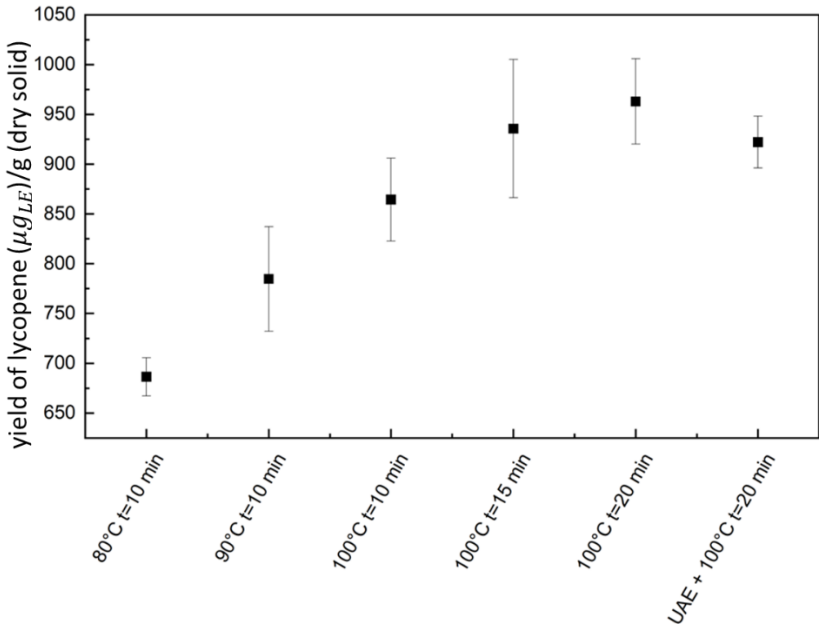

Figure 35. Yield of total lycopene by microwave-assisted extraction or combined with ultrasound-assisted extraction under pressure using ethanol as solvents at different temperature and times.

Figure 35 shows that increasing the temperature of the microwave reaction device can improve the extraction efficiency of lycopene at the same extraction conditions. At the same temperature, increasing the extraction time also increased the extraction efficiency of lycopene but the extraction rate decreased after reaching a certain time. There are many factors leading to this result. One of the factors may be that the combination of the two methods allows the concentration of lycopene to reach the maximum value quickly in a shorter time, while too long time at high temperature causes the degradation of lycopene or isomerization, which may be explained from the chromatogram (Figure 36).

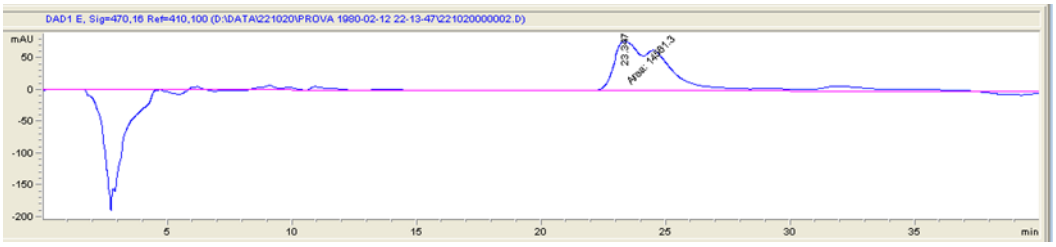

Figure 36. Chromatogram of MASE at condition of UAE + MASE (ethanol as solvent for 20 min) analysed by using HPLC Agilent 1100 series.

From the last point in the graph, it is clear that the combination of the two methods using ultrasound pretreatment followed by microwave-assisted sub critical extraction

did not result in a further increase of the extraction yield of lycopene. Considering the error, there is no obvious difference in the yield of lycopene obtained by using microwave-assisted subcritical ethanol extraction for 15 minutes and 20 minutes and using ultrasound-assisted pretreatment and then using microwave-assisted subcritical ethanol extraction for 20 minutes. This phenomenon may be explained by the fact that microwave-assisted subcritical ethanol extraction is a very efficient extraction method. When the extraction time reaches 15 minutes, the maximum extraction yield of lycopene has been obtained, so there is no appreciable difference in the results between the three.

3.8.4.2 *Trans*-lycopene and *cis*-lycopene content

An interesting phenomenon can be observed from the obtained experimental data, i.e., not all methods and conditions yielded *cis*-lycopene. This evidence was observed also when the SoLVE extraction method was used, where the presence of *cis*-lycopene was not detected under all conditions. As can be seen in Figure 37, the total lycopene obtained using microwave-assisted subcritical extraction with ethanol as the solvent contained about 70 % of *trans*-lycopene. The total lycopene obtained was all *trans*-lycopene when pure water and 20 % ethanol were used solvents, but the extraction efficiency was low. It can also be seen from Figure 38 that a higher proportion of trans-lycopene can be obtained when pure ethanol is used as the solvent.

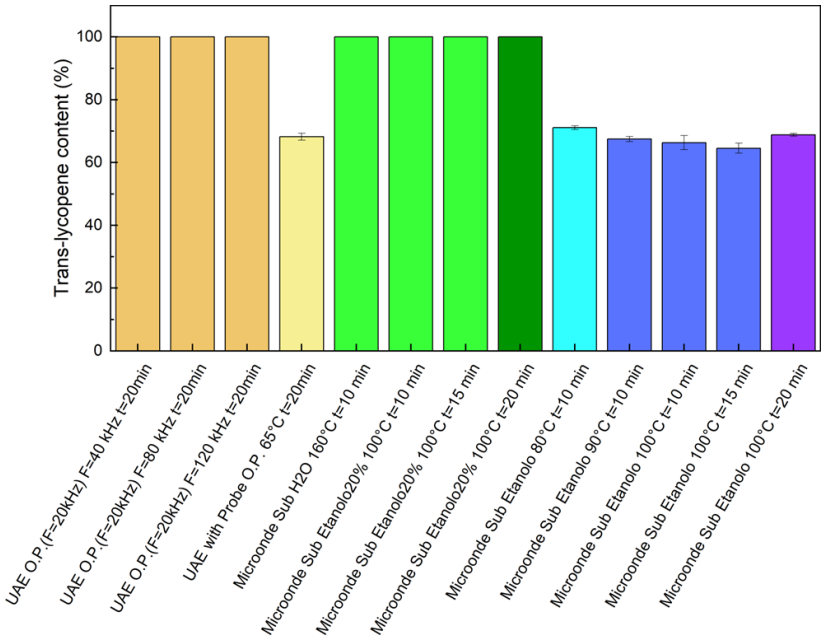

Figure 37. The content of *trans*-lycopene obtained under different extraction methods and conditions.

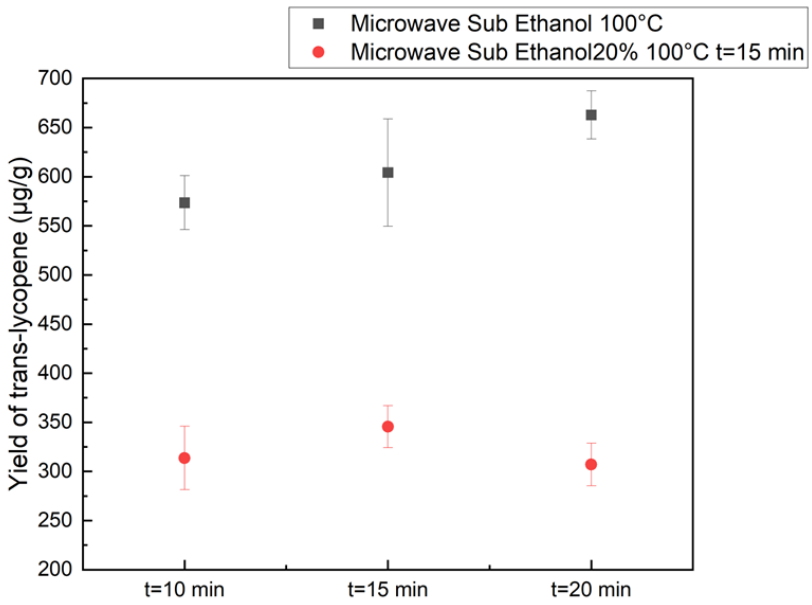

Figure 38. Yield of *trans*-lycopene by microwave-assisted extraction under pressure with two different solvents at different times.

From Figure 38, we can see that as the extraction temperature increases, the yield of *trans*-lycopene also increases. This result is consistent with the study of Ho et al [67]. Moreover, the yield of *trans*-lycopene increased with time. However, it can be clearly seen from Figure 39 that the *trans*-lycopene obtained after ultrasound pretreatment is reduced. This may be due to the degradation caused by ultrasound. There are many similar studies, such as, Xu and Pan's [209] study showed that the extraction rate increased dramatically in the first 30 minutes of ultrasound-assisted extraction. However, longer than 30 min will cause the degradation and isomerization of trans-lycopene, resulting in a decrease in lycopene yield. Zhang and Liu [66] also found similar results in their research. They reported that the optimal extraction time for ultrasonic extraction of lycopene from tomato paste was 29.1 min, but longer time will lead to oxidative decomposition of lycopene.

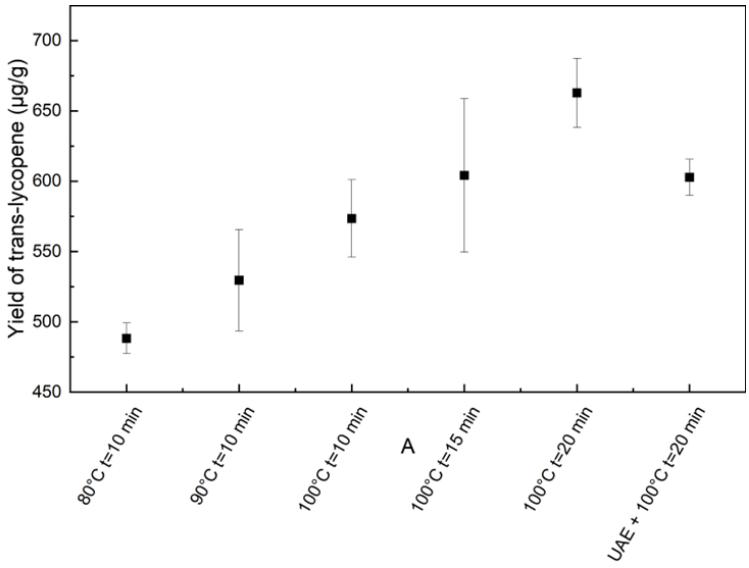

Figure 39. Yield of *trans*-lycopene by microwave-assisted extraction or combined with ultrasound-assisted extraction under pressure using ethanol as solvent at different temperatures and times.

3.8.4.3 Effect of biomass for different methods at different concentrations

An interesting phenomenon can be observed from the obtained experimental data, i.e., extract total solids. The extraction process destroys the epidermal tissue and causes the penetrate on of the solvent ethanol the epidermal tissue. Therefore, different methods and different operating processes have significantly different effects on the extract (Figure 40). Due to the of lycopene affinity towards non polar solvents, the choice of solvent is crucial for its extraction. However, any solvent does not dissolve only one active ingredient. As shown in Figure 38, when water is used as a solvent, the total active substances obtained are much larger than with other solvents. But there was very little of the target compound (lycopene) (Figure 40). The purpose of this experiment is to extract as much lycopene from TW as possible while extracting as little other active ingredients as possible. To minimize subsequent purification, separation and other steps to reduce energy and financial consumption. Among the several methods shown in Figure 40, microwave-assisted subcritical extraction best meets the objectives of this study.

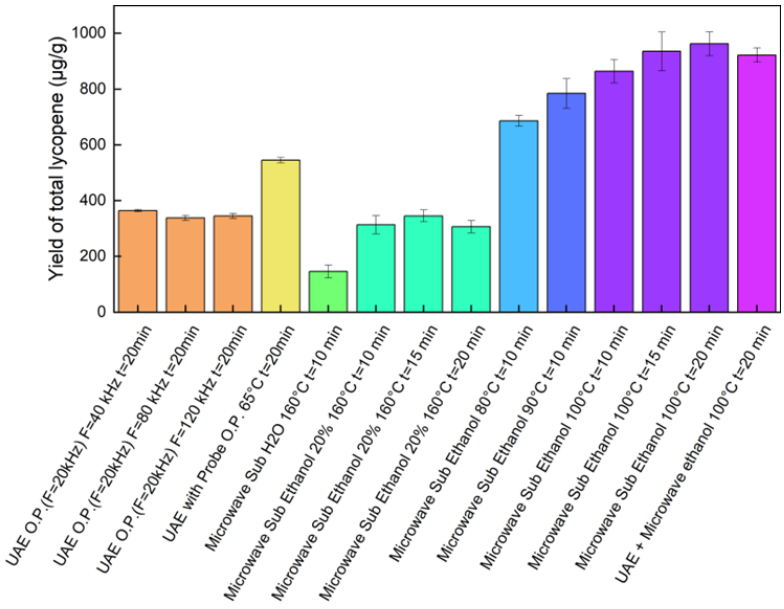

Figure 40. Yield of total lycopene by different methods of extraction and solvents at different temperatures and times.

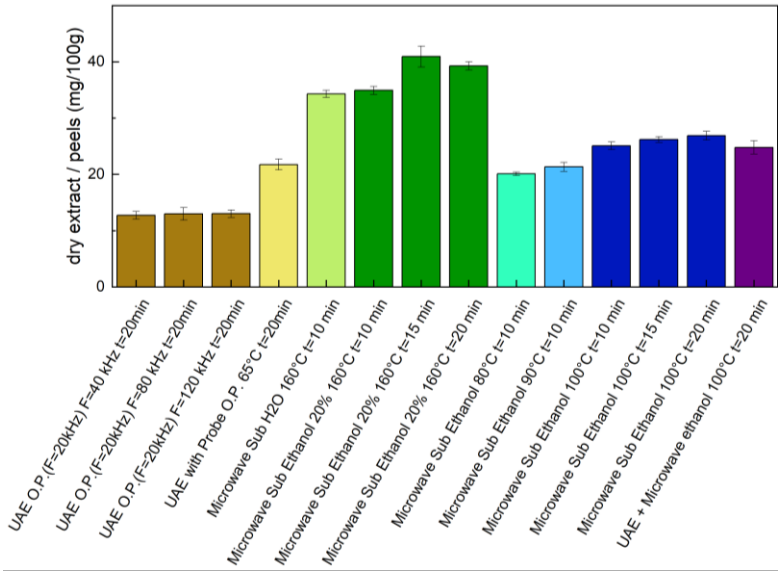

Figure 41. Dry extracts by different methods and solvents at different temperatures and times.

On the other hand, Table 15 shows the overall quality of each part of the biomass after the extraction process is completed. From the data in the table, it can be seen that the remaining tomato waste after the extraction process still accounts for a large part, about 75 %. Therefore, it is still of great significance to continue to study the remaining waste in future work. For example, in recent years, some scholars have used it to develop animal feed or produce green fuel through microbial fermentation [242].

Table 15. Overall mass balance of biomass after the extraction process of MASE at the best conditions (L/S = 72 mL/g, V =30 mL, T(beginning) = 25 °C, P(beginning) =15 bar, t(extraction) = 20 min t(pre-heat)= 5 min, Stirrer = 80 %).

Tomato waste [g]	Biomass extracted [g]	Tomato waste remaining [g]
0.416	0.1083	0.3085

3.9 Conclusion

In this chapter, an experimental study on the recovery of bioactive compounds using tomato peels and seeds from tomato processing was undertaken. The recovery and reintegration of carotenoids in food products in the form of additives fits the strategy for sustainability and the circular economy. The first extraction technique used was SLE. In solid-liquid extraction sunflower oil was used as solvents, extraction temperature, liquid-to-solid ratio and extraction time were evaluated separately. The maximum extraction of lycopene of 1237.32 ± 4.80 μg $_{\text{lycopene equivalent}}$/g (dry solid) was finally obtained as well as the optimum process conditions: T = 45 °C, L/S = 20/3 mL/g, t = 45 min, and stir = 900 rpm. In the second extraction technique, the response surface modelling and desirability methods were applied to evaluate the effect of the operating conditions of ultrasound-assisted extraction using ethanol as solvent. The results showed that in UAE the operating conditions are strongly interconnected, and the dependence of extraction performances from the process variables are more complex when all the process variables are evaluated simultaneously. Optimization was carried out by maximizing lycopene yield, total carotenoids, antiradical power of the extract. The results of the optimization showed that high temperature, amplitude, liquid-to-solid ratio, system volume, short time and on/off pulsed ratio provide a high lycopene recovery of 1536 ± 53 μg/g. Under these conditions, a good desirability value was obtained, which simultaneously maximized all the response variables selected and the optimization constraints. The results of the Pearson correlation coefficient indicated a strong positive correlation ($p < 0.001$) between lycopene yields quantified by UV-vis and HPLC methods, suggesting the operability of both methods.

The following step of the study evaluated the solid-liquid multivariable extractor. This method is a nearly fully automated continuous extractor and was proposed as a novel technique that enables the use and evaluation of several simultaneous process

parameters such as ultrasonic frequency, temperature, pressure, and flow rate, for lycopene and antioxidant extraction from TW. At the same time, the total lycopene yield was evaluated using almost the same experimental conditions as in UAE, with the aim of comparing the results of the two experiments in the same pair. In addition, the extraction process of SoLVE was analyzed for extraction kinetics. Results showed that, the experimental data are well described by the Peleg's model (R^2 is in the range 0.8293 - 0.9991). The yield of lycopene was in the range 92.5 - 546.7 µg/g. The results presented in this study with SoLVE ware satisfying, so the method can be considered an improvement and innovation in the field of non-conventional extraction methods. It should also be noted that different lycopene recoveries depended on the extraction method and type of raw material.

Finally, the extraction by MASE was studied. The same solid-liquid ratio as that of the ultrasound-assisted extraction method was used for the evaluation of the extraction temperature, time and solvent effects on lycopene yield. The results showed that when using ethanol as solvent and at 100 °C for 15 min, the total lycopene content was 962.97 ± 42.87 µg/g (dry solid) a little lower than using UAE.

Combining all the factors and selecting the best extraction method from a large number of methods is a scientific and rigorous process, which can be synthesized through the DECISION MATRIX. While selecting the lycopene extraction methods, one has to review all the relevant influential parameters such as choice of raw material, percentage recovery of lycopene, amount of impurities getting dissolved into the solution, cost of processes, toxic properties of the extraction solvents, amount of raw materials to be processed, extraction temperature, extraction time, liquid-to-solid ratio, particle size, capital and operating costs etc. in order to maximize the extraction efficiency. It can be concluded from the references that some of the parameters discussed in this paper are conflicting with each other in optimizing the extraction process. The optimization process of lycopene extraction becomes complex due to the ambiguity and conflicting nature of all the above-mentioned attributes. For this complex process, techniques such as multi-attribute decision making (MADM) can be used to select the relevant attributes from the available options. Thus, a team of experts can rate the attributes relevant to a typical application and then use the TOPSIS (Techniques for Ranking by Similarity to Ideal Solutions) evaluation method to rank

the selected attributes according to priority. In this way, the most appropriate candidate solution can be selected to maximize lycopene recovery and minimize operating costs. Below is a list (Table 16) of some of the possible attributes that are generally relevant to the lycopene extraction process. The MADM can use this list to help identify the core attributes that are relevant to the particular application under consideration. It is important to note, however, that the list is not exhaustive, and the user may call upon additional attributes depending on their application.

Table 16. Decision Matrix for select the best method of lycopene extraction.

Criteria	**Weight**	**SLE**		**UAE**		**SoLVE**		**MASE**	
		Score	Total	Score	Total	Score	Total	Score	Total
Extraction temperature	**5**	2	10	1	5	2	10	1	5
Extraction time	**4**	1	4	3	12	3	12	3	12
Solvents	**3**	1	3	3	9	3	9	3	9
Solid-to-liquid ratio	**2**	3	6	3	6	3	6	3	6
Yield of lycopene	**5**	2	10	3	15	3	15	2	10
Ease of implementation	**3**	3	9	2	6	2	6	1	3
Ease of scale up and operation	**3**	3	9	3	9	3	9	2	6
Energy consumption	**3**	2	6	2	6	2	6	3	9
Cost of the process	**4**	3	12	2	8	2	8	1	4
Environmental concerns	**3**	1	3	2	6	2	6	2	6
Total			72		82		87		70

Note: The weights are categorized on a scale of 1-5, according to the importance of the parameters for the process. For temperature greater than 60 °C score 1, less than 30 °C score 3; for time greater than 60 minutes score 1, less than 30 minutes score 3; for solvents toxic score 1, clean and renewable score 3; for solid-liquid ratio less than 10 score 1, greater than 30 score 3; for lycopene yield less than 800 score 1, greater than 1200 score 3; for ease of implementation, ease of scale up and operation and cost of the process and energy consumption the more equipment and conditions needed the lower the score; for environmental concerns the more toxic the reagents used the more toxic the reagents used, the lower the score.

Since the object extracted in this experiment was lycopene, whose stability is very sensitive to temperature, the extraction temperature and lycopene yield accounted for a considerable amount of weight, followed by extraction time and cost loss, among others. Comprehensive Table 14 for each extraction time, extraction temperature, solvent type, solid-liquid ratio, lycopene extraction efficiency, operation and can scale up the ease of operation, energy consumption and cost, environmental factors and other aspects of the comprehensive scoring results learned that, among the several extraction methods involved in this study, the SoLVE showed a greater advantage. In terms of extraction efficiency, the difference between UAE and SoLVE is not significant, but SoLVE integrates more operational parameters and can achieve almost continuous extraction without additional improvements. The extraction solution uses ethanol, which is a relatively environmentally friendly solvent that reduces the pollution of harmful gases to the environment. Therefore, SoLVE is the best extraction method in this experiment.

Parts of this section were already published in ***"A Comprehensive Optimization of Ultrasound-Assisted Extraction for Lycopene Recovery from Tomato Waste and Encapsulation by Spray Drying" by Junyang Li,*** *Margherita Pettinato, Alessandro Alberto Casazza, Patrizia Perego.* ***Processes 10.2 (2022): 308.*** *doi.org/10.3390/pr10020308****,*** *and partially presented as "Ultrasound-assisted Extraction of Lycopene from Industrial Tomato Waste", in the international congress "6th Green and Sustainable Chemistry Conference - GREEN2020", online, as poster presentation.*

4 ENCAPSULATION OF BIOACTIVE EXTRACTED FROM TW

ABSTRACT

The main purpose of this section is to study the encapsulation of lycopene-rich extracts using different embedding methods. In fact, many middle embedding techniques have been developed in recent years such as: solvent evaporation, emulsion polymerization, layer-by-layer deposition, liposomes, oil-in-water emulsions, water-in-oil emulsions, vacuum freeze drying, and spray drying. The first major challenge in this part concerned to improve the encapsulation rate of lycopene in oil-in-water nanoemulsions and use appropriate emulsifiers and low-energy consumption preparation processes to maintain long-term stability of the nanoemulsions. Therefore, the stability of the oil-in-water nanoemulsion part at different storage temperatures and the degradation of lycopene were evaluated to verify whether this method can be used as an effective technique to protect lycopene. Based on the conclusions obtained, the optimal operating process conditions for homogeneous emulsification were determined. Another challenge in this chapter was related to the influence of oil on the process during spray drying and drying the nanoemulsions with different coating agents under different conditions by supercritical assisted atomization (SAA). When the drying object is an aqueous solution or organic solvent mixture, it is relatively easy to find the best process due to its volatile characteristics. On the contrary, when the drying object is an oil-in-water nanoemulsion, wall-hanging or coking reactions are prone to occur due to the presence of oil. Therefore, this chapter studies the impact of different coating agents on the process and uses electron microscopy to characterize the surface and particle size of the resulting particles, and ultimately determines the optimal coating agent and process operating conditions.

4.1 Encapsulation by Oil-in-water nanoemulsions methods

4.1.1 Apparatus, Chemicals, Standards and Solvents

4.1.1.1 Chemical and sample preparation

2,2'-azino-bis (3-ethylbenzothiazoline-6-sulphonic acid) diammonium salt (Sigma Aldrich, Milan, Italy); pectin citrus (Thermo scientific, United States); gum arabic (Carlo Erba, France); inulin (Thermo scientific, China); polyvinylpyrrolidone (Sigma Aldrich, China); maltodextrin (Sigma Aldrich, USA); whey from bovine milk (Sigma Aldrich USA); potassium persulfate, iso-propanol, acetonitrile, methanol (Carlo Erba, Cornaredo, Italy), isopropyl tetradecanoate, 98% (Alfa Aesar, Germany); Pluronic F-127 (Sigma Aldrich, USA); all-*trans*-lycopene and standards (Sigma Aldrich, Milan, Italy) employed in this study were of analytical grade and used without further purification. The water was obtained with a Milli-Q system (Merck, Darmstadt, Germany). Tomato peels and seeds were kindly provided by a producer of tomato sauce in northern Italy. The TW was stored at -20 °C for characterization of biomass, and partially dried at 60 °C up to constant weight for extraction experiments.

4.1.1.2 Apparatus

The complete layout of the process proposed in this work is schematized in Figure 42. As shown in this figure, the extraction technology used in this study was ultrasound-assisted technology. The extract obtained was then mixed with the oil phase for the preparation of the emulsion by the ultrasound-assisted technique and then oil-in-water nanoemulsion was prepared by a high-speed rotor stator mixed. The nanoemulsions, to which the coating agent was added, were then dried by spray drying technology to eliminate the inconvenience of storing and transporting the liquid nanoemulsions. Furthermore, in the final stage of this study the verification of the possibility of reconverting the powder obtained by spray-drying into the originary nanoemulsions was studied.

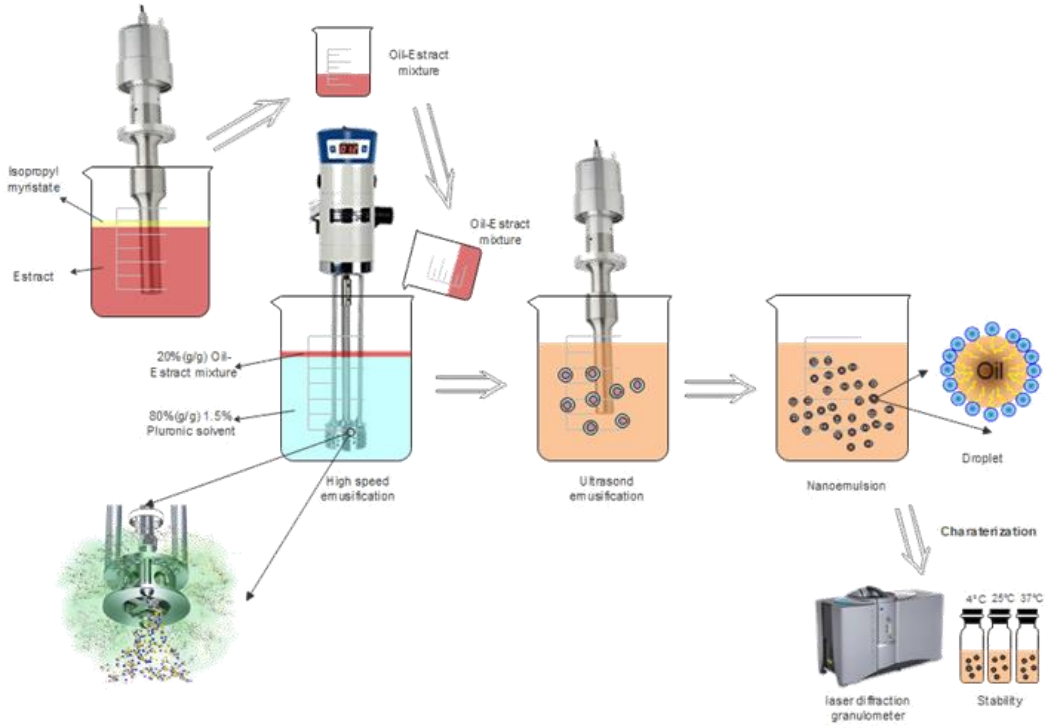

Figure 42. Nanoemulsion production process flow chart and some details are displayed.

4.1.2 Preparation of aqueous phase and O/W emulsion

4.1.2.1 Emulsification of Alcohol Extracts

For the preparation of the emulsion, isopropyl myristate was used as oil phase, whereas the water phase was prepared dissolving Pluronic at concentration of 1.5 % (w/w). The ratio between the water and the oil phase was varied between 10/90 (w/w) and 20/80 (w/w). Briefly, a known amount of isopropyl myristate was mixed with a fixed amount of lycopene enriched extract were using an ultrasonic probe (Sonicator Vibra cell 75115, 750 W, Bioblock Scientific Co., Strasbourg, France) at 40 % amplitude, on/off = 30/30 s/s for 1 min. Then 90 g of Pluronic solution was stabilized at 7000 rpm for 1 min using Silverson L5M-A rotor-stator type emulsifier (Silverson Machines Ltd, Chesham, England). Then the mixed oil/extract phase was slowly added to the water phase and emulsified for 9 min. Empty emulsions were produced using ethanol in place of the extract.

4.1.2.2 Emulsification of Oil Extracts

For the preparation of the emulsion, isopropyl myristate was used as oil phase, whereas the water phase was prepared dissolving Pluronic at concentration of 1.5 % (w/w). The ratio between the water and the oil phase was varied between 10/90 (w/w) and 20/80 (w/w). Briefly, 80 or 90 g of Pluronic solution (1.5 %) was stabilized at 8000 rpm for 1 min using Silverson L5M-A rotor-stator type emulsifier (Silverson Machines Ltd, Chesham, England). Then a known amount of lycopene enriched extracts phase was slowly added to the water phase and emulsified for 9 min. Empty emulsions were produced using sunflower seed oil in place of the extract.

The emulsions obtained were then ultrasonicated at 70 % amplitude with probe for 5 min (on/off = 30/30 s/s). At the end of the process emulsions were analyzed for DSD again. All the process was conducted in ice bath. Emulsions were also characterized using optical microscope (Nikon, ECLIPSE LV 100D, Japan) with a 50-fold mirror. The images were collected using a microscopic camera (Delta Pix, Invenio 6EIII S/N. 26656, Denmark) with an interface (Delta Pix, inSight 6.4).

4.1.3 Analytical methods

4.1.3.1 Droplet size distribution

The produced emulsions were analyzed using Malvern Mastersizer-3000 (Malvern Instruments Ltd., Malvern, UK) for droplet size distribution (DSD) using the methods described by [243] with slight modifications. The emulsions were dispersed in deionized water up to at laser obscuration between 10 % and 12 % using a speed of circulating pump of 1800 rpm. The refractive index and absorption of aqueous phase used were 1.344 (measured by Abbe refractometer) and 0.1 respectively; droplet size data are presented as volume fraction.

The Sauter mean diameter ($d_{3,2}$) was calculated using the Equation (34) and used to represent the droplet size [244].

$$d_{3,2} = \frac{\sum(n_i \cdot d_i^3)}{\sum(n_i \cdot d_i^2)'} \qquad (34)$$

Where n_i is the number of droplets with the size of d_i.

The uniformity, a measure of the absolute deviation from the median, was calculated using the Equation (35) and used to represent symmetry of droplet size distribution.

$$Uniformity = \frac{\sum X_i |d_{(x,o.5)} - d_i|}{d_{(x,0.5)} \sum X_i'} \qquad (35)$$

Where $d_{(x,o.5)}$ is the size of droplet below 50 % of the samples and X_i is the volume of the number of droplets with diameter existing between the two consecutive diameters [245].

4.1.3.2 Lycopene content

Total lycopene amount and free lycopene in nanoemulsions were determined using the procedure adapted from Zhao et al [133]. For total lycopene amount 1 mL of emulsions were dissolved in 4 mL of acetone, vortexed for 1 min to release the lycopene from the oil phase. The emulsions without lycopene were used as a control. The absorbance of the total lycopene amount was measured using a UV-vis spectrophotometer (Lambda 25, PerkinElmer, Wellesley, MA, USA), at 470 nm using a calibration curve, the procedure was adapted from Zhao et al [133]. For free lycopene content 5 mL of emulsions were dissolved in 5 mL of *n*-hexane, shacked for one min, then left for 30 mins to allow solvent separation. After this time the organic liquid separated on top was taken and centrifuged at 5000 rpm for 10 min to obtain the *n*-hexane phase. This operation was repeated twice. The absorbance of the free lycopene amount in n-hexane was measured using UV-vis spectrophotometer essay at 470 nm using a calibration curve, the procedure was adapted from Zhao et al [133].

The encapsulation rate was obtained by the following Equation (36).

$$Encapsulation\ rate\ (\%) = \frac{m_{total} - m_{free}}{m_{initial}} \times 100 \qquad (36)$$

Where m_{total} is the total amount of lycopene in the nanoemulsions, m_{free} is the free lycopene in the nanoemulsions, and $m_{initial}$ the initial amount of lycopene contained in the extract loaded to the nanoemulsions.

4.1.3.3 Stability test

Also, stability tests were performed. Stability studies on empty and loaded lycopene enriched extract nanoemulsions were performed by keeping the sample at 4 °C, 25 °C, and 37 °C. These studies were performed for periods of 1 and 3 months. The DSDs were determined by Malvern Mastersizer-3000 every week. For the chemical stability, the total lycopene content of the samples stored at the different temperatures was determined every week according to the method described in the paragraph **4.1.3.2**.

4.1.3.4 Emulsions total and free lycopene content in nanoemulsions

- **Total lycopene amount in nanoemulsions**

Emulsions (1 mL) were dissolved in 4 mL of acetone, vortexed for 1 min to release the lycopene from the oil phase. The emulsions without lycopene were used as a control. The absorbance of the total lycopene amount was measured using a UV-vis spectrophotometer (Lambda 25, PerkinElmer, Wellesley, MA, USA), at 470 nm using a calibration curve, the procedure was adapted from Zhao et al [246].

- **Free lycopene content**

Emulsions (5 mL) were dissolved in 5 mL of *n*-hexane, shacked for 1min, then stand still for 30 mins, then the organic liquid separated on top was taken and centrifuged at 5000 rpm for 10 min to obtain the *n*-hexane phase. This operation was repeated twice. The absorbance of the free lycopene amount in *n*-hexane was measured using UV-vis spectrophotometer essay at 470 nm using a calibration curve, the procedure was adapted from Zhao et al [246].

4.1.3.5 Lycopene encapsulation rate in nanoemulsions

The encapsulation rate was obtained by the following Equation (37).

$$Encapsulation\ rate\ (\%) = \frac{m_{total} - m_{free}}{m_{initial}} \times 100 \qquad (37)$$

Where m_{total} is the total amount of lycopene in the nanoemulsions, m_{free} is the free lycopene in the nanoemulsions, and $m_{initial}$ the initial amount of lycopene contained in the extract loaded to the nanoemulsions.

4.1.4 Statistical analysis

All experiments were repeated at least three times unless otherwise stated. All data were given as mean ± standard deviation. The statistical analysis was performed using Origin Pro. 8.5 (Origin Lab Co., USA) followed by one-way ANOVA with Tukey test at $p < 0.05$ significance level.

4.1.5 Results and discussion

4.1.5.1 Emulsion production with ethanol

Empty and loaded nanoemulsions were produced using the high-speed rotor stator mixed and ultrasonication. The lycopene extract obtained by UAE (T = 65 °C, t = 20 min, L/S = 72 mL/g, *A* = 65 %, *on*/*off* = 33/30 s/s, V = 90 mL) with interesting properties (total carotenoids of 1408 ± 14 µg $_{\text{lycopene equivalents}}$/g, lycopene yield of 1536 ± 53 µg/g, 36.1 ± 0.9 µg $_{\text{Trolox equivalents}}$ /g as antiradical power, was used and loading was varied between 1 and 14 g. Emulsions were produced at O/W ratio of 10/90 and 20/80. Also, empty emulsions were produced for comparison purpose, in this case pure ethanol was added to the oil phase in the same quantity used for the extract loaded emulsions. Table 13 reports the experimental test conducted and the results in terms of diameter of droplet of nanoemulsions. From Table 13 it is possible to observe that empty emulsions were characterized by mean diameters between 410 and 596 nm, whereas loaded emulsions were characterized by mean diameters between 259 and 632 nm. In all the conditions tested stable nanoemulsions were formed.

Figure 40a shows the macroscopic aspect of nanoemulsions. It can be seen that the nanoemulsion with the addition of lycopene extract was characterized by a noticeable change in color. Optical microscopy measurements indicated that there were small differences in the microstructure of the emulsions loaded with lycopene ascribable to an increase in droplets size (Figure 43b and 43c).

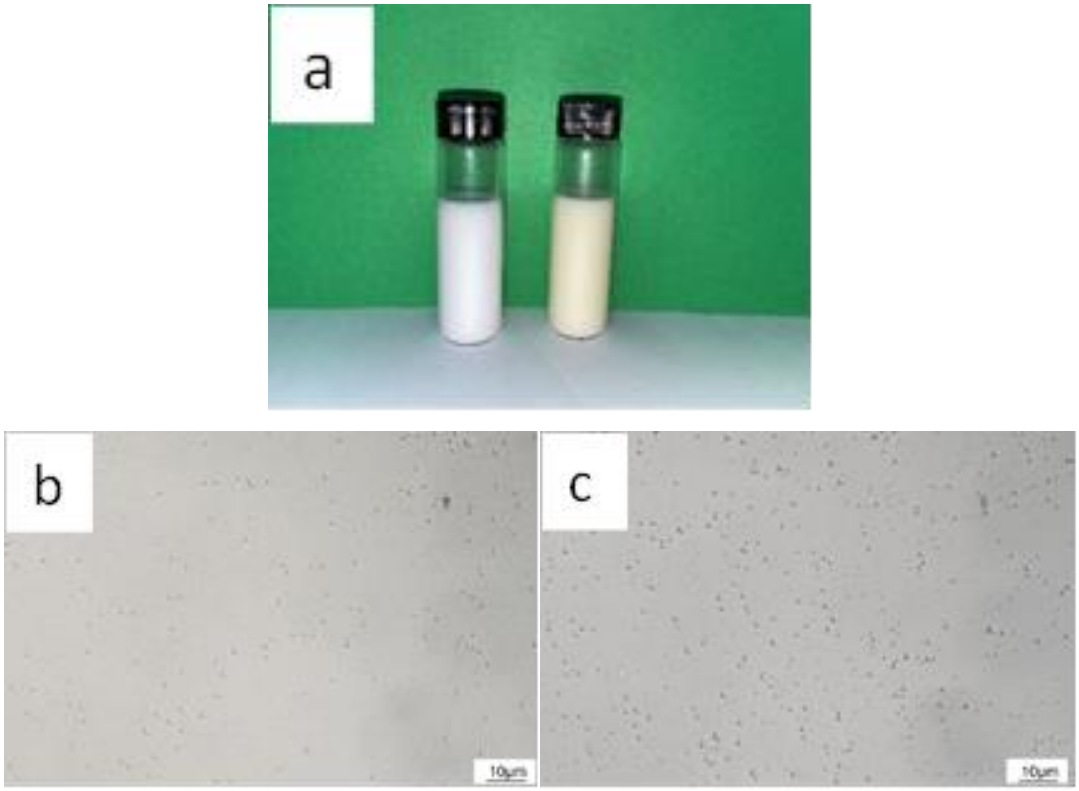

Figure 43. Macro/micro-level photo of empty and loaded nanoemulsions. (a) the empty nanoemulsion (on the left) and the loaded nanoemulsion lycopene enriched extract (on the right); (b) and (c) optical microscope images of empty and loaded nanoemulsions.

Diameters of droplets of different empty and lycopene-loaded nanoemulsion were presented in Table 17 and Figure 44. Physical stability of all the empty emulsions produced was evaluated measuring the PSD and mean diameter of the droplets after storage at 4 °C, 25 °C, 37 °C and at fixed time interval from 0 to 90 days (three months of observation). Data are reported graphically in Figure 44.

Table 17. Emulsions production conditions and results in terms of granulometric data. (-) None or not measured.

Sample	Ethanol [g]	O/W [w/w]	D[3,2] [nm]	Uniformity	Sample	Extract [g]	O/W [w/w]	D[3,2] [w/w]	Uniformity	Total lycopene content theoretical [µg/mL]	Total lycopene content real [µg/mL]	Lycopene encapsulation rate [%]
E_0	0	10/90	410	0.477	L_0	0	10/90	410	0.477	(-)	(-)	(-)
E_1	1	10/90	312	0.353	L_1	1	10/90	345	0.741	7.10	0.68 ± 0.12	89%
E_2	3	10/90	327	0.353	L_2	3	10/90	303	0.57	21.30	2.14 ± 0.25	95%
E_3	5	10/90	413	0.645	L_3	5	10/90	331	0.334	35.49	3.3 ± 0.06	97%
E_4	0	20/80	489	0.432	L_4	0	20/80	489	0.432	(-)	(-)	(-)
E_5	10	20/80	323	0.487	L_5	10	20/80	272	0.615	70.99	6.5 ± 0.15	98%
E_6	14	20/80	306	0.717	L_6	14	20/80	259	0.37	99.38	9.6 ± 0.20	99%

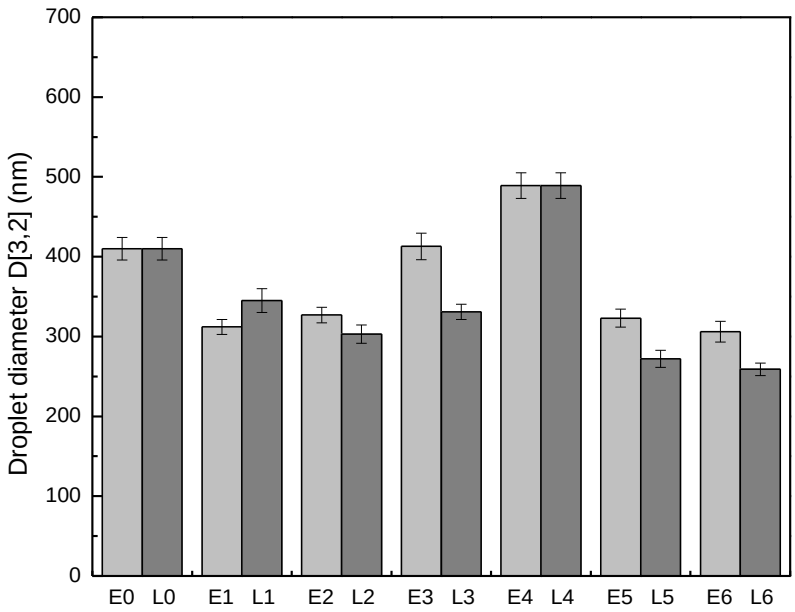

Figure 44. Droplet diameter of empty and loaded nanoemulsions at different conditions.

Figure 44 shows the results in terms of mean diameters of the different nanoemulsions produced comparing the empty and the loaded emulsions at the same process conditions. It can be seen that for the simple O/W emulsions both at 10/90 ratio (sample E0 and L0) and at 20/80 ratio (sample E4 and L4) the droplets mean diameter is larger than that of the nanoemulsion loaded with ethanol or lycopene enriched extract. This result is consistent with the findings of Ferreira et al. [247], who observed that a certain level of ethanol can decrease the size of the nanoemulsion droplets, i.e. ethanol can act as a co-emulsifier. It is also known that the O/W ratio could have an effect on the nanoemulsion droplet diameter, indeed, observing the results obtained for the simple O/W emulsions (sample E0, L0 and sample E4 and L4) it can be observed that the droplet mean diameter was slightly smaller at O/W 10/90 (w/w) than at O/W 20/80 (w/w). Looking at data of empty and loaded emulsions another it is possible to observe that loaded emulsions showed smaller diameters if compared to empty emulsions produced under the same conditions. The addition of the extract did not alterate the stability of the emulsions produced. This demonstrates the feasibility of using the oil-in-water nanoemulsion technique for lycopene enriched extract containment and protection.

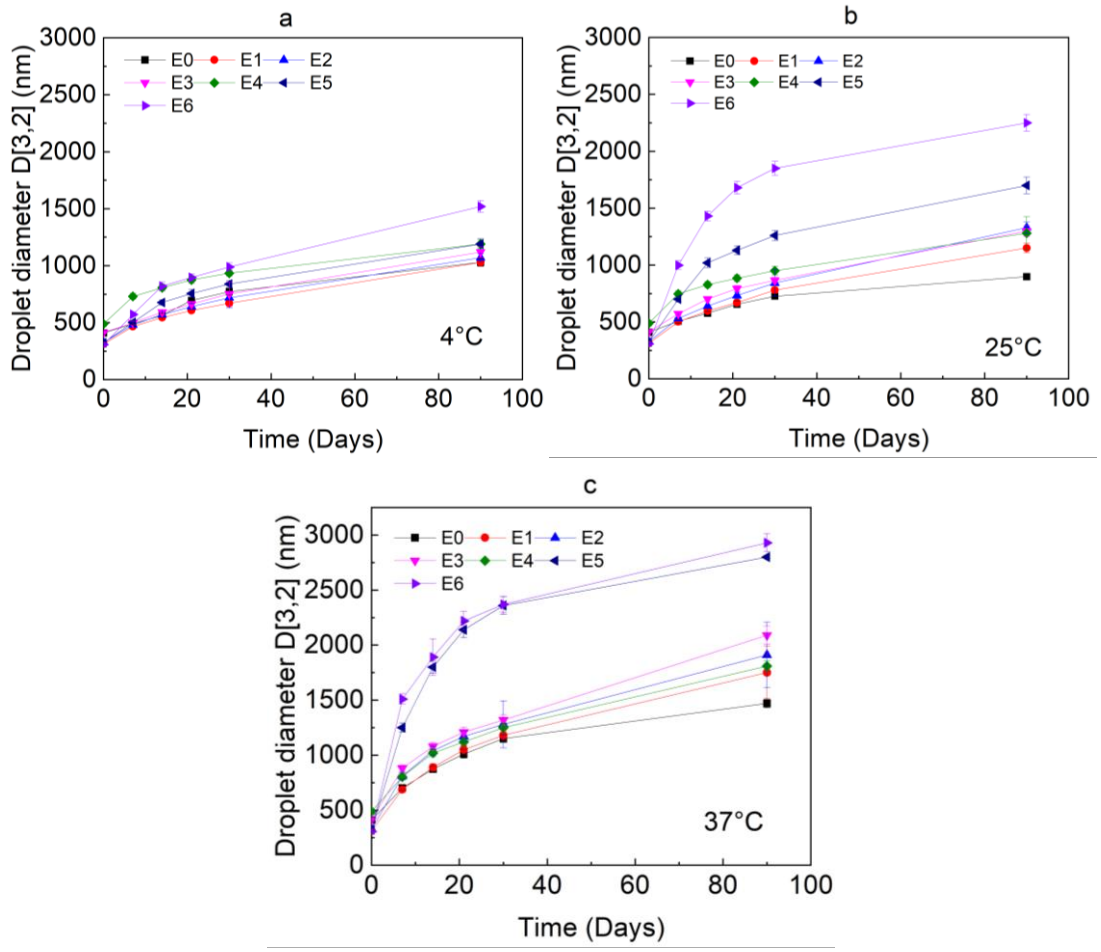

Figure 45. Empty emulsions physical stability evaluated at a) 4 °C, b) 25 °C and c) 37 °C for 90 days.

4.1.5.2 Stability of nanoemulsion

Stability of nanoemulsions was evaluated for three months at different storage temperature at 4 °C, 25 °C, and 37 °C. Results are reported in Figure 45 for empty emulsions. From the stability tests conducted it was noted that the physical stability of the nanoemulsions decreases with increasing temperature; this fact is probably due to the molecular activity more intense with increasing temperature. In addition, the stability of the nanoemulsions decreased at the higher O/W ratio of 20/80 due to the high oil dropltes concentration that favored the droplets induced by temperature. However, the droplet diameter remained in the nanoscale range within a month.

The chemical stability of lycopene was evaluated by monitoring changes in total lycopene retention throughout a 30 days storage period at different temperatures, i.e., 4 °C, 25 °C, and 37 °C.

From the results obtained, Figure 46, it was noted that the lycopene encapsulated in nanoemulsions showed the highest degradation of lycopene at higher temperature (Figure 43a). This can be attributed to the fact that the high temperatures can accelerate lycopene degradation by breaking the oil-in-water system and exposing the lycopene to degradation, resulting in a reduction of its stability [248]. Looking at Figure 46 it can be seen that the nanoemulsions can still contain more than 50 % of lycopene after a month at the lower temperature of 4 °C. This result is in agreement with Kim et al. [170] who reported an increase in stability of lycopene in the encapsulated form over the non-encapsulated form at 4 °C. At the same time, it can also be concluded that this method has a very good protective effect on lycopene, because according to some studies, lycopene degrades very quickly in an unprotected state. Srivastava and Kulshreshtha [249] found 52 % lycopene retention at 60 °C for 10 hours. Lee and Chen [250] found 94 % lycopene was degraded with illumination intensity ranged from 2,000 to 3,000 lx at 25 °C for 6 days. Ax et al. [251] studied the stability of lycopene by dissolving it in the oil phase of oil-in water emulsions, under oxygen saturation or oxygen-free conditions. Study found that at 25 °C, about 25 % of lycopene was degraded within 30 h in the oxygen-removed emulsions, whereas the lycopene degraded about 80 % for oxygen saturation. In addition, it can also be observed from Figure 46b that the diameter of the droplet changes significantly at higher temperature during storage, confirming the results observed for the empty emulsion stability tests. Visual appearance of samples after three months of storage at the different temperature investigated is reported in Figure 47.

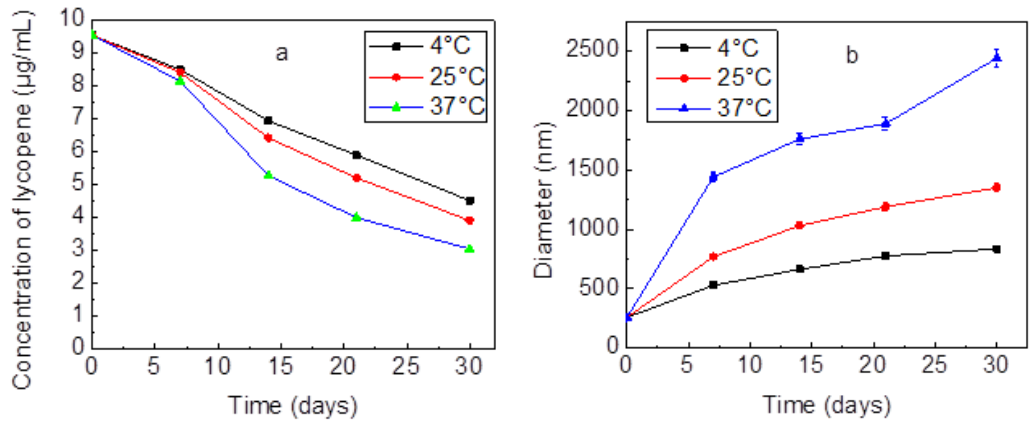

Figure 46. Stability of lycopene content during time in 14g lycopene extract loaded in nanoemulsions at different temperatures; (b) Physical stability of 14g lycopene extract loaded in nanoemulsion during time at different temperatures.

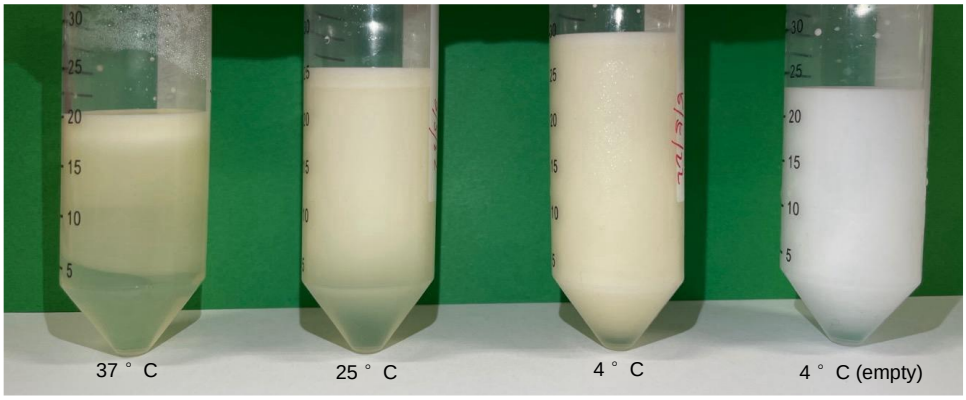

Figure 47. Visual appearance of empty nanoemulsion and nanoemulsion loaded with lycopene extract in ethanol by UAE after 3 months at 4 °C, 25 °C and 37 °C of storage.

In general, oil-in-water emulsions (that consist of spherical oil droplets dispersed within an aqueous continuous phase) are thermodynamically unstable systems because the free energy of the separated oil and water phases is lower than that of the emulsion itself [252]. Although, by adding appropriate stabilizers such as emulsifiers, texture improvers, ripening inhibitors or weighting agents, they can be kept in a metastable state for considerable periods of time. These emulsions typically breakdown over time due to a variety of destabilization mechanisms, e.g., creaming, flocculation, coalescence, and ostwald ripening [253], this phenomenon can be seen from Figure 47.

4.1.5.3 Emulsion production with sunflower seed oil

In this part, lycopene-rich sunflower seed oil extract was used as the oil phase to prepare oil-in-water nanoemulsions to study the stability of emulsion droplets and lycopene of in nanoemulsions during long-term storage at different temperatures. Empty and lycopene loaded nanoemulsions were produced using the high-speed rotor stator mixed and ultrasonication. It can be seen from the starting time in Figures 48 and 48 that the diameter of the nanoemulsion droplets increases as the ratio of oil to water increases. This result is consistent with the study of Zhao et al [246]. Another phenomenon shows that nanoemulsion droplets of all oil-to-water ratios exhibit a high degree of stability whether stored in a low-temperature environment of 4 °C or in a normal temperature environment of 25 °C for long periods of time. Moreover, when

the proportion of oil increased from 10 % to 20 %, the size of the nanoemulsion droplets did not increase significantly, remaining around 500 nm. This starting size is approximately twice the droplet size of the nanoemulsion prepared from the alcohol extract. Comparing the Figures 48, 49, 50, and 51, the result shows that adding a certain proportion of ethanol can reduce the size of nanoemulsion droplets. Literature data shows that surface tension of aqueous alcohol solutions decreases with increasing alcohol concentrations, with the most appreciable reduction occurring at low alcohol concentrations. The presence of 5 - 10 % w/w alcohol leads to the formation of smaller oil droplets compared to equivalent alcohol-free emulsions, a phenomenon that may be attributed to changes in interfacial tension [254,255]. Similar studies, Zeeb et al. [256] found that a certain content of long-chain alcohols can cause significant changes in the physical and chemical properties of the oil and water phases (such as viscosity and interfacial tension), thus affecting changes in droplet diameter. The research by Zhao et al [246]. also confirmed that adding a certain amount of lycopene can reduce the size of nanoemulsion droplets to a certain extent.

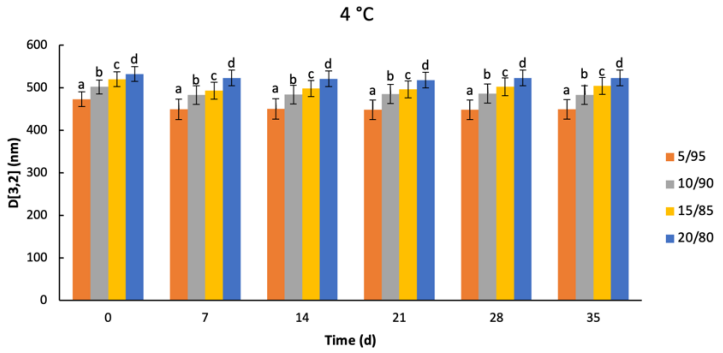

Figure 48. The stability of nanoemulsion droplet diameter with different O/W ratio at 4 °C for a month. Different letters within the same series indicate significant differences among data ($p<0.05$, Tukey HSD Test).

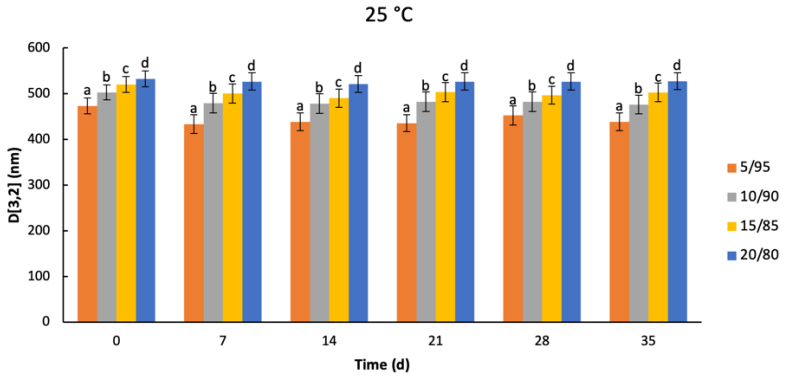

Figure 49. The stability of nanoemulsion droplet diameter with different O/W ratio at 4 °C for a month. Different letters within the same series indicate significant differences among data ($p<0.05$, Tukey HSD Test).

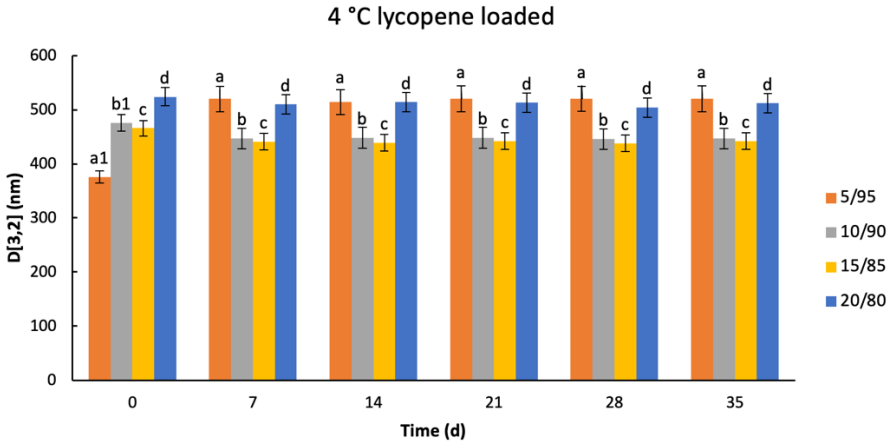

Figure 50. The stability of nanoemulsion loaded lycopene droplet diameter with different O/W ratio at 4 °C for a month. Different letters within the same series indicate significant differences among data ($p<0.05$, Tukey HSD Test).

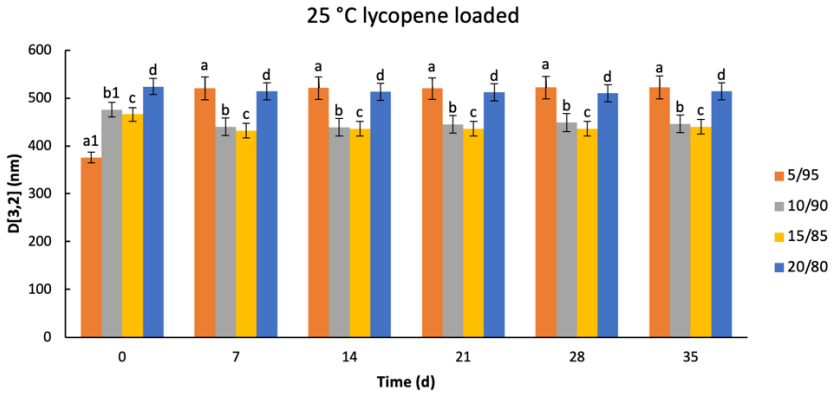

Figure 51. The stability of nanoemulsion loaded lycopene droplet diameter with different O/W ratio at 25 °C for a month. Different letters within the same series indicate significant differences among data ($p<0.05$, Tukey HSD Test).

In this part, lycopene-rich sunflower seed oil extract was used as the oil phase to prepare oil-comparing Figures 52 and 53, the results show that the temperature will affect the size of the nanoemulsion during storage, thereby affecting the stability of the nanoemulsion during storage. The study by Zhao et al [246]. found that when the temperature reaches 37 °C, the size of the nanoemulsion droplets is greatly affected. During 6 weeks of storage, the size of the droplets almost doubled compared to the initial size. It can be seen from Figure 52 that when the storage temperature is 4 °C, the oil-in-water nanosystem has a good protective effect on lycopene.

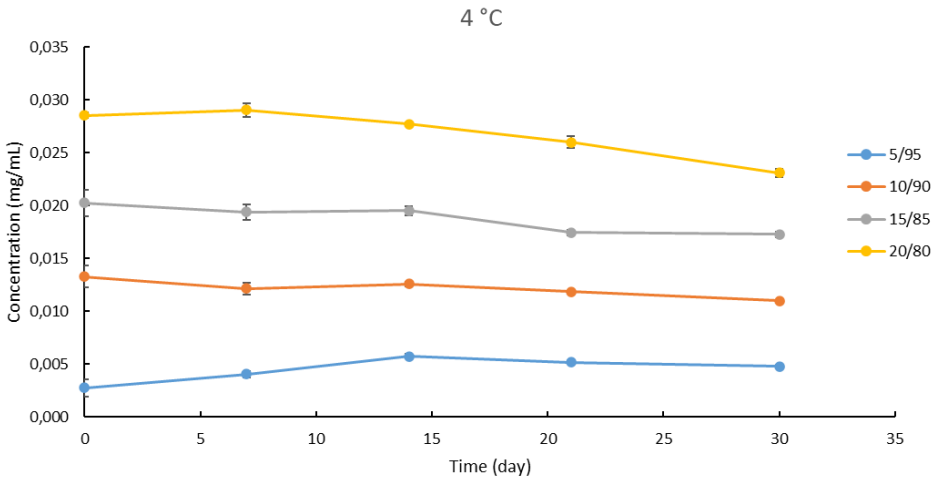

Figure 52. Stability of lycopene in nanoemulsions with different O/W ratios at 4 °C for a month.

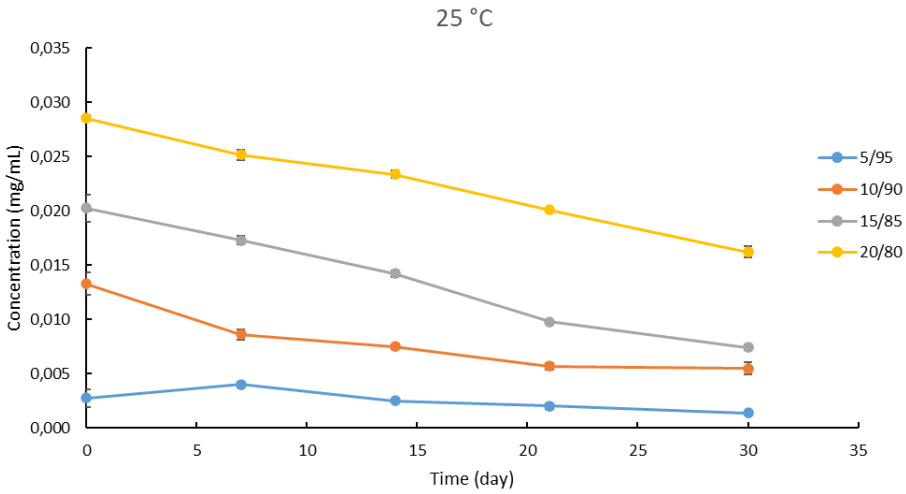

Figure 53. Stability of lycopene in nanoemulsions with different O/W ratios at 25 °C for a month.

4.2 Encapsulation by Spray Drying

4.2.1 Materials and Methods

4.2.1.1 Apparatus, chemicals, standards and solvents

Ethanol (analytical grade, Sigma Aldrich, St. Louis, MO, USA); 2,2′-azino-bis (3-ethylbenzothiazoline-6-sulphonic acid) diammonium salt (Sigma Aldrich, Milan, Italy); potassium persulfate, iso-propanol, acetonitrile, methanol (Carlo Erba, Italy), all-trans-lycopene and the standards (Sigma Aldrich, Milan, Italy) employed in this study were of analytical grade and used without further purification. The water was

obtained with a Milli-Q system (Merck-Millipore, Darmstadt, Germany). Tomato peels and seeds were kindly provided by a producer of tomato sauce in northern Italy. The TW resulting from this process were partially stored at -20 °C for characterization of the biomass, and partially dried at 60 °C up to constant weight for extraction experiments.

4.2.1.2 Extract stabilization by Spray drying

Lycopene is a carotenoid of interest in the food industry, being both a food colorant and a strong antioxidant with functional characteristics. However, considering its susceptibility to isomerization and oxidation, and its hydrophobicity, the microencapsulation process is needed to enhance molecule stability, prevent losses of bioactivity and improve bioavailability [257]. Among the microencapsulation processes, spray drying is a consolidated technique widely used in food industry, due to its efficiency, the possibility of continuous production, versatility, and flexibility. Moreover, this technique is suitable for the treatment of thermosensitive compounds and provides products with enhanced storage stability due to the low water activity of the product [258]. In addition, by the selection of the proper coating agent, the solubility of encapsulated compounds can be improved. The microencapsulation of lycopene-rich ethanolic extract was carried out by a BÜCHI Mini Spray Dryer B-290 (BÜCHI Labortechnik AG, Flawil, Switzerland) (Figure 54), working by a co-current configuration and equipped with a two-fluid nozzle for the dispersion of the liquid body into fine droplets. The extract (50 mL) was diluted with 50 mL of deionized water and homogenized. A mixture of maltodextrins and inulin was used as wall material varying its composition (21.7 %, 50 % and 78.3 % w/w of inulin) in a concentration of 10 % (w/v) with respect to the diluted extract. Maltodextrins are widely used in encapsulation by spray drying, but do not exhibit remarkable nutraceutical properties as inulin. The selection of the proportion between inulin and maltodextrin was determined by preliminary study (data not shown), which showed that values of inulin higher than 78.3 % w/w in the wall material composition provided a significant reduction in process performances. The lower value was selected basing on the will to work in a symmetric interval of values. The coating agent was dissolved into the liquid extract and left under stirring for 30 min, before starting the

microencapsulation tests. The spray dryer worked with an inlet temperature set at 135 °C, an aspiration rate of 32.4 m^3/h, and a feed flow rate of 7.5 mL/min.

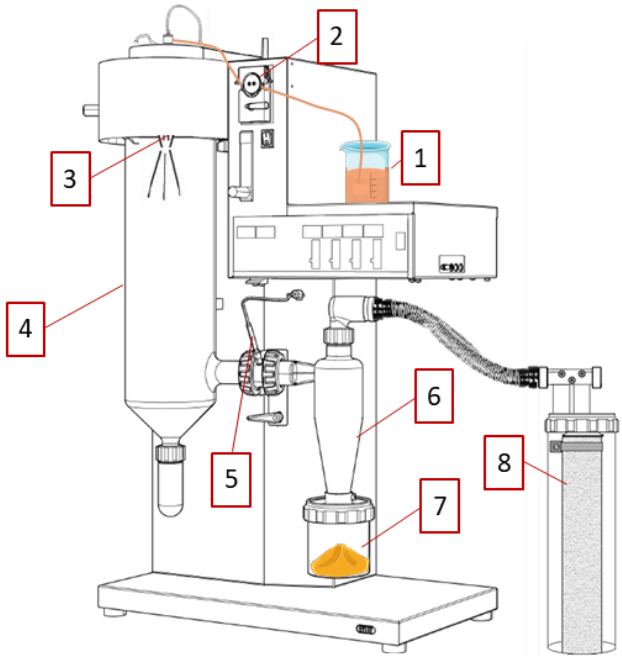

Figure 54. Scheme of spray dryer used for microencapsulation experiments. (1) Liquid feed; (2) peristaltic pump; (3) two-fluid nozzle; (4) drying vessel; (5) thermocouple for outlet temperature detection; (6) cyclone; (7) collection vessel; (8) filter. Adapted from BÜCHI mini spray dryer B-290 operation manual.

After the spray drying process, obtained microparticles were collected, weighed, and stored in water-proof containers under dark conditions at room temperature, for further analyses.

4.2.1.3 O/W nanoemulsions stabilization by Spray drying

The microparticles of O/W nanoemulsion was carried out by a BÜCHI Mini Spray Dryer B-290 (BÜCHI Labortechnik AG, Flawil, Switzerland), working by a co-current configuration and equipped with a two-fluid nozzle (DM = 0.7 mm) for the dispersion of the liquid feed into fine droplets. Detailed description of the apparatus is reported else were [259-261]. Several operative parameters were investigated such as drying vessel temperature (135 °C, 140 °C, 170 °C), outlet temperature (7 °C, 81 °C, 96 °C) and feed flow rate (3 mL/min, 6 mL/min, 9 mL/min), whereas aspiration rate (35 m^3/h) and weight of the nanoemulsions processed (80 g) were kept constant. The coating agent was dissolved directly inside the nanoemulsion until complete dissolution before spray-drying. Six different coating agents were tested: maltodextrin,

inulin, polyvinylpyrrolidone (PVP), pectin citrus, whey from bovine milk and Arabic gum.

The influence of the process operating conditions was evaluated on total lycopene content, product recovery and particles morphology. The coatings were dissolved directly inside the nanoemulsions.

4.2.2 Analytical methods

4.2.2.1 Product recovery

The product recovery (PR) was calculated according to Equation (38), as the ratio between the total solids recovered in the collection vessel of the spray dryer and total solids fed to the process.

$$PR = \frac{\text{mass of dry microparticles}}{mass\ of\ coating\ agent + mass\ of\ extract\ fed} \qquad (38)$$

The mass of extract fed was determined by drying 4 mL of the ethanolic extract at 110 °C up to constant weight and multiplying the concentration of the extract total solids by the volume of extract fed to the process.

4.2.2.2 Determination of particle sizes

Particle Sizes Distributions (PSD) of spray dried particles were carried out using Malvern Mastersizer-3000 granulometer. The powders (1.00 g) were suspended in isopropanol (10 mL), vortexed for one minute; each sample were poured into the small volume cell to obtain a laser obscuration between 10 % and 12 % and the rotate speed of circulating pump was set to 1800 rpm. The refractive index and absorption of alcohol phase were 1.673 (measured by Abbe refractometer) and 0.1 respectively. PSD data were presented as volume fraction. The morphology of dry samples was observed by Field Emission Scanning Electron Microscopy (FESEM, mod. LEO 1525, Carl Zeiss SMT AG, Oberkochen, Germany). Samples were placed on a carbon tab previously fixed to an aluminum stub (Agar Scientific, United Kingdom) and then, coated with gold-palladium (layer thickness 250 Å) using a sputtering coater (mod. 108 A, Agar Scientific, Stansted, United Kingdom). Several FESEM images at different magnifications were taken for each sample.

4.2.2.3 Determination of moisture content

The moisture of the produced microparticles was obtained by drying samples at 110 °C until a constant weight was reached, and it was expressed as mass of water removed by drying per initial mass of wet sample (%, w/w).

4.2.2.4 Determination of water activity

Water activity was measured through a HygroPalm -HP23-AW-A (Rotronic, Crawley, UK).

4.2.2.5 Determination of lycopene content in powders

Total lycopene content in the obtained product was determined after the complete dissolution of the particles. In a glass tube, 15 mL of 8 % (v/v) acetic acid aqueous solution were added to 400 mg of spray dried particles. This dispersion was vortexed for 1 min and placed in an ultrasonic bath (model UTA 90, FALC, Treviglio, Italy), working at 25 °C and 700 W for 5 min. Then, 5 mL of chloroform were added to carry out the liquid–liquid extraction of the lycopene in about 12 h. The hydrophobic phase was recovered, while the aqueous phase was subjected to a second stage of liquid-liquid extraction by adding further 5 mL of chloroform. The non-polar phase was recovered again and added to the previous one. After the chloroform complete evaporation, the dry sample was suspended in 1 mL of pure ethanol, filtered (0.22 µm), and analyzed by HPLC for lycopene quantification. For the determination of superficial lycopene, the method by Robert et al. [262] was adapted, as reported in the following. 400 mg of powder were treated with 1 mL of pure ethanol and the dispersion was agitated in a vortex at room temperature for 1 min and filtered (0.22 µm). Then, superficial lycopene was determined by HPLC.

4.2.2.6 Determination of lycopene content in powders

Total lycopene amount and free lycopene in nanoemulsions were determined using the procedure adapted from Zhao [133]. For total lycopene amount 1 mL of emulsions were dissolved in 4 mL of acetone, vortexed for 1 min to release the lycopene from the oil phase. The emulsions without lycopene were used as a control. The absorbance of the total lycopene amount was measured using a UV-vis spectrophotometer (Lambda 25,

PerkinElmer, Wellesley, MA, USA), at 470 nm using a calibration curve, the procedure was adapted from Zhao [133]. For free lycopene content 5 mL of emulsions were dissolved in 5 mL of n-hexane, shacked for 1min, then left for 30 mins to allow solvent separation. After this time the organic liquid separated on top was taken and centrifuged at 5000 rpm for 10 min to obtain the n-hexane phase. This operation was repeated twice. The absorbance of the free lycopene amount in n-hexane was measured using UV-vis spectrophotometer essay at 470 nm using a calibration curve, the procedure was adapted from Zhao [133].

The encapsulation rate was obtained by the following Equation (39).

$$Encapsulation\ rate\ (\%) = \frac{m_{total} - m_{free}}{m_{initial}} \times 100 \qquad (39)$$

Where m_{total} is the total amount of lycopene in the nanoemulsions, m_{free} is the free lycopene in the nanoemulsions, and $m_{initial}$ the initial amount of lycopene contained in the extract loaded to the nanoemulsions.

4.2.2.7 Water solubility index and water absorption index

Water solubility (WSI) and water absorption (WAI) indexes were determined following the protocol described by Ahmed et al. [263], with some modifications. Briefly, 0.5 g of microparticles and 6 mL of water were vigorously vortexed, the mixture was incubated in a water bath at 30 °C for 30 min, and centrifuged (MF-20-R, Alliance Bio Expertise, Guipry, France) at 2090 × g for 15 min. The pellet obtained was weighed and WAI was calculated according to Equation (40).

$$WAI = \frac{\text{mass of dry microparticles}}{mass\ of\ coating\ agent + mass\ of\ extract\ fed} \qquad (40)$$

Moreover, the supernatant was dried at 110 °C up to a constant weight, and WSI was obtained from Equation (41).

$$WSI = \frac{mass\ of\ solids\ in\ the\ supernatant}{mass\ of\ dry\ sample} \qquad (41)$$

Finally, the swelling capacity (SWC) was determined according to the protocol reported by Lai et al. [264], as described in Equation (42).

$$SWC = \frac{mass_{pellet}}{mass_{initial\ dried\ sample} * (1 - WSI)} \qquad (42)$$

4.2.3 Results and discussion

4.2.3.1 Extract stabilization by Spray drying

Thermo-sensitivity of carotenoids made them highly unstable and susceptible to losses of activity during processing and storage [265]. Encapsulation by spray drying allowed protection against degradation and the modulation of active compound release, providing a dry product suitable for storage.

For this reason, the extract obtained under the optimal condition was spray dried using a mixture of maltodextrins (78.3 %, w/w) and inulin (21.7 %, w/w) as wall material. Maltodextrins are polysaccharides widely used as a food additive and flavor enhancer due to their high-water solubility, low viscosity, and the ability to provide colorless solution [262]. Although they are often employed alone in microencapsulation processes by spray drying, the combination with other wall materials can improve the properties of the obtained products. Indeed, a coating agent enriched by inulin can confer nutritive properties to the product without impacting raw materials costs [265].

As shown in Figure 55, microencapsulation was carried out by setting an inlet temperature of 135 °C, in order to reduce lycopene thermal damage. Heating time, up to the set point temperature, occurred in 8 min; then, the feed started to be spread into the drying chamber. The drying process was conducted for about 14 min, while 5 min were required for the cooling stage up to 55 °C.

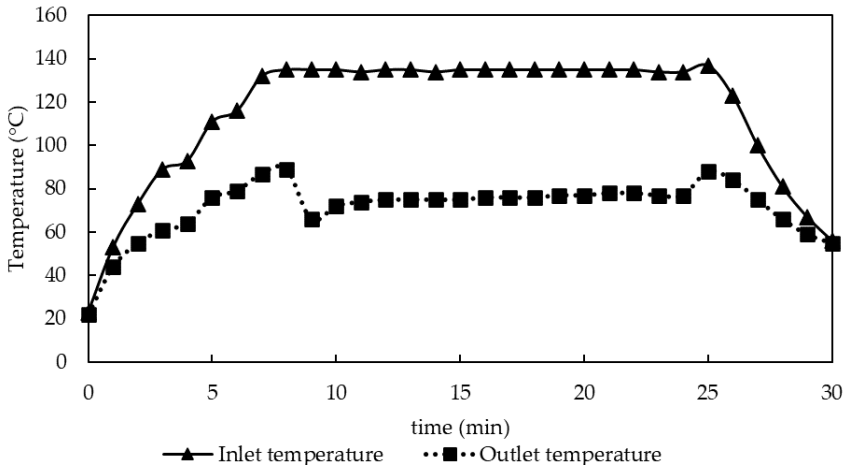

Figure 55. Inlet and outlet temperatures recorded over time during spray drying test.

Results of analyses on the collected dry microparticles are reported in Table 18, as a function of inulin content in the mixture composing the coating agent.

Table 18. Model for total carotenoid yield (TC) as a function of input variables and analysis of variance.

	21.7% Inulin	**50% Inulin**	**78.3% Inulin**
Product recovery (%)	73 ± 4	64 ± 3	63 ± 3
Moisture (%)	3.2 ± 0.1	2.5 ± 0.4	2.9 ± 0.3
Water activity (-)	0.239 ± 0.001	0.217 ± 0.023	0.220 ± 0.000
Total lycopene content (µg/g dry powder)	15.6 ± 2.9	0.8 ± 0.3	1.1 ± 0.1
Superficial lycopene (µg/g dry powder)	0.30 ± 0.02	0.7 ± 0.2	1.1 ± 0.1
Encapsulated lycopene (µg/g dry powder)	15.3 ± 2.9	0.1 ± 0.4	0.0 ± 0.1
Water solubility index (WSI)	0.935 ± 0.007	0.858 ± 0.006	0.643 ± 0.012
Water absorption index (WAI)	0.376 ± 0.027	0.800 ± 0.050	1.78 ± 0.002
Swelling capacity (SWC)	5.79 ± 0.25	5.635 ± 0.315	4.98 ± 0.17

The low moisture and water activity of the microparticles are favorable to ensure a good shelf life of the product at room temperature, away from light. Moisture results in this work are in agreement with the study by Fernandes et al. [164]. Non-significant differences in moisture and water activity were observed by varying the composition of the wall material. The process ensured a good product recovery in comparison with

values reported in the literature for spray drying processes [154,266-269], particularly at the lower inulin content. The same experimental point provided a satisfying amount of encapsulated lycopene compared to the superficial (and unprotected) content, which strongly decreased with the increase in inulin percentage. However, an optimization of the spray drying process could improve the encapsulation of the extract and the amount of active agent in the particles, which resulted lower than that reported in the literature [160,270]. The lycopene losses during the process can be traced back to the low solubility of the compound in the feed, where the extract was diluted with water and a low concentration of coating agent in the feed, rather than being due to degradation effects, considering the low temperature inside the drying chamber. Powder solubility depends on many parameters, such as the coating agent composition and spray drying operating conditions, and it determines the potential applications of the product. WSI gives information about the behavior of the product in the aqueous phase [271], while WAI measures the volume occupied by the wall material after swelling in excess of water [272]. The product presents high water solubility at the lowest inulin concentration, while a decrease was observed as the percentage in the used wall material increased, being the compound less soluble than maltodextrin in aqueous media. However, up to 50 % inulin, WSI was higher than the reported value for lycopene microencapsulation in maltodextrin, whey protein isolate, and modified starch by Souza et al. [270].

4.2.3.2 Encapsulation of nanoemulsion with different coating agent by spray drying

In order to provide an alternative to refrigerated storage of the natural extract encapsulated product nanoemulsions loaded with lycopene extract were dried by spray drying and the comprehensive data analysis of the powdered product was carried out. At the end the possibility of emulsion restoration by simple water dispersion of spray dried particles was investigated. First of all, empty nanoemulsions were subjected to spray drying using maltodextrin as coating agent. For this study nanoemulsion (sample L6) produced at the following operative condition was used: O/W 20/80 (w/w), 14 g of extract and 6 g of isopropyl myristate mixed by ultrasonic (A = 40 % and 1 min), 80 g of pluronic solution (1.5 % (w/w)), results are shown in Table 2. Before the spray

drying experiment the coating agent was dissolved in fixed amount directly in the prepared nanoemulsion until complete dissolution.

Spray drying operative conditions such as temperature, feed flow rate and the concentration of coating agent were varied in order to find the condition at which a good powder recovery was reached. In Table 19 a summary of the preliminary tests conducted is reported.

Table 19. Preliminary spray drying tests of nanoemulsion (sample L6) using maltodextrin as coating agent.

Sample	**Process conditions**	**Coating agent [%]**	**Nanoemulsion mean diameter D [3,2] [nm]**	**Product recovery [%]**	**Powder mean diameter D [3,2] [µm]**
D_1	135 °C,35 m^3/h,3 mL/min	10	267 ± 16	7.4	4.21 ± 0.16
D_2	135 °C,35 m^3/h,6 mL/min	10	235 ± 21	3.7	6.27 ± 0.22
D_3	140 °C,35 m^3/h,6 mL/min	20	249 ± 19	16.6	10.4 ± 0.37
D_4	140 °C,35 m^3/h,6 mL/min	40	246 ± 17	47.7	6.14 ± 0.23
D_5	140 °C,35 m^3/h,9 mL/min	40	256 ± 16	34.6	4.57 ± 0.19
D_6	170 °C,35 m^3/h,3 mL/min	40	252 ± 13	10.7	3.44 ± 0.15
D_7	170 °C,35 m^3/h,6 mL/min	40	236 ± 24	80.3	4.87 ± 0.17
D_8	170 °C,35 m^3/h,9 mL/min	40	251 ± 15	14.5	10.1 ± 0.36
D_9	170 °C,35 m^3/h,6 mL/min	20	253 ± 16	38.4	8.51 ± 0.34

The operating conditions at which spray drying reached the highest recovery were the input temperature 170 °C, the gas flow rate 35 m^3/h, the flow rate of the nanoemulsion 6 mL/min and the coating agent at 40 % w/w. In this condition the recovery of the product reaches 80.3 %.

FESEM images of maltodextrin particles obtained at the best conditions (experiment D7) are reported in Figure 56. Particles are spherical and with regular shape. Particles mean diameter was 4.87 ± 0.17 µm.

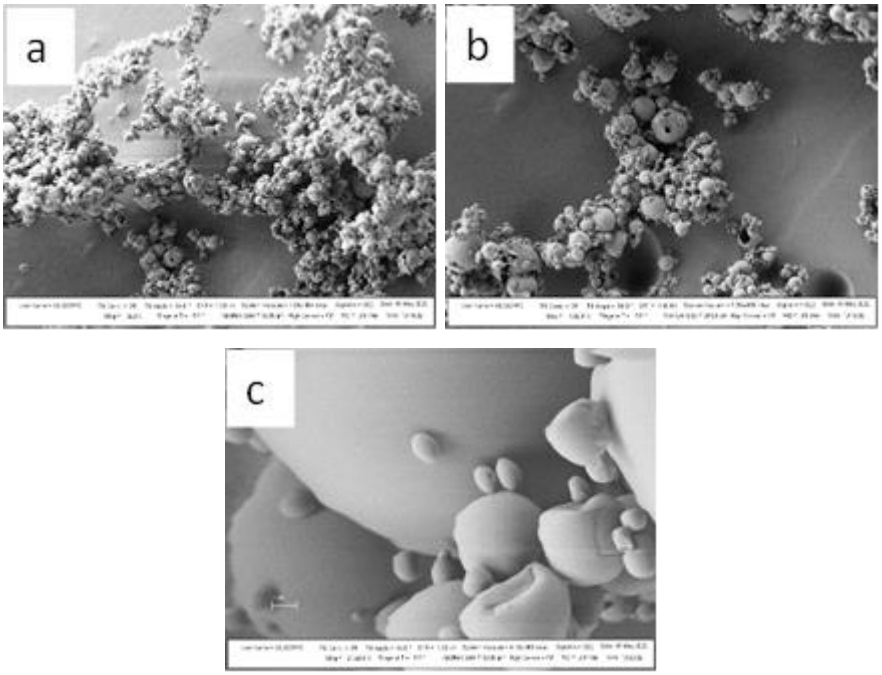

Figure 56. FESEM image of maltodextrin particles at different magnification for sample D7.

Considering the good results obtained with maltodextrin also other coating agent were considered. Spray drying experiments were considered at the operative conditions optimized in the feasibility study. For this study loaded nanoemulsion produced at the condition of sample L6 was used and the different coating agents were added at 40 % (w/w) with respect to the emulsion weight. Table 19 represents the experiments performed and the results obtained in terms of product recovery and particles mean diameters. The data showed that the mean diameter of the starting nanoemulsion was influenced by the addition of the different coating agents. The inulin had a weak effect on the droplet diameter of the nanoemulsion after being fully dissolved, while Pectin Citrus had the most significant effect on the droplet diameter causing an increase of droplets mean diameter up to 1670 nm. The coating agent dissolved in the water phase can have an effect on the hydrodynamic diameter especially for substances that show an affinity with emulsion droplets and thus trend to deposit on droplets surface. The highest product recovery was found for maltodextrin 80.88 %, while the lowest product recovery was found for PVP only about 16.28 % of power was recovered. From Table 20, it can be seen that there is no direct and obvious relationship between

the recovery level of the product and the droplet diameter of the emulsion after the coating agent is completely dissolved.

Table 20. Characteristics of nanoemulsion and product recovery of spray drying with different coating agent. (-) None or not measured.

Coating agent	Emu diameter D [3,2] [nm]	PR (%)	Powder diameter D [3,2] [µm]	EnE [%]	Moisture [%]	WA	WSI	WAI	SCI
Emu	195 ± 6	(-)	(-)	(-)	(-)	(-)	(-)	(-)	(-)
I	386 ± 14	51.02	(-)	(-)	5.4	0.362	0.5623	0.0586	0.1338
M	418 ± 16	80.88	4.87 ± 0,17	99	9.7	0.328	0.7871	0.0013	0.0062
PVP	466 ± 17	16.28	(-)	(-)	6.1	0.348	0.8014	0.6751	3.3987
GA	477 ± 61	59.86	(-)	(-)	10.5	0.204	0.8064	0.4680	2.4177
W	1100 ± 83	40.69	(-)	(-)	7.6	0.287	0.6503	0.1249	0.3571
PC	1670 ± 96	36.35	(-)	14	7.8	0.350	0.1880	0.2950	0.3634

Emu = emulsion only; I = inulin; Ma = maltodextrin; GA = gum arabic; Wh = whey; PeC = pectin citrus; PR = Product recovery; EnE = Encapsulation efficiency; WA = water activity.

Figure 57 shows the powder produced with different coating agents used; there were almost four types of particles observed: 1) smooth spherical (Figure 57g); 2) wrinkled (Figure 57d and 57e); 3) spherical with small particles (Figure 57a and 57b); 4) broken flakes and colloidal particles (Figure 57c, and 57d). From this study also inulin and PVP reveals to be good coating agent. Maltodextrin confirmed the good results of the feasibility study. The dried nanoemulsion containing lycopene appears light red as seen in Figure 54h.

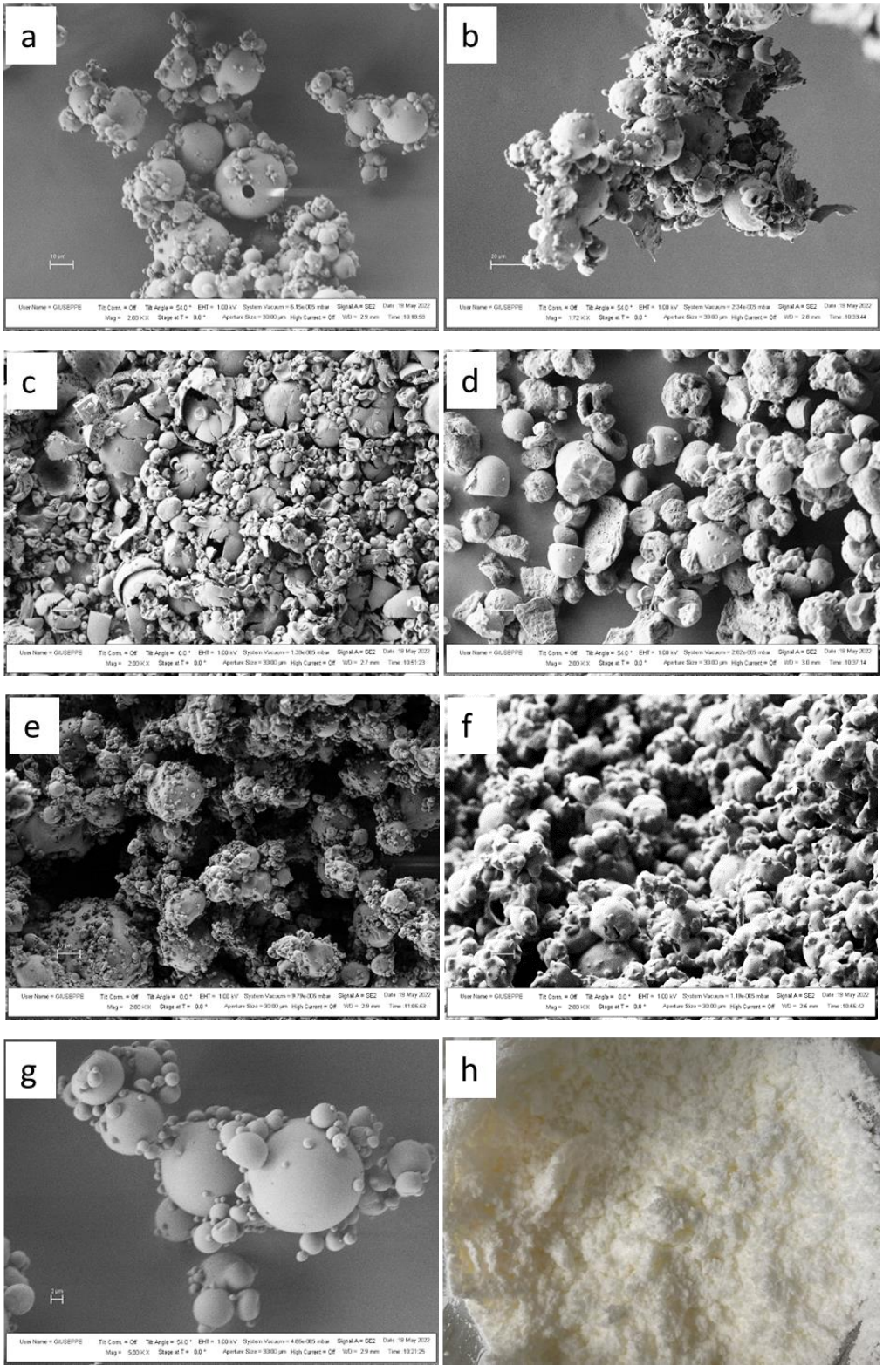

Figure 57. FESEM images of spray drying nanoemulsions produced with different coating agent: (a) Maltodextrin 2000X; (b) Inulin 2000X; (c) Gum Arabic 2000X; (d) Pectin 2000X; (e) PVP 2000X; (f) Whey 2000X, (g) Maltodextrin 5000X, (h) Dried powder for lycopene-loaded nanoemulsions with maltodextrin.

A final experiment was conducted to assess the possibility of dissolving the powder obtained by spray drying and restoring the original emulsion. The perform this proof of concept the powder obtained using maltodextrin as coating agent and lycopene loaded nanoemulsion product at T = 65 °C, t = 20 min, L/S = 72 mL/g, A = 65 %, on =33 s, V = 90 mL was used.

In Figure 58 pictures each step of this proof of concept is reported: A, preparation of the emulsion that contains the coating agent; B, powder production using spray drying; C, powder addition in water; D, emulsion restoration. The powder was dissolved in water fixing a 10/1 (w/w) liquid/solid ration. From Figure 58 it is possible to make the similarity of step A and step D visual appearance, indicating that with good probability the emulsion has been repristinated after powder dissolution. In terms of particle size distribution (PSD) the system was analyzed at each step. Data are reported in Figure 56.

Emulsion after production is characterized by a mean diameter of 276 nm. A small enlargement of the PSD was observed after maltodextrin addition (Figure 59a). The spray drying of emulsion + maltodextrin lead to the formation of particles of 4.87 µm, mean diameter and micrometric PSD (Figure 59b). After the dissolution of the powder in water an opaque liquid system was obtained again with a mean diameter of 394 nm (Figure 59c); i.e., very similar to PSD of Figure 59a (the maltodextrin curve). These results constituted a confirmation of the possibility of drying nanoemulsions using spray drying and restoring the original emulsions by simple water dissolution of the powder.

Figure 58. From emulsion to powder and back to emulsion steps. A) loaded nanoemulsion with 40 % (w/w) of maltodextrin, B) dried powder, C) water, D) nanoemulsion rehydration.

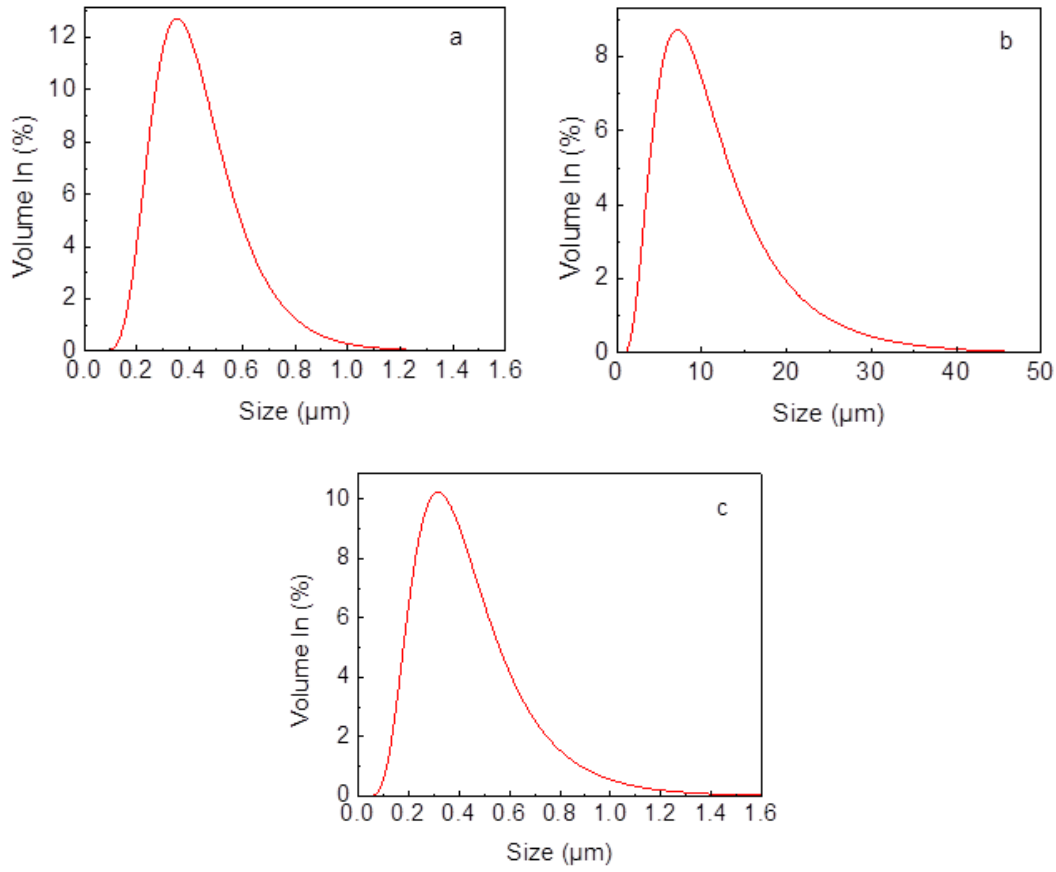

Figure 59. Granulometric data of a) of lycopene-loaded nanoemulsions; b) spray drying product; c) emulsion after rehydration.

4.3 Encapsulation by supercritical assisted atomization (SAA)

4.3.1 Materials and Methods

4.3.1.1 Apparatus, chemicals, Standards and Solvents

Polyvinylpyrrolidone (PVP, average molecular weight of 10 kg/mol), dextran from Leuconostoc mesenteroides (DEX, average molecular weight of 43 kg/mol), hydroxypropyl-β-cyclodextrin (HP-β-CD, purity of 99.9 %), curcumin (CUR, purity > 65 %), and ethanol (99.9 %) were provided by Sigma-Aldrich (Milan, Italy). Carbon dioxide (CO_2, purity 99 %) was supplied by Morlando Group s.r.l. (Sant'Antimo, Naples, Italy), and nitrogen (N_2, purity 99.9 %) by SON (Naples, Italy).

4.3.1.2 SAA Apparatus and Procedure

SAA laboratory apparatus (Figure 60, left), used in this work, consists of two high-pressure pumps (model 305, Gilson) delivering the liquid solution and liquid CO_2 to a heated bath then, to the saturator. The saturator is a high-pressure vessel (internal volume: 25 cm^3) loaded with stainless steel perforated saddles which assure a large contact surface between liquid solution and CO_2, thus enhancing the dissolution of the gaseous stream into the liquid solution. Typically, volumetric flow rates of the liquid solution of about 4 - 5 mL/min are used, that produce long residence times (from 4 to 5 min) in the saturator, leading to near-equilibrium conditions. The solution produced in the saturator is sprayed through a thin wall 80 μm diameter injection nozzle into the precipitator. A controlled flow of N_2 is taken from a cylinder, heated in an electric heat exchanger (mod. CBEN 24G6, Watlow) and sent to the precipitator to facilitate liquid droplets evaporation. The precipitator is a stainless-steel vessel (internal volume: 3 dm^3) operating at atmospheric pressure (Figure 60, right). The saturator and the precipitator are electrically heated using thin-band heaters (Watlow, mod. STB3EA10). A stainless-steel filter located at the bottom of the precipitator allows the powder collection and the gaseous stream flow out.

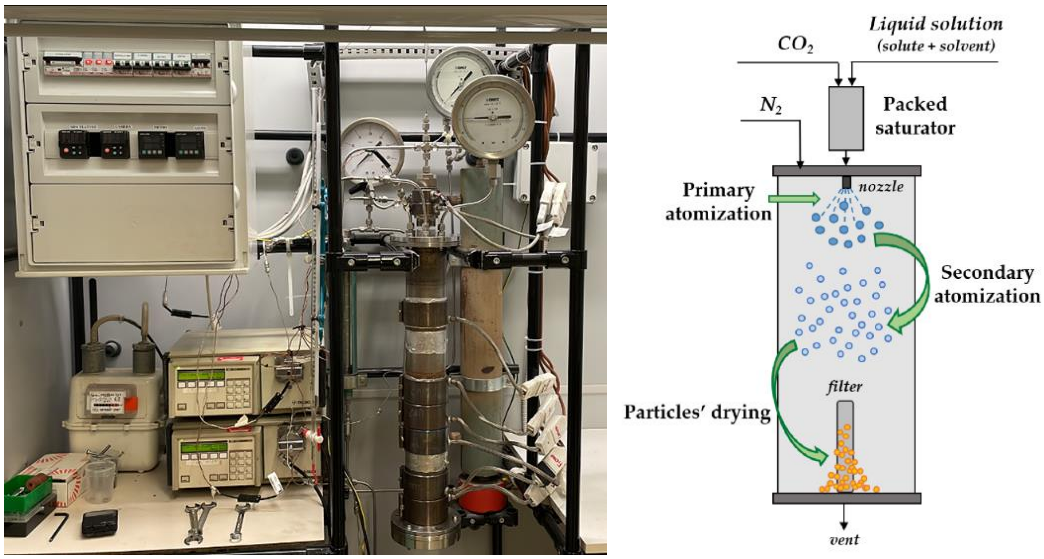

Figure 60. A sketch of supercritical assisted atomization (SAA) [273].

4.3.1.3 Process description

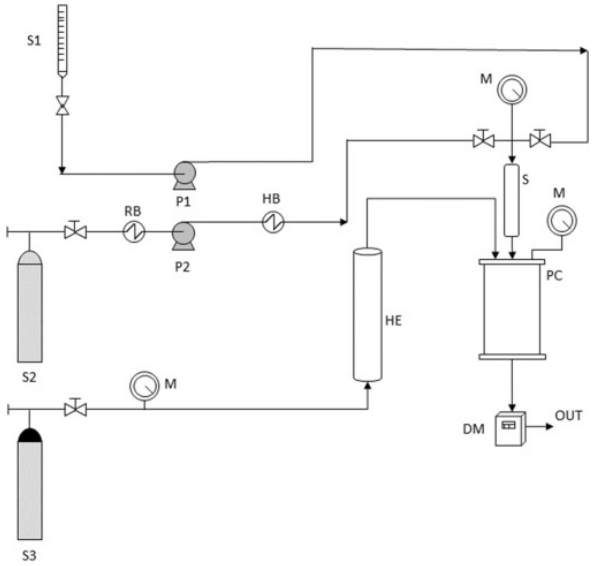

Figure 61. A sketch of the SAA laboratory plant. S1, S2, and S3: CO_2 supply, nitrogen supply, and liquid solution supply; P1 and P2: pumps; RB: refrigerating bath; HB: heating bath; M: manometer; HE: heat exchanger; S: saturator; PC: precipitatvion chamber; DM: dry test meter [274].

Briefly, according to the flow chart in Figure 61, the CO_2 (stored in tank S2) is cooled in a refrigerating bath RB and then pumped by P2; carbon dioxide is pre-heated in HB, before reaching the saturator S, which is a high-pressure vessel (25 cm^3 internal volume). In the saturator, 5 mm perforated Berl saddles are placed to favor optimal contact between the liquid phase and the supercritical phase and allow the thermodynamic equilibrium achievement. Another high-pressure pump (P1) is used for the emulsions with coating agent 40 % (maltodextrin, inulin, polyvinylpyrrolidone (PVP), pectin citrus, whey from bovine milk and arabic gum) (stored in the buret S1), which was pumped 7.5 mL/min. Carbon dioxide (CO_2 flow rate = 16 mL/min) dissolves in the liquid solution, and the mixture formed is sprayed from the saturator S (P_{mixer} = 80 - 90 bar T_{mixer} = 90 °C) to the 0.5 - 1.5 bar precipitation chamber PC (3000 cm^3 internal volume) through an 80 µm internal-diameter stainless-steel nozzle. Nitrogen stored in a tank (S3) and heated in an electric heat exchanger (HE) (T_{N2} = 140 °C) enters in a controlled manner (1200 mL/h) from the top of the precipitation vessel (T_{cell} = 100 - 110 °C) and assured the liquid droplets' evaporation. The temperature control is ensured by controllers connected with electrically thin bands, whereas the pressure is determined by a test gauge manometer (M). The precipitated

powder is collected at the bottom of the precipitation chamber on a stainless-steel filter (size of pores of around 0.1 μm). The total quantity of delivered CO_2 is measured at the exit by a dry test meter (DM). Micronization experiments were performed in triplicates.

4.3.1.4 Product recovery

The product recovery (PR) was calculated according to Equation (43), as the ratio between the total solids recovered in the collection vessel of the spray drying and total solids fed to the process.

$$PR = \frac{\text{mass of dry microparticles}}{mass\ of\ coating\ agent + mass\ of\ extract\ fed} \qquad (43)$$

The mass of extract fed was determined by drying 4 mL of the ethanolic extract at 110 °C up to constant weight and multiplying the concentration of the extract total solids by the volume of extract fed to the process.

4.3.1.5 Determination of particle sizes

Particle Sizes Distributions (PSD) of particles obtained by spray drying were carried out using Malvern Mastersizer-3000 granulometer. The powders (1.00 g) were suspended in isopropanol (10 mL), vortexed for one minute; each sample were poured into the small volume cell to obtain a laser obscuration between 10 % and 12 % and the rotate speed of circulating pump was set to 1800 rpm. The refractive index and absorption of alcohol phase were 1.673 (measured by Abbe refractometer) and 0.1 respectively. PSD data were presented as volume fraction. The morphology of dry samples was observed by Field Emission Scanning Electron Microscopy (FESEM, mod. LEO 1525, Carl Zeiss SMT AG, Oberkochen, Germany). Samples were placed on a carbon tab previously fixed to an aluminum stub (Agar Scientific, United Kingdom) and then, coated with gold-palladium (layer thickness 250 Å) using a sputtering coater (mod. 108 A, Agar Scientific, Stansted, United Kingdom). Several FESEM images at different magnifications were taken for each sample.

4.3.1.6 Determination of moisture content

The moisture of the produced microparticles was obtained by drying samples at 110 °C until a constant weight was reached, and it was expressed as mass of water removed by drying per initial mass of wet sample (%, w/w).

4.3.1.7 Determination of water activity

Water activity was measured through a HygroPalm -HP23-AW-A (Rotronic, Crawley, UK).

4.3.2 Results and Discussion

It can be seen from Figure 62 that the appearance of the powders obtained from the three wall materials does not have much difference, and they all appear milky yellow. However, compared with Gum Arabic (GA) and PVP, the powder obtained by using maltodextrin as a wall material does not have much agglomeration. This may be because maltodextrin forms finer droplets in the drying chamber when used as a wall material, or it may be because gum arabic cannot form dispersed spheroids as a wall material. From the electron microscope photo in Figure 63, it can be seen that the powder obtained by using gum arabic as the wall material has a block structure. The powder obtained by using PVP as the wall material also agglomerates. On the contrary, when maltodextrin was used as the wall material (Figure 63b), the particles obtained are spherical and relatively uniform.

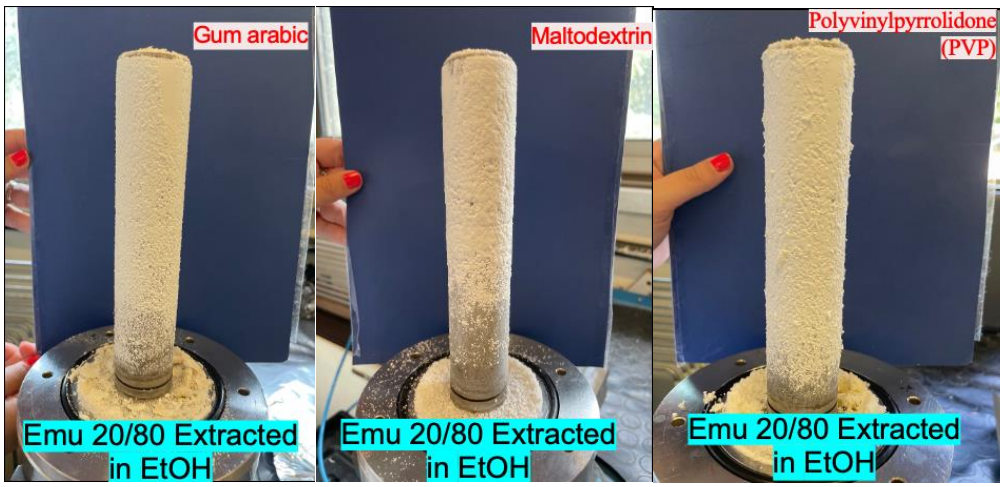

Figure 62. Production images a) with arabic gum; b) with maltodextrin; c) with PVP.

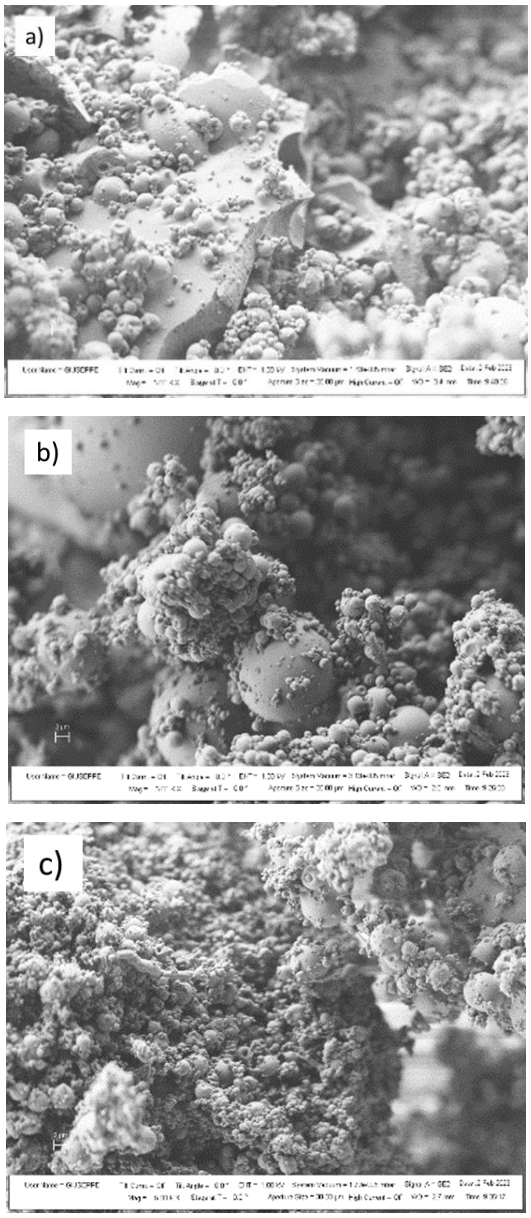

Figure 63. SEM images of powder a) GA; b) Maltodextrin; c) PVP.

Powders production obtained from SAA after Arabic gum addition (Figure 64a) were characterized by a mean diameter of 1.39 ± 0.26 µm. A small enlargement (1.47 µm) of the PSD was observed after maltodextrin addition (Figure 64b).

The SAA drying of emulsion + PVP lead to the formation of particles of 4.87 µm, mean diameter and micrometric PSD.

These results constituted a confirmation of the possibility of drying nanoemulsions using SAA and restoring the original emulsions by simple water dissolution of the powder.

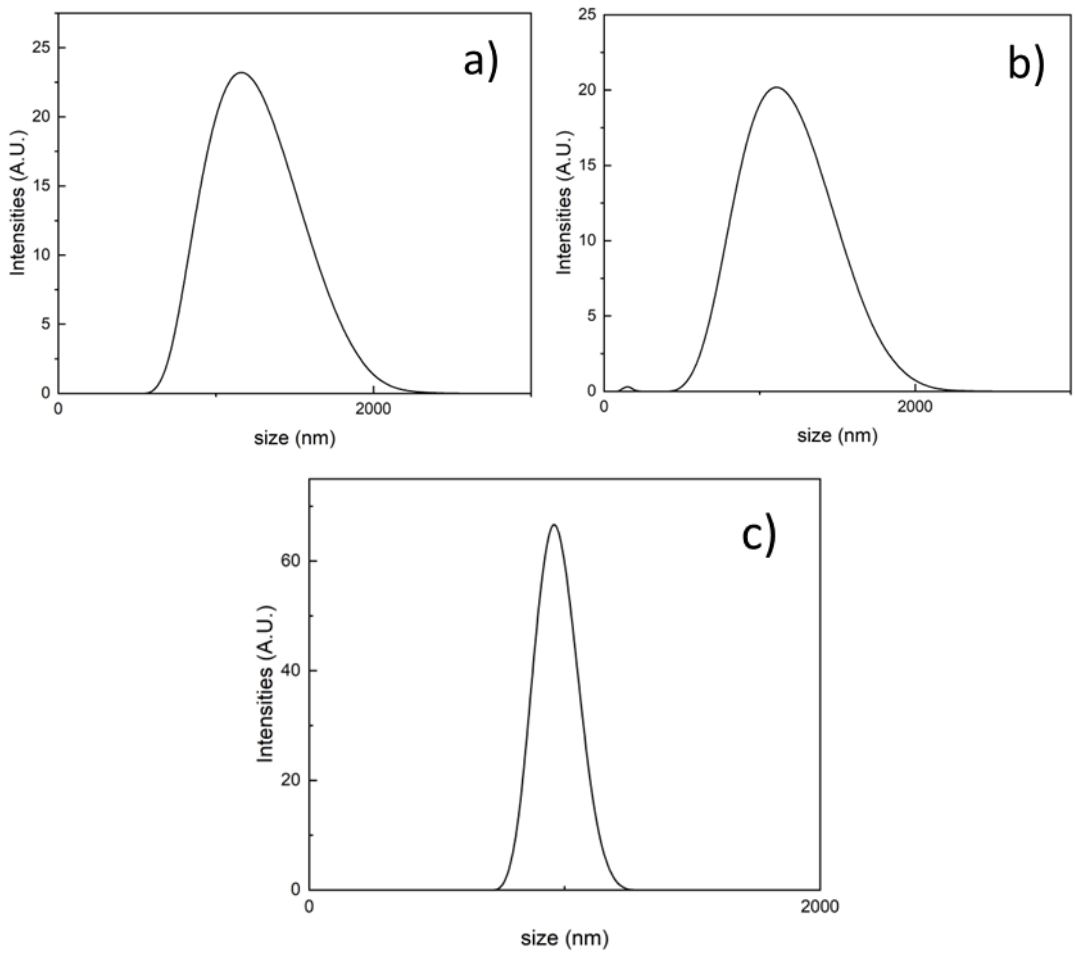

Figure 64. Granulometric data of a) Arabic gum; b) Maltodextrin; c) PVP.

4.4 Conclusion

In this chapter, a convenient method for lycopene enriched natural encapsulation and its preservation in oil-in-water nanoemulsions was proposed. Nanoemulsions were found stable for up to three months at the optimal storage temperature (4 °C) as no significant agglomeration was observed. The addition of extract (ethanol enriched lycopene) was found to significantly reduce the droplet size and increase the stability of nanoemulsions. However, a degradation phenomenon of encapsulated lycopene was observed even at refrigerated conditions. For this reason, the drying of the emulsions was attempted. The spray drying technology was found efficient for transferring the nanoemulsion to solid powder. The operating conditions at which spray drying reached the highest recovery were the input temperature 170 °C, the gas flow rate 35 m^3/h, the flow rate of the nanoemulsion 6 mL/min and the coating agent (maltodextrin) at 40 % w/w. Under the optimal condition, the recovery of the product reaches 80.3 %. The

powder obtained using maltodextrin as coating agent presented a better microstructure property. Obtained microparticles have a good dissolution in water and the reconstituted emulsions maintain in nanosize. Furthermore, as a comparison, a feasibility evaluation of the encapsulation of the obtained extract by spray drying was carried out, investigating the possibility to add inulin in the composition of the wall material. The best results were obtained at the lowest percentage of inulin (21.7 % inulin and 78.3 % of maltodextrins). Despite the high product recovery, low water activity, higher content of encapsulated rather than superficial lycopene of the microparticles, and good water solubility, the spray drying process deserves further investigations to enhance process performances. Finally, a SAA laboratory apparatus was adopted to dry the nanoemulsions, and different coating agents, CO_2 flow rate, temperature, feed flow rate, and production recovery were evaluated. The results showed that the product recovery was relatively low compared to spray drying, but the diameter of the powder particles obtained was smaller than that of the spray dried product. It can be seen from the emulsion results that lycopene was well preserved: after one month more than 50 % lycopene is preserved. While if lycopene has not been protected, most of it degrades in a few days. In summary, solid products usually have the advantages of low moisture content, low water activity, smaller volume and weight. Special non-liquid products are prone to breed microorganisms, which may cause harm to consumers' health. Although spray drying and SAA both dry under high temperature conditions. But the product obtained by spray drying quickly changes from high to low temperature (in fact, the product is collected immediately in a cryogenic container). For the SAA process, the product remains in a high-temperature drying chamber. Therefore, due to the very sensitive nature of lycopene to temperature, the process conditions for spray drying are more suitable. And a large amount of literature has also proved that the protected spray drying process for lycopene is an efficient and good technology.

As shown in the section of extraction, selecting the best encapsulation method from many criteria is a scientific and rigorous process, which also can be synthesized through the DECISION MATRIX. Below is a list (Table 21) of some of the possible attributes that are generally relevant to the lycopene encapsulation process. The MADM can use this list to help identify the core attributes that are relevant to the particular application under consideration. It is important to note, however, that the list

is not exhaustive, and the user may call upon additional attributes depending on their application.

Table 21. Decision Matrix for select the process of lycopene encapsulation.

Criteria	**Weight**	**Emulsion**		**Spray drying**		**SAA**	
		Score	Total	Score	Total	Score	Total
Temperature	**5**	3	15	2	10	2	10
Coating agents	**2**	3	6	3	6	3	6
Yield of production	**5**	3	15	3	15	1	5
Lycopene retention	**5**	3	15	3	15	1	5
Ease of implementation	**3**	2	6	2	6	1	3
Ease of scale up and operation	**3**	2	6	3	9	2	6
Energy consumption	**2**	2	4	2	4	1	2
Cost of the process	**4**	2	8	2	8	1	4
Environmental concerns	**3**	2	6	2	6	2	6
Total			81		79		47

Note: The weights are categorized on a scale of 1-5, according to the importance of the parameters for the process. For temperature greater than 160 °C score 1, less than 60 °C score 3; for coting agents cheap and easy to obtain the higher the score; for yield of production less than 50 % score 1, greater than 80 % score 3; for ease of implementation, ease of scale up and operation and cost of the process and energy consumption the more equipment and conditions needed the lower the score; for environmental concerns the less gas released the higher the score.

As can be seen in Table 21, the highest scores are given to emulsion technology when all aspects of the drying process are considered. Also spray drying scored very high in terms of obtaining the highest yield and lycopene retention while being simple to operate and not polluting the environment. As for, between the two products (liquid and solid), it is difficult to say which method is better, since the type of use of the final product must also be considered.

Parts of this section were already published in ***"A Comprehensive Optimization of Ultrasound-Assisted Extraction for Lycopene Recovery from Tomato Waste and Encapsulation by Spray Drying" by Junyang Li,*** *Margherita Pettinato, Alessandro Alberto Casazza, Patrizia Perego.* ***Processes 10.2 (2022): 308.*** *doi.org/10.3390/pr10020308****,*** *and partially presented as "Ultrasound-assisted Extraction of Lycopene from Industrial Tomato Waste", in the international congress "6th Green and Sustainable Chemistry Conference - GREEN2020", online, as poster presentation. Also, partially presented as "Oil-in-Water Nanoemulsions for Encapsulation of Lycopene from tomato waste", in the national conference " Centralità dell' Ingegneria Chimica in un Mondo che cambia - GRICU2022", Ischia, Italia, as poster presentation, July 3-6, 2022*

CONCLUSIONS

Tomato industrial waste, mainly from peels and seeds, in which fiber is the main compound, accounting for 25.4 - 50.0 % of dry matter, protein 15.4 - 23.7 %, protein 5.4 - 20.5 % fat and 4.4 - 6.8 % minerals. What's more, this byproduct contains important antioxidants (primarily polyphenols), which studies have found to be high in TW, as well as ascorbate and lycopene. What's more important is that the lycopene in tomatoes mainly comes from TW, accounting for more than 80% of the total, and can be efficiently extracted through appropriate extraction methods. Therefore, the high chemical value in TW indicates its great potential commercial application and medicinal value in extracting antioxidants.

In Chapter 2, the characterization of TW was evaluated to get a comprehensive understanding of the target extracts in order to facilitate a clear preparation for the in-depth study of TW. Results showed that initial moisture data at the time of collection were obtained, confirming that TW presented the same moisture content, approximately 84.3 ± 0.83 %. This information allowed the determination that drying for 3 days at 60 °C provided a starting material suitable for antioxidant extraction, with a final moisture of approximately 6 % of residual moisture. Particularly, after the drying process, the TW exhibited a water activity of 0.101 ± 0.042, resulting as suitable for long-term storage in water-proof containers and in the dark for extraction experiments. After crushing, the average diameter of the particles is smaller (732 ± 67 µm), making it possible to directly use TW for extraction. The biomass showed an ash content of 4.1 ± 0.8 % and the obtained value agreed with those reported in literature. Since lycopene recovery processing could involve different extraction technologies, it was of paramount importance to investigate the parameters that can influence the lycopene yield in the extracts during extraction process, as well as effect of different extraction techniques on the results, SLE using hexane as solvent was carried out for the quantification of lycopene as reference. Three consecutive extractions were performed. The total lycopene content was 1438.24 ± 44.3 µg/g (dry solid), measured via HPLC. SLE using Sunflower seed oil as solvent was carried out for a general traditional extraction. The results show that the optimal conditions were T = 45 °C, L/S = 20/3 mL/g, stirring speed = 900 rpm, t = 45 min. The total lycopene content was

1237.32 ± 4.80 µg $_{\text{lycopene equivalent}}$/g (dry solid) measured by UV-vis spectrophotometer. The maximum extraction of lycopene was very close to the total content, indicating that a simple extraction operation using sunflower oil as a solvent could achieve a fairly high extraction rate, and verifying the fat-soluble nature of lycopene. UAE extraction using ethanol as solvent as advanced extraction method was carried out. Response Surface Methodology was used to investigate the effect of the ultrasound-assisted extraction parameters on the extract bioactive content. A Central Composite Design (CCD) was employed as the experimental design. The factors investigated included extraction temperature (35 - 65 °C), time (20 - 50 min), volume of the extraction system (45 - 90 mL), liquid-to-solid ratio (27 - 80 mL/g), amplitude (30 - 65 %) and on/off pulsed ratio (30 - 70 s). The last was defined as the time of applied ultrasounds in a cycle where the relaxation time (ultrasounds were not applied) was fixed to 30 s. The optimal conditions found by the desirability method (CCD) (T = 65 °C, t = 20 min, L/S = 72 mL/g, A = 65 %, on/off = 33/30 s/s, V = 90 mL) were experimentally verified and the total lycopene content was 1536 ± 53 µg/g (dry solid), measured via HPLC. It was also found that the frequency of ultrasonic vibration studied (40 kHz, 80 kHz, 120 kHz) did not significantly improve the lycopene extraction rate. SoLVE extraction using ethanol as solvent was also carried out. The optimal conditions also found by the desirability method (CCD) (T = 65 °C, t = 41 min, L/S = 27 mL/g, A = 39 %, on/off = 32/30 s/s) were experimentally verified. Under optimal conditions, the *trans*-lycopene yield was of 546.7 µg/g and the total lycopene yield was 1193.0 µg lycopene equivalents/g. In addition, the kinetic extraction model was found to be consistent with the Peleg's model. Finally, a new microwave-assisted subcritical extraction method was used to study and compare the extraction of lycopene with the extraction conditions of UAE and SoLVE. The results showed that the extraction rate of lycopene was much greater when pure ethanol was used as solvent than when water was used as solvent. The optimal conditions were T = 100 °C, L/S = 72 mL/g, V = 30mL, t = 15min. The maximum total lycopene content was 962.97 ± 42.87 µg/g (dry solid), the *trans*-lycopene yield was of 662.84 ± 24.55 µg/g (dry solid), measured via HPLC. It was also found that pretreatment with UAE did not significantly change the total lycopene yield but increased the *cis*-lycopene content.

The encapsulation of lycopene was evaluated to protect the lycopene from oxidation by the external environment (temperature, light, pH, oxygen), which can cause it to

lose its activity and efficacy during storage. Regarding all, when we talk about the type of product, the liquid product has a great disadvantage, that of the potential growth of microorganisms, resulting in possible harm to the consumer's health. There are also special problems for transportation. On the other hand, with regard to solid products, they have no such disadvantages, as they generally have a low moisture content, low water activity, lower volume, and weight. As for, however, the two solid products, obtained by spray drying and SAA, the diameter of particles produced by SAA is much smaller than those obtained by spray drying. Another difference consists in the type of process: in spray drying, the product goes quickly from high to low temperature (in fact, the product immediately collects in the container at low temperature). Indeed, for the SAA process, the product remains in the high-temperature dryer cell all the time. As known, lycopene is very sensitive to temperature, so the SAA method is not suggested, because the largest part of lycopene will be degraded. As for the two spray drying products (one dried directly at 135°C and one obtained by drying the emulsion at 170°C), the former is definitely much richer in lycopene than the other. About all, between the two products (liquid and solid), it is difficult to say which method is better, as one must also consider the type of use of the final product.

Future Research Perspectives:

For the extraction part, future research may focus on exploring green solvents, renewable energy, and low-energy production processes to ensure that the research has minimal ecological impact. Explore the development and optimization of new extraction technologies, such as nanomaterial-assisted extraction. By applying these advanced methods, that aim to improve the efficiency and quality of lycopene extraction while minimizing adverse environmental impacts.

For the encapsulation, almost all studies selected the encapsulation method based on past research on similar substances or the availability and cost of equipment. Future research may focus on the effect of microencapsulation on the stability of bioactive substances in the gastrointestinal environment and the release of bioactive substances into the gastrointestinal system including in vivo absorption, transport and targeted release to ensure minimal toxicity and more good bioavailability.

FIGURE

Figure 1. Production/yield quantities of tomatoes in world 1994-2021 (FAO). 1
Figure 2. Average production quantities of tomatoes by country in 2022 [3]. 2
Figure 3. PLE system adapted from [91-93]. (a) Static mode; (b) Dynamic mode. SR, solvent reservoir; FI, flow indicator; PI, pressure indicator; SV, selecting valve; EC, extraction cell; C, cooler system; PV, pressure valve; INV, inlet needle valve; OV, outlet needle valve; R, restrictor. 11
Figure 4. Sketch of the SFE plant. 14
Figure 5. Tomato waste (peels and seeds) thawed, dried and ground..... 23
Figure 6. Mean of cumulative mass fraction (F) of overflow as function of the mean diameter of each interval (D). 30
Figure 7. Solid-liquid multivariate extractor. a) HPLC pump b) A computer that can display and adjust pressure and flow; c) Ultrasonic reactor; d) Reaction vessel; e) Constant temperature water bath; f) Reaction cells. P, pressure sensor; T, temperature sensor. 37
Figure 8. MW multimodal reactor: SynthWAVE, Milestone, Bergamo, Italy. 41
Figure 9. Yield of lycopene vs temperature with 25 min of extraction time using sunflower seed oil and liquid-to-solid ratio equal to 20/3 mL/g by SLE. LE, lycopene equivalents. 45
Figure 10. Yield of lycopene vs liquid-to-solid ratio with 25 min of extraction time and at 45 °C using sunflower seed oil by SLE. LE, lycopene equivalents. 46
Figure 11. Yield of lycopene vs time that extracted at 45 °C using sunflower seed oil and liquid-to-solid ratio was 20/3 mL/g by SLE. LE, lycopene equivalents. 47
Figure 12. Surface plots of desirability as a function of the input variables: temperature (T), time (t), ultra-sound amplitude (A), on/off pulsed ratio (on), liquid-to-solid ratio (L/S), and volume (V). 55
Figure 13. Chromatogram under optimal condition of UAE analysed by using HPLC Agilent 1100 series..... 56
Figure 14. Surface plots of: (a) total carotenoid yield (TC); (b) antiradical power (ARP); and (c,d) lycopene yield as functions of amplitude (A) and total volume (V). 58

Figure 15. Desirability values for the input and response variables. T, temperature; t, time; L/S, liquid to solid ratio; A, amplitude; on, time working of UAE probe; V, volume; TC, carotenoid content; LY, lycopene content; ARP, antiradical power.....59
Figure 16. Yield of total lycopene extracted with ultrasound-assisted extraction (UAE) at different frequencies for 20 min.....60
Figure 17. Surface plots of lycopene yield as function of the input variables: a) on/off pulsed ratio (on, s) and temperature (°C), b) liquid-to-solid ratio (mL/g) and on/off pulsed ratio (on, s), c) liquid-to-solid ratio (mL/g) and temperature (°C). 62
Figure 18. Chromatogram of Optimal condition of SoLVE analysed by using HPLC Agilent 1100 series.....63
Figure 19. Surface plots of inhibition as function of liquid-to-solid ratio (L/S) and temperature (°C).....63
Figure 20. Relationship between inhibition and lycopene concentration under different conditions. 65
Figure 21. Extraction kinetics of lycopene under different experimental conditions fitted by the Peleg's model. 69
Figure 22. Surface plots of k1 as functions of the input variable of time (min) and temperature (°C).....71
Figure 23. Surface plots of k2 as functions of the input variables: a) temperature (°C) and on/off pulsed ratio (on), b) time (min) and on/off pulsed ratio (on).....72
Figure 24. Trans-lycopene isomer percentage in the extract composition and extraction time under different conditions. 73
Figure 25. Trans-lycopene conditions.....74
Figure 26. The calculation of parameters K_1 and K_2 of Peleg's model and fit the extraction kinetic model R^2.....74
Figure 27. Extraction kinetics of lycopene at the best conditions for 3h fitted to the Peleg's model.....75
Figure 28. Relationship between inhibition and lycopene concentration under the best conditions for 3h.....75
Figure 29. Trans-lycopene content and extraction time under the best conditions for 3h.....75
Figure 30. Tomato waste. a) without extraction, b) after 3 hours extraction with ethanol. 76

Figure 31. The lightness, redness and yellowness of TW before (a) and after extraction (b) (The X-axis is the solvent flow direction from 1 [in] to 15 [out]). 77
Figure 32. Association between color parameters and lycopene concentration. a) L* vs lycopene concentration, b) a* vs lycopene concentration, c) b* vs lycopene concentration. 79
Figure 33. Yield of total lycopene by microwave-assisted extraction under pressure with two different solvents at different times by MASE. 79
Figure 34. Yield of total lycopene by microwave-assisted extraction under pressure with three different solvents for 10 min by MASE. 80
Figure 35. Yield of total lycopene by microwave-assisted extraction or combined with ultrasound-assisted extraction under pressure using ethanol as solvents at different temperature and times. 81
Figure 36. Chromatogram of MASE at condition of UAE + MASE (ethanol as solvent for 20 min) analysed by using HPLC Agilent 1100 series. 81
Figure 37. The content of trans-lycopene obtained under different extraction methods and conditions. 82
Figure 38. Yield of trans-lycopene by microwave-assisted extraction under pressure with two different solvents at different times. 83
Figure 39. Yield of trans-lycopene by microwave-assisted extraction or combined with ultrasound-assisted extraction under pressure using ethanol as solvent at different temperatures and times. 84
Figure 40. Yield of total lycopene by different methods of extraction and solvents at different temperatures and times. 85
Figure 41. Dry extracts by different methods and solvents at different temperatures and times. 85
Figure 42. Nanoemulsion production process flow chart and some details are displayed. 93
Figure 43. Macro/micro-level photo of empty and loaded nanoemulsions. (a) the empty nanoemulsion (on the left) and the loaded nanoemulsion lycopene enriched extract (on the right); (b) and (c) optical microscope images of empty and loaded nanoemulsions. 98
Figure 44. Droplet diameter of empty and loaded nanoemulsions at different conditions. 100

Figure 45. Empty emulsions physical stability evaluated at a) 4 °C, b) 25 °C and c) 37 °C for 90 days. 101
Figure 46. Stability of lycopene content during time in 14g lycopene extract loaded in nanoemulsions at different temperatures; (b) Physical stability of 14g lycopene extract loaded in nanoemulsion during time at different temperatures. 103
Figure 47. Visual appearance of empty nanoemulsion and nanoemulsion loaded with lycopene extract in ethanol by UAE after 3 months at 4 °C, 25 °C and 37 °C of storage. 103
Figure 48. The stability of nanoemulsion droplet diameter with different O/W ratio at 4 °C for a month. Different letters within the same series indicate significant differences among data ($p<0.05$, Tukey HSD Test) 104
Figure 49. The stability of nanoemulsion droplet diameter with different O/W ratio at 4 °C for a month. Different letters within the same series indicate significant differences among data ($p<0.05$, Tukey HSD Test) 105
Figure 50. The stability of nanoemulsion loaded lycopene droplet diameter with different O/W ratio at 4 °C for a month. Different letters within the same series indicate significant differences among data ($p<0.05$, Tukey HSD Test) 105
Figure 51. The stability of nanoemulsion loaded lycopene droplet diameter with different O/W ratio at 25 °C for a month. Different letters within the same series indicate significant differences among data ($p<0.05$, Tukey HSD Test). 105
Figure 52. Stability of lycopene in nanoemulsions with different O/W ratios at 4 °C for a month. 106
Figure 53. Stability of lycopene in nanoemulsions with different O/W ratios at 25 °C for a month. 106
Figure 54. Scheme of spray dryer used for microencapsulation experiments. (1) Liquid feed; (2) peristaltic pump; (3) two-fluid nozzle; (4) drying vessel; (5) thermocouple for outlet temperature detection; (6) cyclone; (7) collection vessel; (8) filter. Adapted from BÜCHI mini spray dryer B-290 operation manual. 108
Figure 55. Inlet and outlet temperatures recorded over time during spray drying test. 113
Figure 56. FESEM image of maltodextrin particles at different magnification for sample D7 116

Figure 57. FESEM images of spray drying nanoemulsions produced with different coating agent: (a) Maltodextrin 2000X; (b) Inulin 2000X; (c) Gum Arabic 2000X; (d) Pectin 2000X; (e) PVP 2000X; (f) Whey 2000X, (g) Maltodextrin 5000X, (h) Dried powder for lycopene-loaded nanoemulsions with maltodextrin. 118
Figure 58. From emulsion to powder and back to emulsion steps. A) loaded nanoemulsion with 40 % (w/w) of maltodextrin, B) dried powder, C) water, D) nanoemulsion rehydration. 119
Figure 59. Granulometric data of a) of lycopene-loaded nanoemulsions; b) spray drying product; c) emulsion after rehydration. 120
Figure 60. A sketch of supercritical assisted atomization (SAA) [272]. 121
Figure 61. A sketch of the SAA laboratory plant. S1, S2, and S3: CO_2 supply, nitrogen supply, and liquid solution supply; P1 and P2: pumps; RB: refrigerating bath; HB: heating bath; M: manometer; HE: heat exchanger; S: saturator; PC: precipitatvion chamber; DM: dry test meter [273]. 122
Figure 62. Production images a) with arabic gum; b) with maltodextrin; c) with PVP. 124
Figure 63. SEM images of powder a) GA; b) Maltodextrin; c) PVP. 125
Figure 64. Granulometric data of a) Arabic gum; b) Maltodextrin; c) PVP. 126

TABLE

Table 1. The advantages and disadvantages of various methods for lycopene extraction [52]. 6
Table 2. Extraction of carotenoids by supercritical carbon dioxide. EtOH = ethanol; P = operating pressure; T = operating temperature; t = extraction time. 15
Table 3. The advantages and disadvantages of various methods for lycopene encapsulation. 17
Table 4. Screen opening used during the test on particle size distribution. 25
Table 5. Values of the input variables (T = temperature; t = time; L/S = liquid-to-solid ratio; on = time during which ultrasounds were applied in a cycle (ultrasounds off = 30 s); V = total extraction volume) in the Central Composite Design of the ultrasound-assisted extraction process, and experimental results of the response variables (TC = total carotenoid yield; LY = lycopene yield; ARP = antiradical power). Data are reported as mean value of triplicate analyses ± standard deviation. 48
Table 6. Model coefficients and significance for total carotenoid yield (TC) as a function of input variables and analysis of variance. 50
Table 7. Model coefficients and significance for lycopene yield (LY) as a function of input variables and analysis of variance. 51
Table 8. Model coefficients and significance for antiradical power (ARP) as a function of input variables and analysis of variance. 53
Table 9. Results of numerical optimization and experimental verification. T, temperature; t, time; L/S, liquid to solid ratio; A, amplitude; on, time working of UAE probe; V, volume; TC, carotenoid content; LY, lycopene content; ARP, antiradical power. 59
Table 10. Analysis of variance (ANOVA) for reduced quadratic model for optimization of extraction parameters based on yield of lycopene. 62
Table 11. Analysis of variance (ANOVA) for reduced quadratic model for optimization of extraction parameters based on inhibition. 64
Table 12. Calculated parameters of Peleg's model at different extraction conditions. 67

Table 13. Analysis of variance (ANOVA) for reduced quadratic model for optimization of extraction parameters based on K_1. 70
Table 14. Analysis of variance (ANOVA) for reduced 2FI model for optimization of extraction parameters based on K_2. 71
Table 15. Overall mass balance of biomass after the extraction process of MASE at the best conditions (L/S = 72 mL/g, V =30 mL, T(beginning) = 25 °C, P(beginning) =15 bar, t(extraction) = 20 min t(pre-heat)= 5 min, Stirrer = 80 %). 86
Table 16. Decision Matrix for select the best method of lycopene extraction. 88
Table 17. Emulsions production conditions and results in terms of granulometric data. (-) None or not measured. 99
Table 18. Model for total carotenoid yield (TC) as a function of input variables and analysis of variance. 113
Table 19. Preliminary spray drying tests of nanoemulsion (sample L6) using maltodextrin as coating agent. 115
Table 20. Characteristics of nanoemulsion and product recovery of spray drying with different coating agent. (-) None or not measured. 117
Table 21. Decision Matrix for select the process of lycopene encapsulation. 128

REFERENCES

1. Viuda-Martos, M.; Sanchez-Zapata, E.; Sayas-Barberá, E.; Sendra, E.; Pérez-Alvarez, J.A.; Fernández-López, J. Tomato and Tomato Byproducts. Human Health Benefits of Lycopene and Its Application to Meat Products: A Review. *Critical Reviews in Food Science and Nutrition* **2014**, *54*, 1032-1049, doi:10.1080/10408398.2011.623799.
2. Rocco, C.D.; Morabito, R. Production and logistics planning in the tomato processing industry: A conceptual scheme and mathematical model. *Computers and Electronics in Agriculture* **2016**, *127*, 763-774, doi:10.1016/j.compag.2016.08.002.
3. WPTC. Volume of tomatoes processed in different countries in 2022. https://www.wptc.to/production/.
4. Hayes, W.A.; Smith, P.G.; Morris, A.E.J. The Production and Quality of Tomato Concentrates. *Critical Reviews in Food Science and Nutrition* **1998**, *38*, 537-564, doi:10.1080/10408699891274309.
5. Shi, J.; Le Maguer, M. Lycopene in tomatoes: chemical and physical properties affected by food processing. *Crit Rev Food Sci Nutr* **2000**, *40*, 1-42, doi:10.1080/10408690091189275.
6. Panno, S.; Davino, S.; Caruso, A.G.; Bertacca, S.; Crnogorac, A.; Mandic, A.; Noris, E.; Matic, S. A Review of the Most Common and Economically Important Diseases That Undermine the Cultivation of Tomato Crop in the Mediterranean Basin. *Agronomy-Basel* **2021**, *11*, doi:ARTN 218810.3390/agronomy11112188.
7. Del Valle, M.; Cámara, M.; Torija, M.-E. Chemical characterization of tomato pomace. *Journal of the Science of Food and Agriculture* **2006**, *86*, 1232-1236, doi:10.1002/jsfa.2474.
8. Gheonea, I.; Aprodu, I.; Circiumaru, A.; Rapeanu, G.; Bahrim, G.E.; Stanciuc, N. Microencapsulation of lycopene from tomatoes peels by complex coacervation and freeze-drying: Evidences on phytochemical profile, stability and food applications. *J Food Eng* **2021**, *288*, doi:ARTN 11016610.1016/j.jfoodeng.2020.110166.
9. Carle, A.S.F.C.S.R. By-products of plant food processing as a source of functional compounds — recent developments. *Trends in Food Science & Technology* **2001**, *12*, 401-413, doi:10.1016/S0924-2244(02)00012-2.
10. Ascenso, A.; Pinho, S.; Eleuterio, C.; Praca, F.G.; Bentley, M.V.L.B.; Oliveira, H.; Santos, C.; Silva, O.; Simoes, S. Lycopene from Tomatoes: Vesicular Nanocarrier Formulations for Dermal Delivery. *J Agr Food Chem* **2013**, *61*, 7284-7293, doi:10.1021/jf401368w.
11. Khachik, F.; Pfander, H.; Traber, B. Proposed mechanisms for the formation of synthetic and naturally occurring metabolites of lycopene in tomato products and human serum. *J Agr Food Chem* **1998**, *46*, 4885-4890, doi:DOI 10.1021/jf9803233.
12. Shen, R.P.; Jiang, X.Y.; Ye, W.D.; Song, X.H.; Liu, L.; Lao, X.J.; Wu, C.L. A novel and practical synthetic route for the total synthesis of lycopene. *Tetrahedron* **2011**, *67*, 5610-5614, doi:10.1016/j.tet.2011.05.104.

13. McClain, R.M.; Bausch, J. Summary of safety studies conducted with synthetic lycopene. *Regul Toxicol Pharm* **2003**, *37*, 274-285, doi:10.1016/S0273-2300(03)00004-7.
14. Meeting, J.F.W.E.C.o.F.A.; Organization, W.H. *Evaluation of Certain Food Additives and Contaminants: Sixty-Seventh Report of the Joint FAO/WHO Expert Committee on Food Additives*; World Health Organization: 2007; Volume 67.
15. Starmans, T.B.S.E.D.A.J. Supercritical CO2 Extraction of β-Carotene and Lycopene from Tomato Paste Waste. *J. Agric. Food Chem.* **2000**, *48*, 5507-5511, doi:10.1021/jf000311t.
16. Frusciante, L.; Carli, P.; Ercolano, M.R.; Pernice, R.; Di Matteo, A.; Fogliano, V.; Pellegrini, N. Antioxidant nutritional quality of tomato. *Mol Nutr Food Res* **2007**, *51*, 609-617, doi:10.1002/mnfr.200600158.
17. Romão, M.F.M.D.R.C.D.C. The basis of a policy for minimizing and recycling food waste. *Environmental Science & Policy* **2002**, *5*, 247-253, doi:10.1016/s1462-9011(02)00036-9
18. Kalogeropoulos, N.; Chiou, A.; Pyriochou, V.; Peristeraki, A.; Karathanos, V.T. Bioactive phytochemicals in industrial tomatoes and their processing byproducts. *LWT - Food Science and Technology* **2012**, *49*, 213-216, doi:10.1016/j.lwt.2011.12.036.
19. Peschel, W.; Sanchez-Rabaneda, F.; Diekmann, W.; Plescher, A.; Gartzia, I.; Jimenez, D.; Lamuela-Raventos, R.; Buxaderas, S.; Codina, C. An industrial approach in the search of natural antioxidants from vegetable and fruit wastes. *Food Chemistry* **2006**, *97*, 137-150, doi:10.1016/j.foodchem.2005.03.033.
20. Wang, H.; Wang, S.; Zhu, H.; Wang, S.; Xing, J. Inclusion Complexes of Lycopene and beta-Cyclodextrin: Preparation, Characterization, Stability and Antioxidant Activity. *Antioxidants (Basel)* **2019**, *8*, doi:10.3390/antiox8080314.
21. George, B.; Kaur, C.; Khurdiya, D.S.; Kapoor, H.C. Antioxidants in tomato (Lycopersium esculentum) as a function of genotype. *Food Chemistry* **2004**, *84*, 45-51, doi:10.1016/S0308-8146(03)00165-1.
22. Ha, T.V.; Kim, S.; Choi, Y.; Kwak, H.S.; Lee, S.J.; Wen, J.; Oey, I.; Ko, S. Antioxidant activity and bioaccessibility of size-different nanoemulsions for lycopene-enriched tomato extract. *Food Chem* **2015**, *178*, 115-121, doi:10.1016/j.foodchem.2015.01.048.
23. Ferdosh, S.; Sarker, M.Z.I.; Abd Rahman, N.N.N.; Selamat, J.; Karim, M.R.; Razak, T.A.; Abd Kadir, M.O. Fish Oil Recovery from Viscera of Indian Mackerel (Rastrelliger kanagurta) by Supercritical Fluid: An Optimization Approach. *Journal of the Chinese Chemical Society* **2012**, *59*, 1421-1429, doi:10.1002/jccs.201100235.
24. Sharma, S.K.; LeMaguer, M. Lycopene in tomatoes and tomato pulp fraction. *Ital J Food Sci* **1996**, *8*, 107-113.
25. Dumas, Y.; Dadomo, M.; Di Lucca, G.; Grolier, P. Effects of environmental factors and agricultural techniques on antioxidantcontent of tomatoes. *Journal of the Science of Food and Agriculture* **2003**, *83*, 369-382, doi:10.1002/jsfa.1370.
26. Choudhari, S.M.; Ananthanarayan, L. Enzyme aided extraction of lycopene from tomato tissues. *Food Chemistry* **2007**, *102*, 77-81, doi:10.1016/j.foodchem.2006.04.031.

27. Kalogeropoulos, N.; Chiou, A.; Pyriochou, V.; Peristeraki, A.; Karathanos, V.T. Bioactive phytochemicals in industrial tomatoes and their processing byproducts. *Lwt-Food Sci Technol* **2012**, *49*, 213-216, doi:10.1016/j.lwt.2011.12.036.
28. Herrera, P.G.; Sanchez-Mata, M.C.; Camara, M. Nutritional characterization of tomato fiber as a useful ingredient for food industry. *Innov Food Sci Emerg* **2010**, *11*, 707-711, doi:10.1016/j.ifset.2010.07.005.
29. Cetkovic, G.; Savatovic, S.; Canadanovic-Brunet, J.; Djilas, S.; Vulic, J.; Mandic, A.; Cetojevic-Simin, D. Valorisation of phenolic composition, antioxidant and cell growth activities of tomato waste. *Food Chemistry* **2012**, *133*, 938-945, doi:10.1016/j.foodchem.2012.02.007.
30. Toor, R.K.; Savage, G.P. Antioxidant activity in different fractions of tomatoes. *Food Res Int* **2005**, *38*, 487-494, doi:10.1016/j.foodres.2004.10.016.
31. Alwandawi, H.; Abdulrahman, M.; Alshaikhly, K. Tomato Processing Wastes as Essential Raw-Materials Source. *J Agr Food Chem* **1985**, *33*, 804-807, doi:DOI 10.1021/jf00065a009.
32. Topal, U.; Sasaki, M.; Goto, M.; Hayakawa, K. Extraction of lycopene from tomato skin with supercritical carbon dioxide: Effect of operating conditions and solubility analysis. *J Agr Food Chem* **2006**, *54*, 5604-5610, doi:10.1021/jf0606407.
33. Knoblich, M.; Anderson, B.; Latshaw, D. Analyses of tomato peel and seed byproducts and their use as a source of carotenoids. *Journal of the Science of Food and Agriculture* **2005**, *85*, 1166-1170, doi:10.1002/jsfa.2091.
34. Fierascu, R.C.; Fierascu, I.; Avramescu, S.M.; Sieniawska, E. Recovery of Natural Antioxidants from Agro-Industrial Side Streams through Advanced Extraction Techniques. *Molecules* **2019**, *24*, 4212, doi:10.3390/molecules24234212.
35. Beltrán-Ramírez, F.; Orona-Tamayo, D.; Cornejo-Corona, I.; González-Cervantes, J.L.N.; Esparza-Claudio, J.d.J.; Quintana-Rodríguez, E. Agro-Industrial Waste Revalorization: The Growing Biorefinery. *Biomass for Bioenergy - Recent Trends and Future Challenges* **2019**, 1-20.
36. Pettinato, M.; Trucillo, P.; Campardelli, R.; Perego, P.; Reverchon, E. Bioactives extraction from spent coffee grounds and liposome encapsulation by a combination of green technologies. *Chemical Engineering and Processing - Process Intensification* **2020**, *151*, doi:10.1016/j.cep.2020.107911.
37. Pettinato, M.; Casazza, A.A.; Ferrari, P.F.; Palombo, D.; Perego, P. Eco-sustainable recovery of antioxidants from spent coffee grounds by microwave-assisted extraction: Process optimization, kinetic modeling and biological validation. *Food Bioprod Process* **2019**, *114*, 31-42, doi:10.1016/j.fbp.2018.11.004.
38. Li, J.; Pettinato, M.; Casazza, A.A.; Perego, P. A Comprehensive Optimization of Ultrasound-Assisted Extraction for Lycopene Recovery from Tomato Waste and Encapsulation by Spray Drying. *Processes* **2022**, *10*, doi:10.3390/pr10020308.
39. Nunes, A.N.; Roda, A.; Gouveia, L.F.; Fernández, N.; Bronze, M.R.; Matias, A.A. Astaxanthin Extraction from Marine Crustacean Waste Streams: An Integrate Approach between Microwaves and Supercritical Fluids. *ACS Sustainable Chemistry & Engineering* **2021**, *9*, 3050-3059, doi:10.1021/acssuschemeng.0c06534.

40. Roy, V.C.; Getachew, A.T.; Cho, Y.-J.; Park, J.-S.; Chun, B.-S. Recovery and bio-potentialities of astaxanthin-rich oil from shrimp (Penaeus monodon) waste and mackerel (Scomberomous niphonius) skin using concurrent supercritical CO2 extraction. *The Journal of Supercritical Fluids* **2020**, *159*, doi:10.1016/j.supflu.2020.104773.
41. Ferrari, P.F.; Pettinato, M.; Casazza, A.A.; De Negri Atanasio, G.; Palombo, D.; Perego, P. Polyphenols from Nerone Gold 26/6, a new pigmented rice, via non-conventional extractions: antioxidant properties and biological validation. *Journal of Chemical Technology & Biotechnology* **2021**, *96*, 1691-1699, doi:10.1002/jctb.6694.
42. Spennati, E.; Mirizadeh, S.; Casazza, A.A.; Solisio, C.; Converti, A. Chlorella vulgaris and Arthrospira platensis growth in a continuous membrane photobioreactor using industrial winery wastewater. *Algal Research* **2021**, *60*, doi:10.1016/j.algal.2021.102519.
43. Aliakbarian, B.; Casazza, A.A.; Montoya, E.J.O.; Convert, A. Valorisation of Olive Oil Solid Wastes: Valuable Compounds Recovery Using High Pressure-High Temperature. *Journal of Biotechnology* **2010**, *150*, 332-332, doi:10.1016/j.jbiotec.2010.09.341.
44. Casazza, A.A.; Pettinato, M.; Perego, P. Polyphenols from apple skins: A study on microwave-assisted extraction optimization and exhausted solid characterization. *Sep Purif Technol* **2020**, *240*, doi:10.1016/j.seppur.2020.116640.
45. Ruiz-Domínguez, M.C.; Fuentes, J.L.; Mendiola, J.A.; Cerezal-Mezquita, P.; Morales, J.; Vílchez, C.; Ibáñez, E. Bioprospecting of cyanobacterium in Chilean coastal desert, Geitlerinema sp. molecular identification and pressurized liquid extraction of bioactive compounds. *Food Bioprod Process* **2021**, *128*, 227-239, doi:10.1016/j.fbp.2021.06.001.
46. Rozzi, N.L.; Singh, R.K.; Vierling, R.A.; Watkins, B.A. Supercritical fluid extraction of lycopene from tomato processing byproducts. *J Agr Food Chem* **2002**, *50*, 2638-2643, doi:10.1021/jf011001t.
47. Periago, M.J.; Rincon, F.; Aguera, M.D.; Ros, G. Mixture approach for optimizing lycopene extraction from tomato and tomato products. *J Agr Food Chem* **2004**, *52*, 5796-5802, doi:10.1021/jf049345h.
48. Strati, I.F.; Oreopoulou, V. Effect of extraction parameters on the carotenoid recovery from tomato waste. *Int J Food Sci Tech* **2011**, *46*, 23-29, doi:10.1111/j.1365-2621.2010.02496.x.
49. Leoni, C. Focus on Lycopene. *Acta Horticultutae* **2003**, *613*, 357-363, doi:10.17660/ActaHortic.2003.613.58
50. Carpentieri, S.; Mazza, L.; Nutrizio, M.; Jambrak, A.R.; Ferrari, G.; Pataro, G. Pulsed electric fields- and ultrasound-assisted green extraction of valuable compounds from Origanum vulgare L. and Thymus serpyllum L. *Int J Food Sci Tech* **2021**, *56*, 4834-4842, doi:10.1111/ijfs.15159.
51. Wani, F.A.; Rashid, R.; Jabeen, A.; Brochier, B.; Yadav, S.; Aijaz, T.; Makroo, H.A.; Dar, B.N. Valorisation of food wastes to produce natural pigments using non-thermal novel extraction methods: a review. *Int J Food Sci Tech* **2021**, *56*, 4823-4833, doi:10.1111/ijfs.15267.
52. Deng, Y.; Zhao, S.N.; Yang, X.L.; Hou, F.R.; Fan, L.H.; Wang, W.J.; Xu, E.B.; Cheng, H.; Guo, M.M.; Liu, D.H. Evaluation of extraction technologies of lycopene: Hindrance of extraction, effects on isomerization and comparative

analysis-A review. *Trends in Food Science & Technology* **2021**, *115*, 285-296, doi:10.1016/j.tifs.2021.06.051.

53. Khaw, K.Y.; Parat, M.O.; Shaw, P.N.; Falconer, J.R. Solvent Supercritical Fluid Technologies to Extract Bioactive Compounds from Natural Sources: A Review. *Molecules* **2017**, *22*, 1186, doi:10.3390/molecules22071186.
54. Belwal, T.; Chemat, F.; Venskutonis, P.R.; Cravotto, G.; Jaiswal, D.K.; Bhatt, I.D.; Devkota, H.P.; Luo, Z. Recent advances in scaling-up of non-conventional extraction techniques: Learning from successes and failures. *TrAC Trends in Analytical Chemistry* **2020**, *127*, 115895, doi:10.1016/j.trac.2020.115895.
55. Naviglio, D.; Scarano, P.; Ciaravolo, M.; Gallo, M. Rapid Solid-Liquid Dynamic Extraction (RSLDE): A Powerful and Greener Alternative to the Latest Solid-Liquid Extraction Techniques. *Foods* **2019**, *8*, doi:ARTN 245 10.3390/foods8070245.
56. G. SADLER, J.D., D. DEZMAN. Rapid Extraction of Lycopene and β-Carotene from Reconstituted Tomato Paste and Pink Grapefruit Homogenates. *J Food Sci* **1990**, *55*, 1460-1461, doi:10.1111/j.1365-2621.1990.tb03958.x.
57. Cardenas-Toro, F.P.; Alcazar-Alay, S.C.; Coutinho, J.P.; Godoy, H.T.; Forster-Carneiro, T.; Meireles, M.A.A. Pressurized liquid extraction and low-pressure solvent extraction of carotenoids from pressed palm fiber: Experimental and economical evaluation. *Food Bioprod Process* **2015**, *94*, 90-100, doi:10.1016/j.fbp.2015.01.006.
58. Ashraf, W.; Latif, A.; Zhang, L.F.; Jian, Z.; Wang, C.Q.; Rehman, A.; Hussain, A.; Siddiquy, M.; Karim, A. Technological Advancement in the Processing of Lycopene: A Review. *Food Rev Int* **2022**, *38*, 857-883, doi:10.1080/87559129.2020.1749653.
59. Bakhshabadi, H.; Mirzaei, H.; Ghodsvali, A.; Jafari, S.M.; Ziaiifar, A.M.; Farzaneh, V. The effect of microwave pretreatment on some physico-chemical properties and bioactivity of Black cumin seeds' oil. *Ind Crop Prod* **2017**, *97*, 1-9, doi:10.1016/j.indcrop.2016.12.005.
60. Madia, V.N.; De Vita, D.; Ialongo, D.; Tudino, V.; De Leo, A.; Scipione, L.; Roberto, S.; Costi, R.; Messore, A. Recent Advances in Recovery of Lycopene from Tomato Waste: A Potent Antioxidant with Endless Benefits. *Molecules* **2021**, *26*, doi:ARTN 449510.3390/molecules26154495.
61. Rahimi, S.; Mikani, M. Lycopene green ultrasound-assisted extraction using edible oil accompany with response surface methodology (RSM) optimization performance: Application in tomato processing wastes. *Microchem J* **2019**, *146*, 1033-1042, doi:10.1016/j.microc.2019.02.039.
62. Wang, X.J.; Du, X.D.; Sun, F.L.; Yuan, L. Isolation of Lycopene from Tomato using Microwave-assisted Extraction. *Text Bioeng Inform S* **2014**, 82-88.
63. Zuorro, A.; Fidaleo, M.; Lavecchia, R. Enzyme-assisted extraction of lycopene from tomato processing waste. *Enzyme Microb Tech* **2011**, *49*, 567-573, doi:10.1016/j.enzmictec.2011.04.020.
64. Ranveer, R.C.; Patil, S.N.; Sahoo, A.K. Effect of different parameters on enzyme-assisted extraction of lycopene from tomato processing waste. *Food Bioprod Process* **2013**, *91*, 370-375, doi:10.1016/j.fbp.2013.01.006.
65. Naviglio, D. Naviglio's principle and presentation of an innovative solid-liquid extraction technology: Extractor Naviglio (R). *Anal Lett* **2003**, *36*, 1647-1659, doi:10.1081/Al-120021555.

66. Zhang, L.F.; Liu, Z.L. Optimization and comparison of ultrasound/microwave assisted extraction (UMAE) and ultrasonic assisted extraction (UAE) of lycopene from tomatoes. *Ultrason Sonochem* **2008**, *15*, 731-737, doi:10.1016/j.ultsonch.2007.12.001.
67. Ho, K.K.H.Y.; Ferruzzi, M.G.; Liceaga, A.M.; Martin-Gonzalez, M.F.S. Microwave-assisted extraction of lycopene in tomato peels: Effect of extraction conditions on all-trans and cis-isomer yields. *Lwt-Food Sci Technol* **2015**, *62*, 160-168, doi:10.1016/j.lwt.2014.12.061.
68. Kingston, H.M.; Jassie, L.B.; American Chemical, S. *Introduction to microwave sample preparation : theory and practice*; American Chemical Society: Washington, DC, 1988; pp. xxii, 263 p. : ill.
69. Subhedar, P.B.; Gogate, P.R. Enhancing the activity of cellulase enzyme using ultrasonic irradiations. *J Mol Catal B-Enzym* **2014**, *101*, 108-114, doi:10.1016/j.molcatb.2014.01.002.
70. Amiri-Rigi, A.; Abbasi, S.; Scanlon, M.G. Enhanced lycopene extraction from tomato industrial waste using microemulsion technique: Optimization of enzymatic and ultrasound pre-treatments. *Innov Food Sci Emerg* **2016**, *35*, 160-167, doi:10.1016/j.ifset.2016.05.004.
71. Silva, Y.P.A.; Ferreira, T.A.P.C.; Celli, G.B.; Brooks, M.S. Optimization of Lycopene Extraction from Tomato Processing Waste Using an Eco-Friendly Ethyl Lactate-Ethyl Acetate Solvent: A Green Valorization Approach. *Waste Biomass Valori* **2019**, *10*, 2851-2861, doi:10.1007/s12649-018-0317-7.
72. Kumcuoglu, S.; Yilmaz, T.; Tavman, S. Ultrasound assisted extraction of lycopene from tomato processing wastes. *J Food Sci Tech Mys* **2014**, *51*, 4102-4107, doi:10.1007/s13197-013-0926-x.
73. Andreu, V.; Picó, Y. Pressurized liquid extraction of organic contaminants in environmental and food samples. *TrAC Trends in Analytical Chemistry* **2019**, *118*, 709-721, doi:10.1016/j.trac.2019.06.038.
74. Carabias-Martinez, R.; Rodriguez-Gonzalo, E.; Revilla-Ruiz, P.; Hernandez-Mendez, J. Pressurized liquid extraction in the analysis of food and biological samples. *J Chromatogr A* **2005**, *1089*, 1-17, doi:10.1016/j.chroma.2005.06.072.
75. Dobrincic, A.; Balbino, S.; Zoric, Z.; Pedisic, S.; Bursac Kovacevic, D.; Elez Garofulic, I.; Dragovic-Uzelac, V. Advanced Technologies for the Extraction of Marine Brown Algal Polysaccharides. *Mar Drugs* **2020**, *18*, 168, doi:10.3390/md18030168.
76. Mustafa, A.; Turner, C. Pressurized liquid extraction as a green approach in food and herbal plants extraction: A review. *Anal Chim Acta* **2011**, *703*, 8-18, doi:10.1016/j.aca.2011.07.018.
77. Richter, B.E.; Jones, B.A.; Ezzell, J.L.; Porter, N.L. Accelerated Solvent Extraction: A Technique for Sample Preparation. *Angewandte Chemie* **1996**, *68*, 1033-1039.
78. Hawthorne, S.B.; Grabanski, C.B.; Martin, E.; Miller, D.J. Comparisons of Soxhlet extraction, pressurized liquid extraction, supercritical fluid extraction and subcritical water extraction for environmental solids: recovery, selectivity and effects on sample matrix. *Journal of Chromatography A* **2000**, *892*, 421-433.
79. Schantz, M.M. Pressurized liquid extraction in environmental analysis. *Anal Bioanal Chem* **2006**, *386*, 1043-1047, doi:10.1007/s00216-006-0648-2.

80. Aguilar, L.; Williams, E.S.; Brooks, B.W.; Usenko, S. Development and application of a novel method for high-throughput determination of PCDD/Fs and PCBs in sediments. *Environ Toxicol Chem* **2014**, *33*, 1529-1536, doi:10.1002/etc.2579.
81. Santos, P.H.; Kammers, J.C.; Silva, A.P.; Oliveira, J.V.; Hense, H. Antioxidant and antibacterial compounds from feijoa leaf extracts obtained by pressurized liquid extraction and supercritical fluid extraction. *Food Chem* **2021**, *344*, 128620, doi:10.1016/j.foodchem.2020.128620.
82. Herrero, M.; Sánchez-Camargo, A.d.P.; Cifuentes, A.; Ibáñez, E. Plants, seaweeds, microalgae and food by-products as natural sources of functional ingredients obtained using pressurized liquid extraction and supercritical fluid extraction. *TrAC Trends in Analytical Chemistry* **2015**, *71*, 26-38, doi:10.1016/j.trac.2015.01.018.
83. Gfrerer, M.; Chen, S.; Lankmayr, E.P.; Quan, X.; Yang, F. Comparison of different extraction techniques for the determination of chlorinated pesticides in animal feed. *Anal Bioanal Chem* **2004**, *378*, 1861-1867, doi:10.1007/s00216-004-2492-6.
84. Celeiro, M.; Llompart, M.; Lamas, J.P.; Lores, M.; Garcia-Jares, C.; Dagnac, T. Determination of fungicides in white grape bagasse by pressurized liquid extraction and gas chromatography tandem mass spectrometry. *J Chromatogr A* **2014**, *1343*, 18-25, doi:10.1016/j.chroma.2014.03.057.
85. Sumere, B.R.; de Souza, M.C.; Dos Santos, M.P.; Bezerra, R.M.N.; da Cunha, D.T.; Martinez, J.; Rostagno, M.A. Combining pressurized liquids with ultrasound to improve the extraction of phenolic compounds from pomegranate peel (Punica granatum L.). *Ultrason Sonochem* **2018**, *48*, 151-162, doi:10.1016/j.ultsonch.2018.05.028.
86. Santos, M.P.; Souza, M.C.; Sumere, B.R.; da Silva, L.C.; Cunha, D.T.; Bezerra, R.M.N.; Rostagno, M.A. Extraction of bioactive compounds from pomegranate peel (Punica granatum L.) with pressurized liquids assisted by ultrasound combined with an expansion gas. *Ultrason Sonochem* **2019**, *54*, 11-17, doi:10.1016/j.ultsonch.2019.02.021.
87. Rostagno, M.A.; Palma, M.; Barroso, C.G. Pressurized liquid extraction of isoflavones from soybeans. *Analytica Chimica Acta* **2004**, *522*, 169-177, doi:10.1016/j.aca.2004.05.078.
88. Jiang, Y.; Li, P.; Li, S.P.; Wang, Y.T.; Tu, P.F. Optimization of pressurized liquid extraction of five major flavanoids from Lysimachia clethroide. *J Pharm Biomed Anal* **2007**, *43*, 341-345, doi:10.1016/j.jpba.2006.06.030.
89. Barriada-Pereira, M.; Gonzalez-Castro, M.J.; Muniategui-Lorenzo, S.; Lopez-Mahia, P.; Prada-Rodriguez, D.; Fernandez-Fernandez, E. Comparison of pressurized liquid extraction and microwave assisted extraction for the determination of organochlorine pesticides in vegetables. *Talanta* **2007**, *71*, 1345-1351, doi:10.1016/j.talanta.2006.07.012.
90. Murakami, T.; Kawasaki, T.; Takemura, A.; Fukutsu, N.; Kishi, N.; Kusu, F. Identification of degradation products in loxoprofen sodium adhesive tapes by liquid chromatography-mass spectrometry and dynamic pressurized liquid extraction-solid-phase extraction coupled to liquid chromatography-nuclear magnetic resonance spectroscopy. *J Chromatogr A* **2008**, *1208*, 164-174, doi:10.1016/j.chroma.2008.08.076.

91. Luque-García, J.L.; Luque de Castro, M.D. Comparison of the static, dynamic and static-dynamic pressurised liquid extraction modes for the removal of nitrated polycyclic aromatic hydrocarbons from soil with on-line filtration-preconcentration. *Journal of Chromatography A* **2003**, *1010*, 129-140, doi:10.1016/s0021-9673(03)01106-3.
92. Pitipanapong, J.; Chitprasert, S.; Goto, M.; Jiratchariyakul, W.; Sasaki, M.; Shotipruk, A. New approach for extraction of charantin from Momordica charantia with pressurized liquid extraction. *Sep Purif Technol* **2007**, *52*, 416-422, doi:10.1016/j.seppur.2005.11.037.
93. Wicker, A.P.; Carlton, D.D., Jr.; Tanaka, K.; Nishimura, M.; Chen, V.; Ogura, T.; Hedgepeth, W.; Schug, K.A. On-line supercritical fluid extraction-supercritical fluid chromatography-mass spectrometry of polycyclic aromatic hydrocarbons in soil. *J Chromatogr B Analyt Technol Biomed Life Sci* **2018**, *1086*, 82-88, doi:10.1016/j.jchromb.2018.04.014.
94. Naviglio, D. Naviglio's Principle and Presentation of an Innovative Solid–Liquid Extraction Technology: Extractor Naviglio®. *Anal Lett* **2003**, *36*, 1647-1659, doi:10.1081/al-120021555.
95. Naviglio, D.; Pizzolongo, F.; Ferrara, L.; Aragòn, A.; Santini, A. Extraction of pure lycopene from industrial tomato by-products in water using a new high-pressure process. *Journal of the Science of Food and Agriculture* **2008**, *88*, 2414-2420, doi:10.1002/jsfa.3334.
96. Aliakbarian, B.; Casazza, A.A.; Perego, P. Valorization of olive oil solid waste using high pressure–high temperature reactor. *Food Chemistry* **2011**, *128*, 704-710, doi:10.1016/j.foodchem.2011.03.092.
97. Chienthavorn, O.; Insuan, W. Superheated Water Extraction of Lime Peel: a Comparison with Conventional Methods. *Anal Lett* **2004**, *37*, 2393-2409, doi:10.1081/al-200028189.
98. Ding, W.-H.; Fann, J.C.H. Determination of linear alkylbenzenesulfonates in sediments using pressurized liquid extraction and ion-pair derivatization gas chromatography-mass spectrometry. *Analytica Chimica Acta* **2000**, *408*, 291-297.
99. Herrera, M.C.; Prados-Rosales, R.C.; Luque-García, J.L.; Luque de Castro, M.D. Static–dynamic pressurized hot water extraction coupled to on-line filtration–solid-phase extraction–high-performance liquid chromatography–post-column derivatization–fluorescence detection for the analysis of N-methylcarbamates in foods. *Analytica Chimica Acta* **2002**, *463*, 189-197.
100. Dobrincic, A.; Pedisic, S.; Zoric, Z.; Jurin, M.; Roje, M.; Coz-Rakovac, R.; Dragovic-Uzelac, V. Microwave Assisted Extraction and Pressurized Liquid Extraction of Sulfated Polysaccharides from Fucus virsoides and Cystoseira barbata. *Foods* **2021**, *10*, 1481, doi:10.3390/foods10071481.
101. Vazquez-Roig, P.; Picó, Y. Pressurized liquid extraction of organic contaminants in environmental and food samples. *TrAC Trends in Analytical Chemistry* **2015**, *71*, 55-64, doi:10.1016/j.trac.2015.04.014.
102. Herbst, G.; Hamerski, F.; Errico, M.; L. Corazza, M. Pressurized liquid extraction of brewer's spent grain: Kinetics and crude extracts characterization. *Journal of Industrial and Engineering Chemistry* **2021**, *102*, 370-383, doi:10.1016/j.jiec.2021.07.020.

103. Pronyk, C.; Mazza, G. Design and scale-up of pressurized fluid extractors for food and bioproducts. *J Food Eng* **2009**, *95*, 215-226, doi:10.1016/j.jfoodeng.2009.06.002.
104. Osorio-Tobón, J.F.; Carvalho, P.I.N.; Rostagno, M.A.; Petenate, A.J.; Meireles, M.A.A. Extraction of curcuminoids from deflavored turmeric (Curcuma longa L.) using pressurized liquids: Process integration and economic evaluation. *The Journal of Supercritical Fluids* **2014**, *95*, 167-174, doi:10.1016/j.supflu.2014.08.012.
105. Nathia-Neves, G.; Tarone, A.G.; Tosi, M.M.; Marostica Junior, M.R.; Meireles, M.A.A. Extraction of bioactive compounds from genipap (Genipa americana L.) by pressurized ethanol: Iridoids, phenolic content and antioxidant activity. *Food Res Int* **2017**, *102*, 595-604, doi:10.1016/j.foodres.2017.09.041.
106. Aliakbarian, B.; Fathi, A.; Perego, P.; Dehghani, F. Extraction of antioxidants from winery wastes using subcritical water. *The Journal of Supercritical Fluids* **2012**, *65*, 18-24, doi:10.1016/j.supflu.2012.02.022.
107. Nastić, N.; Švarc-Gajić, J.; Delerue-Matos, C.; Morais, S.; Barroso, M.F.; Moreira, M.M. Subcritical water extraction of antioxidants from mountain germander (Teucrium montanum L.). *The Journal of Supercritical Fluids* **2018**, *138*, 200-206, doi:10.1016/j.supflu.2018.04.019.
108. da Silva, M.F.; Casazza, A.A.; Ferrari, P.F.; Aliakbarian, B.; Converti, A.; Bezerra, R.P.; Porto, A.L.F.; Perego, P. Recovery of phenolic compounds of food concern from Arthrospira platensis by green extraction techniques. *Algal Research* **2017**, *25*, 391-401, doi:10.1016/j.algal.2017.05.027.
109. Posadino, A.M.; Biosa, G.; Zayed, H.; Abou-Saleh, H.; Cossu, A.; Nasrallah, G.K.; Giordo, R.; Pagnozzi, D.; Porcu, M.C.; Pretti, L.; et al. Protective Effect of Cyclically Pressurized Solid(-)Liquid Extraction Polyphenols from Cagnulari Grape Pomace on Oxidative Endothelial Cell Death. *Molecules* **2018**, *23*, doi:10.3390/molecules23092105.
110. Derrien, M.; Aghabararnejad, M.; Gosselin, A.; Desjardins, Y.; Angers, P.; Boumghar, Y. Optimization of supercritical carbon dioxide extraction of lutein and chlorophyll from spinach by-products using response surface methodology. *Lwt* **2018**, *93*, 79-87, doi:10.1016/j.lwt.2018.03.016.
111. Casazza, A.A.; Aliakbarian, B.; Mantegna, S.; Cravotto, G.; Perego, P. Extraction of phenolics from Vitis vinifera wastes using non-conventional techniques. *J Food Eng* **2010**, *100*, 50-55, doi:10.1016/j.jfoodeng.2010.03.026.
112. Hubert, P.; Vitzthum, O.G. Fluid Extraction of Hops, Spices, and Tobacco with Supercritical Gases. *Angewandte Chemie* **1978**, *17*, 710-715.
113. Reverchon, E.; De Marco, I. Supercritical fluid extraction and fractionation of natural matter. *The Journal of Supercritical Fluids* **2006**, *38*, 146-166, doi:10.1016/j.supflu.2006.03.020.
114. Herrero, M.; Cifuentes, A.; Ibanez, E. Sub- and supercritical fluid extraction of functional ingredients from different natural sources: Plants, food-by-products, algae and microalgaeA review. *Food Chemistry* **2006**, *98*, 136-148, doi:10.1016/j.foodchem.2005.05.058.
115. Reverchon, E. Supercritical fluid extraction and fractionation of essential oils and related products. *The Journal of Supercritical Fluids* **1997**, *10*.

116. de Andrade Lima, M.; Kestekoglou, I.; Charalampopoulos, D.; Chatzifragkou, A. Supercritical Fluid Extraction of Carotenoids from Vegetable Waste Matrices. *Molecules* **2019**, *24*, 466, doi:10.3390/molecules24030466.
117. Baysal, T.; Ersus, S.; Starmans, D.A.J. Supercritical CO2 Extraction of â-Carotene and Lycopene from Tomato Paste Waste. *J Agr Food Chem* **2000**, *48*, 5507-5511.
118. Sabio, E.; Lozano, M.; Espinosa, V.M.d.; Mendes, R.L.; Pereira, A.P.; Palavra, A.F.; Coelho, J.A. Lycopene and â-Carotene Extraction from Tomato Processing Waste Using Supercritical CO2. *Industrial & Engineering Chemistry Research* **2003**, *42*, 6641-6646.
119. Longo, C.; Leo, L.; Leone, A. Carotenoids, fatty acid composition and heat stability of supercritical carbon dioxide-extracted-oleoresins. *Int J Mol Sci* **2012**, *13*, 4233-4254, doi:10.3390/ijms13044233.
120. Durante, M.; Lenucci, M.S.; Mita, G. Supercritical Carbon Dioxide Extraction of Carotenoids from Pumpkin (Cucurbita spp.): A Review. *Int J Mol Sci* **2014**, *15*, 6725-6740, doi:10.3390/ijms15046725.
121. Lenucci, M.S.; De Caroli, M.; Marrese, P.P.; Iurlaro, A.; Rescio, L.; Bohm, V.; Dalessandro, G.; Piro, G. Enzyme-aided extraction of lycopene from high-pigment tomato cultivars by supercritical carbon dioxide. *Food Chemistry* **2015**, *170*, 193-202, doi:10.1016/j.foodchem.2014.08.081.
122. Konwarh, R.; Pramanik, S.; Kalita, D.; Mahanta, C.L.; Karak, N. Ultrasonication - A complementary 'green chemistry' tool to biocatalysis: A laboratory-scale study of lycopene extraction. *Ultrason Sonochem* **2012**, *19*, 292-299, doi:10.1016/j.ultsonch.2011.07.010.
123. Ladole, M.R.; Nair, R.R.; Bhutada, Y.D.; Amritkar, V.D.; Pandit, A.B. Synergistic effect of ultrasonication and co-immobilized enzymes on tomato peels for lycopene extraction. *Ultrason Sonochem* **2018**, *48*, 453-462, doi:10.1016/j.ultsonch.2018.06.013.
124. Kha, T.C.; Nguyen, M.H.; Roach, P.D.; Stathopoulos, C.E. Ultrasound-Assisted Aqueous Extraction of Oil and Carotenoids from Microwave-Dried Gac (Momordica cochinchinensis Spreng) Aril. *Int J Food Eng* **2015**, *11*, 479-492, doi:10.1515/ijfe-2014-0220.
125. Hu, W.; Chen, S.; Wu, D.; Zhu, K.; Ye, X. Manosonication assisted extraction and characterization of pectin from different citrus peel wastes. *Food Hydrocolloid* **2021**, *121*, doi:10.1016/j.foodhyd.2021.106952.
126. de Andrades, E.O.; da Costa, J.; de Lima Neto, F.E.M.; de Araujo, A.R.; de Oliveira Silva Ribeiro, F.; Vasconcelos, A.G.; de Jesus Oliveira, A.C.; Sobrinho, J.L.S.; de Almeida, M.P.; Carvalho, A.P.; et al. Acetylated cashew gum and fucan for incorporation of lycopene rich extract from red guava (Psidium guajava L.) in nanostructured systems: Antioxidant and antitumor capacity. *Int J Biol Macromol* **2021**, *191*, 1026-1037, doi:10.1016/j.ijbiomac.2021.09.116.
127. Calvo, T.R.A.; Santagapita, P.R. Encapsulation of a free-solvent extract of lycopene in alginate-Ca(II) beads containing sugars and biopolymers. *Chem Biol Technol Ag* **2017**, *4*, doi:ARTN 1610.1186/s40538-017-0099-3.
128. Bamidele, O.P.; Emmambux, M.N. Encapsulation of bioactive compounds by "extrusion" technologies: a review. *Crit Rev Food Sci Nutr* **2021**, *61*, 3100-3118, doi:10.1080/10408398.2020.1793724.

129. Kaushik, V.; Roos, Y.H. Limonene encapsulation in freeze-drying of gum Arabic–sucrose–gelatin systems. *LWT - Food Science and Technology* **2007**, *40*, 1381-1391, doi:10.1016/j.lwt.2006.10.008.
130. Buljeta, I.; Pichler, A.; Simunovic, J.; Kopjar, M. Polysaccharides as Carriers of Polyphenols: Comparison of Freeze-Drying and Spray-Drying as Encapsulation Techniques. *Molecules* **2022**, *27*, doi:10.3390/molecules27165069.
131. Fang, Z.; Bhandari, B. Spray drying, freeze drying and related processes for food ingredient and nutraceutical encapsulation. In *Encapsulation Technologies and Delivery Systems for Food Ingredients and Nutraceuticals*; 2012; pp. 73-109.
132. Lohith Kumar, D.H.; Sarkar, P. Encapsulation of bioactive compounds using nanoemulsions. *Environmental Chemistry Letters* **2017**, *16*, 59-70, doi:10.1007/s10311-017-0663-x.
133. Zhao, C.; Wei, L.; Yin, B.; Liu, F.; Li, J.; Liu, X.; Wang, J.; Wang, Y. Encapsulation of lycopene within oil-in-water nanoemulsions using lactoferrin: Impact of carrier oils on physicochemical stability and bioaccessibility. *Int J Biol Macromol* **2020**, *153*, 912-920, doi:10.1016/j.ijbiomac.2020.03.063.
134. Wang, X.; Wang, Y.-W.; Huang, Q. Enhancing Stability and Oral Bioavailability of Polyphenols Using Nanoemulsions. In *Micro/Nanoencapsulation of Active Food Ingredients*; ACS Symposium Series; 2009; pp. 198-212.
135. Mahmood, T.; Akhtar, N.; Manickam, S. Interfacial film stabilized W/O/W nano multiple emulsions loaded with green tea and lotus extracts: systematic characterization of physicochemical properties and shelf-storage stability. *Journal of Nanobiotechnology* **2014**, *12(1)*, 20-, doi:doi:10.1186/1477-3155-12-20
136. Parthasarathy, S.; Siah Ying, T.; Manickam, S. Generation and Optimization of Palm Oil-Based Oil-in-Water (O/W) Submicron-Emulsions and Encapsulation of Curcumin Using a Liquid Whistle Hydrodynamic Cavitation Reactor (LWHCR). *Industrial & Engineering Chemistry Research* **2013**, *52*, 11829-11837, doi:10.1021/ie4008858.
137. Gutiérrez, J.M.; González, C.; Maestro, A.; Solè, I.; Pey, C.M.; Nolla, J. Nano-emulsions: New applications and optimization of their preparation. *Current Opinion in Colloid & Interface Science* **2008**, *13*, 245-251, doi:10.1016/j.cocis.2008.01.005.
138. Sarker, D.K. Engineering of Nanoemulsions for Drug Delivery. *Current Drug Delivery* **2005**, *2(4)*, doi:doi:10.2174/156720105774370267.
139. Mihranyan, A.; Ferraz, N.; Strømme, M. Current status and future prospects of nanotechnology in cosmetics. *Progress in Materials Science* **2012**, *57*, 875-910, doi:10.1016/j.pmatsci.2011.10.001.
140. Kumar, N.; Verma, A.; Mandal, A. Formation, characteristics and oil industry applications of nanoemulsions: A review. *Journal of Petroleum Science and Engineering* **2021**, *206*, doi:10.1016/j.petrol.2021.109042.
141. Silva, H.D.; Cerqueira, M.Â.; Vicente, A.A. Nanoemulsions for Food Applications: Development and Characterization. *Food and Bioprocess Technology* **2011**, *5*, 854-867, doi:10.1007/s11947-011-0683-7.

142. Gupta, A.; Eral, H.B.; Hatton, T.A.; Doyle, P.S. Nanoemulsions: formation, properties and applications. *Soft Matter* **2016**, *12*, 2826-2841, doi:10.1039/c5sm02958a.
143. Ray, S.; Raychaudhuri, U.; Chakraborty, R. An overview of encapsulation of active compounds used in food products by drying technology. *Food Biosci* **2016**, *13*, 76-83, doi:10.1016/j.fbio.2015.12.009.
144. Etzbach, L.; Meinert, M.; Faber, T.; Klein, C.; Schieber, A.; Weber, F. Effects of carrier agents on powder properties, stability of carotenoids, and encapsulation efficiency of goldenberry (
L.) powder produced by co-current spray drying. *Curr Res Food Sci* **2020**, *3*, 73-81, doi:10.1016/j.crfs.2020.03.002.
145. Malik, N.; Muttakin, S.; Lopez-Quiroga, E.; Watson, N.J.; Fryer, P.J.; Bakalis, S.; Gouseti, O. Microstructure and reconstitution of freeze-dried gum Arabic at a range of concentrations and primary drying temperatures. *Food Hydrocolloid* **2020**, *104*, doi:ARTN 105712
10.1016/j.foodhyd.2020.105712.
146. Lu, W.; Kelly, A.L.; Miao, S. Emulsion-based encapsulation and delivery systems for polyphenols. *Trends in Food Science & Technology* **2016**, *47*, 1-9, doi:10.1016/j.tifs.2015.10.015.
147. Martín, A.; Cocero, M.J. Micronization processes with supercritical fluids:: Fundamentals and mechanisms. *Adv Drug Deliver Rev* **2008**, *60*, 339-350, doi:10.1016/j.addr.2007.06.019.
148. Shi, J.; Xue, S.J.; Wang, B.; Wang, W.L.; Ye, X.Q.; Quek, S.Y. Optimization of formulation and influence of environmental stresses on stability of lycopene-microemulsion. *Lwt-Food Sci Technol* **2015**, *60*, 999-1008, doi:10.1016/j.lwt.2014.10.066.
149. Shariffa, Y.N.; Tan, T.B.; Uthumporn, U.; Abas, F.; Mirhosseini, H.; Nehdi, I.A.; Wang, Y.H.; Tan, C.P. Producing a lycopene nanodispersion: Formulation development and the effects of high pressure homogenization. *Food Res Int* **2017**, *101*, 165-172, doi:10.1016/j.foodres.2017.09.005.
150. Mao, L.K.; Xu, D.X.; Yang, J.; Yuan, F.; Gao, Y.X.; Zhao, J. Effects of Small and Large Molecule Emulsifiers on the Characteristics of beta-Carotene Nanoemulsions Prepared by High Pressure Homogenization. *Food Technol Biotech* **2009**, *47*, 336-342.
151. Shinoda, K.; Shinoda, K. *Solvent properties of surfactant solutions*; Edward Arnold: 1968; p. 365 pages : illustrations.
152. Rocha-Filho, D.S.B.T.A.P.N.R.M.J.B.G.S.V.G.C.O.P.A. Formation and stability of oil-in-water nanoemulsions containing rice bran oil: in vitro and in vivo assessments. *Journal of Nanobiotechnology* **2011**, *9(1)*, doi:doi:10.1186/1477-3155-9-44.
153. Kim, S.O.; Ha, T.V.; Choi, Y.J.; Ko, S. Optimization of homogenization-evaporation process for lycopene nanoemulsion production and its beverage applications. *J Food Sci* **2014**, *79*, N1604-1610, doi:10.1111/1750-3841.12472.
154. Correa, L.C.; Lourenco, S.C.; Duarte, D.F.; Moldao-Martins, M.; Alves, V.D. Microencapsulation of Tomato (Solanum lycopersicum L.) Pomace Ethanolic Extract by Spray Drying: Optimization of Process Conditions. *Appl Sci-Basel* **2019**, *9*, doi:ARTN 61210.3390/app9030612.

155. Bakry, A.M.; Abbas, S.; Ali, B.; Majeed, H.; Abouelwafa, M.Y.; Mousa, A.; Liang, L. Microencapsulation of Oils: A Comprehensive Review of Benefits, Techniques, and Applications. *Compr Rev Food Sci F* **2016**, *15*, 143-182, doi:10.1111/1541-4337.12179.
156. Salaün, F. Microencapsulation technology for smart textile coatings. *Woodhead Publ Ser Te* **2016**, 179-220, doi:10.1016/B978-0-08-100263-6.00009-5.
157. Chuyen, H.V.; Roach, P.D.; Golding, J.B.; Parks, S.E.; Nguyen, M.H. Encapsulation of carotenoid-rich oil from Gac peel: Optimisation of the encapsulating process using a spray drier and the storage stability of encapsulated powder. *Powder Technol* **2019**, *344*, 373-379, doi:10.1016/j.powtec.2018.12.012.
158. Geranpour, M.; Assadpour, E.; Jafari, S.M. Recent advances in the spray drying encapsulation of essential fatty acids and functional oils. *Trends in Food Science & Technology* **2020**, *102*, 71-90, doi:10.1016/j.tifs.2020.05.028.
159. Gheonea, I.; Aprodu, I.; Cîrciumaru, A.; Râpeanu, G.; Bahrim, G.E.; Stanciuc, N. Microencapsulation of lycopene from tomatoes peels by complex coacervation and freeze-drying: Evidences on phytochemical profile, stability and food applications. *J Food Eng* **2021**, *288*, doi:ARTN 110166 10.1016/j.jfoodeng.2020.110166.
160. Shu, B.; Yu, W.L.; Zhao, Y.P.; Liu, X.Y. Study on microencapsulation of lycopene by spray-drying. *J Food Eng* **2006**, *76*, 664-669, doi:10.1016/j.jfoodeng.2005.05.062.
161. Rocha-Selmi, G.A.; Favaro-Trindade, C.S.; Grosso, C.R.F. Morphology, Stability, and Application of Lycopene Microcapsules Produced by Complex Coacervation. *J Chem-Ny* **2013**, *2013*, doi:10.1155/2013/982603.
162. Souza, A.L.R.; Hidalgo-Chávez, D.W.; Pontes, S.M.; Gomes, F.S.; Cabral, L.M.C.; Tonon, R.V. Microencapsulation by spray drying of a lycopene-rich tomato concentrate: Characterization and stability. *Lwt-Food Sci Technol* **2018**, *91*, 286-292, doi:10.1016/j.lwt.2018.01.053.
163. Botrel, D.A.; Borges, S.V.; Fernandes, R.V.D.; Viana, A.D.; da Costa, J.M.G.; Marques, G.R. Evaluation of spray drying conditions on properties of microencapsulated oregano essential oil. *Int J Food Sci Tech* **2012**, *47*, 2289-2296, doi:10.1111/j.1365-2621.2012.03100.x.
164. Fernandes, R.V.; Borges, S.V.; Botrel, D.A. Gum arabic/starch/maltodextrin/inulin as wall materials on the microencapsulation of rosemary essential oil. *Carbohydr Polym* **2014**, *101*, 524-532, doi:10.1016/j.carbpol.2013.09.083.
165. Zhang, L.Q.; Zeng, X.H.; Fu, N.; Tang, X.; Sun, Y.; Lin, L. Maltodextrin: A consummate carrier for spray-drying of xylooligosaccharides. *Food Res Int* **2018**, *106*, 383-393, doi:10.1016/j.foodres.2018.01.004.
166. Nair, K.K.; Kharb, S.; Thompkinson, D.K. Inulin Dietary Fiber with Functional and Health AttributesA Review. *Food Rev Int* **2010**, *26*, 189-203, doi:Pii 91879471510.1080/87559121003590664.
167. Tonyali, B.; Sensoy, I.; Karakaya, S. The effect of extrusion on the functional components and in vitro lycopene bioaccessibility of tomato pulp added corn extrudates. *Food Funct* **2016**, *7*, 855-860, doi:10.1039/c5fo01185j.

168. Tapiero, H.; Townsend, D.M.; Tew, K.D. The role of carotenoids in the prevention of human pathologies. *Biomed Pharmacother* **2004**, *58*, 100-110, doi:10.1016/j.biopha.2003.12.006.
169. dos Santos, P.P.; Paese, K.; Guterres, S.S.; Pohlmann, A.R.; Costa, T.H.; Jablonski, A.; Flores, S.H.; Rios, A.D. Development of lycopene-loaded lipid-core nanocapsules: physicochemical characterization and stability study. *J Nanopart Res* **2015**, *17*, doi:ARTN 10710.1007/s11051-015-2917-5.
170. Kim, S.O.; Ha, T.V.A.; Choi, Y.J.; Ko, S. Optimization of Homogenization-Evaporation Process for Lycopene Nanoemulsion Production and Its Beverage Applications. *J Food Sci* **2014**, *79*, N1604-N1610, doi:10.1111/1750-3841.12472.
171. Boon, C.S.; McClements, D.J.; Weiss, J.; Decker, E.A. Role of Iron and Hydroperoxides in the Degradation of Lycopene in Oil-in-Water Emulsions. *J Agr Food Chem* **2009**, *57*, 2993-2998, doi:10.1021/jf803747j.
172. Jain, A.; Sharma, G.; Ghoshal, G.; Kesharwani, P.; Singh, B.; Shivhare, U.S.; Katar, O.P. Lycopene loaded whey protein isolate nanoparticles: An innovative endeavor for enhanced bioavailability of lycopene and anti-cancer activity. *Int J Pharm* **2018**, *546*, 97-105, doi:10.1016/j.ijpharm.2018.04.061.
173. Salimi, A.; Maghsoudlou, Y.; Jafari, S.M.; Mahoonak, A.S.; Kashaninejad, M.; Ziaiifar, A.M. Preparation of Lycopene Emulsions by Whey Protein Concentrate and Maltodextrin and Optimization by Response Surface Methodology. *J Disper Sci Technol* **2015**, *36*, 274-283, doi:10.1080/01932691.2013.879833.
174. Tan, C.; Feng, B.; Zhang, X.M.; Xia, W.S.; Xia, S.Q. Biopolymer-coated liposomes by electrostatic adsorption of chitosan (chitosomes) as novel delivery systems for carotenoids. *Food Hydrocolloid* **2016**, *52*, 774-784, doi:10.1016/j.foodhyd.2015.08.016.
175. Rostamabadi, H.; Falsafi, S.R.; Jafari, S.M. Nanoencapsulation of carotenoids within lipid-based nanocarriers. *J Control Release* **2019**, *298*, 38-67, doi:10.1016/j.jconrel.2019.02.005.
176. Rocha, G.A.; Favaro-Trindade, C.S.; Grosso, C.R.F. Microencapsulation of lycopene by spray drying: Characterization, stability and application of microcapsules. *Food Bioprod Process* **2012**, *90*, 37-42, doi:10.1016/j.fbp.2011.01.001.
177. Bouchemal, K.; Briancon, S.; Perrier, E.; Fessi, H. Nano-emulsion formulation using spontaneous emulsification: solvent, oil and surfactant optimisation. *Int J Pharm* **2004**, *280*, 241-251, doi:10.1016/j.ijpharm.2004.05.016.
178. Aboofazeli, R. Nanometric-Scaled Emulsions (Nanoemulsions). *Iran J Pharm Res* **2010**, *9*, 325-326.
179. Singh, Y.; Meher, J.G.; Raval, K.; Khan, F.A.; Chaurasia, M.; Jain, N.K.; Chourasia, M.K. Nanoemulsion: Concepts, development and applications in drug delivery. *J Control Release* **2017**, *252*, 28-49, doi:10.1016/j.jconrel.2017.03.008.
180. Marete, E.N.; Jacquier, J.C.; O'Riordan, D. Feverfew as a source of bioactives for functional foods: Storage stability in model beverages. *J Funct Foods* **2011**, *3*, 38-43, doi:10.1016/j.jff.2011.01.004.
181. Jizomoto, H.; Kanaoka, E.; Sugita, K.; Hirano, K. Gelatin-Acacia Microcapsules for Trapping Micro Oil Droplets Containing Lipophilic Drugs

and Ready Disintegration in the Gastrointestinal-Tract. *Pharmaceut Res* **1993**, *10*, 1115-1122, doi:Doi 10.1023/A:1018951814939.
182. Re, M.I. Formulating drug delivery systems by spray drying. *Dry Technol* **2006**, *24*, 433-446, doi:10.1080/07373930600611877.
183. Borel, T.; Sabliov, C.M. Nanodelivery of Bioactive Components for Food Applications: Types of Delivery Systems, Properties, and Their Effect on ADME Profiles and Toxicity of Nanoparticles. *Annu Rev Food Sci T* **2014**, *5*, 197-213, doi:10.1146/annurev-food-030713-092354.
184. Patel, S.; Goyal, A. Applications of Natural Polymer Gum Arabic: A Review. *Int J Food Prop* **2015**, *18*, 986-998, doi:10.1080/10942912.2013.809541.
185. Pk, S.; P, S. Novel Encapsulation of Lycopene in Niosomes and Assessment of its Anticancer Activity. *Journal of Bioequivalence & Bioavailability* **2016**, *8*, doi:10.4172/jbb.1000300.
186. dos Santos, P.P.; Andrade, L.D.; Flres, S.H.; Rios, A.D. Nanoencapsulation of carotenoids: a focus on different delivery systems and evaluation parameters. *J Food Sci Tech Mys* **2018**, *55*, 3851-3860, doi:10.1007/s13197-018-3316-6.
187. Nazemiyeh, E.; Eskandani, M.; Sheikhloie, H.; Nazemiyeh, H. Formulation and Physicochemical Characterization of Lycopene-Loaded Solid Lipid Nanoparticles. *Adv Pharm Bull* **2016**, *6*, 235-241, doi:10.15171/apb.2016.032.
188. Davis, A.R.; Fish, W.W.; Perkins-Veazie, P. A rapid spectrophotometric method for analyzing lycopene content in tomato and tomato products. *Postharvest Biol Tec* **2003**, *28*, 425-430, doi:Pii S0925-5214(02)00203-X Doi 10.1016/S0925-5214(02)00203-X.
189. Anguelova, T.; Warthesen, J. Lycopene stability in tomato powders. *J Food Sci* **2000**, *65*, 67-70, doi:DOI 10.1111/j.1365-2621.2000.tb15957.x.
190. Mangut, V.; Sabio, E.; Ganan, J.; Gonzalez, J.F.; Ramiro, A.; Gonzalez, C.M.; Roman, S.; Al-Kassir, A. Thermogravimetric study of the pyrolysis of biomass residues from tomato processing industry. *Fuel Process Technol* **2006**, *87*, 109-115, doi:10.1016/j.fuproc.2005.08.006.
191. Rossini, G.; Toscano, G.; Duca, D.; Corinaldesi, F.; Pedretti, E.F.; Riva, G. Analysis of the characteristics of the tomato manufacturing residues finalized to the energy recovery. *Biomass Bioenerg* **2013**, *51*, 177-182, doi:10.1016/j.biombioe.2013.01.018.
192. Celma, A.R.; Cuadros, F.; Lopez-Rodriguez, F. Characterization of pellets from industrial tomato residues. *Food Bioprod Process* **2012**, *90*, 700-706, doi:10.1016/j.fbp.2012.01.007.
193. Poojary, M.M.; Passamonti, P. Extraction of lycopene from tomato processing waste: Kinetics and modelling. *Food Chemistry* **2015**, *173*, 943-950, doi:10.1016/j.foodchem.2014.10.127.
194. Nour, V.; Panaite, T.D.; Ropota, M.; Turcu, R.; Trandafir, I.; Corbu, A.R. Nutritional and bioactive compounds in dried tomato processing waste. *Cyta-J Food* **2018**, *16*, 222-229, doi:10.1080/19476337.2017.1383514.
195. Pettinato, P.P.A.A.C.M. Process and System For Extracting Molecules From Solid Particle Matrices. 15/05/2021 2021.
196. Kumar, K.; Srivastav, S.; Sharanagat, V.S. Ultrasound assisted extraction (UAE) of bioactive compounds from fruit and vegetable processing by-products: A review. *Ultrason Sonochem* **2021**, *70*, doi:ARTN 10532510.1016/j.ultsonch.2020.105325.

197. Khuri, A.I.; Mukhopadhyay, S. Response surface methodology. *WIREs Computational Statistics* **2010**, *2*, 128-149, doi:10.1002/wics.73.
198. El Hami, A.; Pougnet, P. *Embedded Mechatronic Systems 2: Analysis of Failures, Modeling, Simulation and Optimization*; Elsevier: 2020; Volume 2.
199. DelCastillo, E.; Montgomery, D.C.; McCarville, D.R. Modified desirability functions for multiple response optimization. *J Qual Technol* **1996**, *28*, 337-345, doi:Doi 10.1080/00224065.1996.11979684.
200. Costa, N.R.; Lourenco, J.; Pereira, Z.L. Desirability function approach: A review and performance evaluation in adverse conditions. *Chemometr Intell Lab* **2011**, *107*, 234-244, doi:10.1016/j.chemolab.2011.04.004.
201. Vojnovic, D.; Moneghini, M.; Rubessa, F.; Zanchetta, A. Simultaneous-Optimization of Several Response Variables in a Granulation Process. *Drug Dev Ind Pharm* **1993**, *19*, 1479-1496, doi:Doi 10.3109/03639049309047186.
202. Pettinato, M.; Casazza, A.A.; Ferrari, P.F.; Perego, P. Optimization and modeling of solid-liquid multivariable extractor (SoLVE): A new solution for tomato waste valorization. *Chem Eng Res Des* **2022**, *182*, 465-477, doi:10.1016/j.cherd.2022.04.025.
203. Nagarajan, J.; Krishnamurthy, N.P.; Ramanan, R.N.; Raghunandan, M.E.; Galanakis, C.M.; Ooi, C.W. A facile water-induced complexation of lycopene and pectin from pink guava byproduct: Extraction, characterization and kinetic studies. *Food Chemistry* **2019**, *296*, 47-55, doi:10.1016/j.foodchem.2019.05.135.
204. Francis, F.J. Quality as Influenced by Color. *Food Qual Prefer* **1995**, *6*, 149-155, doi:Doi 10.1016/0950-3293(94)00026-R.
205. Cravotto, C.; Grillo, G.; Binello, A.; Gallina, L.; Olivares-Vicente, M.; Herranz-Lopez, M.; Micol, V.; Barrajon-Catalan, E.; Cravotto, G. Bioactive Antioxidant Compounds from Chestnut Peels through Semi-Industrial Subcritical Water Extraction. *Antioxidants-Basel* **2022**, *11*, doi:ARTN 98810.3390/antiox11050988.
206. Ferreira, D.F.; Barin, J.S.; Binello, A.; Veselou, V.V.; Cravotto, G. Highly efficient pumpkin-seed extraction with the simultaneous recovery of lipophilic and hydrophilic compounds. *Food Bioprod Process* **2019**, *117*, 224-230, doi:10.1016/j.fbp.2019.07.014.
207. Re, R.; Pellegrini, N.; Proteggente, A.; Pannala, A.; Yang, M.; Rice-Evans, C. Antioxidant activity applying an improved ABTS radical cation decolorization assay. *Free Radical Bio Med* **1999**, *26*, 1231-1237, doi:Doi 10.1016/S0891-5849(98)00315-3.
208. Yagmur, N.; Sahin, S. Encapsulation of ellagic acid from pomegranate peels in microalgae optimized by response surface methodology and an investigation of its controlled released under simulated gastrointestinal studies. *J Food Sci* **2020**, *85*, 998-1006, doi:10.1111/1750-3841.15085.
209. Xu, Y.; Pan, S.Y. Effects of various factors of ultrasonic treatment on the extraction yield of all-trans-lycopene from red grapefruit (Citrus paradise Macf.). *Ultrason Sonochem* **2013**, *20*, 1026-1032, doi:10.1016/j.ultsonch.2013.01.006.
210. Ying, Z.; Han, X.X.; Li, J.R. Ultrasound-assisted extraction of polysaccharides from mulberry leaves. *Food Chemistry* **2011**, *127*, 1273-1279, doi:10.1016/j.foodchem.2011.01.083.

211. Srivastava, S.; Srivastava, A.K. Lycopene; chemistry, biosynthesis, metabolism and degradation under various abiotic parameters. *J Food Sci Tech Mys* **2015**, *52*, 41-53, doi:10.1007/s13197-012-0918-2.
212. Luengo, E.; Condon-Abanto, S.; Condon, S.; Alvarez, I.; Raso, J. Improving the extraction of carotenoids from tomato waste by application of ultrasound under pressure. *Sep Purif Technol* **2014**, *136*, 130-136, doi:10.1016/j.seppur.2014.09.008.
213. Priyadarsani, S.; Patel, A.S.; Kar, A.; Dash, S. Process optimization for the supercritical carbondioxide extraction of lycopene from ripe grapefruit (Citrus paradisi) endocarp. *Sci Rep-Uk* **2021**, *11*, doi:ARTN 1027310.1038/s41598-021-89772-6.
214. Xi, J. Effect of high pressure processing on the extraction of lycopene in tomato paste waste. *Chem Eng Technol* **2006**, *29*, 736-739, doi:10.1002/ceat.200600024.
215. Grassino, A.N.; Pedisic, S.; Dragovic-Uzelac, V.; Karlovic, S.; Jezek, D.; Bosiljkov, T. Insight into High-Hydrostatic Pressure Extraction of Polyphenols from Tomato Peel Waste. *Plant Food Hum Nutr* **2020**, *75*, 427-433, doi:10.1007/s11130-020-00831-1.
216. Szabo, K.; Dulf, F.V.; Diaconeasa, Z.; Vodnar, D.C. Antimicrobial and antioxidant properties of tomato processing byproducts and their correlation with the biochemical composition. *Lwt-Food Sci Technol* **2019**, *116*, doi:ARTN 10855810.1016/j.lwt.2019.108558.
217. Ummat, V.; Tiwari, B.K.; Jaiswal, A.K.; Condon, K.; Garcia-Vaquero, M.; O'Doherty, J.; O'Donnell, C.; Rajauria, G. Optimisation of Ultrasound Frequency, Extraction Time and Solvent for the Recovery of Polyphenols, Phlorotannins and Associated Antioxidant Activity from Brown Seaweeds. *Mar Drugs* **2020**, *18*, doi:ARTN 25010.3390/md18050250.
218. Eh, A.L.S.; Teoh, S.G. Novel modified ultrasonication technique for the extraction of lycopene from tomatoes. *Ultrason Sonochem* **2012**, *19*, 151-159, doi:10.1016/j.ultsonch.2011.05.019.
219. Ali, M.C.; Chen, J.; Zhang, H.J.; Li, Z.; Zhao, L.; Qiu, H.D. Effective extraction of flavonoids from Lycium barbarum L. fruits by deep eutectic solvents-based ultrasound-assisted extraction. *Talanta* **2019**, *203*, 16-22, doi:10.1016/j.talanta.2019.05.012.
220. Borras-Enriquez, A.J.; Reyes-Ventura, E.; Villanueva-Rodriguez, S.J.; Moreno-Vilet, L. Effect of Ultrasound-Assisted Extraction Parameters on Total Polyphenols and Its Antioxidant Activity from Mango Residues (Mangifera indica L. var. Manililla). *Separations* **2021**, *8*, doi:ARTN 9410.3390/separations8070094.
221. Ferrari, P.F.; Pettinato, M.; Casazza, A.A.; Atanasio, G.D.; Palombo, D.; Perego, P. Polyphenols from Nerone Gold 26/6, a new pigmented rice, via non-conventional extractions: antioxidant properties and biological validation. *J Chem Technol Biot* **2021**, *96*, 1691-1699, doi:10.1002/jctb.6694.
222. Liao, J.Q.; Zheng, N.; Qu, B.D. An Improved Ultrasonic-Assisted Extraction Method by Optimizing the Ultrasonic Frequency for Enhancing the Extraction Efficiency of Lycopene from Tomatoes. *Food Anal Method* **2016**, *9*, 2288-2298, doi:10.1007/s12161-016-0419-4.
223. Grassino, A.N.; Ostojic, J.; Miletic, V.; Djakovic, S.; Bosiljkov, T.; Zoric, Z.; Jezek, D.; Brncic, S.R.; Brncic, M. Application of high hydrostatic pressure

and ultrasound-assisted extractions as a novel approach for pectin and polyphenols recovery from tomato peel waste. *Innov Food Sci Emerg* **2020**, *64*, doi:ARTN 10242410.1016/j.ifset.2020.102424.

224. Mao, Y.J.; Robinson, J.; Binner, E. Understanding heat and mass transfer processes during microwave-assisted and conventional solvent extraction. *Chem Eng Sci* **2021**, *233*, doi:ARTN 11641810.1016/j.ces.2020.116418.
225. Chemat, F.; Rombaut, N.; Sicaire, A.G.; Meullemiestre, A.; Fabiano-Tixier, A.S.; Abert-Vian, M. Ultrasound assisted extraction of food and natural products. Mechanisms, techniques, combinations, protocols and applications. A review. *Ultrason Sonochem* **2017**, *34*, 540-560, doi:10.1016/j.ultsonch.2016.06.035.
226. Oliveira, V.S.; Rodrigues, S.; Fernandes, F.A.N. Effect of high power low frequency ultrasound processing on the stability of lycopene. *Ultrason Sonochem* **2015**, *27*, 586-591, doi:10.1016/j.ultsonch.2015.04.016.
227. Goula, A.M.; Ververi, M.; Adamopoulou, A.; Kaderides, K. Green ultrasound-assisted extraction of carotenoids from pomegranate wastes using vegetable oils. *Ultrason Sonochem* **2017**, *34*, 821-830, doi:10.1016/j.ultsonch.2016.07.022.
228. Preece, K.E.; Hooshyar, N.; Krijgsman, A.J.; Fryer, P.J.; Zuidam, N.J. Pilot-scale ultrasound-assisted extraction of protein from soybean processing materials shows it is not recommended for industrial usage. *J Food Eng* **2017**, *206*, 1-12, doi:10.1016/j.jfoodeng.2017.02.002.
229. Kulkarni, V.M.; Rathod, V.K. Mapping of an ultrasonic bath for ultrasound assisted extraction of mangiferin from Mangifera indica leaves. *Ultrason Sonochem* **2014**, *21*, 606-611, doi:10.1016/j.ultsonch.2013.08.021.
230. Mizrach, A. Ultrasonic technology for quality evaluation of fresh fruit and vegetables in pre- and postharvest processes. *Postharvest Biol Tec* **2008**, *48*, 315-330, doi:10.1016/j.postharvbio.2007.10.018.
231. Kaur, D.; Wani, A.A.; Oberoi, D.P.S.; Sogi, D.S. Effect of extraction conditions on lycopene extractions from tomato processing waste skin using response surface methodology. *Food Chemistry* **2008**, *108*, 711-718, doi:10.1016/j.foodchem.2007.11.002.
232. Shi, J.; Yi, C.; Xue, S.J.; Jiang, Y.M.; Ma, Y.; Li, D. Effects of modifiers on the profile of lycopene extracted from tomato skins by supercritical CO2. *J Food Eng* **2009**, *93*, 431-436, doi:10.1016/j.jfoodeng.2009.02.008.
233. Dewanto, V.; Wu, X.Z.; Adom, K.K.; Liu, R.H. Thermal processing enhances the nutritional value of tomatoes by increasing total antioxidant activity. *J Agr Food Chem* **2002**, *50*, 3010-3014, doi:10.1021/jf0115589.
234. Hackett, M.M.; Lee, J.H.; Francis, D.; Schwartz, S.J. Thermal stability and isomerization of lycopene in tomato oleoresins from different varieties. *J Food Sci* **2004**, *69*, C536-C541.
235. Alonso, M.J.C.S.G.S.P.E. Supercritical extraction of unsaturated products. Degradation of β-carotene in supercritical extraction processes. *The Journal of Supercritical Fluids* **2000**, *19*, 39-44, doi:10.1016/S0896-8446(00)00077-2.
236. Bucic-Kojic, A.; Planinic, M.; Tomas, S.; Bilic, M.; Velic, D. Study of solid-liquid extraction kinetics of total polyphenols from grape seeds. *J Food Eng* **2007**, *81*, 236-242, doi:10.1016/j.jfoodeng.2006.10.027.
237. Odriozola-Serrano, I.; Soliva-Fortuny, R.; Gimeno-Ano, V.; Martin-Belloso, O. Modeling changes in health-related compounds of tomato juice treated by

high-intensity pulsed electric fields. *J Food Eng* **2008**, *89*, 210-216, doi:10.1016/j.jfoodeng.2008.04.019.

238. Boileau, A.C.; Merchen, N.R.; Wasson, K.; Atkinson, C.A.; Erdman, J.W. Cis-lycopene is more bioavailable than trans-lycopene in vitro and in vivo in lymph-cannulated ferrets. *J Nutr* **1999**, *129*, 1176-1181, doi:DOI 10.1093/jn/129.6.1176.
239. Vallecilla-Yepez, L.; Ciftci, O.N. Increasing cis-lycopene content of the oleoresin from tomato processing byproducts using supercritical carbon dioxide. *Lwt-Food Sci Technol* **2018**, *95*, 354-360, doi:10.1016/j.lwt.2018.04.065.
240. Hatami, T.; Ciftci, O.N. A step-by-step technoeconomic analysis of supercritical carbon dioxide extraction of lycopene from tomato processing waste. *J Food Eng* **2023**, *357*, doi:ARTN 111639 10.1016/j.jfoodeng.2023.111639.
241. Calvo, M.M.; Dado, D.; Santa-Maria, G. Influence of extraction with ethanol or ethyl acetate on the yield of lycopene, beta-carotene, phytoene and phytofluene from tomato peel powder. *Eur Food Res Technol* **2007**, *224*, 567-571, doi:10.1007/s00217-006-0335-8.
242. Lu, Z.Q.; Wang, J.J.; Gao, R.P.; Ye, F.Y.; Zhao, G.H. Sustainable valorisation of tomato pomace: A comprehensive review. *Trends in Food Science & Technology* **2019**, *86*, 172-187, doi:10.1016/j.tifs.2019.02.020.
243. Ushikubo, F.Y.; Cunha, R.L. Stability mechanisms of liquid water-in-oil emulsions. *Food Hydrocolloid* **2014**, *34*, 145-153, doi:10.1016/j.foodhyd.2012.11.016.
244. Sansone, F.; Mencherini, T.; Picerno, P.; d'Amore, M.; Aquino, R.P.; Lauro, M.R. Maltodextrin/pectin microparticles by spray drying as carrier for nutraceutical extracts. *J Food Eng* **2011**, *105*, 468-476, doi:10.1016/j.jfoodeng.2011.03.004.
245. Amid, B.T.; Mirhosseini, H. Emulsifying Activity, Particle Uniformity and Rheological Properties of a Natural Polysaccharide-Protein Biopolymer from Durian Seed. *Food Biophysics* **2012**, *7*, 317-328, doi:10.1007/s11483-012-9270-3.
246. Zhao, C.C.; Wei, L.P.; Yin, B.B.; Liu, F.G.; Li, J.Y.; Liu, X.B.; Wang, J.G.; Wang, Y.T. Encapsulation of lycopene within oil-in-water nanoemulsions using lactoferrin: Impact of carrier oils on physicochemical stability and bioaccessibility. *Int J Biol Macromol* **2020**, *153*, 912-920, doi:10.1016/j.ijbiomac.2020.03.063.
247. Ferreira, A.C.; Sullo, A.; Winston, S.; Norton, I.T.; Norton-Welch, A.B. Influence of Ethanol on Emulsions Stabilized by Low Molecular Weight Surfactants. *J Food Sci* **2020**, *85*, 28-35, doi:10.1111/1750-3841.14947.
248. Zhou, Q.X.; Yang, L.; Xu, J.; Qiao, X.; Li, Z.J.; Wang, Y.M.; Xue, C.H. Evaluation of the physicochemical stability and digestibility of microencapsulated esterified astaxanthins using in vitro and in vivo models. *Food Chemistry* **2018**, *260*, 73-81, doi:10.1016/j.foodchem.2018.03.046.
249. Srivastava, S.; Kulshreshtha, K. Development and physic chemical characterization of tomato powder. *Beverage & Food World* **2012**, *39*, 56-59.
250. Lee, M.T.; Chen, B.H. Stability of lycopene during heating and illumination in a model system. *Food Chemistry* **2002**, *78*, 425-432, doi:Pii S0308-8146(02)00146-2 Doi 10.1016/S0308-8146(02)00146-2.

251. Ax, K.; Mayer-Miebach, E.; Link, B.; Schuchmann, H.; Schubert, H. Stability of Lycopene in Oil-in-Water Emulsions. *Eng Life Sci* **2003**, *3*, 199-201, doi:10.1002/elsc.200390028.
252. Walstra, P.; ProQuest. *Physical chemistry of foods*; Marcel Dekker: New York, 2003.
253. McClements, D.J.; Rao, J. Food-Grade Nanoemulsions: Formulation, Fabrication, Properties, Performance, Biological Fate, and Potential Toxicity. *Critical Reviews in Food Science and Nutrition* **2011**, *51*, 285-330, doi:Pii 935269214 10.1080/10408398.2011.559558.
254. Burgaud, I.; Dickinson, E. Emulsifying Effects of Food Macromolecules in Presence of Ethanol. *J Food Sci* **1990**, *55*, 875-876, doi:DOI 10.1111/j.1365-2621.1990.tb05257.x.
255. Agboola, S.O.; Dalgleish, D.G. Effects of pH and ethanol on the kinetics of destabilisation of oil-in-water emulsions containing milk proteins. *Journal of the Science of Food and Agriculture* **1996**, *72*, 448-454.
256. Zeeb, B.; Herz, E.; McClements, D.J.; Weiss, J. Impact of alcohols on the formation and stability of protein-stabilized nanoemulsions. *J Colloid Interf Sci* **2014**, *433*, 196-203, doi:10.1016/j.jcis.2014.07.034.
257. Aguiar, J.; Estevinho, B.N.; Santos, L. Microencapsulation of natural antioxidants for food application - The specific case of coffee antioxidants - A review. *Trends in Food Science & Technology* **2016**, *58*, 21-39, doi:10.1016/j.tifs.2016.10.012.
258. Mujumdar, A.S. *Handbook of industrial drying*, 3rd ed.; CRC Press: Place of publication not identified, 2006.
259. Pralits, J.O.; Atzori, M.; Colli, M.; Pettinato, M.; Drago, E.; Perego, P. Unsteadiness and resolution effects in experimentally verified simulations of a spray drying process. *Powder Technology* **2022**, *404*, doi:10.1016/j.powtec.2022.117482.
260. da Costa, R.S.; Teixeira, C.B.; Gabbay Alves, T.V.; Ribeiro-Costa, R.M.; Casazza, A.A.; Aliakbarian, B.; Converti, A.; Silva Junior, J.O.C.; Perego, P. Optimization of spray drying conditions to microencapsulate cupuassu (Theobroma grandiflorum) seed by-product extract. *Nat Prod Res* **2019**, *33*, 2600-2608, doi:10.1080/14786419.2018.1462178.
261. Margherita Pettinato; Bahar Aliakbarian; Alessandro A. Casazza; Perego, P. Encapsulation of Antioxidants from Spent Coffee Ground Extracts by Spray Drying *CHEMICAL ENGINEERING TRANSACTIONS* **2017**, *57*, doi:10.3303/CET1757204.
262. Robert, P.; Gorena, T.; Romero, N.; Sepulveda, E.; Chavez, J.; Saenz, C. Encapsulation of polyphenols and anthocyanins from pomegranate (Punica granatum) by spray drying. *Int J Food Sci Tech* **2010**, *45*, 1386-1394, doi:10.1111/j.1365-2621.2010.02270.x.
263. Ahmed, M.; Akter, M.S.; Lee, J.C.; Eun, J.B. Encapsulation by spray drying of bioactive components, physicochemical and morphological properties from purple sweet potato. *Lwt-Food Sci Technol* **2010**, *43*, 1307-1312, doi:10.1016/j.lwt.2010.05.014.
264. Lai, H.M.; Cheng, H.H. Properties of pregelatinized rice flour made by hot air or gum puffing. *Int J Food Sci Tech* **2004**, *39*, 201-212, doi:DOI 10.1046/j.0950-5423.2003.00761.x.

265. Eun, J.B.; Maruf, A.; Das, P.R.; Nam, S.H. A review of encapsulation of carotenoids using spray drying and freeze drying. *Critical Reviews in Food Science and Nutrition* **2020**, *60*, 3547-3572, doi:10.1080/10408398.2019.1698511.
266. Ballesteros, L.F.; Ramirez, M.J.; Orrego, C.E.; Teixeira, J.A.; Mussatto, S.I. Encapsulation of antioxidant phenolic compounds extracted from spent coffee grounds by freeze-drying and spray-drying using different coating materials. *Food Chemistry* **2017**, *237*, 623-631, doi:10.1016/j.foodchem.2017.05.142.
267. Nishad, J.; Mir, S.A.; Walia, K. Optimization of Spray Drying Technology for Sugarcane Juice Using Natural and Synthetic Encapsulating Agents. *Sugar Tech* **2019**, *21*, 749-755, doi:10.1007/s12355-018-0696-x.
268. Ma, W.Y.; Zhang, J.; Shu, L.; Tan, X.Q.; An, Y.; Yang, X.D.; Wang, D.P.; Gao, Q. Optimization of spray drying conditions for the green manufacture of gamma-aminobutyric acid-rich powder from Lactobacillus brevis fermentation broth. *Biochem Eng J* **2020**, *156*, doi:ARTN 10749910.1016/j.bej.2020.107499.
269. Chasekioglou, A.N.; Goula, A.M.; Adamopoulos, K.G.; Lazarides, H.N. An approach to turn olive mill wastewater into a valuable food by-product based on spray drying in dehumidified air using drying aids. *Powder Technol* **2017**, *311*, 376-389, doi:10.1016/j.powtec.2017.02.008.
270. Souza, A.L.R.; Hidalgo-Chavez, D.W.; Pontes, S.M.; Gomes, F.S.; Cabral, L.M.C.; Tonon, R.V. Microencapsulation by spray drying of a lycopene-rich tomato concentrate: Characterization and stability. *Lwt-Food Sci Technol* **2018**, *91*, 286-292, doi:10.1016/j.lwt.2018.01.053.
271. Jafari, S.M.; Ghalenoei, M.G.; Dehnad, D. Influence of spray drying on water solubility index, apparent density, and anthocyanin content of pomegranate juice powder. *Powder Technol* **2017**, *311*, 59-65, doi:10.1016/j.powtec.2017.01.070.
272. Nargis Yousf, F.N., Rehana Salim, Hafiza Ahsan and Adnan Sirwal. Water solubility index and water absorption index of extruded product from rice and carrot blend. *Journal of Pharmacognosy and Phytochemistry* **2017**, *6*, 2165-2168.
273. Franco, P.; De Marco, I. Nanoparticles and Nanocrystals by Supercritical CO2-Assisted Techniques for Pharmaceutical Applications: A Review. *Appl Sci-Basel* **2021**, *11*, doi:ARTN 147610.3390/app11041476.
274. De Marco, I.; Franco, P. Effect of the Carrier on the Coprecipitation of Curcumin through Supercritical-Assisted Atomization. *Chemengineering* **2021**, *5*, doi:ARTN 5910.3390/chemengineering5030059.

RINGRAZIAMENTI

During my whole PhD journey, I am always very grateful and happy to be a member of UNIGE. I knew many interesting and wise people here and they made an indelible impression on me. I feel fully supported by my families, colleagues and friends. Importantly, many thanks to my supervisors, Prof. Patrizia Perego and Dr. Margherita Pettinato, it is hard to imagine that I can finish my PhD project so efficiently without their supports. Your academic expertise and appreciated personal characteristics have been keeping impressing and benefiting me which is so vital to my life. You give me confidence and courage to achieve this important milestone. I still remember that prof. Patrizia perego showed me the way and attitude to deal with project issues in a point of professional view. You are always there whenever I need you and made sure that everything went well. Thank you very much for your guidance, and also for accompanying me from work to life.

Also many thanks to Prof. Iolanda De Marco, Prof. Giancarlo Cravotto, and Prof. Chenggang Cai, and Prof. jingtao Zhang, I am so glad to collaborate with all of you. My experiment or manuscript would not have been as they are without your broadened scope. My best colleagues – Prof. Roberta Campardelli, Prof. Alessandro Alberto Casazza, Emanuala Drago, Pier Francesco Ferrari, Chiara Bufalini, Maria Bolla, Giuglia D'agostino, Shabnam Mirizadeh and Fatemeh Ahmadpoor, thank you so much for studying and working together to exchange knowledge and inspire discussion, even though we are in the separate projects. You took some of the work that needs strength off my hands since you came. Your humorous and personality makes our lab-life so bright and happy. It was a pleasure to be one of our groups over the last three years. Also, many thanks to everyone in Chemical Engineering department and I wish all the bests to you.

Last but not the least, I really appreciate Enrico Franceschi and Maria Augusta Carpineti who gave me a grand help for working and living in Italy.

Thanks to all of you – supervisors, colleagues, families and friends. I am so grateful to have you in my life.